

**Agbomerie Charles Odijie** BEng, MSc.

## DESIGN OF PAIRED COLUMN SEMISUBMERSIBLE HULL

Thesis submitted for the degree of Doctor of Philosophy

November 2016



Faculty of Science and Technology, Department of Engineering

Engineering Building

Lancaster University

Lancaster,

United Kingdom.

LA1 4YW

Email: [engineering@lancaster.ac.uk](mailto:engineering@lancaster.ac.uk)

Tel: +44(0)1624 593314

## **Abstract**

There is a constant effort to reconfigure column stabilized semisubmersible unit to meet the challenging demands associated with deep water exploration. Paired column semisubmersible platform is one of the recent column stabilized semisubmersible hull configured to allow top-deck well head compatibility for oil reserves in deep waters. Its unique ability to maintain reduced vertical motion in extreme weather conditions despite its hull size and payload create a high payload to motion ratio, as compare to conventional semisubmersible hulls. This unique feature makes it recommendable for other hull applications in ocean engineering. A study has been carried out to harness this high payload to motion ratio offered by this new hull concept in the development of drilling and production platforms in deep waters, support and foundation systems.

Numerical models were developed to understand the semisubmersible hull (dynamics of the reduced vertical motion and its ability to withstand bending and twisting behaviour from extreme wave conditions). Prior to this, a preliminary CFD model was developed in to understand the vortex shedding effect on the arrayed columns. An experimental setup was also put together to understand this motion behaviour, alongside a detailed review of the first model. The motion response of a scaled hull model was studied in a wave tank with a Digital Image Correlation (DIC) system known as Imetrum. To further investigate its application for other ocean depths and support systems, series of hydrodynamic models were developed in ANSYS AQWA with weather conditions as recommended by API, DNV, and ABS. The AQWA model was validated with results recorded by Imetrum system from the wave tank experimental test. The wave forces and moments were studied for different draft sizes and ocean conditions, and their response where checked in ORCAFLEX. A finite element model was finally developed in APDL to understand the nature and effect of stresses from wave, current and wind loads, alongside topside integration.

The results obtained from the FE model was use to postulate reinforcement during scantling, for different hull applications. The results for motion response showed favourable heeling moment for smaller draft sizes as recommended by regulatory bodies, but a reconfiguration for heave displacement might be required for smaller draft size. In such case, an increase in pontoon area or an additional heave plate attachment has been recommended. Furthermore, the effect of wave-current interactions was observed to create unique motion behaviour for all draft sizes at resonance frequency range. A fluid-structure interaction model of multi-phase flow will be required to understand this behaviour. The stress concentration on the columns generated from hydrodynamic loads was observed to be higher on the inner columns, relative to the outer ones.



## **Contributions**

- i. A new standard for estimating the draft size for paired column semisubmersible hull application has been postulated, for an inclusion of top tension production risers.
- ii. The motion response of a PC-Semi has been characterized, and hull optimization will be necessary to improve its rotational behaviour at the resonant frequency in the horizontal plane (roll and pitch motions).
- iii. Insight into the effect of wave-current interaction on the multiple column arrangements of a PC-Semi has been recorded.
- iv. Contributions of wave drift phenomenon to PC-Semi hull motion.
- v. Column shape configuration and inner/outer column spacing for future design of PC-Semi have been developed. Spacing less than three times the diameter of the columns will generate a highly uneven drag around the hull. This will create a level of instability.
- vi. The reasons behind the low VIM amplitude have been discovered to be the collision of shed vortexes from inner and outer columns. This finding can be applied in subsequent applications of multi-columns arrangement where reciprocating vortexes resonate with the structure's natural frequencies.
- vii. A novel concept for formulating boundary conditions for complex floating bodies under hydrodynamic loads for finite element analysis has been developed. It involves the coupling of hydrostatic translational and rotational stiffness with the hydrodynamic response properties of the body.
- viii. An insight into the unique nature of stress distribution around the hull of a PC-Semi has also been presented in this chapter. The contributions of hydrodynamic loads, alongside mooring and riser loads, to the level of stress and possible buckling tendencies of the columns were discussed. This contribution is very significant in selecting materials and their sizes for scantling, and general hull reinforcement.

## **List of Publications and Presentations**

- Presentation on Stress Distribution from Vortex Interactions on a PC-Semi at the International Conference on Light Weight Design of Marine Structures (LIMAS), Glasgow, United Kingdom. November 2015.
- Presentation of Vortex Shedding Effect on paired Column Semisubmersible Hull at The International Conference on Advances in Steel Structures (ICASS), Lisbon, Portugal. July 2015.
- Odijie, A.C. and Ye, J., 2015. Effect of vortex induced vibration on a paired-column semisubmersible platform. *International Journal of Structural Stability and Dynamics*, 15(08), p.1540019. **Published**
- Odijie, C. and Ye, J., 2015. Understanding Fluid-Structure Interaction for high amplitude wave loadings on a deep-draft paired column semi-submersible platform: a finite element approach. In *International Conference on Light Weight Design of Marine Structures*. **Published**
- Odijie, A.C., Wang F., and Ye, J., 2016. A Review of Floating Semisubmersible Hull Systems: Column Stabilized Unit. *Ocean Engineering*, October 2016. *Ocean Engineering*. **Accepted for publication**
- Odijie, A.C., Quayle, S. and Ye, J., 2017. Wave Induced Stress Profile on a Paired Column Semisubmersible Hull Formation for Column Reinforcement. March 2017. *Journal of Engineering Structures*, 143 (2017) 77-90. **Published**
- Odijie, A.C. and Ye, J., 2017. Experimental and Numerical Study of Hydrodynamic Behaviour of an Unstiffened Deep-Draft Paired-Column Semisubmersible Hull from Biaxial Combined Hydrodynamic Loads: Response and Elastic Study. **Draft**

## **Acknowledgement**

The time I spent studying for my Ph.D. degree at Lancaster University was a combination of both academic work and building relationships with industry experts in ocean engineering. My life and engineering career have received a huge boost not only because I was able to design my hull as earlier projected, but because I gain other skills in the process, alongside building relationships.

Special thanks to Professor Jianqiao Ye for giving me the option to work on ocean structures and availing me the opportunity to be his research student. Outside the routine meetings and updates on my research progress, he taught me other aspects of engineering including structural and material designs. I was able to learn how to critically analyse engineering problems, how to develop a research, and how to work on constructive criticisms to improve my work. I will always be grateful to him for his moral and academic support to the successful development of this project.

I also want to thank Dr. Stephen Quayle with his help and assistance on the wave tank; as it was the only way I was able to get a complete understanding of the working principles and conditions of the Lancaster University wave tank. Thanks to Dr. Geoffrey Turvey for his academic advice and direction. Andrew Gavriluk was very helpful in optimizing the computer capacity for developing the numerical models; I am particularly grateful to him. I also want to acknowledge the contributions from the workshop staff; particularly Mark Salisbury, for their help in fabricating the hulls, making alterations at different stages of the experiment. I also want to thank my colleague Mohammed Milad, for his assistance with calibrating the Imetrum system.

I also want to thank my best friends, Elisabeth Roy and Akhademe Ferdinand, they were the source of inspiration I had during my lonely and difficult times. I want to thank some of my colleagues; Adeayo Sotayo, Yakubu Itsado, Naley Alobari, Opeyemi Ehimiaghe, Animashaun Fasasi Olatunde, and Aghogho Ohwoka for their contributions to the successful completion of this project. I will always be grateful to them.

Finally, I would like to thank my family for their financial and moral support; Eromosele, Andrew, Louis, Kingsley, Irene, Fidelis, Helen, Grace, Ehis, Adrienn, Fred, Ebosetale, mum and dad. It is their care, love, and kindness that brought me this far.

**Dedicated to my parents**

Joseph Osaobho Odijie

and

Victoria Odijie

# Contents

<b>Contributions</b> .....	<b>iii</b>
<b>List of Publications and Presentations</b> .....	<b>iv</b>
<b>Acknowledgement</b> .....	<b>v</b>
<b>List of Figures</b> .....	<b>xv</b>
<b>List of Tables</b> .....	<b>xxi</b>
<b>Regulatory Bodies</b> .....	<b>xxiii</b>
<b>List of Abbreviations</b> .....	<b>xxiv</b>
<b>Nomenclature</b> .....	<b>xxvi</b>
Chapter 2.....	xxvi
Chapter 3.....	xxvi
Chapter 4.....	xxvi
Chapter 5.....	xxvii
Chapter 6.....	xxvii
<b>Chapter One: Introduction</b> .....	<b>1</b>
<b>1.1 Background of Study</b> .....	<b>1</b>
<b>1.2 Scope</b> .....	<b>3</b>
<b>1.3 Aim and Objectives of Study</b> .....	<b>4</b>
1.3.1 Aim.....	4
1.3.2 Objectives.....	4
<b>1.4 Design Approach</b> .....	<b>5</b>
1.3.1 Design for motion and stability.....	6
1.3.2 Design for strength .....	8
<b>1.5 Methodologies</b> .....	<b>8</b>



<b>1.6 Thesis Outline .....</b>	<b>9</b>
1.6.1 Chapter Two: Review of Semisubmersible Hull Systems: Column Stabilized Unit .....	9
1.6.2 Chapter Three: Experimental Study of Motion Characterises of PC-Semi: VIM and Global Performance .....	10
1.6.3 Chapter Four: Numerical Simulation of Hydrodynamic Loading on a PC-Semi for Motion Characterization .....	10
1.6.4 Chapter Five: Effect of Vortex Shedding on a PC-Semi Hull formation.....	10
1.6.5 Chapter Six: Finite Element Modelling of PC-Semi for Hull Reinforcement.....	11
1.6.6 Chapter Seven: Recommendations for Design Improvement .....	11
1.6.7 Chapter Eight: Conclusion.....	11
<b>Chapter Two: Review of Floating Semisubmersible Hull Systems; Column Stabilized Unit .....</b>	<b>13</b>
<b>2.1 Introduction.....</b>	<b>13</b>
<b>2.2 Background of Semisubmersible Hull .....</b>	<b>13</b>
2.2.1 Brief History and Development .....	13
2.2.2 Evolution of Design .....	15
2.2.3 Degree of Freedom .....	19
2.2.4 Structural Attachments .....	21
2.2.4.1 Mooring Lines.....	21
2.2.4.2 Risers.....	22
<b>2.3 Dynamics .....</b>	<b>23</b>
<b>2.4 Strength .....</b>	<b>26</b>
<b>2.5 Applications for Drilling and Production Systems: Dry-Trees Concepts .....</b>	<b>28</b>
2.5.1 Development of Paired Column Semisubmersible Hull .....	29
2.5.2 The Extendable Draft Platform .....	31
2.5.3 E-Semi and T-Semi .....	32
2.5.4 Aker Deep Draft Concept (ADTS) .....	32
<b>2.6 Offshore Wind Turbine Foundation.....</b>	<b>33</b>

<b>2.7 Future Application: Luxury Cruise .....</b>	<b>34</b>
<b>2.8 Other Types of Floating Hull Systems .....</b>	<b>35</b>
2.7.1 Tension Leg Platform.....	35
2.7.2 Spar Platform .....	36
2.7.3 Floating Production Storage and Offloading Platform (FPSO).....	38
<b>2.9 Chapter Summary .....</b>	<b>38</b>
<b>Chapter Three: Experimental Study of Motion Characteristics of PC-Semi; Global Performance.....</b>	<b>41</b>
<b>3.1 Introduction.....</b>	<b>41</b>
<b>3.2 Experimental Study of Vortex Induced Motion .....</b>	<b>42</b>
<b>3.3 Experimental Study of Global Performance .....</b>	<b>45</b>
<b>3.4 Lancaster University Wave Tank Test.....</b>	<b>47</b>
3.4.1 Model description.....	48
3.4.2 Limitation .....	49
3.4.3 Test.....	49
3.4.4 Post-processing: Result analysis .....	50
<b>3.5 Chapter Summary .....</b>	<b>51</b>
<b>Chapter 4 Numerical Simulation of Hydrodynamic Loading on a PC-Semi for Motion Characterization .....</b>	<b>53</b>
<b>4.1 Introduction.....</b>	<b>53</b>
<b>4.2 Methodology: Theory Formulation .....</b>	<b>55</b>
4.2.1 Wave Kinematics .....	56
4.2.1.1 Definition of Surface Wave .....	56
4.2.1.2 Boundary Conditions: Boundary Value Problem.....	57
4.2.1.3 Diffraction and Radiation .....	58
4.2.1.4 Regular Wave Potential (Linear and Stokes 2 <sup>nd</sup> order theories) .....	58
4.2.2 Hydrodynamic Forces .....	59

4.2.2.1 First Order Wave Exciting Forces (from linear wave potential).....	60
4.2.2.2 Second Order Pressure Forces (from nonlinear wave potential).....	60
4.2.2.3 Drift Forces.....	61
4.2.2.3 Motion Equation.....	62
4.2.3 Response Formulation.....	62
4.2.4 Hydrodynamic Approximations.....	63
<b>4.3 Model Description .....</b>	<b>64</b>
4.3.1 Definition of Case Study.....	64
4.3.2 Hydrodynamic Model.....	65
4.3.3 Hydrostatics.....	66
4.3.3.1 Centre of Gravity and Centre of Buoyancy (COG and COB).....	67
4.3.3.2 Hydrostatic Equilibrium.....	69
4.3.4 Response Model.....	69
<b>4.4 Environmental Conditions.....</b>	<b>71</b>
4.4.1 Regular Wave.....	71
4.4.2 Irregular Waves.....	71
4.4.3 Current Calibration.....	72
4.4.4 Wind Load.....	73
<b>4.5 Validation.....</b>	<b>73</b>
4.5.1 Mesh Study.....	73
4.5.2 Validation with Experimental Study by RPSEA.....	74
4.5.3 Validation with Model Test.....	75
4.5.4 Comparing numerical models.....	75
<b>4.6 Results and Discussion.....</b>	<b>76</b>
4.6.1 Response Amplitude Operator (RAO).....	76
4.6.2 Wave Forces.....	79
4.6.2.1 First order forces.....	79
4.6.2.2 Second Order Drift Forces.....	81
4.6.3 Added Mass.....	85

4.6.4 Motion Test (Extreme and Survival Conditions).....	86
4.6.4.1 Heave offset.....	87
4.8.4.2 Surge Offset.....	88
4.8.4.4 Maximum rotation: pitch and roll offset.....	89
4.8.5 Current Effect.....	90
4.8.5.1 Effect on RAO.....	91
4.9.6.2 Effect on first order forces.....	95
<b>4.7 Chapter Summary.....</b>	<b>99</b>
<b>Chapter 5: Effect of Vortex Shedding on a PC-Semi Hull Formation.....</b>	<b>103</b>
<b>5.1 Introduction.....</b>	<b>103</b>
<b>5.2 Background Work.....</b>	<b>104</b>
5.2.1 VIM in Offshore Industry.....	104
5.2.2 VIM in Semisubmersibles.....	105
5.2.3 VIM in Paired Column Semisubmersible.....	106
<b>5.3 Mathematical Formulation.....</b>	<b>107</b>
<b>5.4 CFD Model.....</b>	<b>107</b>
5.4.1 Description.....	107
5.4.2 Case Study.....	108
5.4.3 Flow Domain and Setup.....	109
5.4.4 Mesh Study.....	110
5.4.5 Boundary Conditions.....	111
5.4.6 Model Validation.....	111
<b>5.5 Drag Study.....</b>	<b>111</b>
5.5.1 Relationship between average hull drag, current velocity and inner/outer column spacing.....	112
5.5.2 Relationship between flow angle and average hull drag.....	113
5.5.3 Individual column drag at 0° flow angle: staggered pattern.....	113
5.5.4 Individual column drag at 45° flow angle: diamond pattern.....	115
5.5.5 Individual column drag at 15° and 30° flow angles: inclination.....	116

5.5.6 Pair Analysis .....	117
5.5.2 Contour Study .....	119
<b>5.6 Summary .....</b>	<b>121</b>
<b>Chapter Six: Non-Linear Finite Element Modelling of PC-Semi for Hull Reinforcement</b> .....	<b>123</b>
<b>6.1 Introduction.....</b>	<b>123</b>
<b>6.2 Component Description.....</b>	<b>123</b>
<b>6.3 Load calibration .....</b>	<b>125</b>
6.3.1 Mass calibration (Static loads).....	125
6.3.1.1 Buoyancy mass.....	126
6.3.1.2 Deck mass (Materials and Facilities).....	126
6.3.1.3 Mass of hull.....	126
6.3.1.4 Topside steel (Deck structure) .....	126
6.3.1.5 Additional mass .....	127
6.3.1.6 Steel Properties .....	127
6.3.2 Environmental load .....	127
6.3.3 Yield Assessment .....	128
<b>6.4 Modelling .....</b>	<b>128</b>
6.4.1 Description of ANSYS Finite Element Model .....	128
6.4.2 Developing Boundary Conditions.....	130
6.4.2.1 Displacement .....	130
6.4.2.2 Hydrostatic Stiffness: Cut-Water Plane, COG, and Column Base .....	131
6.4.3 Joint Design .....	133
6.4.4 Mesh Study .....	134
<b>6.5 Loads on Columns .....</b>	<b>136</b>
<b>6.6 Stress Assessment: Working Stress Design (WSD) .....</b>	<b>137</b>

<b>6.7 Analysis and Description of the Hull Structure Finite Element Models: Column Stresses.....</b>	<b>139</b>
6.7.1 Case 1 Hull Type .....	139
6.7.2 Case 2 Hull Type .....	140
<b>6.8 Column Stress Assessment .....</b>	<b>141</b>
<b>6.9 Chapter Summary .....</b>	<b>142</b>
<b>Chapter Seven: Recommendations for Design Improvement .....</b>	<b>144</b>
<b>7.1 Introduction.....</b>	<b>144</b>
<b>7.2 Improving Stability .....</b>	<b>144</b>
7.2.1 Design alteration for roll improvement .....	145
7.2.2 Design alteration for heave improvement.....	147
<b>7.3 Strength Improvement.....</b>	<b>149</b>
7.3.1 Design for Columns under Uniaxial Compressive Loads .....	150
7.3.2 Joint Assessment and Recommendation .....	151
<b>7.4 Recommendation for Payload .....</b>	<b>152</b>
<b>7.5 Postulated Reinforcement .....</b>	<b>154</b>
<b>7.6 Applications .....</b>	<b>155</b>
7.6.1 Application for Support Systems; Accommodation and Luxury Cruise.....	155
7.6.1 Application for FPS (Floating Production System) .....	156
7.6.2 Application for Foundation System .....	156
7.6.3 Application for Drilling Rig.....	156
<b>7.7 Chapter Summary .....</b>	<b>157</b>
<b>Chapter Eight: Conclusions and Recommendations for Future Studies .....</b>	<b>158</b>
<b>8.1 Conclusion.....</b>	<b>158</b>
<b>8.2 Recommendation for Future Studies.....</b>	<b>161</b>

8.2.1 Effect of fluid-structure interaction on column stress profile and hull deformation	161
8.2.2 Design and sizing of Tee-Butt joint for column-pontoon connection .....	161
8.2.3 Design and development of PC-Semi for wind turbine foundation system .....	162
8.2.4 Hull Scantling.....	162
<b>Reference .....</b>	<b>163</b>

## List of Figures

Figure 1.1 Photo of Eirik Raude	2
Figure 1.2 Photo of Blind-Faith, during topside construction	2
Figure 1.3 Wave and vortex induced motion response	7
Figure 2.1 Semisubmersible depth	14
Figure 2.2 Concept of deep draft semisubmersible	16
Figure 2.3 Description of six degrees of freedom system	20
Figure 2.4 Mooring illustration	22
Figure 2.5 Recent designs of semisubmersible heave natural periods	26
Figure 2.6 Top tension riser: Courtesy of JAMSTEC	28
Figure 2.7 Dry Tree Semisubmersibles	29
Figure 2.8 Paired Column Semisubmersible: Courtesy of Houston Offshore Technology 2009	31
Figure 2.9 Extendable-Draft Semisubmersible. Courtesy: Technip France	31
Figure 2.10 E-Semi Courtesy FloaTEC	32
Figure 2.11 T-Semis. Courtesy FloaTEC	32
Figure 2.12 Aker deep-draft hull	33
Figure 2.13 Semisubmersible Mini Island ( <a href="http://www.migaloo-submarines.com">www.migaloo-submarines.com</a> )	34
Figure 3.1 Test model from MARIN, Netherlands	42
Figure 3.2 Comparing Max A/D of PC-Semi and conventional deep draft semisubmersible [1, 2]	44
Figure 3.3 Underwater view of PC-Semi Test Model for Global performance: Courtesy, Houston Offshore Engineering	45
Figure 3.4 Definition of coordinate system	47
Figure 3.5 Side view of Lancaster University wave tank	48
Figure 3.6 Imetrum cameras	49
Figure 3.7 Test model	49
Figure 3.8 Data collection	50



Figure 4.1 Wave definition	56
Figure 4.2 Hull Dimension	65
Figure 4.3 Definition of flow angles	65
Figure 4.4 Mesh size 1.15m	66
Figure 4.5 Front view	66
Figure 4.6 Model ocean view	66
Figure 4.7 Complete View (Orcaflex model)	70
Figure 4.8 Orcaflex model for free response study	70
Figure 4.9 Orcaflex model for response study; with mooring. (Underwater view)	70
Figure 4.10 Spectrum study	72
Figure 4.11 Hydrodynamic Mesh Study	74
Figure 4.12 Heave RAO for free floating hull	77
Figure 4.13 Pitch RAO for free floating hull	77
Figure 4.14 Surge RAO for free floating hull	78
Figure 4.15 First order surge force	80
Figure 4.16 First-order heave forces	80
Figure 4.17 First order pitch moment	81
Figure 4.18 Surge drift forces	82
Figure 4.19 Sway drifts force	82
Figure 4.20 Heave drifts force	83
Figure 4.21 Drift roll moment	83
Figure 4.22 Drift pitch moment	84
Figure 4.23 Drift yaw moment	84
Figure 4.24 Surge added mass	85
Figure 4.25 Roll added mass	85
Figure 4.26 Sway added mass	86
Figure 4.27 Pitch added mass	86

Figure 4.28 Heave added mass	86
Figure 4.29 Yaw added mass	86
Figure 4.30 Comparison between ANSYS and Orcaflex	87
Figure 4.31 Heave offset for survival conditions	88
Figure 4.32 Heave offset for extreme conditions	88
Figure 4.33 Surge offset for survival conditions	89
Figure 4.34 Surge offset for extreme conditions	89
Figure 4.35 Snap shot from ANSYS AQWA model for maximum rotation; 1000years	90
Figure 4.36 Effect of current velocity on the surge response of a PC-Semi of 44.65m draft size	91
Figure 4.37 Effect of current velocities on the heave response of a PC-Semi of 44.65m draft size	91
Figure 4.38 Effect of current velocities on the pitch rotation of a PC-Semi of 44.65m draft size	92
Figure 4.39 Effect of current velocities on the surge response of a PC-Semi of 49m draft size	92
Figure 4.40 Effect of current velocities on the heave response of a PC-Semi of 49m draft size	92
Figure 4.41 Effect of current velocities on the pitch rotation of a PC-Semi of 49m draft size	93
Figure 4.42 Effect of current velocity on the surge response of a PC-Semi of 53.34m draft size	93
Figure 4.43 Effect of current velocity on the heave response of a PC-Semi of 53.34m draft size	93
Figure 4.44 Effect of current velocities on the pitch rotation of a PC-Semi of 53.34m draft size	94
Figure 4.45 Effect of current velocities on the first order surge force on a PC-Semi for 44.65m draft size	95
Figure 4.46 Effect of current velocity on the first order surge force on a PC-Semi for 44.65m draft size	95
Figure 4.47 Effect of current velocities on the first order pitch moment on a PC-Semi for 44.65m draft	96

Figure 4.48 Effect of current velocities on the first order surge forces on a PC-Semi for 49m draft size	96
Figure 4.49 Effect of current velocities on the first order heave forces on a PC-Semi for 49m draft size	96
Figure 4.50 Effect of current velocities on the first order pitch moment on a PC-Semi for 49m draft	97
Figure 4.51 Effect of current velocities on the first order surge forces on a PC-Semi for 53.34m draft size	97
Figure 4.52 Effect of current velocities on the first order heave forces on a PC-Semi for 53.34m draft	97
Figure 4.53 Effect of current velocities on the first order pitch moment on a PC-Semi for 53.34m draft	98
Figure 5.1 Schematic Diagram of a PC-Semi	107
Figure 5.2 Definition of current angle	108
Figure 5.3 Definition of inner/outer column spacing	109
Figure 5.4 Column numbering	109
Figure 5.5 CFD mesh study	110
Figure 5.6 Relationship between hull drag and high current velocity	112
Figure 5.7 Flow angle and column drag	113
Figure 5.8 Column $C_d$ at $\alpha = 0^0$	114
Figure 5.9 Column $C_d$ at $\alpha = 45^0$	115
Figure 5.10 Column $C_d$ at $\alpha = 15^0$	117
Figure 5.11 Column $C_d$ at $\alpha = 30^0$	117
Figure 5.12 $C_d$ on Pairs at $\alpha = 0^0$	118
Figure 5.13 $C_d$ on Pairs at $\alpha = 45^0$	118
Figure 5.14 $C_d$ on Pairs at $\alpha = 15^0$	118
Figure 5.15 $C_d$ on Pairs at $\alpha = 30^0$	118
Figure 5.16 Velocity direction for $0^0$ flow heading, 32m inner/outer column spacing, and 1.8m/s current velocity	119
Figure 5.17 Vorticity magnitude for $0^0$ flow heading, 32m inner/outer column spacing, 1.8m/s current velocity	119

Figure 5.18 Rectangular-rectangular	120
Figure 5.19 Circular-rectangular	120
Figure 5.20 Wake vortex identification at 0 <sup>0</sup> flow angle	121
Figure 5.21 Wake vortex identification for 45 <sup>0</sup> flow angle	121
Figure 6.1 Case 1 Topside	124
Figure 6.2 Case 2 Topside	124
Figure 6.3 CONTA173 Element	129
Figure 6.4 Quadratic triangular target	129
Figure 6.5 Quadrilateral target	129
Figure 6.6 X, Y and Z response for 100 seconds	130
Figure 6.7 Nonlinear boundary displacement in X, Y and Z direction for 0 <sup>0</sup> flow angle	131
Figure 6.8 Displacement in the X-direction; Snap shot from ANSYS time response analysis	131
Figure 6.9 Hull mesh	134
Figure 6.10 Element size 1.15m	134
Figure 6.11 Element size; 0.25m	134
Figure 6.12 Column Mesh Study	135
Figure 6.13 External force illustration of inner columns	136
Figure 6.14 External force illustration on outer columns	137
Figure 6.15 Column stress study for case 1 topside.	140
Figure 6.16 1.15m Mesh Size	140
Figure 6.17 0.70m Mesh Size	140
Figure 6.18 0.25m Mesh Size	140
Figure 6.19 Hull stress distribution from case 2 topside	141
Figure 7.1 Calculating for rotation	145
Figure 7.2 Relationship between flow angles and roll motion for 53.34m draft size.	146
Figure 7.3 Drift roll-moment at 90 <sup>0</sup> flow angle	146

Figure 7.4 Draft effect on roll RAO for 90 <sup>0</sup> flow angle.	147
Figure 7.5 Heave offset study for hurricane conditions; extreme and survival conditions	148
Figure 7.6 Column design presented by [3]	148
Figure 7.7 Hull frame	150
Figure 7.8 Connections and braces	150
Figure 7.9 Stress on inner columns braces	150
Figure 7.10 Inner column stress from case 1 topside	151
Figure 7.11 Inner column stress from case 2 topside	151
Figure 7.12 Column-pontoon assembly postulated by [4]. Tee-fillet joint	152
Figure 7.13 [4] recommended joint design	152
Figure 7.14 Recommended joint from current study	152
Figure 7.15 Effect of topside weight on the maximum stress on columns	154
Figure 7.16 Reinforcement for inner columns	155
Figure 7.17 Ring and straight stiffeners	155

## List of Tables

Table 1.1 Sea weather conditions around the world	6
Table 1.2 Stability criteria	8
Table 2.1 Contributions to the development of semisubmersible hull system	19
Table 2.2 Degrees of freedoms	20
Table 2.3 Plane motions	21
Table 2.4 Tension leg platforms	35
Table 3.1 Summary of global response test results [4]	46
Table 3.2 Particulars of test models	48
Table 3.3 Wave calibration	49
Table 3.4 Result summary for maximum displaced amplitude	51
Table 4.1 Case study	64
Table 4.2 Buoyancy force	66
Table 4.3 Centre of gravity and buoyancy	68
Table 4.4 Hull natural frequencies and periods	68
Table 4.5 Parameters for small angle stability	69
Table 4.6 parameters for survival and extreme conditions	71
Table 4.7 Case study for irregular waves	72
Table 4.8 Current Parameters	73
Table 4.9 Mean wind speed (m/s)	73
Table 4.10 Heave RAO Study	74
Table 4.11 Validation with [4]	75
Table 4.12 Comparing experimental and numerical results	75
Table 4.13 Comparing model with [5]	76
Table 4.14 Maximum offset summary	90
Table 5.1 Geometric parameters of semisubmersible platform and $V_R$	106
Table 5.2 Pair definition	118

Table 6.1 Loading conditions for MODU and FPI	125
Table 6.2 Summary of mass calibration	127
Table 6.3 Properties of steel	127
Table 6.4 Stiffness matrixes	133
Table 6.5 Column mesh study for dynamic analysis	135
Table 6.6 Basic usage factors	138
Table 6.7 $\beta$ for shell buckling as presented in [14]	138
Table 6.8 Working stresses for static and dynamic load cases.	142
Table 7.1 Summary of global performance	144
Table 7.2 Effect of topside weight on maximum stress on columns	153

## **Regulatory Bodies**

International Maritime Organization	<b>IMO</b>
Det Norske Veritas	<b>DNV</b>
Det Norske Veritas and Germanischer Lloyd	<b>DNV-GL</b>
American Petroleum Institute	<b>API</b>
America Bureau of Shipping	<b>ABS</b>
Health and Safety Executive	<b>HSE</b>
International Organization for Standardization	<b>ISO</b>



## List of Abbreviations

---

MODU	Mobile Offshore Drilling Unit
FPU or FPI or FPS	Floating production Unit/Installation/System
TLP	Tension Leg Platform
CFD	Computational Fluid Dynamics
BEM	Boundary Element Method
FEM	Finite Element Model
CAD	Computer Aided Design
VLFS	Very Large Floating Structure
BOP	Blowout Preventer
GOM	Gulf of Mexico
P-55	Petrobrass 55
RP	Recommend Practice
WSD	Working Stress Design
OS	Offshore Standard
LRFD	Load Resistance Factor Design
PC-Semi	Paired Column Semisubmersible
EDP	Extendable Draft Semisubmersible
ROV	Remotely Operated Vehicle
T-Semi	Truss Semisubmersible
E-Semi	Extendable Semisubmersible
TTR	Top Tension Riser
ADTS	Akear Deep Draft Semisubmersible
GWEC	Global Wind Energy Council
LNG	Liquefied Natural Gas
FPSO	Floating Production Storage and Offloading Platform
DD-Semi	Deep Draft Semisubmersible
RPSEA	Research Partnership to Secured Energy for America
QTF	Quadratic Transfer Function
WAMIT	Wave Analysis At Massachusetts Institute of Technology
HVS	Heave Vortex Suppressed
COG	Centre of Gravity
COB	Centre of Buoyancy
JONSWAP	Joint North Sea Wave Observation Project
RAO	Response Amplitude Operator
VIM	Vortex Induced Motion
VIV	Vortex Induced Vibration
MARIN	Maritime Research Institute of the Netherlands
OTC	Offshore Technology Conference
OMS	Offshore Monitoring System

2D

Two Dimension

3D

Three Dimension

---

# Nomenclature

## Chapter 2

---

$C_D$	Drag coefficient
$D$	Diameter of the structure
$u$	Velocity of the fluid particle
$\dot{u}$	Acceleration of fluid particle
$\rho$	Density of water
$C_m$	Initial coefficient of the structure
$C_{dmp}$	Damping coefficient
$\dot{x}$	Velocity of structure
$\ddot{x}$	Acceleration of structure
$K_i$	Stiffness parameter
$\omega_n$	Natural frequency
$T_n$	Natural period
$W_{hull}$	Total hull weight
$W_{Pontoon}$	Pontoon weight
$W_{Columns}$	Weight of columns
$W_{Braces}$	Weight of braces
$M_a$	Added mass parameter
$F_d$	Hydrodynamic force

---

## Chapter 3

---

$V_c$	Ocean current velocity
$V_R$	Reduced velocity
$A_{max}$	Maximum displaced amplitude from point 0
$A_{min}$	Minimum displaced amplitude from point 0

---

## Chapter 4

---

$\zeta$	Wave elevation
$\alpha_\theta$	Wave phase angle
$\theta$	Wave propagating direction
$A_w$	Wave amplitude
$A_i$	Unit amplitude
$\phi$	Wave potential
$K_w$	Wave number ( $\omega^2/g$ )
$\omega$	Wave frequency
$z$	Draft size
$\nabla$	Laplace grad factor
$\vec{F}_j^1, \vec{M}_j^1$	First order forces and moment

$\vec{F}_j^2, \vec{M}_j^2$	Second order forces and moment
$n_{ij}$	Cosine function of normal direction
$S_{avg}$	Average submerged area during motion response
$S_w$	Area of submerged hull; wetted surface.
$P$	Flow pressure
$P_{hyst}$	Hydrostatic pressure
$F_{hyst}$	Hydrostatic force
$F_j^w$	Wave excitation force
$F_{dft}$	Second order drift force
$C$	Damping parameter
$ M $	Hydrodynamic mass matrix
$H_c^e$	Exposed column
$H_c^s$	Submerged column
$Tp$	Maximum spectral period
$\omega_p$	Highest spectral frequency
$S(\omega)$	Spectral parameter for a particular frequency
$\gamma$	Spectral enhancement factor
$\alpha$	Relationship between wind speed and $\omega_p$

---

## Chapter 5

$R_e$	Reynolds Number
$KC$	Keulegan Carpenter number
$H_p$	Pontoon height
$S$	Distance between outer column centres
$L$	Diagonal width thickness of outer columns
$\theta$	Flow angle or flow direction.

---

## Chapter 6

$M_b$	Buoyancy mass
$Vol$	Volume of displaced hull
$\sigma_x$	Stress in X direction
$\sigma_y$	Stress in Y direction
$\sigma_e$	Equivalent Stress; von-Mises stress
$\tau_{xy}$	Shear stress on the XY plane
$\delta x ; \delta y$	Distance between centre of gravity and cut-water plane in X and Y direction
$A_{wsx}$ also $A_{wsy}$	Submerged area in X and Y plane
$A_{ws}$ also $s_w$	Area of wetted surface
$\delta_{zcg}$	Vertical distance from centre of gravity

$\eta_p$	Permissible usage factor
$\eta_0$	Basic usage factor
$\beta$	Buckling parameter
$\lambda$	Slenderness parameter
$f_Y$	Minimum yield stress
$f_E$	Elastic buckling stress

---



# Chapter One: Introduction

## 1.1 Background of Study

Over the years the demand for fossil fuel products have increased and this has expanded the search for crude deposit to remote sea areas where the weather/sea conditions are not favourable for conventional oil platforms [6]. The production capacity of oil reserves situated in these areas of the sea is usually prolific, making them targets for oil companies. And because of the high consumption rate of these products, there is a constant search for resources, to keep the prices affordable. The basic challenge in exploring (drilling and production) reserves situated in such areas is 'how to design structures that can meet with safety standards set by regulatory bodies. Floating platforms have been harnessed over the years for this purpose. As a result of this, the demand for floating offshore structures has gradually increased in the oil and gas industry. The increase in demand can also be tied to the prolific production capacity of oil fields situated in the deep sea. The nature of the weather conditions (wave, current, tide, and wind) requires high safety standards for structures designed to operate in them. Although they are of different types and are used for different reasons; they are practically exposed to almost the same sea state conditions in any particular geographical location, which varies from normal operating conditions, hurricane conditions and tsunami conditions. This is the basic reason why the design standards of a drilling platform are different from that of a production platform. Since they are expected to be stable during drilling operation and still be under the same loading conditions as production platforms (which are allowed to move within a certain range), the design for their plate thickness, braces connection, and the general stress distribution, will be completely different from that of production platforms. In summary, the design engineer pays more attention to the operating and environmental forces (wave, current, and wind) when designing a drilling rig, while he concentrates on the motion response when building a production system. Using 'Erick Raude and Blind Faith' as a typical example, Erick Raude is a mobile offshore drilling unit, while Blind Faith is a production platform (Figure 1.1 and Figure 1.2). From both images, we can see that the hull of Erick Raude was designed using more columns and more braces (more materials). This is to enable it withstand the forces and still gain stability during operation.

Apart from exploration purpose, there are other applications of floating platforms such as offshore crane systems and support structures [7]. Generally, in the oil & gas industry, floating platforms are mainly used in situations where it is impossible to use a fixed structure; jacket type, jack-up or gravity based. [8]described the evolution of floating structures from the conventional

compliant tower. The contrast of this type of structure as compared to the old ones is that its floating/flexible state makes the response analysis of outmost importance as compared to the fixed/rigid structures that tends to attract more forces. Concerning the fatigue analysis between fixed structures and floating structures, [9] concluded that as a result of their low stiffness, they are more likely to make sea working conditions safer.



**Figure 1.1 Photo of Eirik Raude: Courtesy of Riglogix**



**Figure 1.2 Photo of Blind-Faith, during topside construction: Courtesy of Aker Akaerner**

There are different factor that affects the functionality of floating structures including payload integration, motion characteristics, stability criteria, and size. Of all these factors, ‘motion characteristics’; (how they respond to the environment they are used) is the most critical of all. For instance, the reduced vertical motions offered by tension leg platforms makes them suitable for



FPS (Float Production System) application in deep waters; especially in oil fields where top-deck well-heads integration are required.

The oil and gas industry has a huge task in offsetting the depth challenges associated with oil reserves situated in very deep regions of the ocean [10] [11] [12]. Some of the challenges include well design, unique drilling and production operations, design of structure and regulatory policies. As a result of these challenges, the industry has gradually developed its rudimentary processes and equipment to sophisticated ones.

## **1.2 Scope**

In this project, we have designed a paired column semisubmersible hull. The research is primarily aimed at recommending this hull formation for different applications in deep waters, other than the floating production system with dry trees installation for which it was designed. For us to be able to draw up any form of recommendation of this hull for any form of application; (drilling unit, wind turbine suspension system, offshore crane system,) the effects of hydrodynamic interactions for different draft conditions have to be known. The complexity associated with achieving our desired goal was designing for the loading condition set by recommended standards for the above-mentioned applications. Three set of numerical models was developed to understand the behaviour of the hull;

- **Hydrodynamic model:** This was setup to calculate the response of the hull under wave, current and wind loads.
- **CFD model:** The nonlinear drag parameter was modelled
- **Finite element model:** The stress concentration around the columns under static and dynamic load cases was studied.

The CFD model was developed in the early stage of the project, to understand the nature of flow around the hull. Reciprocating shed vortexes were identified and investigated on, and the oscillating and drag effect on the hull was recorded. The results were compared with experimental findings recorded in previous experiments. The component of pressure and viscous drag was computed for to estimate the fluid force on the hull; considering Morison's formulation. The CFD model also gave insight into the nature of fluid-structure interaction from the complex column arrangement. A more sophisticated model was developed in comsol to understand this behaviour,

but no precise conclusion was reached; as a result, the finding has not been documented in this thesis.

A hydrodynamic model was built from diffraction principles, to characterize the hull's motion response from wave, current and wind loads; as required by industrial standards. An aqua packaged formulated on Boundary Element Method (BEM) was employed to perform this task. The AQWA solver resolves series of complex partial differential equations of the flow potential around the incidence, diffraction and radiation boundaries. The resolution of these equations enables computation of the pressure, force and moment parameters. Complex and irregular wave behaviours were analysed using a spectrum. The drift second order parameters were investigated to understand their influence in response behaviour of the hull in complex wave flow. The effect of wave and current interactions was also studied. The response of the hull was studied in time and frequency domain using basic motion equation for single degree of freedom system, and multiple line matrixes were developed to compute for subsequent degrees of freedom. Results from different software packages were compared. An experimental investigation was set up in a wave tank to validate and measure the accuracy of our hydrodynamic model. The motion of the scaled-down hull model was recorded using a digital image capturing system; Imetrum. The model response was calculated for different wave frequencies, and the results were compared with that of the aqua model. The finite element model was developed to estimate the strength of the hull during bending, twisting and buckling, for static and combined loadings. The model took into account the effect of the hull response on the strength of its components. Results for hull stress distribution were reported for different topside designs, and static/operating loading conditions and recommendations for hull columns scantling (internal reinforcement) were postulated considering industrial standards.

## **1.3 Aim and Objectives of Study**

### **1.3.1 Aim**

The aim of this research is to design a paired column semisubmersible hull system to function in multiple applications in ocean engineering.

### **1.3.2 Objectives**

- To understand the dynamics of a paired column semisubmersible hull system, and study how much it can carry out the task to which it was designed (dry-trees application).

- To understand the nature of different environmental loading conditions on this unique hull system, and be able to circumvent the challenges that may arise from the complexity of the internal column arrangement.
- To investigate the nature of vortex shedding phenomenon created from a stream of reciprocating vortices in the wake, when high current velocities passes through the hull.
- To investigate the wave-induced motion response of this hull for different sea conditions, and postulate recommendations for formulating design standards for its application in deep waters.
- To evaluate its strength through understanding the stress distribution from operating and environmental loads, and identify regions where reinforcement will be required.
- To recommend the stiffener and girder sizes for internal reinforcement of the columns and pontoon section, in the process creating useful spaces within for ballasting, oil and mud storage.

## **1.4 Design Approach**

For us to effectively harness the advantages of a paired column semisubmersible hull in developing drilling platforms and support vessels, we have to gain a complete knowledge of how the system works. There is no literature on its dynamic behaviours apart from the reports presented by the original patent owner (Jun Zou) because it is a new hull type. Therefore, the first stage of our design process was to reproduce the design of the first PC-Semi (considering the same weather conditions and structural attachments), to gain a full knowledge of its dynamics, and to understand the reasons for their recommendations regarding the topside, moorings, risers, column connections, braces, pontoon type (centralized), and draft size. We also designed based on the applications we intend to recommend the hull for. Example; to enable us to make recommendations for support systems such as wind turbine foundation, we designed for a fully submerge hull, as wind turbine foundations are completely submerged. We have therefore adopted a ‘flexible design approach’; wide range of design parameters was introduced to guarantee recommendation for multiple application of hull concept.

We have categorized our design process into two phases; design for motion/stability, and design for strength. For the hull motions, we looked into the wave induced motion and the self-excited vibration generated from the reciprocating vortices created within the wake formation of the flow stream, while the stress distribution and column buckling were assessed when designing for strength. Preliminary design was carried out for the mooring system, but we haven’t recorded the complete results in this thesis; only where it was required for validation purpose.

### 1.3.1 Design for motion and stability

In designing for motion and stability, we investigated the required standards for motion offset for each of the applications we intend to recommend this hull for. Different weather conditions were studied for different seas around the world (as shown in Table 1.1), to enable us to understand the extent of motion response in applying the hull system in different regions. Weather conditions for the Gulf of Mexico were observed to have the highest effect on the motion response, as suggested in Table 1.1. We also considered some industrial standard, some of which include;

DNV-RP-205 Recommended Practice: Environmental Conditions and Environmental Loads (2010)

DNV-OS-J101 Offshore Standard: Design of Offshore Wind Turbine Structures (2013)

DNV-RP-C103 Recommended Practice: Column-Stabilised Units (2012)

ABS Rules for Building and Classing Floating Production Installations (2014)

**Table 1.1 Sea weather conditions around the world**

	<b>Africa</b>	<b>The Gulf of Mexico</b>	<b>East Asia</b>
<b>Waves</b>	Squalls and trade winds	Hurricanes and winter storms	Typhoons, monsoons, and squalls
<b>Currents</b>	Long period swells and Bi-modal state	Hurricane and winter storms	Typhoons and monsoons
<b>Winds</b>	River flow	Loop current	Monsoon and internal waves

The designs for investigating the wave induced motions were carried out using hydrodynamic diffraction analysis. The wave parameters were developed using the potential theory of flow; representing the dynamics of the flow with a velocity potential which changes with distance and time. With this, we were able to calculate the energy or force parameters of the flow. This eliminated the challenges associated with the complexity of flow separation and rotation. In designing for the vortex-induced motions, we carried out a detailed study into what was presented in [2, 13]. This gave us insight into the challenges that are likely to arise from the complex nature of the shed vortices, for different applications of this hull. We also reviewed the effect of vortex induced vibration of conventional deep-draft semisubmersible (this is presented in the fifth chapter of this thesis). After these reviews, we decided to develop a CFD model to understand the nature of flow around eight columns arranged in form of a PC-Semi. To the best of our knowledge, this study has not been previously carried out. From the CFD model, we were able to investigate;

- The drag coefficient on each column and on each pair.
- Correlation between the inner/outer column spacing and the drag distribution on the pairs.
- Vortex identification; flow pattern around the structure
- Effect of column shapes; square and rectangle

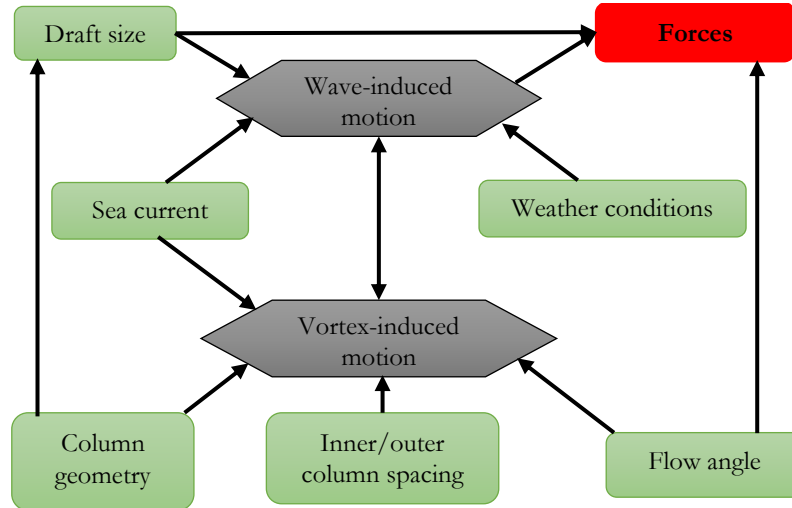


Figure 1.3 Wave and vortex induced motion response

The wave and current induced motions sometimes occur simultaneously, and some researchers [14] have concluded that for deep-draft semisubmersibles, the extent of one depends on the another. The sea current velocities alongside its column geometry, flow angle and draft size are responsible for the vortex induced motions. The wind and wave conditions directly affect the wave-induced motions. All these parameters determine the forces acting on the hull, which is used for selecting the materials and accessing the strength of the hull, for the proposed applications.

The stability of the hull was accessed using ABS, IMO and DNV standards for accessing the stability of column stabilized semisubmersibles. Table 1.2 shows the criteria for intact and damage conditions for assessment.

Table 1.2 Stability criteria

	Requirement	DNV	ABS	IMO
Intact stability	Minimum GM	$\geq 1.3$	$\geq 1.3$	$\geq 1.3$
		N.A.	$\geq 0.0\text{m}$	$\geq 1.0\text{m}$ for operating and survival conditions and $\geq 0.3\text{m}$ for other temporary conditions

	Minimum righting moment	Positive over range from upright to second intercept		
<b>Damaged stability</b>		$\geq 2$	$\geq 2$	$\geq 2$
	Maximum rotation with wind loads	$\leq 7^\circ$	N.A.	$\leq 7^\circ$
<b>CURRENT STUDY</b>				
<b>Intact</b>			<b>Damage</b>	
<ul style="list-style-type: none"> <li>○ The metacentric height has to be positive for all weather conditions.</li> <li>○ The heeling angle at its equilibrium position should not be greater than <math>15^\circ</math>.</li> </ul>			<ul style="list-style-type: none"> <li>○ Not considered for free floating state</li> <li>○ One line damage for 16 mooring integration.</li> </ul>	

### 1.3.2 Design for strength

[15] and [16] were primarily considered in the design and assessment of the hull’s strength. In this process, a finite element modelling approach was adopted. The wave, current and wind loads were extracted from the hydrodynamic analysis and used for loading conditions in the FE-model. The static loads (which include the upward buoyancy force, the hull steel weight, the topside weight, the operating loads, facilities, weight of liquid stored in the columns, mooring weight, riser weight, and so on) were also considered. Results from the FE model were used to make conclusion on the following;

- The nature of steel material to use
- The topside design
- Recommendation for plate thickness
- Stiffeners and girders designs
- Sizing and positioning of braces
- Recommend joint size

## 1.5 Methodologies

In the cause of carrying out our design, we made use of different commercial software’s, some of which are currently used in the industry. In some cases, where the software couldn’t perform the task, we had to write our own programs to get our desired results.

### Setup for numerical analysis

- For CFD analysis, the numerical setup was developed in ANSYS FLUENT
- For hydrodynamics diffraction and response analysis, the numerical setup was developed in ANSYS AQWA and Orcaflex.
- The CAD models were built in SolidWorks and CATIA. In some cases, we made use of ANSYS design modeller.
- Numerical setup for FEA.: ANSYS APDL
- The investigation into the fluid-structure interaction from flow separation within the centralized area of the hull was carried out using Comsol Multiphysics. It is important to mention that details of the results of this investigation have not been presented in this thesis.
- Numerical setup for mooring and riser analysis were developed in Orcaflex

### **Experimental setup**

- Lancaster University wave tank.
- Regular waves : sinusoidal wave and sea-state
- Electronic wave gauges
- Imetrum Digital Image Capturing System.

## **1.6 Thesis Outline**

### **1.6.1 Chapter Two: Review of Semisubmersible Hull Systems: Column Stabilized Unit**

In the second chapter of this thesis, we presented a literature review on semisubmersible platforms. Brief histories into its origin, alongside some significant hull optimizations that have been introduced over the years, were also discussed. We also reviewed the different types of dry trees semisubmersible concepts that have been postulated so far and discussed the reasons why they were not successful in the oil and gas industry. The concept of deep draft semisubmersibles was discussed; their advantages and challenges were also addressed. The design and development of paired column semisubmersible platform were presented. Its comparative advantages over other dry-trees semis were highlighted and useful conclusions were made on the possible high demand of this hull system in the nearest future.

### **1.6.2 Chapter Three: Experimental Study of Motion Characterises of PC-Semi: VIM and Global Performance**

The experimental setups for calculating the wave and current induced motions were presented in this chapter. For VIV, the experimental results presented were extracted from [1, 13]. No further experimental setup was needed to design for VIM of this hull, as the results presented in both reports were enough. Experimental setup developed at the Lancaster University wave tank for investigating the effect of wave-induced motion was also presented in this chapter.

### **1.6.3 Chapter Four: Numerical Simulation of Hydrodynamic Loading on a PC-Semi for Motion Characterization**

The hydrodynamic response of this hull system was presented in chapter 4. This study was done in accordance with regulatory standards (DNV, ABS, and API). The cases were defined with the intention of recommending this hull formation for drilling units and support system. Three cases were defined varying the draft sizes and the hull of the fourth case was totally submerged for wind turbine replication. Results for response amplitude operator were computed for in the vertical plane, the effect of added mass and viscous damping were also investigated and recorded. The wave calibration was done for regular and irregular waves, for a sea depth of 2400meters. The current and wind effect on the hydrodynamic parameters were recorded for the different cases, and further recommendations were done based on the results. The first and second order hydrodynamic forces were computed for at different weather conditions; survival, extreme, severe and hurricane, as recommend by regulatory bodies. The results were used to compare recommended standards for MODU forces, and alteration of the hull geometric properties was recommended to achieve this purpose.

### **1.6.4 Chapter Five: Effect of Vortex Shedding on a PC-Semi Hull formation**

The effect of vortex shedding on an array of eight columns, arranged in a PC-Semi configuration was investigated in chapter 5. The numerical model was validated using experimental results obtained from tow tests carried out at the University of California and MARIN in the Netherlands. The results and conclusions were reported in chapter 3. In this chapter, parameters in which VIV depends on (such as flow angle, current velocity, and column geometry) are varied over a considerable range, and the results were computed for.



### **1.6.5 Chapter Six: Finite Element Modelling of PC-Semi for Hull Reinforcement**

A finite element model of the hull was developed to estimate its stress level from different loading conditions. To carry out the static analysis, APDL codes were developed to integrate hydrodynamic loads (wave, current and wind) and the hull's mass distribution. The effects of different topsides were investigated on the stress distribution on the columns, and the results were used to stiffeners and girders for reinforcement.

### **1.6.6 Chapter Seven: Recommendations for Design Improvement**

In this chapter, the results obtained from hydrodynamic loadings, drag distribution from vortex effect, and nonlinear stresses from combine loads was used to postulate recommendations for the future design of PC-Semis. Design alterations for column and pontoon geometry were recommended to circumvent the effect of roll and heave motions at different water depths. Stiffeners were also designed and recommended for internal reinforcement from stress study.

### **1.6.7 Chapter Eight: Conclusion and Recommendations**

A summary of the findings and recommendations recorded in all the previous chapters have been recorded in this chapter, alongside recommendations for future research.

# CHAPTER 2

## CHAPTER HIGHLIGHTS

- History and Evolution of Modern Semisubmersible Hull Design
- Motion, Degrees of Freedom and Structural Attachments of Semisubmersibles
- Hydrodynamic and Hydrostatic Behaviour, alongside the Strength Assessment of Semisubmersibles.
- Dry-Trees Semisubmersibles Concepts, Development of Paired Column Semisubmersibles
- Winder Turbine Foundation and Mini-Cruise Application of Semisubmersible Hull.
- Other Forms of Floating Hull Systems, including Spar, Tension Leg Platform, and Floating Production Storage & Offloading Platform.

# Chapter Two: Review of Floating Semisubmersible Hull Systems; Column Stabilized Unit

## 2.1 Introduction

Background literatures on floating semisubmersible hull systems have been presented in this chapter. Their dynamics, degrees of freedom, and applications have been discussed. The concept and development of dry-tree semisubmersibles were discussed, and the progress made so far was highlighted. The complexities associated with the hulls were discussed alongside other reasons why dry-trees semisubmersible did not record early success in the oil and gas industry. It is important to note that bulk of the literature on dry trees semisubmersibles (including paired column semisubmersible) that are presented in the thesis was extracted from company and conference reports, as there is no much academic documentation on the invention and dynamics of these hulls and their applications.

At the end of this chapter, we will be able to understand the extent of study that has been varied out in ocean engineering in the following areas:

- i. Their types, operating mechanism and functionalities.
- ii. The progressive growth of semisubmersible application in deep-waters.
- iii. What are dry-tree installation and the structural requirement for this application in deep waters
- iv. The types of dry trees semisubmersible hull concept that has been designed over the years, and reasons why they did not successfully get to stage apart from paired column semisubmersible.

## 2.2 Background of Semisubmersible Hull

### 2.2.1 Brief History and Development

The development and design of semisubmersible hull can be traced back to the 1960s when there was rapid need to increase the stability of floating systems. Bruce Collipp was credited by [17] for designing the first semisubmersible platform. His early design and development of this structure were inspired from the stability obtained by partially submerging a floating structure to avoid capsizing in rough sea conditions. He called his first design the *Bluewater-1*. Since then the use of semisubmersible hull systems in the oil and gas industry has grown tremendously. It has

been used for designing mobile drilling units, floating production systems, barges, crane systems, support vessels, transportation vessels and many other applications. Although it has different forms, the column stabilized form is generally accepted to be the most effective design for drilling purpose, which was later adopted for production. This platform consists of a top-deck section, columns and a pontoon. Originally, the buoyancy was provided by the pontoon, which helps to keep the structure floating. The buoyancy of the recent semisubmersibles is provided by the amount of submerged draft which includes both the pontoon and the columns. Like all floating structures, semisubmersibles have six degrees of freedom and are flexible in all directions. These movements cause fatigue on the risers, mooring lines and other structural attachments and, therefore, they need to be controlled in both normal and harsh sea conditions. Over the years, the use of semisubmersible hull systems has been extended to deep waters; from the first one (Bluewater 1) to the modern semisubmersibles designed by Petrobras, Technip, Shell, Chevron, Transocean, Total, Maersk, Aker Solutions, and many others.

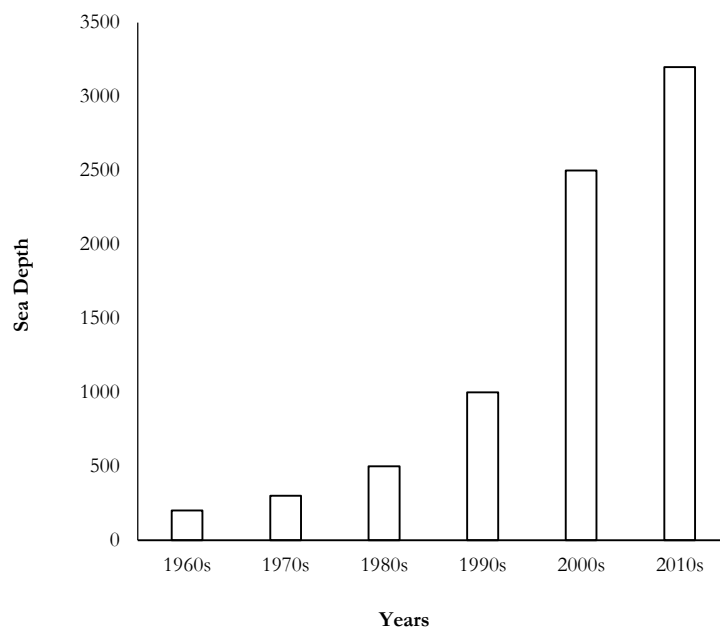


**Figure 2.1 Sea depth for semisubmersible hulls**

Figure 2.1 shows a progressive growth in the application of semisubmersible hulls over the last 50 years. The conceptualization and designs that triggered this growth were carried out by researchers from both academic and industrial environment, which has helped to increase the performance and functionalities in ocean engineering. These investigations were mainly done to understand the response and strength of the hulls under different environmental loading conditions.

## **2.2.2 Evolution of Design**

In the early 80s, Akagi and Ito, presented a motion optimized design of the conventional semisubmersible platform used in the 1970s. These conventional semisubmersibles (example: Argy II FPU and Buchan A) were characterized with much higher motion response than what we have now, because of the amount of steel present in their cut-water plane area (more inline columns and braces). Their design was focused on reducing the natural frequencies of the hull on its vertical plane to prevent lock-in phenomenon due to resonance with the wave oscillating frequencies in the heave DOF. To achieve this, they increased the displaced volume of the semisubmersible, and reduced its cut-water plane area. Six circular columns arranged in-line (three on each side) were designed alongside two large circular pontoon sections (see Table 2.1). The pontoon size guaranteed a high displaced volume, while the small diameter of the columns maintained a small area in the water plane. The mathematical formulation of this relates the water-plane stiffness, added mass and natural frequency of the hull. Considering the wave frequency conditions, the technicality involved was how to determine the size of the displacement and the accurate dimension of the columns that could satisfy the frequency requirement. This was a revolutionary idea that increased the application of semisubmersible hulls in the oil and gas industry, because a great reduction in the motions on the vertical plane of a traditional semisubmersible was achieved. This method has been also implemented in some boat and vessel designs to increase their stability [19].

In the late 1990s, [20] made a series of presentations on some of their findings from experimental test carried out on different shapes and sizes of semisubmersible platforms. They tested on how to increase the stability of semisubmersibles during rough sea conditions. There was an urgent need for this, because commercial operators in deep sea reported high level of instability for tidal conditions, because of the increase in water level; which was specifically due to global warming. At the end of their work, they built a three-column semisubmersible system using the basic principle for stability of all floating bodies, i.e., if a floating system is designed in a way its centre of gravity is below its centre of buoyancy, the system will be stable for any weather condition. Hence they increased the length of the submerged part of the hull, to keep weight further away from the water plane. They called it, a deep-draft semisubmersible (see Table 2.1). Its patent right was issued in 2001 [20]. This was another turning point in the development of modern day offshore floating systems; semisubmersibles. The design and development of the MinDOC3 semisubmersible was attributed to this idea [21]. The idea was also applied in spar platform, keeping the hard tank at the very bottom of the hull. Increase in the total draft size often

leads to total increase in the length of the structure, therefore making it behave as a slender body; Figure 2.2. The major problem encountered by slender bodies under wave motion is vortex induced vibration. The motion is sometimes called vortex induced movement ‘VIM’ when the time it takes for the structure to respond in a complete cycle is longer than 21seconds or more. This is mostly the case for large bodies, such as paired column semisubmersible hull).

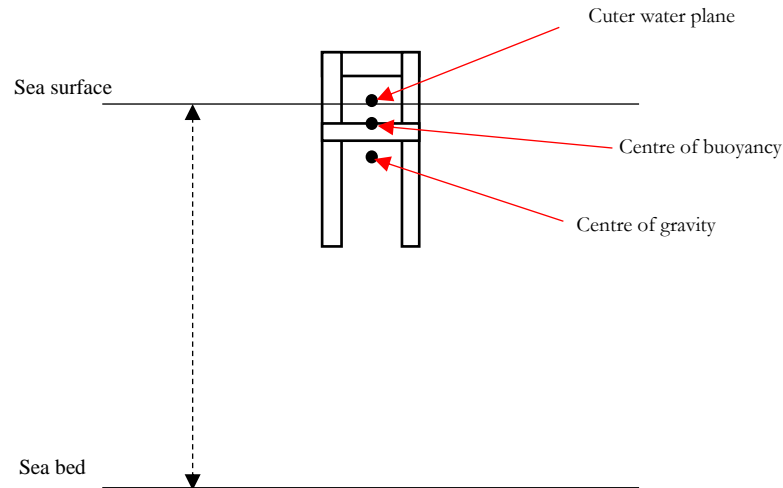


**Figure 2.2 Concept of deep-draft semisubmersible**

The nature of the draft also requires structural attachments (risers and moorings) to be configured in a certain way to suit its application as recorded in [22] and [23]. The length of the draft also makes them behave as slender bodies, and this can be of massive disadvantage during high sea current situations. When fluid flows through a blurred body, a stream of vortexes are formed on the wake of the disturbance. These vortexes oscillate at a particular frequency called the vortex shedding frequency  $f_v$ . As the vortex shedding frequency gradually equals the natural frequency of the structure, a resonant phenomenon sets in; i.e, the structure starts to move in an excessive vibratory manner. This movement is known as vortex induced movement or vortex induced vibration (VIV). VIV is a major problem that is observed in most offshore slender bodies such as risers, mooring lines, etc.; and the evolution of deep draft semisubmersible has added to that list. Different researchers have made conscious attempt to investigate the effect of this phenomenon on deep-draft semis. [24], [14, 25, 26], [27] are some of the recoded reports (experimental and numerical methods) on how deep draft semisubmersible respond to shed vortexes. The extent of this effect was greatly influenced by the in-line motions (surge motions) induced by the hydrodynamic wave loadings [26]. DD-Semi (deep draft semisubmersible) is of different forms. [28] and [29] explained the concept of a DD-Semi with moveable heave plates. This is an imitation of the truss spar conceptual design. The inclusion of the heave plates has a

massive reduction in vertical/heave response of the structure, making it suitable for ultra-deep well operation. Other forms of DD-Semi include paired column semi and conventional four columns DD-Semi (e.g. Petrobras 55).

Irrespective of the numerous advantages associated with deep-draft semisubmersible concept, there are series of challenges associated with them. The issue of vortex shedding phenomenon resulting in destructive oscillating amplitude is of key interest, and operators of this sort of structures employ strakes and other vortex suppressing devices in circumventing the effect of this phenomenon. One of the objectives of this study is to investigate the hydrodynamic behaviour of this hull system with moderate and shallow draft condition. The knowledge of this will help increase its functionality (shallow and moderate sea depths). Deep draft semisubmersibles hulls systems are mainly used for designing drilling and production units in the oil and gas industry and the recently developed paired column semisubmersible platform for dry tree use has been added to the fleet.

In 2010, Qi Xu carried out CFD analysis on different semisubmersibles hull types, to investigate their VIM response. From his simulations, he discovered that any form of alteration on the reciprocating vortexes shed from an arrangement of columns will reduce its amplitude of oscillation. That is; the oscillating vortexes shed from a column with two different diameters is likely to have lesser amplitude when compared to if it had a single diameter. In his investigation, he also compared the RAO plots (Response Amplitude Operator) for cases and recorded favourable wave forces, moments and motions from his novel semisubmersible configuration. To achieve this concept, the size of the pontoon section was reduced, and additional material was added to the base of the columns proportionately; keeping the same displacement (See Table 2.1). [30] explained the formation, and the model test results from series of test carried out from this hull model. Its comparative advantages in reducing the centre of gravity of deep draft semi [20] were explained, alongside with advantages in the reduction of the rotational motions (roll and pitch) in the horizontal plane. This hull has been named the future of deep-draft semisubmersibles because of these advantages. Recently, Diamond Offshore Drilling and other design companies have been optimizing their old semis to meet with the contemporary challenges associated with deep water operations. This method has been very effective in achieving that goal. The recent reconstruction of Ocean Apex and Ocean Onyx are a good example of the application of Xu's method of optimizing semisubmersibles for deep water operations [31].

The three columns semisubmersible hull concept postulated for deep draft by [20] was developed by Bruce Malcolm and Paul Dixon as a semisubmersible vessel that can function as

foundation system (see Table 2.1). This method was not very successful in the oil and gas industry because of some reasons that centres around the amount of displacement it offers[32] presented a representation of this concept in a column-stabilized form. This concept has been greatly harnessed in the development of the large wind turbine foundation systems because of the nature of stability offered by the three legged structured components. Despite the advantage offered by this hull concept, [33] clearly stated ‘low deck space’ as a significant disadvantage of the three column semisubmersible hull.

Another important contribution to the development of semisubmersible is the introduction of the truss pontoon semi. The concept has received very significant attention in the oil and gas industry, but has not been implemented. Some of work on truss pontoon semi can be found in [34-37]. The work presented in [35] explained the fundamental effects of response performance of the hull by adding the truss section that contain heave plates. The recorded significant improvement in the heave and pitch motions, which was attributed to the added mass in the heave DOF offered by the heave plates. They compared results from diffraction method, Morison equation and their test setup, and recorded reasonable agreements in their findings.

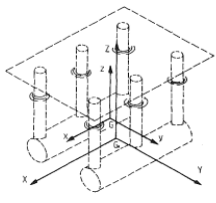
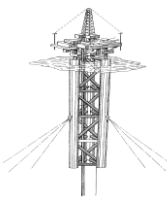
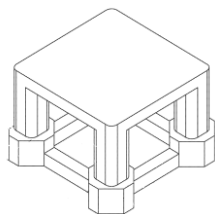
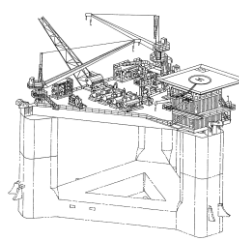
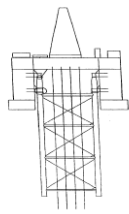
Table 2.1 shows some recent improvements that have been carried out by different researchers on semisubmersibles platform. Each of these novel concepts for semisubmersible hull optimization has its comparative advantages as relating to the operational requirements in deep and ultra-deep sea. They also have their respective shortcomings, which makes it impossible to have a single standard hull concept for all semisubmersibles applications. One unique characteristic of these semisubmersible hull forms is that at the time each of them was conceptualized, they were all designed to function at a greater sea depth than the existing ones. This is usually the trend in the offshore industry; floating structures are design to operate in rough weather conditions.

There are other contributions that have been developed to increase the functionality of this hull system, such as the centralized pontoon system, plate-like pontoon, truss hull, rectangular column formation, and so on. In this thesis, we have restricted our discussion to the contributions to our study; as presented in Table 2.1

**Table 2.1 Contributions to the development of semisubmersible hull system**

	Structure	References	Function(s)
--	-----------	------------	-------------



A		[18]	Reduction in cut-water plane area, to reduce the hydrostatic stiffness.
B		[20]	Redistributing the hull weight; concentrating more weight below the cut-water plane to keep the centre of gravity below the centre of buoyancy,
C		[30]	Heave and vortex suppressed semisubmersible. (HVS)
D		[32]	Three column semisubmersible
E		[37]	Inclusion of heave plates on the pontoon section helps to reduce heave motions.

### 2.2.3 Degree of Freedom

Semisubmersibles are floating hulls, and are therefore flexible bodies; they are free to move. This dynamic behaviour is of primary interest during their design stage. [38] explained the six different directions (degree of freedoms) in which a floating structure (ships, barges, boats or platforms) responds when environmental or operating loadings are placed on them. The translational response in the X, Y & Z directions are called surge, sway and heave, while the rotational response are called roll, pitch and yaw (Table 2.2, and Figure 2.3).

**Table 2.2 Degrees of freedoms**

Direction	Translational	Rotational
X	Surge	Roll
Y	Sway	Pitch
Z	Heave	Yaw

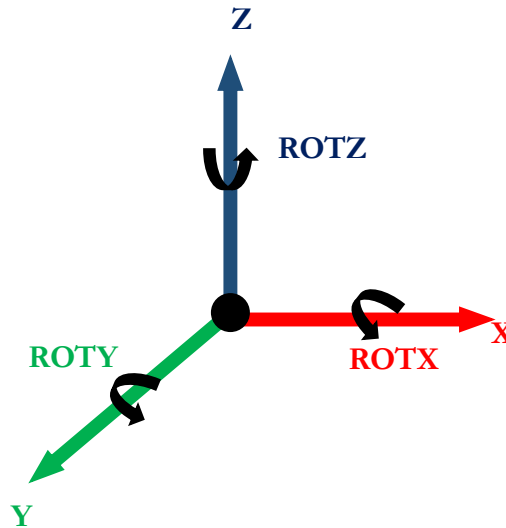


**Figure 2.3 Description of six degrees of freedom system**

$UX$  = Movement in the X direction: surge

$UY$  = Movement in the Y direction; sway

$UZ$  = Movement in the Z direction; heave

$ROTX$  = Rotation about the X direction; roll

$ROTY$  = Rotation about the Y direction; pitch

$ROTZ$  = Rotation about the Z direction; yaw

These six degrees of freedom takes place on two planes; the vertical and the horizontal plane, as presented in Table 2.3. The water surface is on the XY plane, and the X is the direction of flow. The Z direction is normal to the XY plane. It is important to understand the relationship between the six degree of freedoms and the planes they operate, the nature of the hydrostatic behaviour of semisubmersibles (and most floating bodies) is relative to the plane.

**Table 2.3 Plane motions**

Vertical	Horizontal

Heave	Surge
Roll	Sway
Pitch	Yaw

## 2.2.4 Structural Attachments

Floating platforms do not exist as single units as they are designed for a wide range of applications, and semisubmersibles are not an exception to that. Applications such as drilling and production requires risers, crane system application requires anchors, positioning require moorings, and so on. There are various structural attachments for floating structures, but we only discussed the two main attachments in this study;

- Mooring lines and
- Risers

### 2.2.4.1 Mooring Lines

Mooring lines and tethers are used to keep floating platforms in place. They act as the foundation (flexible) system, and are connected from the base of the submerged part of the hull to the seabed. Mooring lines are basically applied in different forms, depending on the extent of response the floating structure is allowed to have. For deep draft semisubmersibles, there are two conventional types of mooring applications; taut mooring and centenary or slack mooring, as illustrated in Figure 2.4.

The responses of floating structures are therefore directly affected by the stability, stiffness, fatigue, and life cycle of the moorings. Researchers have carried out series of investigations to analyse the extent of this influence. In conventional practice, mooring designs are done alongside with hull design, considering recommended standards (API, DNV), as the benchmark. There is no ‘generally acceptable design system for mooring lines’, as each hull is design to meet the environmental and operational loading condition for the particular task it is expected to perform.

[39]demonstrated the dynamics of deep water mooring systems. They presented a comparison between numerical analysis and experimental investigations on the force response of mooring lines attached to a floating buoy. [40]described a technique for analysing the dynamics of mooring cables and its boundary excitations. [41]demonstrated that an increase in the damping of mooring lines helps to reduce surge and pitch motions of spar platforms operating in deep waters. It is important to mention that the conventional way of altering the damping factor of mooring lines is in its

material selection. [42] identified the nonlinear behaviours of moorings, generating some correlations that describes the behaviour of moorings in viscous environments

Apart from the challenges associated with the dynamic positioning of mooring lines, “getting them fixed to the seabed and the structure” was also a problem, because the joints tend to wobble after a while. This is commonly called *coupling effect*. The coupling effect of mooring lines and offshore platforms is a fundamental area of study in the oil & gas industry. Its dynamic complexity varies along the entire mooring chain; from the seabed pegs, to the contact point on the platform. Recently, suction cans have been employed to circumvent the effect of this challenge. This technique was used to anchor the mooring lines of *the Perdido Spar* (world biggest spar platform) to the sea bed in G.O.M, replacing the conventional concrete piles. The effect of this improves the safety and life span of the lines with reduced maintenance cost.

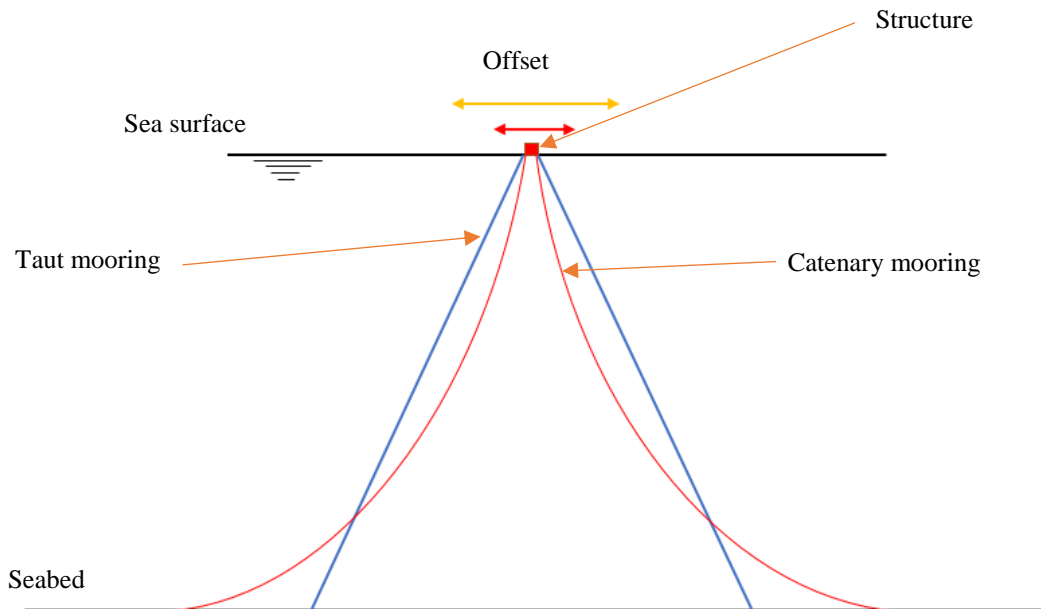


**Figure 2.4 Mooring illustration**

Recently, a non-uniform mooring configuration (material selection) has been adopted in the industry because of the high stiffness they offers. Steel-polyester-steel is the most commonly used configuration. The short steel chains are connected to the anchors and the fairleads, while a significant part of the line is made from polyester rope. The effect of this on the dynamic behaviour of semisubmersible hull will be discussed at the latter part of this thesis

#### **2.2.4.2 Risers**

Risers are pipeline structures used to transport fluid in and out of the well. They come in different sizes, shapes and materials. [43] explained the types, usage and dynamics of drilling and

production risers. Because risers are directly connected to wellheads or blowout preventers (BOPs), which are in direct contact with the seabed, they are affected not only by the structural response of the platform and ocean waves, they also respond to seismic and earthquake conditions [44]. The design of risers and subsea pipe structures is recorded in [45]. The nonlinear behaviour of risers under vibratory motion was investigated by [46]. They later concluded from series of experimental and numerical analysis that increasing the speed of the fluid carried by risers reduces their natural frequencies

A major challenge faced by risers in the offshore industry is ‘vortex induced vibration’, which is a result of the vortexes formed when fluid passes through them. Because this effect is not directly caused by the floating structure, it is of less interest in this research.

## 2.3 Dynamics

Semisubmersibles hulls are classified as VLFS (Very Large Floating Structure). Their applications are restricted almost exclusively in the oil and gas industry, and thus are exposed to extreme weather conditions. As a result, different researchers have tried to remodel this structure to reduce the effect of sea waves and optimize their dynamic behaviour. Modern column stabilized semisubmersibles are designed with small cut-water plane area. This means less area is exposed to wave loads, and less motion is generated in the vertical plane; heave roll, and pitch DOF. The hydrodynamic force parameter ( $F_d$ ) of semi submerged body is calculated using conventional methods as shown in Equation [2-1] and Equation [2-2], [47]. Morison’s equation and 3D diffraction method are generally the acceptable way to determine the nature of hydrodynamic loadings on a floating body, although recommended standards require the use of developed experimental model tow test setups. These tests are normally scaled down, and cannot represent the actual loading scenarios of these structures.

$$F_d = \rho C_m A \dot{u} + \frac{1}{2} \rho C_D D |u|u \quad [2-1]$$

For a hull in motion under wave and current interactions, the hydrodynamics force is represented as the summation of the forces from the drag, the hydrodynamic damping, added mass and fluid acceleration (as presented in Equation 2-2) [47].

$$F_d = \frac{1}{2} \rho C_D D |u|u - \frac{1}{2} \rho C_{dmp} D |\dot{x}|\dot{x} - \rho A \dot{u} C_m + \rho A \ddot{x} (1 + C_m) \quad [2-2]$$

Where;

$\rho$  = Density of sea water

$C_D$  = Drag coefficient

$D$  = Diameter of the structure

$u$  = velocity of fluid particle

$\dot{u}$  = Fluid acceleration

$C_{dmp}$  = Damping coefficient

$\dot{x}$  = Velocity of structure

$C_m$  = Inertia coefficient of the structure

$\ddot{x}$  = Acceleration of the structure

$A$  = Area of the submerged body

The parameters presented in Equation 2-2 (added mass and damping) exist in complex forms, because of the unsteady behaviour of ocean conditions. Different researchers have employed the use of numerical and experimental means in calculating for them. [48] calculated the effect of wave loadings on a typical semisubmersible platform. They developed a computer program to calculate the wave loadings; using finite element method to analyse the deformation at each point of the structural member. The strength of the structure was tested by investigating into the response at different flow incidence angles. A better knowledge of this can be found in the investigation that was carried out by [49]. In the former, a model test was conducted in extreme weather conditions, and the amplitude of the surge and heave response were recorded. The effect on the moorings (mooring force) was also established. The amplitude was plotted against the frequency, on each DOF; considering the varying wave force. The effect of the mooring line damping factor was also investigated, and it was concluded that the mooring damping only have significant effect on the translational response in the horizontal plane (sway and surge) during low and moderate weather conditions, and little or negligible effect during extreme weather conditions.

The nature of the hydrodynamic motion of the hull is relative to a resonant phenomenon between the flow properties (wave frequencies, vortex shedding frequencies) and the natural frequency/oscillating period of the hull. Although the hull motion increases with increase in the wave amplitude, but maximum motions are generally recorded at the resonant frequencies. Semisubmersibles are therefore designed to operate with natural periods that are far away from the oscillating periods of the wave. The natural frequency of the hull is basically a function of its stiffness and mass properties as shown in Equation 2-3.

$$\omega_n = \sqrt{\frac{K_i}{M + M_a}} \quad [2-3]$$

$$T_n = \frac{1}{\omega_n} \quad [2-4]$$

$K_i$  = The stiffness of the hull in  $i$  degree of freedom.

$M$  = Mass of the hull; details will be discussed in subsequent chapters.

$M_a$  = Added-mass parameter

$T_n$  = Natural period

The wave parameters are recorded in weather buoys and recommended documents such as [50] from ocean study, the operating range for 100-years and 1000-years wave periods for hurricane conditions falls between 1s and 17.2s. Very high periods (close to 21s) have perilously been recorded for tsunami cases, but this wasn't recorded in deep waters. As earlier cited, the natural periods of deep draft semisubmersibles in each DOF are therefore designed to operate outside this this range. Example, [51] presented the parameters of Petrobras-52 deep draft semisubmersible hull, and recorded 23.7s, 33.0, and 31.5s as the natural oscillating periods of its heave, roll and pitch DOF. The prototype of Glomar Artic 3 semisubmersible presented in [49] cited the natural heave period of the hull as 20.5s. [52] presented a model of a heave and vortex suppressed deep draft semisubmersible. The hull was designed with heave natural period of 19.1s, while 29.4s and 29.3s for the roll and pitch DOF respectively. They also cited 18.4s, 25.8s and 25.8s for the heave, roll and pitch natural period for conventional semisubmersibles in south East Asia. [53] presented the natural periods derived from a decay test of conventional deep draft semisubmersibles used in the GOM. The heave, roll and pitch natural periods are 20.0s, 28.4s, and 27.3s respectively. In our current study the natural periods were computed in relation with the added mass parameters as described in Equation 2-3. Details of this are presented in the chapter 4 of this thesis. The heave natural periods for different draft cases are between 21s and 22s. Figure 2.5 shows a relationship between the maximum wave periods recorded from weather buoys, and the heave natural periods of recently developed semisubmersibles.

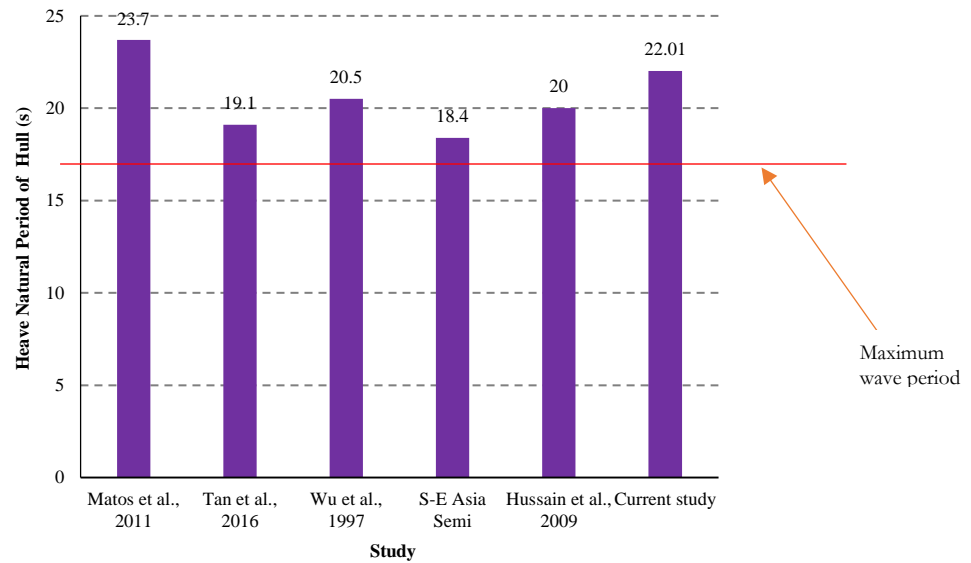


**Figure 2.5 Recent designs of semisubmersible heave natural periods**

It is important to mention that we have only compared the heave natural periods because all other periods are further away from the wave period because of their high added mass parameter during oscillation. There are similarities between the studies recorded in [53] and [51], as they show the nature of deep draft semisubmersibles used in GOM over the last decade. The variation in their heave periods is due to the hull mass and the geometric parameters of the columns used. [51] presented a study of P-52 semisubmersible operating in the GOM. Details of other result obtained from this report is recorded in the chapter 4 of this thesis. Our current study and that presented by [52] are the future recommended hull designs for deep draft semisubmersibles for improved motion behaviour.

## 2.4 Strength

The design of early semisubmersibles had issues with their strength estimation. It was complex to calculate the effect of wind and wave loads on the structural integrity of the hull. Over the last 30 to 40 years, sophisticated numerical and experimental techniques have been developed to calculate the strength of multiple column arrangements in deep waters. In this review we will be discussing on the most conventional method in modern times; Finite Element Analysis. Recently developed software packages make it possible to account for the weight distribution around the hull, from operational and environmental loading. This means we can calculate for stresses at the joints subjected to any load cases, we can select the type and grade of steel preferable for hull construction, and we can resize/re-dimension any of the components of the structure to reduce the effect of loads on them. Apart from the challenges associated with estimating the environmental loads, the hull weight distribution is also a



fundamental property that affects the hull's strength. The mean weight of the hull is estimated from the weight summation of the columns, pontoon, and braces, as shown in Equation 2-5.

$$W_{hull} = W_{Pontoon} + W_{Columns} + W_{Braces} \quad [2-5]$$

where  $W_{hull}$  is the weight of the hull,  $W_{pontoon}$  is the weight of the pontoon,  $W_{columns}$  is the weight of the columns and  $W_{braces}$  is the weight of the braces.

This flexural behaviour has different effect on the structural members of the hull, and the stresses are unevenly distributed. [15], [16, 54, 55] discussed ways of classifying and estimating the level of allowable stresses and buckling level of all offshore floating structures; semisubmersibles inclusive. Design methods such as the Load Resistance Factor Design (LRFD) and Working Stress Design (WSD) were recommended; depending on which is more appropriate for the loading conditions the structure is designed for. During rough weather, the hull experiences bending and twisting (torsional behaviour), [56]. There is a wide range of literature in the ships catalogue that explains this elastic behaviour. The hydro-elastic behaviour in semisubmersible is generally estimated in relation to their response. The theoretical background of this was discussed in [57] in a review of hydro-elastic theories for the response of marine structures. This review explained in a broad view the development of two and three dimensional (linear and nonlinear) theories used in evaluating fluid-structure interactions of deformable parts in marine structures. [58] studied the motions and deformation experienced in barges and columns under regular wave loading. This was not possible without considering some basic assumptions for the flow as incompressible, inviscid, non-rotational and small amplitude. With these assumptions, mathematical models were generated to understand the bending and continuous deformation at different mode shapes of a free-free (both ends) submerge floating column and barge. For the column, high resonant deflection was noticed within the range of occurring wave energy. Comparison for hinge joints and free conditions were analysed for the problem of a floating barge, and the effect of constraints were investigated for some degree of freedoms. [59] further developed a method for estimating the wave induced bending moment on a ship from its motion characteristics. They developed a set of mathematical models describing the bending moment of a floating body and used a network of cellular computational structures (*neural network algorithm*) to understand the bending tendencies of bodies under wave loading. An experimental setup was also put together to validate the accuracy of their model, and significant conclusions were made on incorporating the model into hull response monitoring systems. Although the future development of this technique has been proposed for monitoring reasons, this method does not provide structural design engineers with enough information on how to determine regions around

the hull were steel reinforcement might be required. [60] numerically investigated the impact load of sloshing on a cylinder using finite element method based on Hamilton's principle. It developed a flow domain around a circular cylinder, calculated it based on Einstein's notations, and carried out a time history analysis. Considering finer mesh grid around the column surface, it was concluded that increase in water depth was very likely to lead to a corresponding increase in wave impact load. [61] described the hydrodynamic nature of fluid interactions between a set of arranged columns supporting a large flexible structure (pontoon). With this numerical model, the motion equations of the topside integral part was resolved by studying the effect of the trapped wave and flow circulation within the columns, and the possible effects of elastic deflection of these on the topside. Any of these above mentioned technique can be used evaluate the strength of conventional fifth-generation semisubmersible.

## **2.5 Applications for Drilling and Production Systems: Dry-Trees Concepts**

For oil and gas production, dry-trees technology is predominately used on Spar and TLP because they offer restricted motions in their vertical plane. (Conventional Spar was further reconfigured into Truss Spar and Cell Spar to increase its compatibility with technologies such as dry-trees, while TLP has a vertically taut foundation; tethers). Over the last decade there has been an urgent need to reconfigure the existing semisubmersible floating hull platforms used in deep waters to suit newly developed regulatory policies, to suit newly discovered well depths and to reduce cost of drilling and production operations [62].



**Figure 2.6 Top tension riser: Courtesy of JAMSTEC**

Dry trees systems are possible with the use of tensioners (top-tension-risers). This type of risers are used for both drilling and production purposes. The top of the riser carries the tensioner, which

is traditionally supported by the deck system of the hull (see Figure 2.7). At the top (the main tensioner), it has multiple column system arranged at an angle to each other, moving with different stroke limits, controlling the fluid passage in and out of each of the riser. Its vertical nature exposes it to VIV phenomenon. Some applications involves the inclusion of strakes, to alter the frequency of the shed vortexes. Recent development of TTR in deep sea are designed using recommend standards [63], for 1000-years hurricane condition. The environmental loading is usually developed from the structural response of the hull in which it is to be installed. The application of dry-tree concepts for production operations has been tested in different oil fields, and tremendous successes have been recorded over the years. But because of the complexities associated with them (TLP and Spar) in ultra-deep waters, various design concepts of semisubmersible platforms are currently under screening, in other to get a replacement. Some of these concepts include:

- Paired Column Semisubmersible; PC-Semi
- Extendable Draft Platform (EDP)
- E-Semi and T-Semi
- Aker Dry Tree Semi

Each of the above listed hull concepts comes with its advantages. But of all of them, paired column semisubmersible hull formation is the most realistic and generally accepted concept for this purpose, because of the high payload it offers, and the absence of any moveable part within the hull, as compare the EDP, E-semi and T-semi.

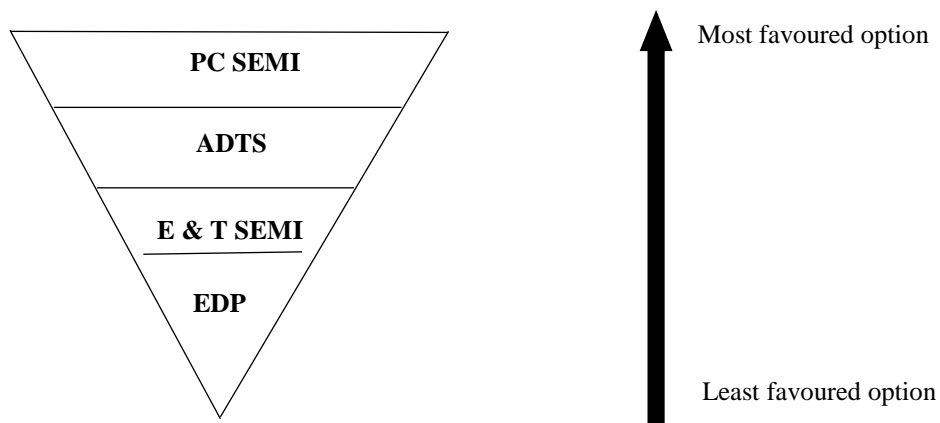


**Figure 2.7 Dry tree semisubmerisbles**

### **2.5.1 Development of Paired Column Semisubmersible Hull**

In the oil and gas industry, there is a constant need to increase the safety level of deep water operations because of the nature of damage caused by any form of failure. BP oil spillage in the

Gulf of Mexico in 2010 is a good example of this. An effective way of improving safety is *reducing subsea operations*. Subsea operations do not allow direct access of wellheads, and other drilling/production equipment's, as they are done with Remotely Operated Underwater Vehicles (ROVs). For safety and cost effectiveness, top-deck well-heads are therefore more advantageous for production operations. TLP and Spar platforms are more favourable to semisubmersible hull for design of production platforms in deep waters, because they are compatible with top deck well head installation, while convention semisubmersibles are not, despite the fact that they offer higher stability and more deck area. Spar and TLP are not as flexible as semisubmersible hulls. As discussed earlier, the problems associated with restoring stiffness of TLP and the complexities with the tethers makes it less economical and unsafe for ultra-deep operations (beyond 2000meter sea depth). Spar platforms have very small working, as they are suspended by a single column (SPAR). This acts as a disadvantage when selecting hulls for deep water production. Design engineers are forced to increase the size of the hull to create enough space for the equipment and staffs needed for deep sea operation. The Perdido Spar is a good example of this.

The development of a suitable structure that suits the requirement of production operation in ultra-deep sea regions therefore falls on semisubmersible hulls because of their wide surface area, stability, and installation convenience. Although semisubmersible have excessive heave displacement and vortex induced vibration for deep-draft, but reconfiguring its hull and deck compartment helps in reducing/eliminating the effect of these disadvantages. Paired Column Semisubmersible was developed to serve this purpose. Designed in 2006 by Jun Zou of Houston Offshore Engineering, the paired column semisubmersible platform (popularly known as PC-Semi) is the most realistic concept of all the semisubmersibles designed with dry-trees installation. Unlike the hull concept postulated by Technip, the PC-Semi has a stationary stable hull, making it safer and more reliably for ultra-deep; Figure 2.6. It has a significant reduction on the RAO heave curve as compare to conventional semisubmersible platforms which makes it suitable for TTR installation. Although the massive size of the hull makes its construction less cost effective, its stability and reduced motion response makes it very viable for ultra-deep water drilling and production operations.

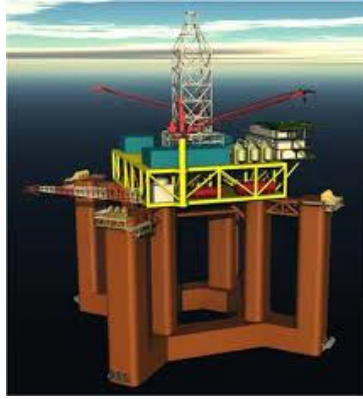


**Figure 2.8 Paired Column Semisubmersible Courtesy of Houston Offshore Technology**

### **2.5.2 The Extendable Draft Platform**

This structure was first designed in 2002 (Technip France), with the idea of combining the advantages of jack-up rig and their deep draft semisubmersible as shown in Figure 2.9. The columns are designed to penetrate the topside, making it possible to control the size of the draft. With a plate-like shape pontoon design, it has reduced motion on its horizontal plane. Although its implementation wasn't very successful in the oil & gas industry; results from the experimental and numerical analysis showed that it has a high stability advantage, coupled with its wide deck space that can accommodate both drilling and production units. [Offshore mag. (2004). Other researchers have made conscious attempts to continue developing this hull concept to make the design more feasible for fabrication/construction.[64] and [65] are some of the notable work that has been presented. Figure 2.9 shows an early sketch of the workability of this hull presented by Technip. The pontoon section acts as a heave reducing mechanism (heave plate), which helps in reducing the vertical motions during hydrodynamic wave and current loading. The movable nature of the hull system made it to be unattractive in ocean engineering; not much is known about the extendable draft platform, since its design has not been implemented in the industry.

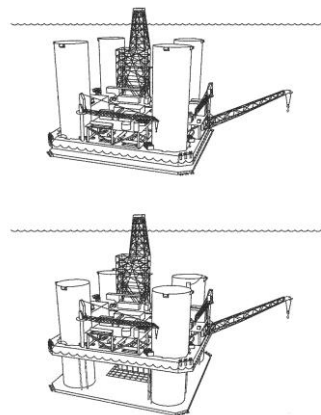


**Figure 2.9 Extendable-Draft Semisubmersible. Courtesy: Technip France**

### 2.5.3 E-Semi and T-Semi

The extended and truss semis are two deep draft concepts that employ conventional *heave plate* method is reducing the motions in the vertical plane in order to allow compatibility with TTRs. These plate inclusions make their hull configuration more complex and will definitely increase the overall maintenance of the structures. The difference between them is the moveable single heave plate on E-semi, and the fixed truss set of plates on T-semi. [66] described these concepts as a hybrid design, combining the advantages of a truss spar and a conventional semisubmersible platform. [67] studied the dynamics of E-Semi and T-Semi (Figure 2.10 and Figure 2.11). The investigation was carried out for 100 years wave return period for post Katrina sea state in the Gulf of Mexico. Eight TTRs of total weight  $4.5 \times 10^5 \text{ Kg}$  was fitted on each of the hull, and their vertical motions were studied for each hull configuration. The results obtained for the vertical motion of the TTR were observed to be less than 9m, which is the recommended standard for stroke limit of TTR. The development of E and T semis can be attributed to FloaTEC

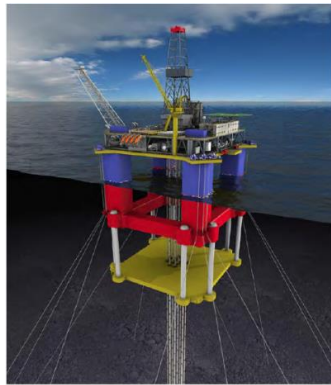


Figure 2.10 E-Semi Courtesy FloaTEC

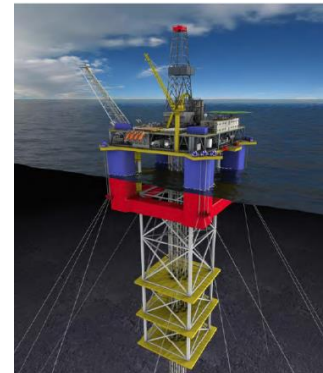


Figure 2.11 T-Semis. Courtesy FloaTEC

The idea of E and T Semis for dry-trees operations in deep waters wasn't really successful in the industry. The reason for this is that movable components on the hull of these structures make them less attractive to operators in this industry, because an ideal structure for deep and ultra-deep sea wells should have stable and stationary hull configuration

### 2.5.4 Aker Deep Draft Concept (ADTS)

The Aker Kvaerner deep draft is one of the practical ways of designing dry-tree semisubmersibles. This design was conceptualized with the intention of not altering the design of traditional semisubmersible. The motion suppressing mechanism is achieved with the plate shape pontoon design placed beneath the columns. The plate acts as heave suppressing device. It functions with a set of tensioners, array in ram style which helps to support the top tension riser

during operation [66]. The method was employed in the design and development of a Chevron operated structure called Blind Faith in 2007 [68].

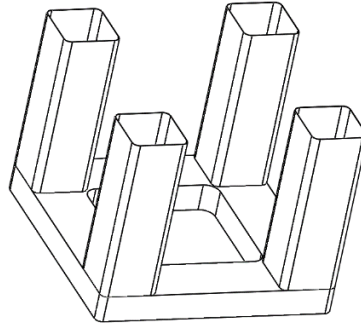


**Figure 2.12 Aker deep-draft hull**

The advantage the PC-Semi offers when compared to Aker semisubmersible is the high payload integration. The eight columns arrangement of the PC-Semi displaces huge amount of water, in turn offers high amount of payload. Aker semisubmersibles don't offer this. An increase in the columns and pontoon sizes for more payloads will increase its motion, and this might eliminate its dry-tree compatibility.

## **2.6 Offshore Wind Turbine Foundation**

Over the last 20years, there has been a significant increase in the generation of energy from offshore wind farms, because of the high demand for renewable energy. Between 1993 and 2014, the Global Wind Energy Council (GWEC) estimated the energy production from wind farms to be 5MW and 8045MW respectively. This rapid increase was made possible by the introduction of bigger and more efficient wind turbines. As the size increases, more weigh is displaced. More displacements imply a bigger foundation system. To resolve this complication, design engineers employed the use of semisubmersibles and TLPs, in place of the floating spar cylinders. The unfavourable conditions associated with TLP and water depth implies that engineers are left with the option of semisubmersible hull suspend these gigantic wind turbines in deep waters. This is why there has been a high research attention in understanding the stability of semisubmersible hull in rough sea weather, subject to maximum wind turbine rotation. [69]looked into the dynamic response of a three column semisubmersible foundation system of a wind turbine in frequency and time domain. Their tripod semisubmersible was anchored with six mooring cables; two on each column, and the turbine was designed to sit in the middle, supported with a frame of triangular trusses. Results from their study showed that a higher stability is required from the foundation (semisubmersibles), to effectively reduce the turbine motion, optimizing the energy

extraction from the blade rotation. The wind load on the turbine was also observed to be influential in calculating the strength of the semisubmersible foundation system. A more recent study presented by [70] compared experimental and numerical results of the design described in [69] with the incorporation of three wave energy converters (WEC) on each pontoon section of the tripod. The results for the motion response were presented in relation to the energy generated from these converters. For the purpose of this study, we have only discussed the response of the hull in relation to the displaced weight. [71] looked into the dynamic response of a V-shaped semisubmersible foundation system for an offshore wind turbine. The result showed that the motion of the system was greatly affected by the wind loads (unlike MODU and FPS) application. This implies that the hydrostatic parameters of the v-shaped semi have to be accurately selected to determine its functionality. The motion test for different cases for wave and wind loads suggested a possible application of this hull for wind turbine foundation. Other literatures and background for designing offshore wind turbine foundation systems can be found in [72-74].

## **2.7 Future Application: Luxury Cruise**

Deep-draft semisubmersibles are the future of ocean engineering, because of the level of stability they can offer from reconfiguration. In September of 2015, [75] reported a documentary into a new form of luxury cruise, designed as a mini-island [75]. The floating system was designed by Migaloo Private Submarine Yachts [75]. The hull of the floating mini island was built with a column stabilized semisubmersible. This hull will be required to function as a yacht or a cruise ship, with extremely high level of stability.



**Figure 2.13 Semisubmersible Mini Island (www.migaloo-submarines.com)**



## 2.8 Other Types of Floating Hull Systems

Apart semisubmersibles, there are other different types of floating hulls systems. Although this thesis is focused on semisubmersible platforms, but we have documented a brief review of other commonly used ones in the industry for better understanding. Spar, TLP Semisubmersible and FPSO are the most conventional types use for commercial drilling and production operations in the industry. Outside their motion characterization, other criteria for selecting which of these is to be use in exploring a particular oil field include the sea depth, the distance from field to land, production capacity, weight of topside (drilling unit, machinery), sea conditions and budget.

### 2.7.1 Tension Leg Platform

This is the most widely used platform for production operation in the oil and gas industry. It can produce over 45 wells simultaneously. It is held vertically downwards to the seabed by tethers, restricting the motions in the vertical plane (Heave, Roll and Pitch), giving it hydrodynamic advantages when compared to other floating platforms. [76] compared the hydrodynamic behaviour of spar platform, TLP and semisubmersible platform. They highlighted the heave and pitch motion of TLP to be over ten times lesser than that of spar and semisubmersible platforms respectively. Magnolia is the world's tallest tension leg platform. It is situated in the Gulf of Mexico, with a total depth of 1432 meters. Some other very deep TLPs are listed in Table 2.3.

**Table 2.4 Tension leg platforms**

Structure	Date	Operators	Sea Depth	Location
Neptune	2008	BHP Billiton	1295m	G.O.M, USA
Marco Polo	2004	Anadarko Petroleum	1310m	G.O.M, USA
Kizomba A	2004	Exxon Mobil	1177m	Angola
Ursa	1991	Shell, BP,	1219m	USA

A lot of researchers have analysed the dynamics of TLP, with the aim of improving its functionality in the oil and gas industry. A good background of the aerodynamic loadings on a typical TLP can be seen in [77]. Their investigation was focused on the wind loadings on the deck of a typical TLP. [78, 79] investigated the linear and nonlinear restoring stiffness in the behaviour of TLP, putting into account the discrepancies faced when using the conventional stiffness matrix method. [80] described the response analysis of TLP, using a set of nonlinear equations that expressed axial and transverse vibration of a tower subjected to tension, and the relationship

between the sea wave conditions, the frequency and amplitude of vibration of the tethers were also analysed. The total restoring stiffness of a typical TLP presented in [78], is the summation of the conventional tendon stiffness, the platform nonlinear restoring stiffness and the tendon geometric stiffness. TLP has some disadvantages in deep waters. Because it functions under the excessive buoyancy provided by the hull, an increase in operating load leads to a corresponding increase in hull size, and with a direct effect on the tethers and riser systems. This makes it less economical for well situated in very deep and harsh environments.

Tethers are another type of structural attachment. They are vertical cables used to keep tension leg platforms in place. They carry out the same function on a TLP just as mooring does for semisubmersibles, spar, FPSO, etc. They are usually made of steel wires and are held to the seabed by means of anchors. Because they are vertically tensioned, they automatically help to reduce the motions in the vertical plane (heave, roll and pitch), and this is why the hull of a conventional tension leg platform do not require any form of reconfiguration for top tension riser compatibility; unlike semisubmersibles and spar. There are different challenges associated with the installation and operation of tethers, as TLP is not favourable structure for ultra-deep oil exploration because of the complexities associated with its tethers as the sea depth increases. One of the major challenges is its 'restoring stiffness'. The detail review of this is outside the scope of this thesis.

There is a broad literature on the study of tethers. There are experimental, numerical and company recorded reports on the dynamic behaviour of tethers at different ocean conditions. [80]presented a simple demonstration of the behaviour of tethers under axial loading for a tension leg platform. [81]studied the stability parameters of tethers under loading

### **2.7.2 Spar Platform**

It is made of a single cylinder hull and a deck. It is the simplest form of floating structure, but its application is very recent. Although different companies have used spar cylinders in storing petroleum products and transporting materials for a very long time, the official first spar used from drilling and production in the oil & gas industry was installed in the Gulf of Mexico in the mid-90s, and since then the industry has witnessed a significant increase in the demand of this structure. Spar platform functions with the basic floatation principles offered in Archimedes' floating theories. [82]described the conceptual frame work behind the operating abilities of a conventional spar platform. In his description he highlighted the contributions of Ed Horton, who he attributed the successful invention of spar platform to. As he rightly pointed out, it functions under the

principle of a floating cylinder, with more of its body submerged into the water; just like an iceberg, creating stability. The cylindrical spar provides buoyancy for the deck section.

Since the design and installation of the first spar platform (Neptune) in the Gulf of Mexico, the structure has gradually developed into different types, with each design gearing towards reducing the effect of floating a cylinder under sea wave conditions. As a result of this, three generations of spar platforms have been developed; conventional spar, truss spar and cell spar. The major issues encountered in operating the earliest spar platforms (Neptune and Genesis) was the increase in heave displacement during extreme weather conditions and vortex induced movement, when vortices are shed. Although strakes were used to reduce the effect of VIM, there was no direct way to reduce the heave movement for a conventional spar, which was what brought about the concept of *truss spar*. The concept of truss spar was financed and developed by Chevron. The idea was to divide the spar tank into two sections, placing a set of heave plates that are attached with trusses in between them. These plate acts as a damping mechanism when high flow tides flows through it; helping to reduce the vertical/heave displacement. After a series of numerical and experimental investigations into the possibility of this sort of structure, final conclusion was made in the mid-90s, and the first truss spar was built by Technip in 1995. The major challenges faced in the design of a spar platform are the enormous time it takes to build the hull, and the cost of fabricating it. In 2001, Ed Horton came up with the idea of eliminating the stiffening process associated in strengthening the metal plates used for fabrication, and also to reduce the time duration faced by oil & gas serving firms in constructing it. He achieved this by bringing a set of tubes together; in a circular configuration, to provide enough buoyancy to support the deck weight of a truss spar. This concept is what brought about the *cell spar*.

It is installed through a process called ballasting and de-ballasting. The cylinder section is normally installed before placing the topside on it. After conveying it to the point where it's to be used, the soft tank is filled with water to make it incline at an angle. When this is achieved, water is finally pumped into the hard tank which eventually brings the spar to a vertical position. The mooring lines are then connected to piles screwed to the seabed, to keep the spar in position. Water is pumped out of the soft tank to achieve weight balance. This process of pumping water into and out of the tanks is called ballasting and de-ballasting. After the hull has finally been installed, the topside is placed on it with the aid of a crane lift, before integrating both compartments together. [83]described the dynamic analysis of a typical offshore spar platform. They explained (from a literal view) the nature of sea state conditions (wave loadings) on a spar platform, describing the response analysis as a function of the hydrostatic force, the nonlinear

restoring stiffness of the mooring cables, which controls the horizontal displacements (surge and sway motions).

### **2.7.3 Floating Production Storage and Offloading Platform (FPSO)**

This type of platform is design to have drilling, production and storage units. It is built in form of a ship, sometimes moored at one extreme end (turret mooring), and have a wide deck space for other activities such as processing unit, offloading and storage. With its streamline (curved) outer surface, it has the ability to conform to different wave movements, which makes it suitable for waters with harsh weather conditions. It has a great advantage in oil fields where there is no piping transportation network. FPSO helps in storing products, prior to when tankers and offloading barges are provided. These storage facilities provided by FPSO can be very useful in countries where oil installations are not safe (Pirate attack and militancy). Its excessive movement makes it impossible for TTR installation; not permitting top deck well heads. FPSOs are the most commonly used platforms in Nigeria and west-Africa region because of their favourable weather conditions. They are not expensive to operate and expertise for maintenance is readily available because of the similar features if shares with hull systems in the shipping industry. FPSO design is also applied to the building and construction of LNG tankers (Liquefied Natural Gas).

There is little or no comparison between FPSOs and deep-draft semisubmersible platforms, so we have not recorded much documentation on the dynamics and operation of FPSO in this thesis.

## **2.9 Chapter Summary**

The origin and background of semisubmersible hull were presented in this chapter, and the progress made so far in optimizing its functionalities/usefulness, and increasing its application in ocean engineering was recorded. A brief summary of some contributions made by the industrial and academic researcher in the improving its motion response was reported and the technique adopted for each invention was discussed. The rapid proliferation of deep-draft semisubmersible for deep water operations was discussed, and the challenges (such as vortex induced vibration) that have been recorded so far by operators were also highlighted, and present recommendations for circumventing some of these challenges were also discussed. The application of deep-draft semisubmersible hull in the design of drilling and production units

It is evident from the brief review presented on the application of semisubmersible for wind turbine foundation system that there is an urgent need to develop a semisubmersible foundation system for offshore wind turbine that has a favourable payload and reduced motion characteristics.

Furthermore, there is a concern on the influence of wind loads and turbine rotation on the strength of the proposed semisubmersible hull. As a result, there is a need for further research into its dynamic behaviour, alongside understanding its stress pattern from wave and wind loads for future application for wind turbine foundation system.

# CHAPTER 3

## HIGHLIGHTS

- Experimental Reports on the Effect of Vortex Phenomenon on a PC-Semi.
- RPSEA Experimental Study on the Hydrodynamic Response of a Paired Column Semisubmersibles Hull.
- Reduced Hull's Response Amplitude for PC-Semi Relative to Conventional Deep-Draft Semisubmersibles
- Lancaster University Experimental Setup for Response Study of PC-Semi.

# Chapter Three: Experimental Study of Motion Characteristics of PC-Semi; Global Performance

## 3.1 Introduction

An experimental study into the effect of vortex induced movement and wave motion of a PC-Semi hull at different flow orientations and draft sizes have been presented in this chapter. For the VIM phenomenon, results from two experimental set-ups developed to estimate the effect of vortex shedding on a paired column semisubmersible hull has been presented. The first experiment was carried out at the University of California, Berkeley (UCB), in 2012 while the other experiment was conducted at the Marine Research Institute Netherland (MARIN) in 2013. Similar results were recorded from both experiments. The results obtained for these experiments were enough to develop numerical models that can predict the behaviour of further application of this hull system. In the cause of this study, no further experimental investigation was carried out to investigate VIM effect on this hull system. Two experimental studies for wave motion from hydrodynamic loads have also been presented. Results from the first experiment was carried by Houston Offshore Engineering (H.O.E) and recorded in [4]. The second experimental study was carried out at the Lancaster University wave tank for different draft sizes, assuming regular wave conditions. Details of these investigations are discussed in the body of this chapter. Although these experiments were carried out using models scaled to 100 times and above, the results are of extremely high integrity as the setups were developed in reputable companies and institutions, considering recognized industrial standards. At the end of this chapter we will be able to draw conclusions on the following;

- i. The level and extent of experimental work carried out so far in investigating the effect of complex flow dynamics around the hull of the newly developed paired column semisubmersible hull system.
- ii. The reciprocating amplitude of shared vortexes developed from eight column arrangement (in the form of a PC-Semi).
- iii. Drag effect on the hull as a fundamental part of the wave forces on actin on the entire structures.
- iv. The relationship between the pontoon and column drag, which is required for strength and buckling assessment.

v. Recommendations for future experimental work require for the application of this hull formation for support structures (Wind turbine foundation and residential quarters).

### 3.2 Experimental Study of Vortex Induced Motion

The conventional way of studying vortex effect on a floating body is the use of a tow test. The same method was used in investigating the VIM effect on this hull formation as shown in Figure 3.1. The results obtained from this study were recorded in [1, 13]. They were developed for the same weather conditions, draft appendage, flow orientation and hull geometric parameters. Analysis was carried out for  $0^\circ$  flow angle. [13] presented VIM test of a free floating PC-Semi hull for a scale of 1:160, using a tow speed range between 0.1m/s and 0.6m/s. Investigation was carried out for two draft conditions; 50.3m and 48.8m, and the results were recorded. Comparison was also made between traditional four columns deep draft semisubmersibles, and PC-Semi. VIM amplitudes were computed using the Equation 3-1, and the reduced velocity was computed as in equation 3-2. D was measured as the diagonal distance of each outer column, which span to 19.4m.

$$\text{Max} \frac{A}{D} = \frac{A_{\max} - A_{\min}}{2D} \quad [3-1]$$

$$V_R = \frac{v_c}{D * f_n} \quad [3-2]$$

$$C_d = \frac{2F_d}{\rho A v_c^2} \quad [3-3]$$

Where  $A_{\max}$  and  $A_{\min}$  are the maximum and minimum values of the displaced amplitude, D is the characteristic length of the column; the outer column's diagonal length,  $V_R$  is the reduced, A is the surface area,  $v_c$  is the current velocity  $C_d$  is the coefficient of drag and  $F_d$  is the hydrodynamic force.



Figure 3.1 Test model from MARIN, Netherlands.



The relationship between the reduced velocity and the oscillating amplitude (Max A/D) was observed to be linear between  $0^\circ$  and  $45^\circ$ . This linearity was experienced for reduced velocity value greater than 3.5. For  $V_R$  range between 4 and 11, the reciprocating amplitude of the shed vortices/the hull gradually reduces from  $0^\circ$  to  $45^\circ$ . The maximum value for Max A/D was recorded as 04. It is important to mention that between a reduced velocity range of 4.5 to 11, there was no significant variation observed between the reciprocating amplitude; i.e., for a specific flow angle, a change in the reduced velocity (natural frequency of the hull) do not amount to any significant change in the reciprocating amplitude of the hull. This is a very useful parameter for motion characteristics of the vibrating tendencies of this hull system from vortex shedding. Similar  $V_r$  was observed for the hull drag, but the relation it has with the flow angle was observed to be different. The maximum value of hull drag was recorded at  $22.5^\circ$  flow angle. There was a gradual increase between  $0^\circ$  and  $22.5^\circ$ , and a drastic decrease between  $22.5^\circ$  and  $45^\circ$ . This irregularity experienced on the nature of drag coefficient around the hull is relative to the surface area exposed to the incident flow.

An experimental study in understanding the effect of hull appendage /draft size on the drag coefficient around a deep draft semisubmersible hull system is reported in [14]. In the report, results were documented for drag coefficient, which was observed to be relative to submerged hull area. The major contributor to this phenomenon is the *inclusion of the pontoon section*. Drag effect on multiple array of column presented in [84], [85, 86] do not necessarily show this phenomenon. The drag variation around the columns is basically subject to whether a specific column is buried in the wake formed from the flow separation from a leading column or not. Maximum drag from the summation of all columns is mostly recorded at  $45^\circ$  flow angle. From this assessment, we can therefore speculate that the inclusion of the centralized pontoon section plays a significant role in understanding the drag distribution around the hull a typical PC-Semi. This unique behaviour have been investigated using CFD method in [87] where it was stated that the pontoon section was observed to be responsible for one-third of the entire drag around this hull. Details of this study will be discussed in later section of this thesis. The maximum value for hull drag was recorded between 1.1 and 1.2, at a reduced velocity of 5.57. Similar behaviour recorded for Max. A/D between  $V_R$  range of 4 and 11 was also recorded for drag. Results were also recorded for a reduced draft size of 48.8m. The draft size was observed to have effect on the Max A/D, for a reduced velocity range of 3.6 and 8.8. Maximum values were recorded at the middle of the range. The drag effect for both draft sizes was more significant. The variation in the average value of the horizontal line graph for drag coefficient recorded for 53.34m and 48.8m are over 0.2m apart. This is huge, considering the fact that the average value of drag coefficient of 53.3m draft size, recorded at

different reduced velocities is 1.0, while the average value recorded for 48.8m draft size is 0.8. From this, we can assume a 20% reduction in drag coefficient for a draft size reduction of 8.5% (53.34m to 48.8m). This is another useful parameter that might be required in controlling the wave forces acting on the hull during tow, installation or transportation. The extent of the columns and pontoon contributions to this reduction was not clearly defined in this experiment study. A numerical study into the drag effect on eight arrays of columns (without the pontoon section) will be presented in the later part of this thesis; to understand the contribution of the columns and pontoon section to this reduction. The parameters (drag and Max A/D) were also checked with conventional four columns arrangement for 0° and 45° and good agreements were recorded.

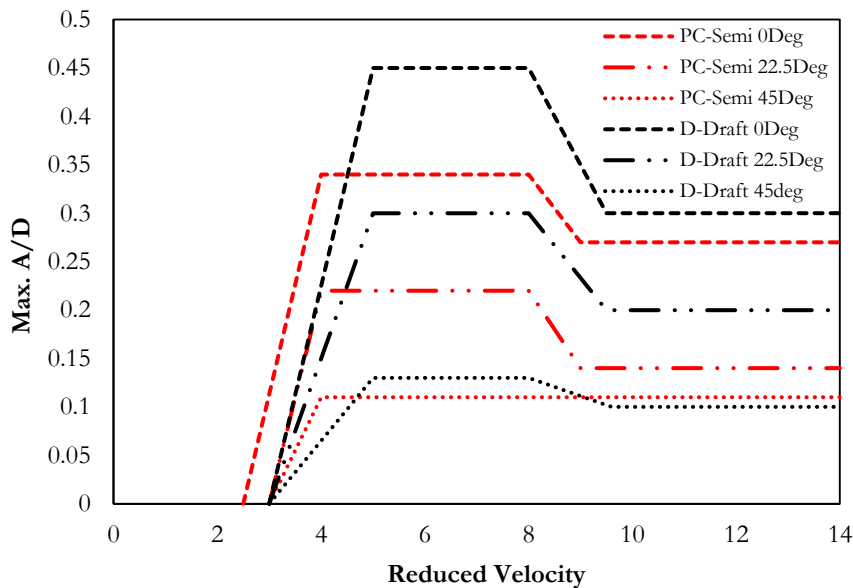


**Figure 3.2 Comparing Max A/D of PC-Semi and conventional deep draft semisubmersible [1, 2]**

A better understanding of how VIM effect on PC-Semi can be compare to VIM in conventional deep draft semisubmersible was recorded in [1]. Comparison was made between the results obtained in [13] for PC-Semi and that of conventional deep-draft semisubmersible. An envelope system was introduced for the Max A/D parameter for 0°, 22.5°, and 45°; as shown in Figure 3.3. For the four columns deep draft system, square columns were used, with a draft size of 45.7m, characteristics length of 30.2m, column length of 21.3m, and slender ratio of 1.5. The setup was developed in MARIN for a scale of 1:54. 16 mooring lines were incorporated into the system to study the effect of fatigue on this new hull system. For free floating condition, the same results were obtained as in [13]. This was a significant indication that scaling does not affects the result integrity of VIM study of ocean structures, as pointed out in the test. The mooring integration system was steel-polyester-steel. Details of the result obtained for mooring fatigue system can be

found in the test. DNV S-N curves and API T-N curves were used to test for the fatigue life of the lines, and PC-Semi was observed to have longer life span for the mooring lines when compared to conventional deep draft semisubmersibles, which is as a result of its reduced response as shown in Figure 3.3.

### **3.3 Experimental Study of Global Performance**

The invention of PC-Semi was done relative to the application of top-tensioned-riser system, as discussed in the previous chapter. The early study for global response was therefore carried out relative to that. Not much of the results obtained from that series of experiments are available in the public domain. [4] is the only report available on the global performance of this hull system, and not much conclusion can be made from the results, as they were recorded for an unconventional design case. Numerical simulation for free body response will provide a more dynamic set of results that can help design engineers to draw up conclusions on the global performance of this hull. A more detailed analysis into this is presented in the next chapter of this thesis. The test setup presented in [4] was done for a scale 1:76.56. The analysis was carried out in a wave basin considering four loading conditions; survival, extreme, operating and one-line damage. Hull parameters measured include maximum offset, minimum downward motion, maximum rotation, minimum airgap, and maximum accelerations. In [50], 100 years wave return period was used for extreme design and one-mooring damage conditions, 1000-years wave return period was used for survival conditions, and 10 years winter storm was used for operation conditions. Figure 3.3 shows the underwater view of the experimental setup.

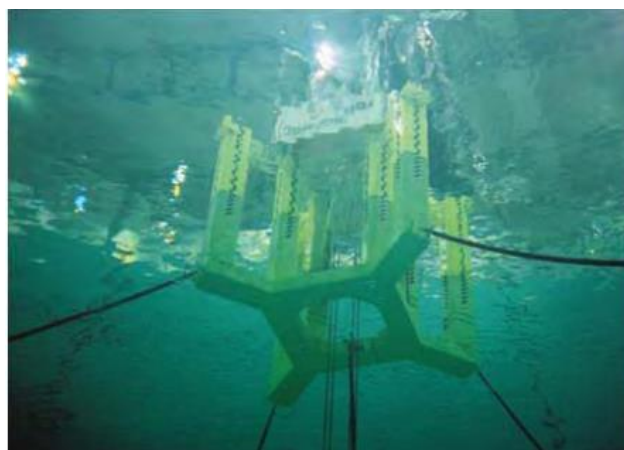


**Figure 3.3 Underwater view of PC-Semi Test Model for Global performance: Courtesy, Houston Offshore Engineering**

The test setup was developed for waves dominate cases, considering unidirectional flow incidence. Effect of current and wind forces were considered in the test setup. There was a direct integration of the steel catenary risers, mooring lines, top-tensioned risers and umbilicals, as shown in Figure 3.3. An asymmetric mooring system was used in this report, as the design was for a specific oilfield in the Gulf of Mexico. 14 mooring lines were used; eight on one side, and 6 on the other side. There was an uneven weight balance on the topside; the mooring was used to create a balance on the hull. As the experimental investigations carried out at the Lancaster University wave tank was carried out for regular wave conditions, the validation of our numerical model for irregular wave condition was done with the result presented in Table 3.1. The effect of the weight and mooring discrepancies was taken into account, as the results for global performance is dependent on the hull’s structural attachments. Maximum offset was recorded to be less than 120meters for all four cases, which falls below the five to seven percent offset limit standard (for a water depth of 2400m) required for a deep-draft semisubmersible platform in the Gulf of Mexico. Very high offsets were recorded for survival and one-mooring damage conditions. 12.07m was recorded for maximum offset for operating conditions, which shows very favourable motion for this hull system as compare to conventional semisubmersible hulls [88].

**Table 3.1 Summary of global response test results [4]**

Parameters	Result	Flow Orientation
<b>SURVIVAL</b>		
Maximum offets (m)	116.19	135Deg
Max. downward motion (m)	5.69	180Deg
Max. Rotation (Deg)	7.75	135Deg
Min. Air gap (m)	3.32	135Deg
Max. Acceleration (g)	0.29	135Deg (Horizontal)
<b>EXTREME</b>		
Maximum offets (m)	74.16	135Deg
Max. downward motion (m)	3.62	135Deg
Max. Rotation (Deg)	6.66	135Deg
Min. Air gap (m)	6.43	135Deg
Max. Acceleration (g)	0.22	135Deg (Horizontal)
<b>OPERATING</b>		
Maximum offets (m)	12.07	135Deg
Max. downward motion (m)	0.55	180Deg
Max. Rotation (Deg)	2.16	135Deg
Min. Air gap (m)	16.79	135Deg
Max. Acceleration (g)	0.06	135Deg (Horizontal)
<b>ONE LINE DAMAGE</b>		
Maximum offets (m)	101.77	135Deg
Max. downward motion (m)	3.33	135Deg
Max. Rotation (Deg)	7.06	135Deg
Min. Air gap (m)	6.28	135Deg
Max. Acceleration (g)	0.22	180Deg (Horizontal)

The maximum downward displacement (heave motion) was recorded as 5.69m for 1000-years wave return period. The effect of the tensioners on this motion is recorded in [5]. For a time series analysis with 15 top tension risers arranged in ram style configuration, a reduction from 5.69m to 4.63m was recorded. The displacement (hull heave motion) was also observed to be less than the stroke limit of the tensioners. Other results from this report will be discussed in chapter four of this thesis.

Results for maximum offset and maximum rotation were recorded for the same weather conditions as expected; i.e., maximum rotation was also recorded for survival and one mooring line damage conditions,  $7.75^\circ$  was observed to be the maximum rotation. The direction of rotation was not recorded at the time of this test, but this will be investigated on in the next chapter of this thesis, using numerical methods.

### 3.4 Lancaster University Wave Tank Test

A test setup was put together at the Lancaster University wave facility to investigate the motion response in the X and Z direction as illustrated in in Figure 3.4. The Lancaster University wave tank is an ultramodern test facility designed to study the behaviour /energy of waves for different weather conditions. The tank is 12.5m long, 2.5m wide and 1.7m deep. It has eight paddles at the extreme right and two carrier platforms; as shown in Figure 3.5. When the paddles are fully engaged, the facility has the capacity of achieving wave amplitude of 0.1m.

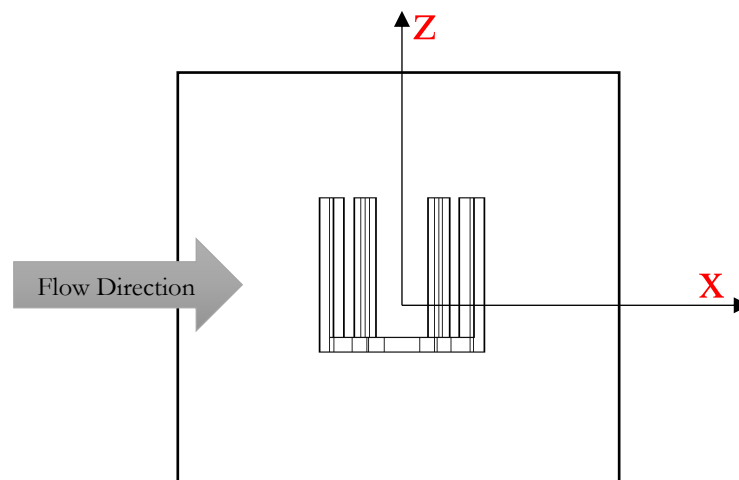


Figure 3.4 Definition of coordinate system



Figure 3.5 Side view of Lancaster University wave tank

### 3.4.1 Model description

The model was developed for a scale of 1:146.68, as shown in Table 3.2. The inner and outer columns are 0.093m x 0.0693m, and 0.093m x 0.0893m respectively. The inner columns are 0.343m apart from the column centre, with a height of 0.5m (see Figure 3.7). The pontoon section is 0.0528m thick, and constructed as water proof. The column sections are hollow and are used for ballasting during experiment. The results for these motions were analysed by a digital image capturing mechanism called the Imetrum system. It is a non-contact system made of two cameras (as shown in Figure 3.6), which capture structural properties such as displacement, compression, tension, strain and deformation. In our study, we have concentrated on the vertical and horizontal displacements (heave and surge motions: Z and X) of the hull during wave motion. The study was carried out for a single wave direction;  $0^0$  with no current study, and the flow was calibrated for regular waves.

Table 3.2 Particulars of test models

Particulars	Full Scale	Model Test
Inner columns (m)	14 x 10.4	0.09545 x 0.07090
Outer columns	14 x 13.4	0.09545 x 0.09136
Inner column dist (m)	50.30	0.34292
Outer column dst (m)	95.98	0.65435
Pontoon height	7.92m	0.0540
Draft size	53.34m	0.36365
Displaced volume (m <sup>3</sup> )	94449.46	0.02945
Displaced Mass (Kg)	96500 x10 <sup>3</sup>	29.1

Centre of Buoyancy	-30.1m	-0.223
Centre of Gravity	35m	-0.13
$K_{xx}$ (m)	56.31	0.3269
$K_{yy}$ (m)	56.31	0.3269
$K_{zz}$ (m)	62.48	0.3522
$I_{xx}$ (Kg.m <sup>2</sup> )	305940047373.97	3.11
$I_{yy}$ (Kg.m <sup>2</sup> )	305940047373.97	3.11
$I_{zz}$ (Kg.m <sup>2</sup> )	376745020975.15	3.61

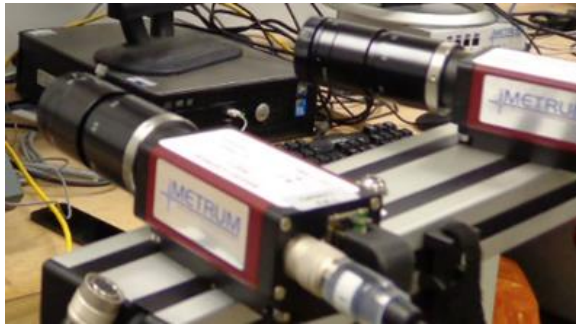


Figure 3.6 Imetrum cameras

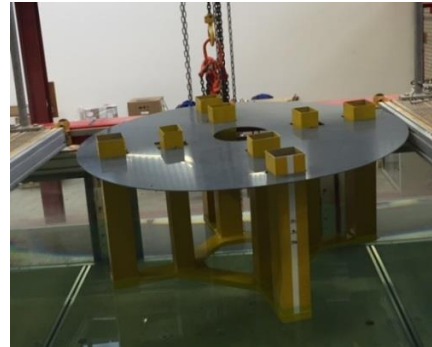


Figure 3.7 Test model

### 3.4.2 Limitation

The size of the wave tank facility generated reflected waves from the wall of the tank, (backward). This affected the force parameters which include the added mass and damping, but not necessarily *the motion* parameters, generated from the height and frequency of the waves. As we will observe from Figure 3.1, the experimental setup developed in MARIN for extracting the vortex induced motion (flow current), the backward hydrodynamic reflection for the side wall was not taken into account.

### 3.4.3 Test

The digital image capturing calibrator records motions referenced from a black background. A dark board with white dots was therefore attached to one end of the hull model, as shown in Figure 3.8. Two high powering lamps where focused on the area of concentration to help increase accuracy.

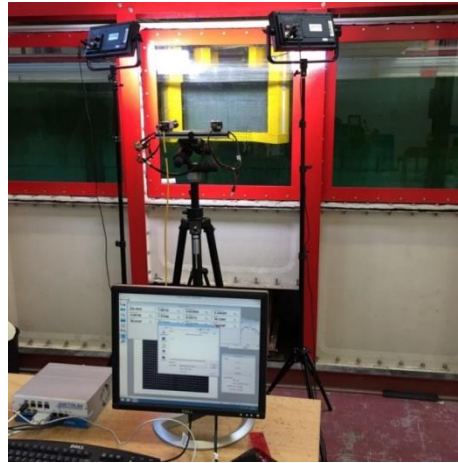
Table 3.3 presents the wave calibration adopted for this study. The wave frequency ( $f_w$ ) was varied between 1Hz and 0.5Hz, for estimated wave amplitude of 0.040m.

Table 3.3 Wave calibration

$f_w$ (Hz)	T (s)
1	1

0.9	1.11
0.8	1.25
0.7	1.43
0.6	1.67
0.5	2

The paddles were engaged for about 120 seconds, and the time was slowly reduced to 25 seconds, and no effect was recorded on the maximum hull displacement for any of the degrees of freedoms.



**Figure 3.8 Data Collection**

#### **3.4.4 Post-processing: Result analysis**

Results from the experimental test showed a decreasing relationship between the motion response and the wave oscillating frequencies for both heave and surge degree of freedoms. Low wave frequencies (below 0.6Hz) showed more influence on the heave response than the surge response. It is speculated that a further reduction in the wave frequency (sea state condition) will lead to a wider disparity between the heave and surge motions. The surge motion experienced a gradual and proportional decrease between 0.5Hz and 1Hz, but was not necessarily the case for the heave motion. Table 3.4 showed that increase in wave frequency leads to a corresponding increase in the hull oscillating frequency, but a decrease in the displaced amplitude; both in the heave and surge degrees of freedom. The oscillation observed for some wave frequencies is nonlinear. A careful analysis of the process (surge response for  $0.9H_f$ ) showed different range of amplitude for every 5s; 0.00618m and 0.00705m. This observation demanded we increase the time limit to 180, and the phenomenon was evident all through. A visual study on the video recordings confirmed our observation. This was taken into account in the development out numerical model. Time series analysis was carried out for a wide range of wave frequencies (from ocean conditions), with little interval between them. A summary of the results for maximum displaced amplitude in presented in Table 3.4.



**Table 3.4 Result summary for maximum displaced amplitude**

Wave Parameters		Maximum Displacement	
$f_w$ (Hz)	$T$ (s)	Heave (m)	Surge (m)
0.5	2	0.0484	0.01609
0.6	1.67	0.0281	0.0140
0.7	1.43	0.00018	0.01136
0.8	1.25	0.0025	0.00943
0.9	1.11	0.0027	0.0071
1.0	1	0.00215	0.00483

### 3.5 Chapter Summary

Experimental studies on the motion characteristics of a paired column semisubmersible hull system have been presented. Two types of motion analysis were studied; vortex induced motion generated by resonance phenomenon from reciprocating shed vortices, and wave induced motion, which is as result of the dynamism of the wave properties. Results presented for current induced motion are from experiments carried out in U.C and MARIN, while the motions from hydrodynamic loads were investigated at the Lancaster University wave tank. We can conclude that PC-Semi has a better VIM response when compared with conventional deep draft semisubmersibles because it has smaller reciprocating amplitude. This is can be due to the combination of different reasons which include the geometric properties of the columns and the manner they are arranged. Results from the wave induced motions showed low response under regular wave, and the heave motion was observed to be inversely proportional to the draft size.

It is important to mention that the results obtained from the experiment carried out that the Lancaster University wave tank was only used for validation purpose.

# CHAPTER 4

## HIGHLIGHTS

- Motion Characterization
- AWQA Utilizes Boundary Element Method
- Mathematical Resolution of Wave Potential Problems, Applying Diffraction and Radiation Theories.
- Forces and Moment Formulation, Introducing Perturbation Formulation; Linearizing the Scattered Wave properties.
- Development of Drift Wave.
- Response Formulation in Time Domain, from Motion Equation
- RAOs Relationships with Draft Size.
- Current Effect on RAOs and Forces.
- Maximum Offset Study, for Survival and Extreme Conditions.

# Chapter 4 Numerical Simulation of Hydrodynamic Loading on a PC-Semi for Motion Characterization

## 4.1 Introduction

The design and recommendation of paired column semisubmersible hull formation for a floating production system (FPS) in the Gulf of Mexico is as a result of its favourable motion characteristics in the vertical plane. The configuration of conventional semisubmersible hull system into pc-semi involved the incorporation of additional components and the modification of the already existing ones such as pontoon modification into a centralized system, draft size, use of slender rectangular columns and the introduction of inner columns. The extent to which these parameters affect the global performance is not known, as a result design standards have not been developed for this hull formation for motion characterization. Early study of motion characteristics from hydrodynamic loading on conventional semisubmersible is recorded in [89] [90]. The effect of mooring lines and damping coefficient investigated on the structural response of eight column semisubmersible arrange in-line (two pairs; four in each pair) with one another. The results showed over 40% reduction in hull surge motion from mooring integration, but no significant reduction (below 7%) for extreme and irregular wave conditions. [49] advanced the study in regular waves by analysing the internal forces of the hull from hydrodynamic loading. The mooring lines were discovered to be negligible in analysing the amplitude response of the hull for wave period of 18s and above, despite the regular nature of the waves. From these studies, it can be said that irregular wave study of the motion response of semisubmersible provide almost the same result for free floating state and structural attachments (moorings and risers). Since the inception of conventional deep-draft semisubmersibles there have been different studies on its motion properties.

[51] investigated the second order resonant heave, roll and pitch motions of deep-draft semisubmersible platforms using Petrobras 52 as a case study. Results from hydrodynamic approximations in WAMIT were checked with that of a test model scaled to 1:100 of P-52. It was observed that the selected approximations (Newman's approximations, White-nose approximations and QTF approximations) showed reduced computational time and cost, in estimating the second order heave, roll and pitch motions. The results from the numerical setup were also checked for different levels of damping. The heave spectrum for 1.5%, 2%, and 2.5% viscous damping showed a gradual reduction in maximum spectral values, for the same natural

oscillating period (23.7s). The average pitch rotation from different degree of freedoms obtained from experimental model was also checked with results from numerical studies for different percentage of viscous damping (3%, 3.5%, and 4%), and precise agreement with the experimental result was observed for viscous damping slightly below 3.5%. Details of other results obtained from this study can be found in the report. Our major interest in this study is the correlation obtained between the experimental and numerical setups for the heave and pitch/roll DOF. This finding was useful in the development of our numerical setup.

[52] presented the results obtained also from experimental and numerical study of the hydrodynamic behaviour of a new concept of deep-draft semisubmersible that has a suppressed heave and VIM amplitude. The compared the result with that of conventional deep-draft semis. The hydrodynamic response study was also developed in WAMIT, the VIM check was build using CFD codes in StarCCM+ and MLTSIM, and the model test was built for 1, 10, and 100year wave return periods. (In this chapter, we will only be discussing the result form the model test and the WAMIT model. The CFD study is out of the scope of this chapter). The result showed almost 20% reduction in heave amplitude (2.5m and 2.1m), and an increase in maximum rotation ( $4^{\circ}$  and  $3.3^{\circ}$ ) for the new semisubmersible concept when compared to conventional deep-draft semisubmersibles. The effect of mooring damage (one line and two lines) was also investigated for both cases, (for a set of 12 mooring lines; 3 at each end of the hull), and the same relationship was recorded for both cases. I line damage had to effect in heave amplitude, for 100-years wave return period for both hull forms, but 2 line damages had about 40% reduction in heave and pitch DOF for 10-year wave return period. These results were also important to our study at the newly develop Heave and Vortex Suppressed semisubmersible hull (HVS) is have the ability tom perform similar task in deep water as PC-Semi.

The prerequisite of the analysis that was carried out in this chapter is documented in [5]. In the report, the dynamic response of a paired column semisubmersible hull system (with tensioners arranged in ram-style) was analysed in post-Katrina irregular sea conditions. Results presented showed that the heave motion for 1000s time series is very small when compared to the tensioner stroke limits. Structural response were discovered to be negligible for extreme conditions if the hull satisfies the response for survival conditions (1000 years return), as set in [50]. The limitation of this study is that it was done for a particular sea condition, for a particular riser application and a particular semisubmersible hull application (floating production system). This limits the knowledge of the motion characteristics of the unique and novel hull system. In this study we have carried out investigations on the hull performance in its free floating state, and have developed

relationships between motion characteristics and the geometric properties on which its configuration was done.

In this chapter we have discussed issues relating with the motion response and general global performance of a pc-semi, and the structural design parameters to which they depend. Recommendations (on draft size, column size and column spacing) were postulated for future application of this hull structure for MODU, support structures and floating wind turbines. Mathematical models for basic consideration for design standards were also formulated in this chapter. At the end of this chapter, we will be able to make conclusions on the following;

- i. The relationship between the draft size and the motion response of a typical paired column semisubmersible hull system,
- ii. The first and second order forces acting on the hull during extreme and survival weather conditions
- iii. The current effect on the response amplitude operator (RAO) plots, and how this vary with the flow orientation,
- iv. Make suggestion for the application of this hull system for drilling unit considering recommended standards.
- v. Compare the motion response of conventional deep draft semisubmersible floating system to deep-draft paired column semisubmersible hull, and make conclusions based on our findings.
- vi. Develop correlations between the surface wave parameters and the hull response for different weather conditions.
- vii. Understand the factors affecting the maximum hull offset.

## **4.2 Methodology: Theory Formulation**

In solving the complication associated with the motion condition of floating systems, [91] employed the use of a three dimensional system in calculating the forces and motions of a floating marine vehicle in waves. We have adopted similar method in this study. Two coordinate systems (Cartesian) were defined; the first is at the cut-water plane level, and the other at the centre of gravity of the hull. The first coordinate is define in relation with the space in which the body occupies, and is measured from the centre of the hull 'O', in three dimensions;  $x, y, z$ ; with  $z$  been the axis normal to the water surface. The second coordinate is measured in relation with the mass of the hull located at the centre of gravity (COG), which enables us to measure the mass properties of the hull during wave loading. With these coordinated, the relative diffraction of the flow

properties can be calculated. Different AQWA packages employed to perform this task. The AQWA codes employ the use of Boundary Element Method (BEM) in resolving diffraction problems. The complex integral and differential equations developed around the sea and structural boundaries as a result of the unsteady behaviour of the flow are solved numerically.

## 4.2.1 Wave Kinematics

### 4.2.1.1 Definition of Surface Wave

The wave (regular and irregular) elevation creates an angle on the XY plane. This angle is generally referred to as the ‘wave direction’ (see Figure 4.1)

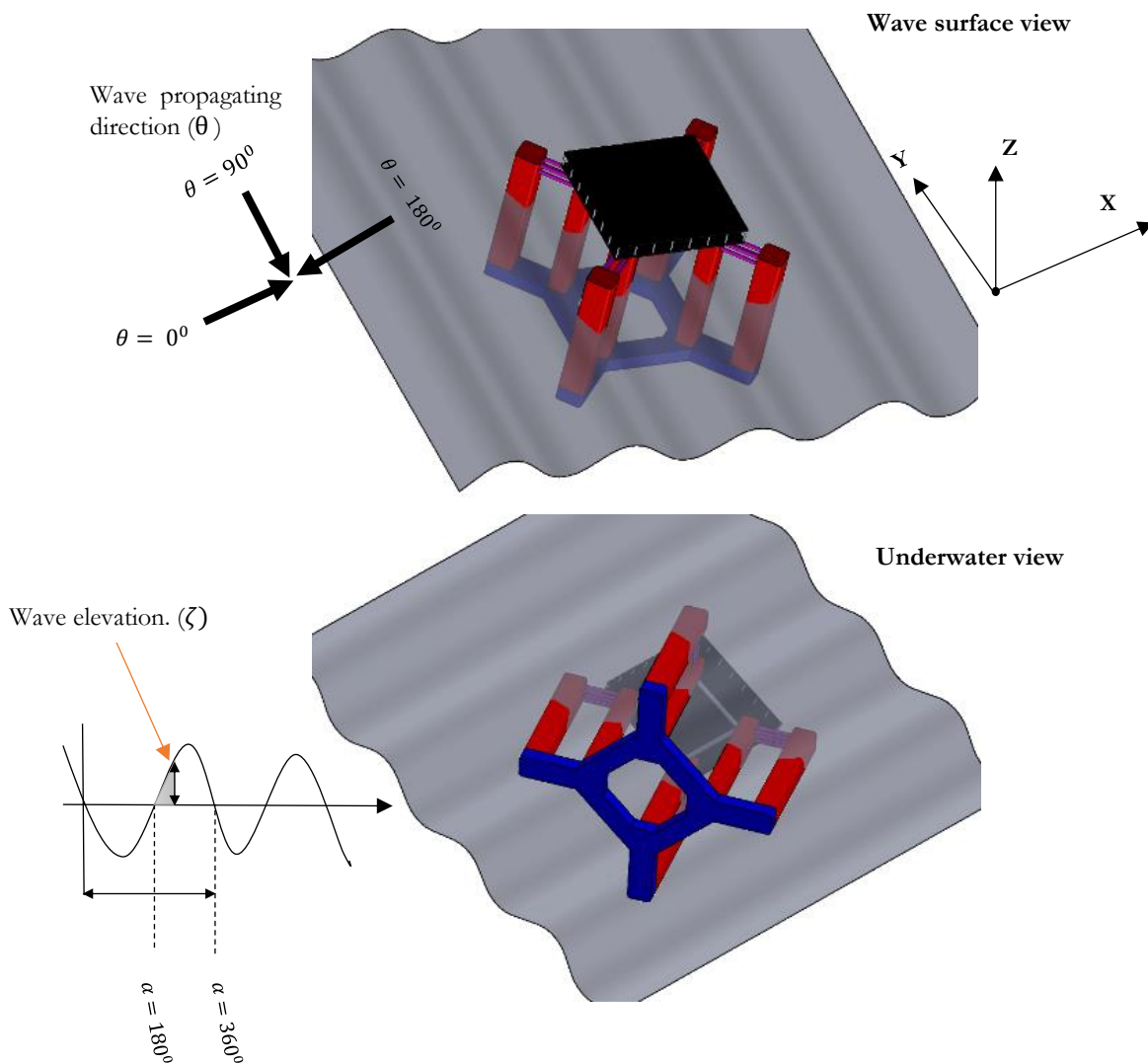


Figure 4.1 Wave definition

Where  $\theta$  is the wave propagating direction,  $\alpha$  is the wave phase and  $\zeta$  is the wave elevation which changes with time along the X and Y axis. Equation [4-1] shows the relationship between the wave elevation and the wave amplitude.

$$\zeta(x; y; t) = A_w \cos(-\omega t + \alpha) \quad [4-1]$$

$A_w$  is the wave amplitude. For regular waves (Airy theory),  $\zeta$  is calculated as

$$\zeta = A_w e^{i[K(x \cos \theta + y \sin \theta) - \omega t + \alpha]} \quad [4-2]$$

#### 4.2.1.2 Boundary Conditions: Boundary Value Problem

With the sea condition as the external boundary condition of the hull, the density of the fluid, its motion and viscosity will need to be analysed for this coordinate systems to be valid. Some assumptions were made in solving these problems, which led to the introduction of fluid potential theory.

- i. The fluid is considered to be irrotational, incompressible and inviscid
- ii. The hull is considered to be impermeable and rigid
- iii. In equilibrium, both planes (the sea surface and the sea bed) are parallel to each other.

The movement of the fluid can therefore be expressed in Laplace formation as;

$$\nabla^2 u = 0 \quad [4-3]$$

Where  $\nabla$  is the Laplace grad operator and u is the flow velocity. Equation 4-3 can be written as

$$\nabla^2 \phi = \frac{\partial^2 \phi}{\partial x^2} + \frac{\partial^2 \phi}{\partial y^2} + \frac{\partial^2 \phi}{\partial z^2} = 0 \quad [4-4]$$

$\phi$  is the velocity potential of the flow.

In resolving Equation [4-4], two conditions were considered; the conditions at the seabed, and the conditions at the free surface. At the seabed, it is assumed that a change in the velocity potential is zero, i.e., not permeable.

$$\frac{\partial \phi}{\partial z} = 0 \quad \text{for } z = \text{seabed} \quad [4-5]$$

Considering the boundary conditions at the free surface, [92] assumed the pressure at the surface equals the atmospheric pressure and the water particles do not leave the surface, satisfying Bernoulli's equation

$$\frac{\partial \phi}{\partial t} + \frac{1}{2}(\nabla \phi * \nabla \phi) + gz = 0 \quad [4-6]$$

### 4.2.1.3 Diffraction and Radiation

The wave experiences two changes as it travels around the hull. It changes its behaviour when it reaches the hull and when it goes out of the hull. In deep waters; where the seabed has no effect on the properties of the travelling wave, the forces on the hull as a result of the flow can be calculated with these changes (diffraction and radiation). The potential of the wave can therefore be calculated by adding whatever alteration occurred as a result of its diffraction, and radiation. The initial potential is referred to as the incidence wave potential ( $\phi_I$ ), while the other two are referred to as the diffraction and radiation wave potentials respectively ( $\phi_D, \phi_R$ ).

$$\phi = \phi_I + \phi_D + \phi_R \quad [4-7]$$

On the hull, the normal component of the diffraction and radiation component are always the same; Equation 4-8

$$\frac{\partial \phi_D}{\partial n} = - \frac{\partial \phi_R}{\partial n} \quad [4-8]$$

Evaluating the radiation potential can be a little bit more complex as compared to the incident and diffraction wave potentials because of the motion of the body, which include added mass and damping parameters. Considering the motion of the body, the radiation potential in each DOF is therefore the product of the unit amplitude of displace in the DOF, and the wave potential in the DOF. That is;

$$\phi_R^{surge} = A_{surge} * \phi_{surge} \quad [4-9]$$

Where  $A_i$  is the unit amplitude; therefore,

$$\phi_R = \sum_{i=1}^6 A_i \phi_i \quad [4-10]$$

On the hull,  $A_i$  exist in a complex form, because of the motion behaviour. It is the change of  $\phi_i$  in the normal direction;

$$\frac{\partial \phi_i}{\partial n} = i\omega n_i \quad [4-11]$$

The total velocity potential defined in Equation

$$\phi = \phi_I + \phi_D + \sum_{i=1}^6 A_i \phi_i \quad [4-12]$$

### 4.2.1.4 Regular Wave Potential (Linear and Stokes 2<sup>nd</sup> order theories)

In solving the equation of Laplace formation of the flow domain, we solved for the velocity potential; as defined in Equation 4-4. From linear wave theory (Airy wave),



$$\phi(\vec{x}; t) = \phi(\vec{x})e^{-i\omega t} \quad [4-13]$$

[93] derived the regular wave potential from linear theory as

$$\phi = -\frac{igA_w \cosh[k(z+h)]}{\omega \cosh(kh)} e^{i(kx \cos \theta + ky \sin \theta - \omega t)} \quad [4-14]$$

For  $\theta = 0$ ,  $\phi$  is

$$\phi = -\frac{igA_w \cosh[k(z+h)]}{\omega \cosh(kh)} e^{i(kx - \omega t)} \quad [4-15]$$

$K$  is the wave number which can be expressed as  $2\pi/L$ , where  $L$  is the wavelength and  $\omega$  is the wave frequency.

Equation 4-15 is only used in scenarios where linear waves are considered. Ocean waves are known for their nonlinear behaviour in which case the correlations for wave potential postulated from Stokes 2<sup>nd</sup> wave was adopted. The wave is considered to progressively change from a steady to an unsteady state. [94-96] recorded the mathematical derivation of wave potential from Stokes 2<sup>nd</sup> order wave theory. The wave potential is presented as;

$$\phi = -\frac{3\omega A_w^2 \cosh 2k(z+h)}{8 \sinh^4 kh} e^{i(kx \cos \theta + ky \sin \theta - \omega t)} \quad [4-16]$$

## 4.2.2 Hydrodynamic Forces

The motion of the hull transfers energy to the water, (which leads to the motion of the water), which in turn varies the pressure around the hull, generating reaction forces. The effect of these forces on the deformation of the hull will be discussed in chapter 6 of this thesis. This chapter will only address the hull motions. The motion response of the hull is as a result of the movement generated on the water surface, which in turn exerts hydrodynamic pressure forces on the wetted surface and reaction/restoring forces. The forces in each of the degree of freedom or mode of deformation can be resolved by integrating the pressure around the submerged or wetted surface [97].

$$F_j = - \int_{s_w} p n_j ds \quad [4-17]$$

Where  $P$  is the fluid pressure,  $s_w$  wetted surface,  $F$  is the hydrodynamic force and  $n$  is the cosine function of the direction

#### 4.2.2.1 First Order Wave Exciting Forces (from linear wave potential)

The motion of the body is relative to  $s_w$  as the hull oscillates the submerged area/surface changes, and also experiences a level of deformation as illustrated in [98]. The force on the wetted surface can therefore be estimated from the summation of the pressure due to the average wetted surface area  $s_{avg}$  and the change created due to the motion  $\delta s_{avg}$ .

$$F_j = -\rho g \iint_{s_w} p n_j ds = -\rho g \left[ \iint_{s_{avg}} p n_j ds + \iint_{\delta s_{avg}} p n_j ds \right] \quad [4-18]$$

Bernoulli's equation is a generally accepted representation of the fluid pressure exerted on a floating body. For a hull system, this pressure can be expressed in terms of the flow total velocity field, and the fluctuating hydrostatic and dynamic pressure. [99] defined the pressure for unsteady

$$P = -\rho \left( \frac{\partial \phi}{\partial t} + \frac{1}{2} |\nabla \phi|^2 - \frac{1}{2} u^2 + gz \right) \quad [4-19]$$

Integrating the pressure;

$$\vec{F}_j^1; \vec{M}_j^1 = -\rho g \iint_{s_w} z n_j ds - i\rho \omega A_{ij} e^{-\omega t} \iint_{s_w} \phi_j n_j ds - i\rho \omega A_w e^{-\omega t} \iint_{s_w} (\phi_I + \phi_D) n_j ds \quad [4-20]$$

For the translational components,  $j=1, 2, 3$ ,  $n = n_1, n_2, n_3$ . For rotational components;  $j = 4, 5, 6$ ,  $n = (r_4 \times n_4), (r_5 \times n_5)$ , and  $(r_6 \times n_6)$ .  $A_{ij}$  is the displaced amplitude of the body, which can be either translational or rotational.

The third component of Equation 4-20 represents the exciting force component. It is a function of the incidence and diffraction wave potentials. The first term of Equation 4-20 represent restoring force, due to hydrostatic pressure  $P_{hyst} = -\rho g z$ , where  $z$  is the draft size of the hull (submerged part). This is generally calculated from the cut-water plane stiffness and the amplitude of displacement  $(-|K|A_{ij})$ . Details of this parameter will be discussed in the chapter 6 of this study. The middle term is the force contribution due to radiation, which is a function of the motion of the body. The summation of all three components is termed first order force.

$$\vec{F}_j^1 = F_j^{hyst} + F_j^d + F_j^w \quad [4-21]$$

#### 4.2.2.2 Second Order Pressure Forces (from nonlinear wave potential)

These forces are further integrated around the submerged part of the hull from the cut-water plane (wetted surface), incorporating the acceleration and momentum parameters into equation. The velocity potential defined in Equation 4-8 can therefore be expressed in steady and unsteady state;

$$\phi = \phi_{st} + \phi_{unst} \quad [4-22]$$

From basic Bernoulli's equation fluid pressure due to unsteady waves can be calculated as

$$P = -\rho \left[ \frac{\partial \phi_{unst}}{\partial t} + \frac{1}{2} v^2 + gh \right] \quad [4-23]$$

Where the velocity is expressed relative to the fluid velocity potential in Laplace form as  $\nabla \phi$ ,

$$P = -\rho \left[ \frac{\partial \phi_{unst}}{\partial t} + \frac{1}{2} \nabla \phi_{unst} * \nabla \phi_{unst} + gh \right] \quad [4-24]$$

If we compute for pressure in respect to its static, velocity and acceleration components, Equation 4-24 can be more complex.

$$P_{total} = P_{st} + P_{vel} + P_{acc} \quad [4-25]$$

$$P_{St} = -\rho gh$$

$$P_{vel} = -\rho [\rho gh^1 + \phi_t^1] \quad [4-26]$$

$$P_{acc} = -\rho \left[ \frac{1}{2} |\nabla \phi_t^1|^2 + h^1 * \nabla \phi_t^1 + (\phi_t^2) + gh^2 \right]$$

From basic integration of pressure over the wetted surface as presented in Equation 4-18, the second order force is derived.

It is important to mention that the second force derivation is carried out with respect of the average wetted surface during the hull oscillation  $S_{avg}$  and the part that is depended on the change experienced during the oscillation  $s_o$ . After integration, the second order force is

$$\vec{F}^2; \vec{M}^2 = -\frac{1}{2} \rho g \oint_L \zeta^2 \vec{n} dl + \frac{1}{2} \rho \iint_{s_o} (\nabla \phi^{(1)2}) \vec{n} ds + \rho \iint_{s_o} (h^1 * \nabla \phi_t^1) \vec{n} ds + \vec{\delta} * \vec{F}^1 + \rho \iint_{s_o} \phi_t^2 \vec{n} ds \quad [4-27]$$

The moment component of the moment equation is a direct representation the force equation with the normal component  $\vec{n}$  replaced by  $(\vec{x} * \vec{n})$ .

### 4.2.2.3 Drift Forces

The technique used for estimating the second order drift forces is based on two groups of regular waves, travelling with different phase angles, amplitudes, directions and frequencies (See [100-102]). The resolution of the forces in the far-field due to the drift between the wave phases result to a set of second order forces.

The drift second order wave forces were generated in respect to the two groups of regular waves generating different amplitudes ( $A_i$  and  $A_j$ ), frequencies, damping and phase angles. Their resulting forces are therefore different.

$$F_{dft} = A_i A_j P_{ij} \cos(\omega_i - \omega_j)t + A_i A_j Q_{ij} \sin(\omega_i - \omega_j)t \quad [4-28]$$

### 4.2.2.3 Motion Equation

Basic equation of motion of a moving body is  $F = ma$ , where 'a' is the acceleration of the body. For a body with 6DOF,

$$F_j = \sum_{j=6}^6 M_j \ddot{A}_j \quad [4-29]$$

With the inclusion of the stiffness and damping parameters;

$$= |M|\ddot{A}_j + |C|\dot{A}_j + |K|A_j \quad [4-30]$$

C and K are the damping and the stiffness of the body, and M is the mass parameter of the body, defined by a 6 X 6 matrix:

$$[M] = \begin{bmatrix} m & 0 & 0 & 0 & mz_g & -my_g \\ 0 & m & 0 & -mz_g & 0 & -mx_g \\ 0 & 0 & m & my_g & -mx_g & 0 \\ 0 & -mz_g & my_g & I_{44} & I_{45} & I_{46} \\ mz_g & 0 & -mx_g & I_{54} & I_{55} & I_{56} \\ -my_g & mx_g & 0 & I_{64} & I_{65} & I_{66} \end{bmatrix} \quad [4-31]$$

The mass of the body is generally calculated from the density of the volume of the displaced or submerged part. Steel material was used in the analysis; with a density of 7850kg/m<sup>3</sup>. Mathematically, m is

$$\iiint_v \rho_b dV \quad [4-32]$$

Where  $\rho_b$  is the density of the hull

### 4.2.3 Response Formulation

The response of the hull is formulated from the unit amplitude parameter  $A_i$  and the wave elevation  $\zeta$  described in section 4.2.2 above.

The response of the hull can be calculated using a time-response analysis for equation of motion. Equation 4-30 can further be

$$[M + M_a]\ddot{A}_i(t) + C\dot{A}_i(t) + KA_i = F(t) \quad [4-33]$$

For regular wave study, the amplitude and degrees of response were computed directly from Equation 4-33. The value of  $A_i$  is computed using basic linear wave theories.

If we are to investigate the response of the hull for irregular wave scenarios, we have to develop a relationship between the frequencies of the different groups. This is conventionally done by comparing the frequencies of the different groups; representing them in a spectrum. Equation 4-33 further becomes

$$[-\omega^2 M - i\omega C + K]A_i = F_i \quad [4-34]$$

$K$  is the hydrostatic stiffness. We can rewrite Equation 4-34 as;

$$\{-\omega^2[M + M_a(\omega)] + i\omega C + K\}A_i = F(\omega) \quad [4-35]$$

$$\frac{F_i(\omega)}{\{-\omega^2[M + M_a(\omega)] - i\omega C + K\}} = A_i \quad [4-36]$$

$$A_i = F_i(\omega)\{-\omega^2[M + M_a(\omega)] - i\omega C + K\}^{-1} \quad [4-37]$$

The response amplitude  $A_i$  exists in a complex form; and it's a function of the wave amplitude.

#### 4.2.4 Hydrodynamic Approximations

Second order motions in irregular waves were computed based on the wave drift force  $F_d$ .

$$F_d = \sum_{i=1}^n \sum_{j=1}^n A_i A_j P_{ij} \cos(\omega_i - \omega_j)t + A_i A_j Q_{ij} \sin(\omega_i - \omega_j)t \quad [4-38]$$

Where  $P_{ij}$  and  $Q_{ij}$  are the resultant forces computed in phase with the wave groups and out of phase with the wave groups respectively. The complexities associated with irregular wave formulation makes it difficult to compute for these forces. [101] assumed negligible forces for long crested waves, making the wave group a function of the drift forces. This assumption also eliminated the contribution of high wave frequencies, assuming sole contribution from *low frequency motions*. I.e.,  $\omega_n \approx \omega_i$ , and  $\omega_i \approx \omega$ .

$$F_{dft} = \sum_{i=1}^n \sum_{j=1}^n A_i A_j P_{ij} \cos(\omega_i - \omega_j)t \quad [4-39]$$

The application of this approximation is mostly valid for cases where the structure is operating in deep waters because for the shallow waters, the relative amplitudes ( $A_i$  and  $A_j$ ) of the superposed waves are distinctively different from each other.

### 4.3 Model Description

PC-Semi has a simple hull system, with a complex column arrangement; as discussed in the chapter two of this thesis. Because of this, it will be difficult to describe / characterize the entire hydrodynamic behaviour of this hull with a single model (a single approach), because of the multiple behaviours of the flow within and outside the hull. Flow behaviours such as shear, separation, wave elevation, backward flow, vortex formation, solid interactions, all take place within and outside this hull. The boundary element method employed in this study can effectively predict the effect of the wave parameters on the response of this hull. The model used for this study was therefore developed in-line with this.

#### 4.3.1 Definition of Case Study

The cases were defined relative to the hull draft size and the sea current velocity, as shown in Table 4.1. The requirements for motion characterization for semisubmersibles are different depending on their functionality. The motion requirement of a conventional deep draft semisubmersible for a floating production system with subsea well-heads is different from that with top-deck well-heads integration. A semisubmersible MODU system has its own unique standard for motion response, same goes to a semisubmersible suspending an offshore wind turbine. The cases studied in this thesis have been based on the application of these hull concept requirements in deep waters for drilling unit, production system and support systems (wind turbine foundation). Figure 4.2 shows the geometry adopted for this study, and it was extracted from [4]. Figure 4.3 shows the definition of flow angle used in this study

**Table 4.1 Case study**

Case	Draft Size	Exposed column $H_c^e$	Submerged Column $H_c^s$	Position
1	44.65m	36.73m	36.73m	Mid surface
2	49.0m	32.38m	41.08m	Intermediate
3	53.34m	28.02m	45.42m	Base case (deep-draft)

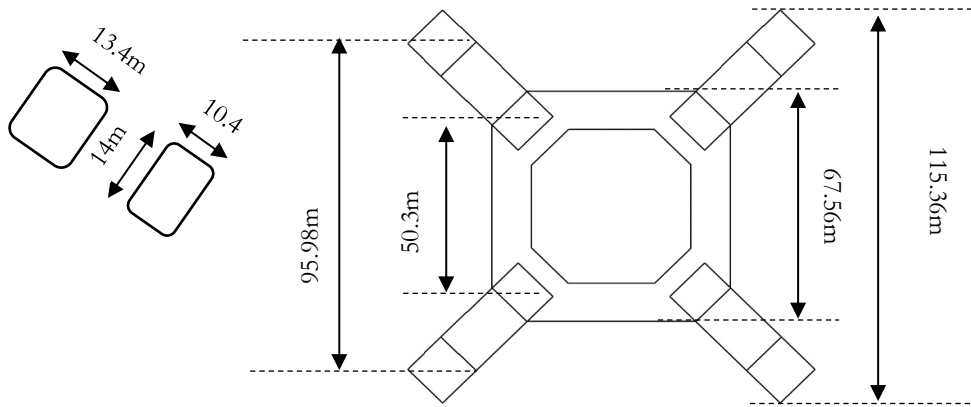


Figure 4.2 Hull Dimensions

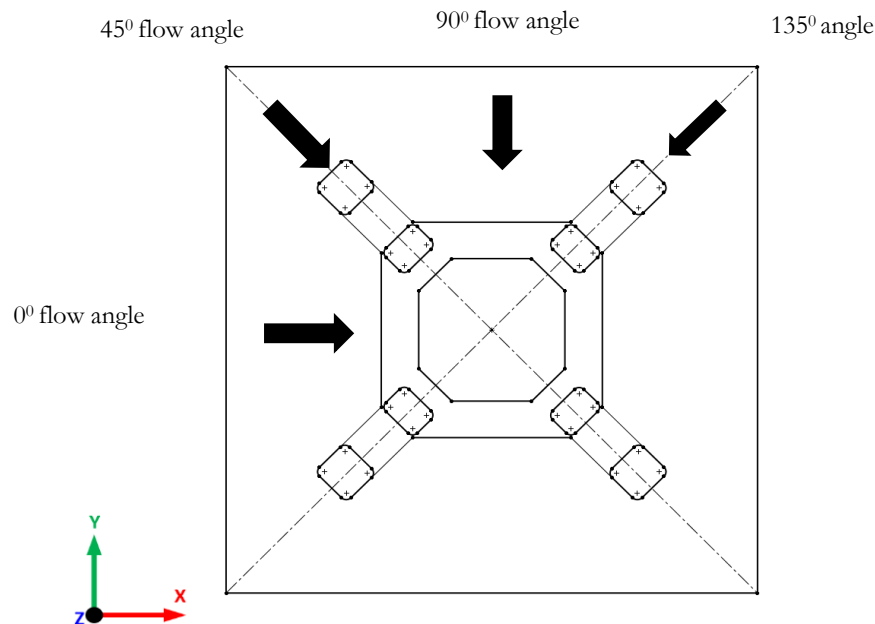


Figure 4.3 Definition of flow angles

### 4.3.2 Hydrodynamic Model

The model was developed in ANSYS AWQA and validated with results obtained from series of experimental studies presented in chapter 3. The full-scale model dimension was extracted from (RPESA, 2009) with little alteration for the column height and edges, to help increase result accuracy. ANSYS AWQA utilized diffraction/radiation methods in resolving the three-dimensional problem associated with floating bodies. This is a generally acceptable method in ocean engineering, as it eliminates the complexity associated with the water viscosity, flow separation, and circulation. There is an extensive report documentation in the use of this method for resolving the behaviour of large floating bodies some of which include [61], [103], [104], [105],

and [106]. Apart from this method, offshore engineers sometimes employ experimental and analytical methods. These methods are restricted.



Figure 4.4 Mesh size 1.15m

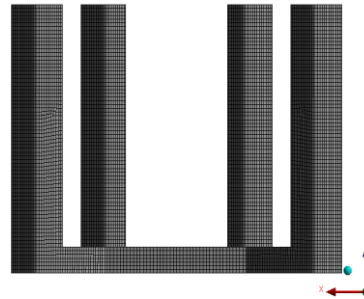


Figure 4.5 Front view

The hull was designed to operate in water depth up to about 3000m. For realistic estimations, we have adopted a water depth of 2400m in this study. The X and Y direction of the sea were represented by 7000m wide to replicate a fully developed flow as shown to in Figure 4.6.

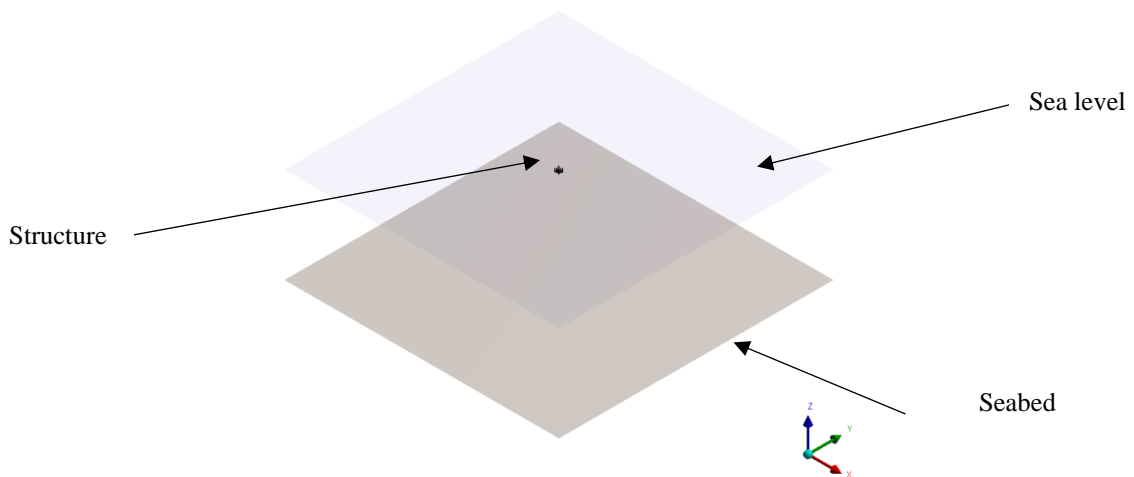


Figure 4.6 Model ocean view

### 4.3.3 Hydrostatics

The hydrostatics of the hull described the effect of fluid on the structure in its static position, which is relative to the area of the submerged part. The hull hydrostatics forces are therefore computed in relation to the fluid pressure and the area of the submerged part. Table 4.2 shows the effect of hull's geometric properties and its hydrostatic parameters (buoyancy force), assuming the density of sea water; 1025kg/m<sup>3</sup>.

Table 4.2 Buoyancy force

	Case 1	Case 2	Case 3



<b>Area (m<sup>2</sup>)</b>	28485.29	30168.44	31847.72
<b>Volume (m<sup>3</sup>)</b>	83656.63	89334.82	94999.96
<b>Displaced mass (Kg)</b>	84640 x 10 <sup>3</sup>	90500 x 10 <sup>3</sup>	96500 x 10 <sup>3</sup>
<b>Buoyancy force (N)</b>	8.3233 x 10 <sup>8</sup>	8.8879 x 10 <sup>8</sup>	9.4511 x 10 <sup>8</sup>

#### 4.3.3.1 Centre of Gravity and Centre of Buoyancy (COG and COB)

The relationship between these two points in the hull describes how stable this hull will be under static and combine loadings. As sited in chapter 2, the idea of deep-draft semisubmersible is to keep the centre of gravity below the centre of buoyancy to guarantee stability at both operating and extreme conditions. For the fact that the surface area of the submerged part is a direct function of its hydrostatics, the gravity and buoyancy centres are therefore affected by this parameter. The study of hull heeling and trimming is based on these points. These parameters (COG and COB) were studied for all four cases assuming free-floating conditions, and case 4 was observed to be the only that has its COG below its COB without the incorporation of the topside or any other structural attachments. The relative masses incorporated on this hull were analysed and estimated to determine an acceptable COG of each of the cases. Since buoyancy is directly related to volume, the buoyancy centre is therefore the centre of area of the draft. On the other hand, the centre of gravity is the centre of mass of the hull. This is determined by different components;

- i. Mass of the hull plate
- ii. Mass of reinforcement within the hull
- iii. Position of ballast liquid
- iv. Arrangement of the topside facilities

Different components of the hull were designed and their masses were estimated considering what is obtainable in the industry (as will be discussed in chapter 6 of this thesis), and the COG of the entire hull was reported for the different cases as shown in Table 4.3. The weight of risers carrying liquids was considered for production platforms, which is applicable for cases 1, 2 and 3, for the COG adopted for this study. Drilling rigs do not necessarily have this advantage, as it is more complex to increase the level of the COG of a drilling rig. Therefore case 1 might not really be applicable for a drilling rig.

The application of the design system presented in Table 4.3 in the optimization of this hull system will be discussed in the later stage of this thesis. The effect of the parameters presented in Table 4.2 and Table 4.3 is presented in Table 4.4. The area of the submerged part of the hull (for a specific draft size) amounts to a given displaced volume. The product of the volume and the

density of water amounts to the mass of the hull displaced; as presented in Table 4.2. This mass alongside the added mass parameters (which is relative to the area) is used to derive the natural frequencies (periods) using Equation 2-3 and Equation 2-4.  $K$  in the equations represents the hydrostatic stiffness of a floating body in the vertical plane (heave, roll and pitch), as described in Table 2.3. Details of the derivation of this stiffness are discussed in chapter 6. The natural oscillating periods for the three cases are presented in Table 4.4.

**Table 4.3 Centre of gravity and buoyancy**

	Cases		
	One	Two	Three
<b>Submerged volume</b>	83656.63m <sup>3</sup>	89334.82 m <sup>3</sup>	94999.96 m <sup>3</sup>
<b>Centre of gravity</b>	≤ -27m	≤ -31.3m	≤ -35m
<b>Centre of buoyancy</b>	-27.96m	-30.34m	-32.52m
<b>Comment</b>	Applicable for FPS as the risers carries heavy liquid	Applicable for MODU and FPS study	Applicable for MODU and FPS study

**Table 4.4 Hull natural frequencies and periods**

	Case 1		Case 2		Case 3	
	$\omega_n$ (Hz)	$T_n$ (s)	$\omega_n$ (Hz)	$T_n$ (s)	$\omega_n$ (Hz)	$T_n$ (s)
<b>Heave</b>	0.0472	21.20	0.0463	21.60	0.0454	22.01
<b>Roll</b>	0.0388	25.79	0.0383	26.11	0.0372	26.89
<b>Pitch</b>	0.0388	25.79	0.0383	26.11	0.0372	26.89

### 4.3.3.2 Hydrostatic Equilibrium

During fluid motion, the frequency and time-dependent parameters are calculated with reference to positions where the summation of all the applied and reactions forces sums to zero. This is defined as the ‘hydrostatic equilibrium position’ of the hull. The stability of the hull can be estimated with these parameters [107]. The criteria for equilibrium is that the summation of all the weight in and around the hull equals the buoyancy force  $F_b$  generated from the submerged volume; the resultant of the forces at the cut-water plane equals zero, as shown in Equation 4-40.

$$\vec{F}_{hyst} - g \sum M_{total} = 0 \quad [4-40]$$

Where  $M_{total}$  is the summation of the all the masses on the hull and  $F_{hyst}$  is the hydrostatic which include the buoyancy parameter. It is important to mention that for this study, the hydrostatic equilibrium was measured from the cut-water plane.

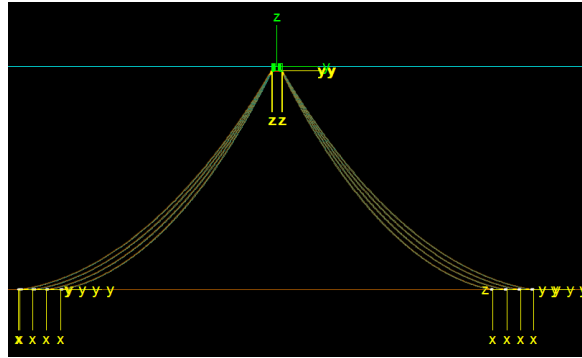
The stability of the hull was tested in all three cases and stable conditions were recorded in survival, extreme and hurricane weather conditions.

**Table 4.5 Parameters for small angle stability**

	Cases		
	One	Two	Three
<b>C.O.G to C.O.B</b>	1m	1m	2.26m
<b>Metacentric height</b>	23.89m	24.17	24.09m
<b>C.O.B to metacentre</b>	24.79m	23.21m	21.83m
<b>Restoring moment</b>	$3.47 \times 10^8 \text{ N.m/}^0$	$3.75 \times 10^8 \text{ N.m/}^0$	$3.97 \times 10^8 \text{ N.m/}^0$

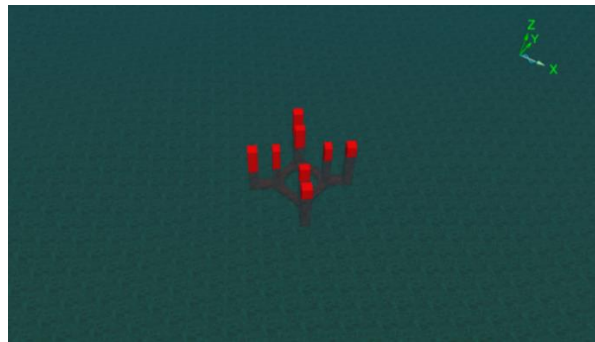
### 4.3.4 Response Model

The models for calculating the hull offset were developed in [139] and Orcaflex. Mathematical formations used by the solvers are described in section 4.2.3. The offset of the hull was studied with a time series analysis computed from the solution of the hydrodynamic diffraction analysis (free floating hull). Risers and mooring integration were developed for validation purpose (Figure 4.7 and Figure 4.9).



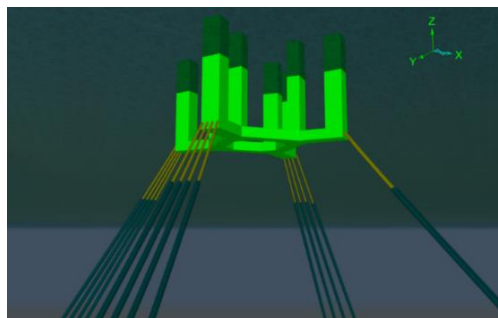
**Figure 4.7 Complete View (Orcaflex model)**

Image of the Orcaflex model for time-response analysis is shown Figure 4.7 developed for a sea depth of 2400m, and 16 mooring lines of steel-polyester-steel configuration. In the diagram, the orange line represents the seabed while the blue line is the sea surface developed for the x and y coordinate. The coordinate system for the mooring points on the seabed is different; this will be discussed during the analysis of the mooring dynamics.



**Figure 4.8 Orcaflex model for free response study**

For our case study, the equation was developed with respect to the external forces created by wave, current, and wind, which varies with the position of the structure, its velocity, and acceleration. For free-floating state condition as shown in Figure 4.8, only the hydrodynamic damping was considered for 'C' during computation. External damping offered by the moorings and risers are considered for subsequent analysis.



**Figure 4.9 Orcaflex model for response study; with mooring. (Underwater view)**

## 4.4 Environmental Conditions

This study was carried out using recommended standards for environmental loading conditions on offshore structures, and with a close study of weather buoys, some of which include [47, 50, 55]. Different regions of the same ocean (Atlantic) recorded different weather conditions. For the Gulf of Mexico, API standard [50] presented conditions for west (between  $97.5^{\circ}$  and  $95^{\circ}$ ), west-central (between  $94^{\circ}$  and  $90.5^{\circ}$ ), central (between  $89.5^{\circ}$  and  $86.5^{\circ}$ ) and east (between  $85.5^{\circ}$  and  $82.5^{\circ}$ ). The variation between values recorded played a significant role in our selection process for estimating values for our weather conditions. Conventional designs are studied for different load conditions depending on what standard are adopted. The conditions include survival, extreme, severe, damage, tow, accident, and operating. Our decision is based on the conclusion made from literature reviews and company reports that maximum values for *structural response* are recorded for these two cases. Table 4.6 shows the design values adopted for this study; after careful consideration of the four regions presented in [50] and other available standards. Values for survival conditions are the wave data for 1000-years return period while the extreme conditions are wave data for 100-years return period.

**Table 4.6 Parameters for survival and extreme conditions**

Parameters	Survival condition	Extreme condition
Significant wave height (m)	16.4	13.1
Maximum wave height (m)	30.1	24.2
Peak spectral period (s)	16.7	15.1
Period of maximum wave (s)	15.1	13.6

NB:  $\gamma = 2.2$

### 4.4.1 Regular Wave

Results for the global analysis presented in this thesis are for irregular wave conditions because floating bodies' response more in irregular waves, but the model validation, experimental setup and current effect of hull response were all studied for regular wave conditions. For the effect of ocean current, the regular wave conditions were calibrated using a forward current speed range from 0.5m/s to 2.5m/s for wave heights less than 34.9meters. The calibrations were done based on 1000 years, and the periods were estimated from weather buoys statistics.

### 4.4.2 Irregular Waves

As this hull application was for open deep waters, the idealization of a complete developed wave spectrum was adopted, for this reason; JONSWAP spectrum was used to study the behaviour of the hull in irregular waves.

$$S(\omega) = \frac{\alpha g^2 \gamma^a}{\omega^5} \exp\left(-\frac{5 \omega_p^4}{4 \omega^4}\right) \quad [4-41]$$

The spectrum plot was studied for four different case as shown in Figure 4.7;  $H_s = 16.8\text{m}$ ,  $16.4\text{m}$ ,  $13.1\text{m}$  and  $12.6\text{m}$ ; and  $T_p = 15.6, 16.7\text{s}, 15.1\text{s}$  and  $14.0\text{s}$ .

**Table 4.7 Cases for irregular waves**

Study	$H_s$ (m)	$T_z$ (s)
A	16.8	15.6
B	16.4	16.7
C	13.1	15.1
D	12.6	14.0

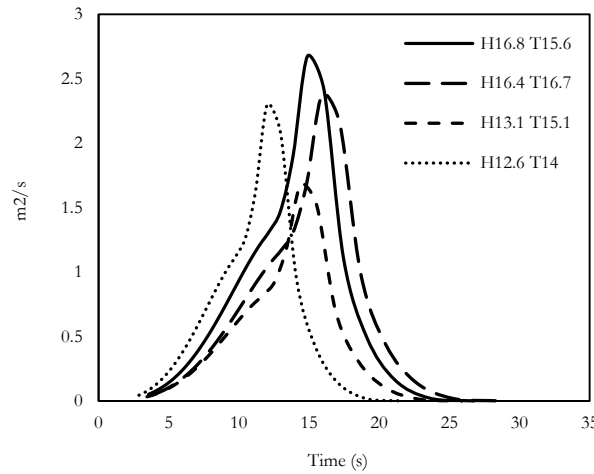


**Figure 4.10 Spectrum study**

Table 4.7 and Figure 4.10 show the different spectral studies that were considered in the analysis. Studies ‘A’ and ‘D’ are the case studies for 1000-years and 100-years wave return period adopted in [5] for survival and extreme conditions respectively. These spectrum studies were used to compare results from our model and [5]. Study B and study C are the cases for 1000-years and 100-years wave return periods adopted for this (as presented in Table 4.7). It is the average range of all four weather conditions presented in [50]

### 4.4.3 Current Calibration

The effect of sea current on the hull has been discussed in the previous chapter; its velocity affects the reciprocating frequencies of the shed vortices as the flow travels through the hull. These velocities also affect the response of the structure, and they’ve been calibrated to recommended standards. Current varies with the sea depth, and eventually amount to zero at the seabed. Its vertical profile for irregular wave scenario is calculated based on this premise. Table 4.8 show the current data adopted in this study.

**Table 4.8 Current parameters**

Extreme condition		Survival condition	
Velocity (m/s)	Depth (m)	Velocity(m/s)	Depth (m)
2.4	0	3	0
1.8	50.4	2.25	63
0	100.8	0	126
0	2400	0	2400

It is important to calibrate the current velocities because the interaction between the wave and current on the sea-surface is a fundamental criterion to which the diffraction properties depend on. The current effect on the RAO plots is presented in the discussion section of this chapter.

#### 4.4.4 Wind Load

The speed of sea wind is a highly changing parameter and therefore the standards are measured in minutes and hours; as presented in Table 4.9. Calibrating wind parameters (speed, direction, and height) is done by coagulating results from satellite data and developing models to predict wind performance. The wind speed used in this study were extracted from API standards.

**Table 4.9 Mean wind speed (m/s)**

Time	Extreme	Survival
1min	62.8	81.6
10min	54.5	69.5
1hr	48	60

## 4.5 Validation

The numerical model used in this study was developed in-line with the experimental results presented in chapter 3 of this thesis. RPSEA experimental setup was modelled in ANSYS AQWA for the same conditions and the result were compared with findings obtained. Models were also developed with the results obtained from experimental response analysis carried out in this in this study. A mesh study was also done during this process.

### 4.5.1 Mesh Study

Despite the validation of our numerical model from experimental results discussed in chapter 3, a mesh/grid independence study was carried out to understand the relationship between the mesh size and results obtained. For the effectiveness of mesh density and tolerance, the element

size was varied between 2 and 1.15 and the effects on the maximum values obtained on the response amplitude operator (RAO) curve at  $0^\circ$  incidences for Z direction were recorded. No mesh refinement was done; uniform mesh distribution around all faces as shown in Figures 4.3 and 4.4. The results in Table 4.10 showed no significant variation in the RAO value for heave motion at  $0^\circ$  flow angle for the same range of wave frequencies. This indicates that the degree of mesh refinement does not have a significant effect on results from hydrodynamic diffraction study.

**Table 4.10 Heave RAO Study**

Element size (m)	No. of elements	No. of nodes	Max. RAO (m/m)
2.0	8948	9058	1.747
1.8	11252	11374	1.738
1.6	13925	14061	1.740
1.4	18061	18215	1.736
1.2	24055	24237	1.731
1.15	25861	26045	1.711

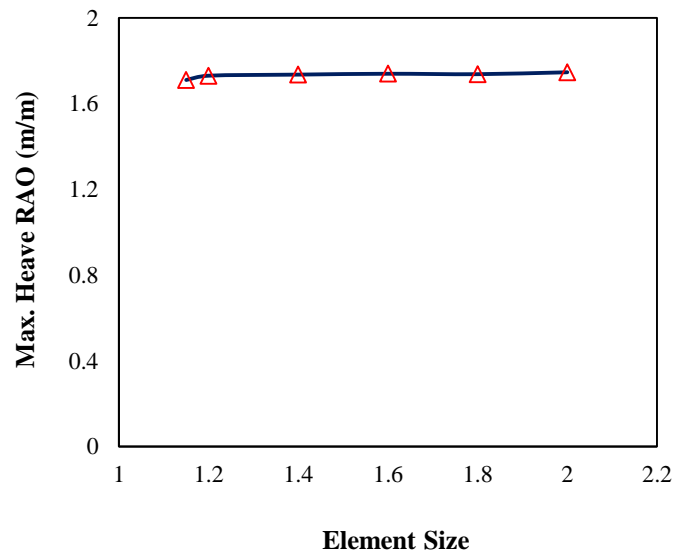


**Figure 4.11 Hydrodynamic Mesh Study**

Figure 4.11 shows the graphical representation of the element and maximum heave RAO represented in Table 4.10.

#### **4.5.2 Validation with Experimental Study by RPSEA**

The accuracy of this model in prediction the motion characteristic of this unique hull was also checked with the result presented in [4], as shown in Table 4.11. The maximum rotation was recorded as  $7.75^\circ$  at a flow incidence angle of  $135^\circ$ , for survival weather conditions. The maximum downward vertical motion was reported as 5.69m for  $0^\circ$  or  $180^\circ$  flow angle. The response model



described in section 4.3.4 was used to predict these parameters, for the same weather conditions, and structural attachments, as shown in Figure 4.9.

The results from our model showed agreement with that of the experimental data.

**Table 4.11 Validation with [4]**

Studies	Conditions	Max. downward	Max. Rotation
[4]	Wave parameters : $H_s = 19.8\text{m}$ , $T_p = 17.2\text{s}$ , With mooring integration.	5.69m	7.75deg
Current study	✓	4.601m	7.23deg

### 4.5.3 Validation with Model Test

The study for the global performance carried out at the Lancaster University wave tank was performed for three draft sizes, assuming free-floating conditions, while [4] documented the effect of mooring lines. A hydrodynamic model was setup in ANSYS AQWA for the same conditions obtained at the Lancaster University wave tank (as described in chapter 3, section 3.4), to compare results from both analysis. A frequency range of 1.1Hz and 0.2Hz was adopted for maximum and minimum values respectively, and motion tests were carried out for 0.05Hz intervals. The wave frequency range in the AQWA solver was set with this parameter. The effect of reflected waves from the edges of the wave tank was studied using a set of wave gauges and significant contributions were observed. The experimental setup was therefore used strictly for model validation. Table 4.11 show the results of the time response analysis of both cases. For wave frequencies, 0.8Hz, 0.9Hz, and 1Hz, the results obtained for both cases were almost the same.

**Table 4.12 Comparing experimental and numerical results**

Wave Parameters		Maximum Displacement			
		Heave (m)		Surge (m)	
$f_w$ (Hz)	T (s)	Experimental	Numerical	Experimental	Numerical
0.5	2	0.0484	0.03958	0.01609	0.01617
0.6	1.67	0.0281	0.01956	0.0140	0.01402
0.7	1.43	0.00018	0.00059	0.01136	0.001181
0.8	1.25	0.0025	0.0025	0.00943	0.00947
0.9	1.11	0.0027	0.00273	0.0071	0.007095
1.0	1	0.00215	0.00225	0.00483	0.00480

### 4.5.4 Comparing numerical models

[5] recorded 4.572m for maximum heave offset (downward displacement), 5.30deg for maximum roll rotation, and 5.06deg for maximum pitch rotation for a 16.8m significant wave

height and 15.6s period, as shown in Table 4.13. Similar results were obtained from the model developed in this study, considering same weather conditions.

**Table 4.13 Comparing model with [5]**

Studies	Weather conditions	Max. heave	Max. roll	Max. pitch
[5]	$H_s = 16.8\text{m}$ , $T_p = 15.6\text{s}$ , $V_c = 2.3\text{m/s}$	4.572m	5.30deg	5.06deg
Current study	✓	4.601m	5.31deg	5.06deg

The maximum surface current velocity is denoted as ' $V_c$ '.

## 4.6 Results and Discussion

### 4.6.1 Response Amplitude Operator (RAO)

The RAO of the hull was investigated for  $0^\circ$  wave orientation and a dominant response was observed for the heave, surge and pitch degree of freedoms. The sea depth was kept constant at about 2400m with weather conditions as presented in Tables 4.6, 4.7, 4.8, and 4.9. The study was done for regular and irregular waves, extreme and survival conditions, free response; and results were recorded for hurricane conditions, as they depict the worst case scenarios.

Figure 4.12, Figure 4.13, and Figure 4.14 shows the RAO for the heave, surge and pitch motions respectively, for free-floating condition. The results were recorded for irregular wave, for a wave frequency range of 0.033Hz to 0.417Hz. [4] reported the surge, heave and pitch RAOs for the first designed PC-Semi. The results were presented in relation to the wave spectral curve for 100-years wave return period. The RAO curves were checked for 53.34m draft size; with and without riser integration. The natural periods were plotted against the spectral density and the RAO(s). The results showed significant riser effect (reduced with riser) on the heave RAO at resonance period, and no much effect was recorded for the surge and pitch RAOs. In this study, we have studied the effect of the draft size on a free-floating PC-Semi by plotting RAO(s) against the wave frequencies, with no riser integration; since maximum heave RAO from [4] was recorded without riser system.

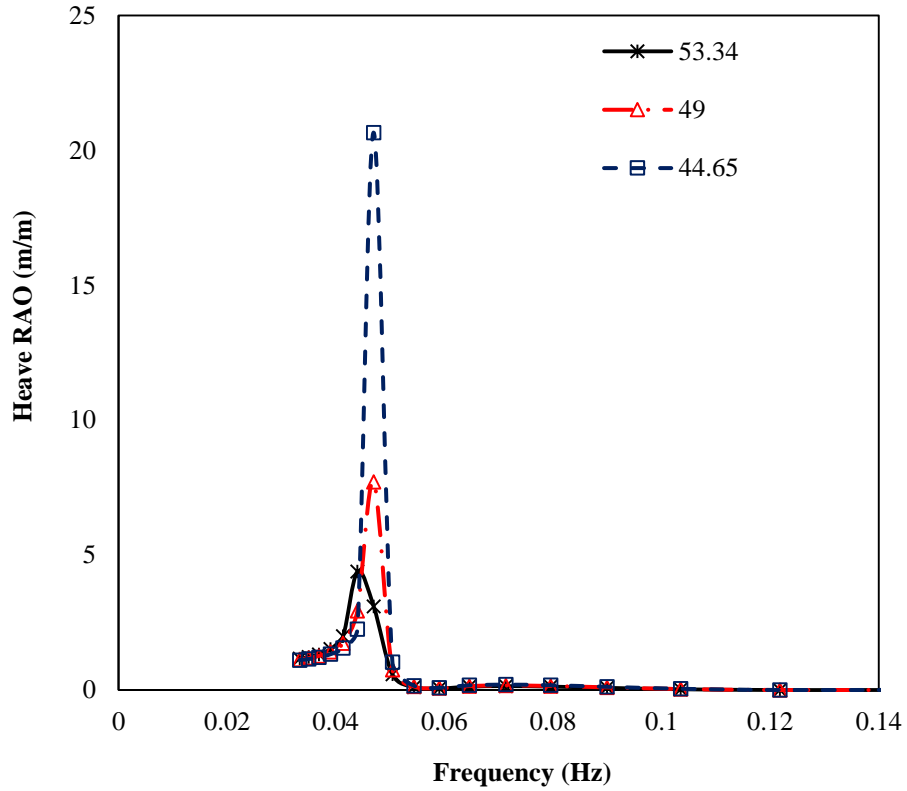


Figure 4.12 Heave RAO for free floating hull

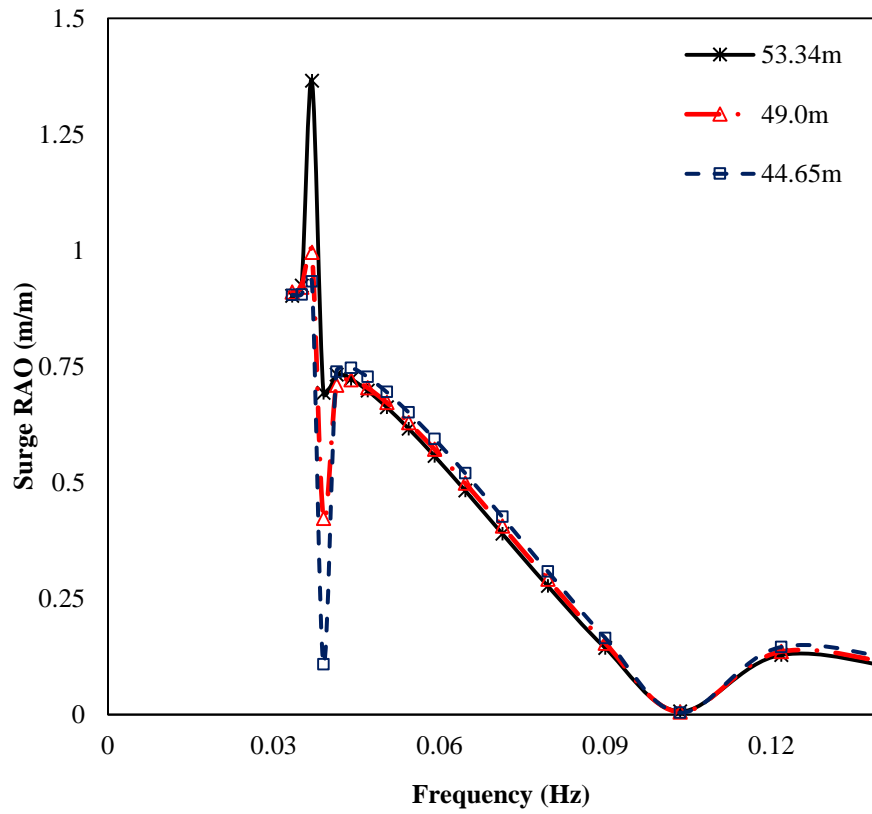
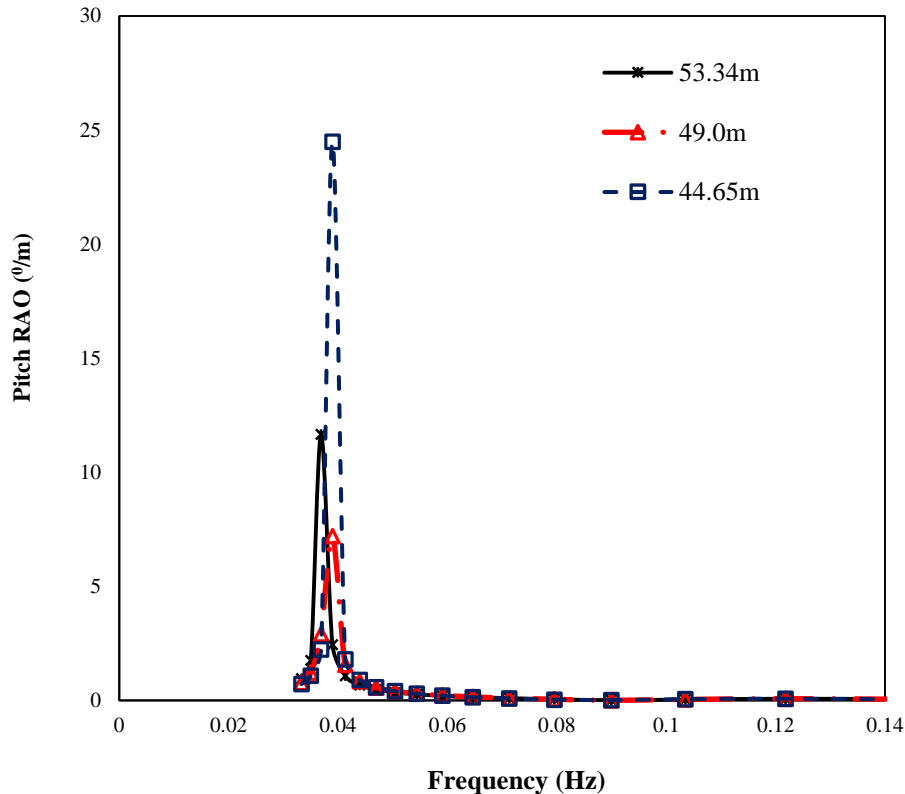


Figure 4.13 Pitch RAO for free floating hull



**Figure 4.14 Surge RAO for free floating hull**

The results from the heave motions showed that the draft size is inversely proportional to the RAO behaviour of the hull (see Figure 4.12). This behaviour was observed for all weather conditions and column geometries. The reason for this can be explained by understanding the effect of added mass on the response of a submerged body. As the submerged part (draft) increases, the weight (acts vertically downwards) helps to reduce the movement in the Z plane, in addition to the central pontoon plate-like system. [108] came up with similar findings on an investigation of heave response and excitation forces of a semisubmersible hull system. For all three draft cases, no significant motion was observed on the hull for high-frequency waves (low periods), as shown in Figure 4.12. Maximum motions were observed at the heave natural periods (between 21.2s and 22s). The hull motions for very low wave frequencies (below resonance frequencies), were observed to be independent of the draft size. The wave frequency was observed to have less effect on the maximum RAO for surge motions, when compared with the heave motions as the experimental results earlier suggested. Figure 4.13 showed that lesser RAO values, when compared with Figure 4.12, despite the fact that the hull has no hydrostatic stiffness on this plane; free to move (zero natural frequency), in its free floating state. The variation observed at resonance frequency range for surge RAO showed an increase in surge motions for deep-draft condition (case 3), for the low-frequency response, although this behaviour changes for wave

frequencies outside resonance range. There is uniformity in the plots outside this range, suggesting that the draft size might have little or no significant effect on the surge response. Surge motions tend to damp away at a higher frequency when compared with heave motions. This unique surge motion response will be a deterministic factor in estimating the draft size during the recommendation of this hull system for drilling unit and support systems in ocean engineering.

Apart from the surge and heave RAOs, a significant response was also recorded for pitch motions. The variation experienced on the pitch RAO plot is unique. 49m hull draft had the lowest response at the resonance frequency, which indicates a nonlinear curve for draft effect on pitch motion. A further investigation into this behaviour will give a better understanding.

## **4.6.2 Wave Forces**

### **4.6.2.1 First order forces**

The first order wave forces were computed for three draft sizes for the same sea conditions used in computing for the RAOs recorded in section 4.6.1. The surge, heave and pitch forces were observed to have different relationships with the wave frequencies. Figure 4.15 shows that at low wave frequency, the first order surge force increases with the draft size. But as the wave frequency increases, the effect of the draft size gradually becomes negligible, reducing the overall value of the surge force.

The heave studies presented in Figure 4.16 do not show this behaviour. The variation for heave force recorded took place within the range of wave frequencies; 0.07Hz to 0.225Hz, and the wave frequency is inversely proportional to the draft size within, unlike for surge forces. As a result of this increase in heave force observed for shallow draft, a corresponding motion increase can be suggested. A confirmation of this phenomenon will be discussed during its motion test, which might result to design alteration of this hull for shallow and moderate draft application. Figure 4.17 presents the relationship between the first order pitch moment and the hull draft size. As suggested by the pitch RAO presented in Figure 4.14, the relationship between the draft size and its pitch behaviour is non-linear. As expected, the pitch moment was observed to be of high values, with the least values recorded for shallow draft.

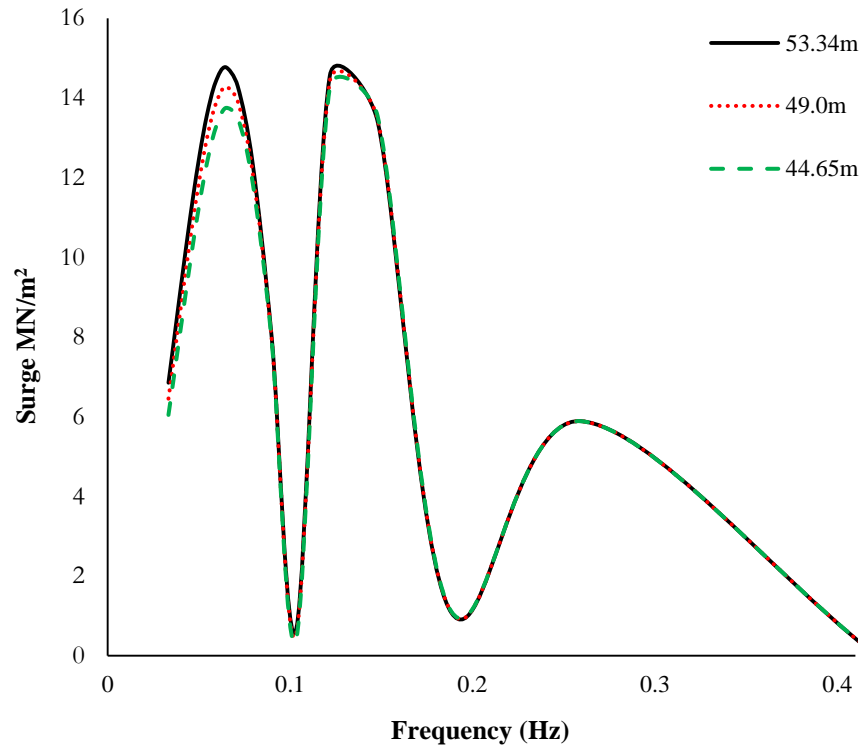


Figure 4.15 First order surge force

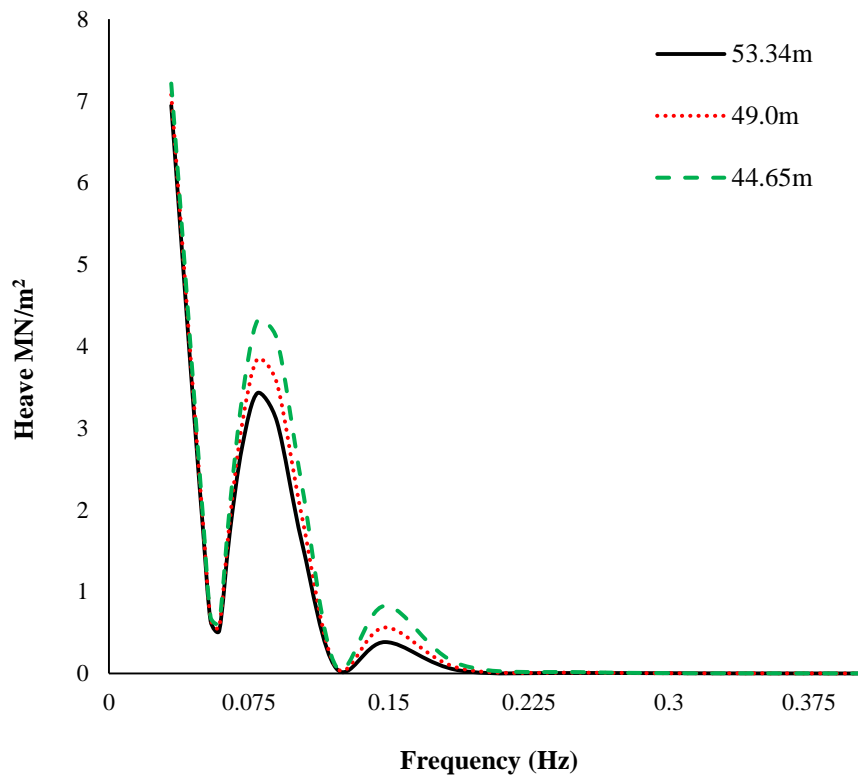


Figure 4.16 First-order heave forces

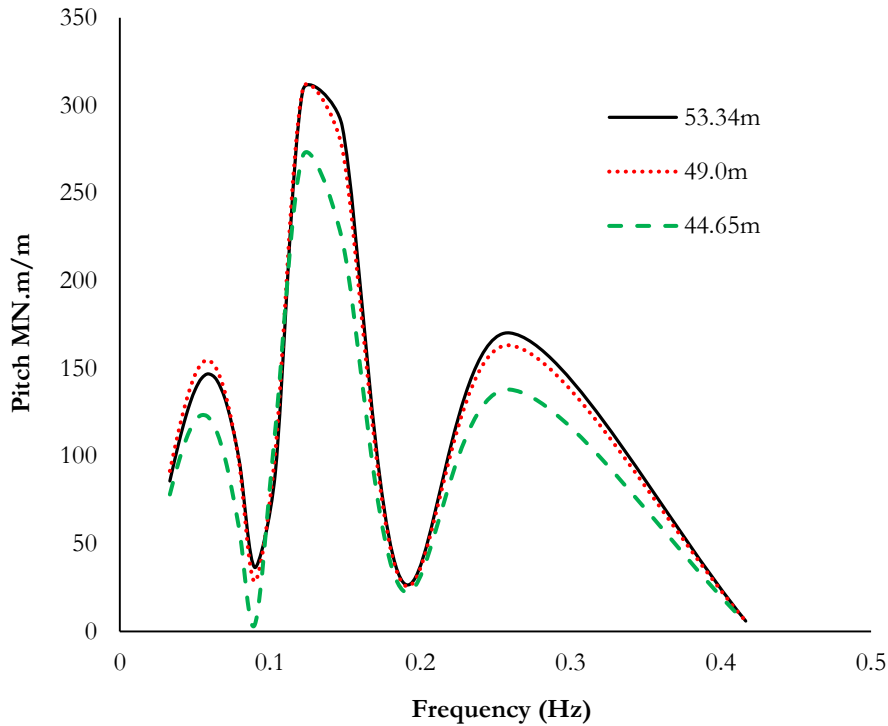


Figure 4.17 First order pitch moment

#### 4.6.2.2 Second Order Drift Forces

The drift forces were studied using the near-field method, and the results have been presented from Figure 4.18 to Figure 4.23. Drift forces were observed to be least for sway DOF, with little or no force for high wave frequencies (Figure 4.20). Forces from resonating motions for three draft sizes were observed to occur for frequencies less than 0.05Hz. For 53.34m draft condition, the drift force for sway motion is very small, almost negligible. The results recorded for the surge and sway drift forces are mostly negative values; especially for the surge force. [109] obtained similar findings in his investigation of drift forces in a double layer of fluid with finite depth. He discovered negative drift forces for free floating bodies, which was as a result of the long surface waves created from the interface between the two set of waves. He concluded that if the wave interface is deeper than the bottom of the structure of the body, the drift force will be negative. This is exactly the situation that was observed of the cases studied in this thesis. More negative values were recorded at low frequencies/high periods (long crested waves) for 44.65m draft size for all DOF, as the reduction in the draft size implies higher effect of the wave interface.

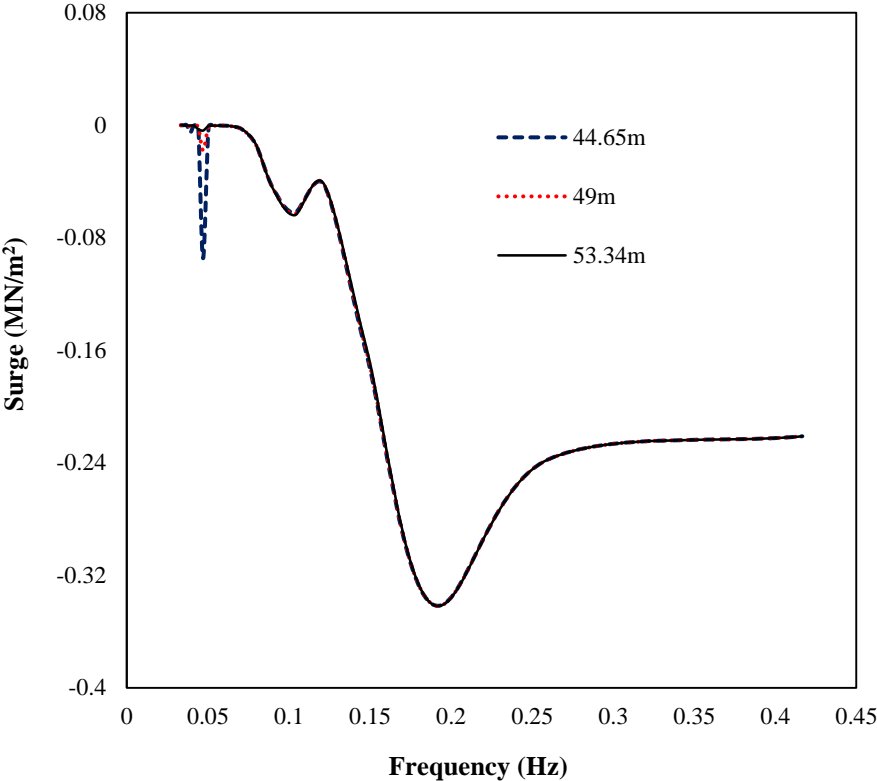


Figure 4.18 Surge drift forces

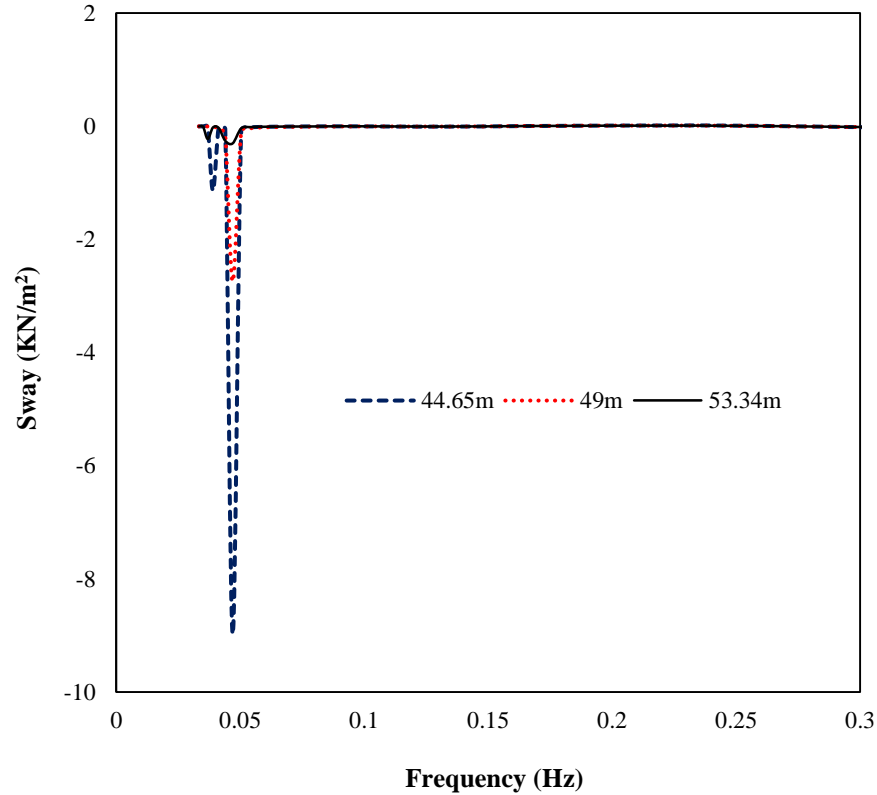


Figure 4.19 Sway drifts force



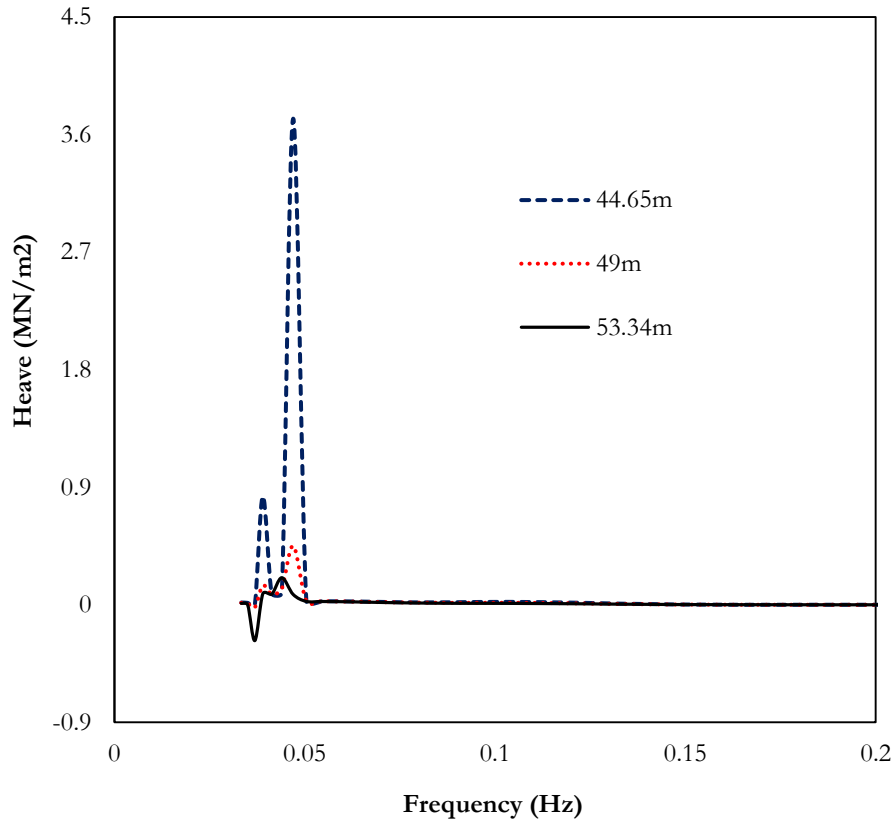


Figure 4.20 Heave drifts force

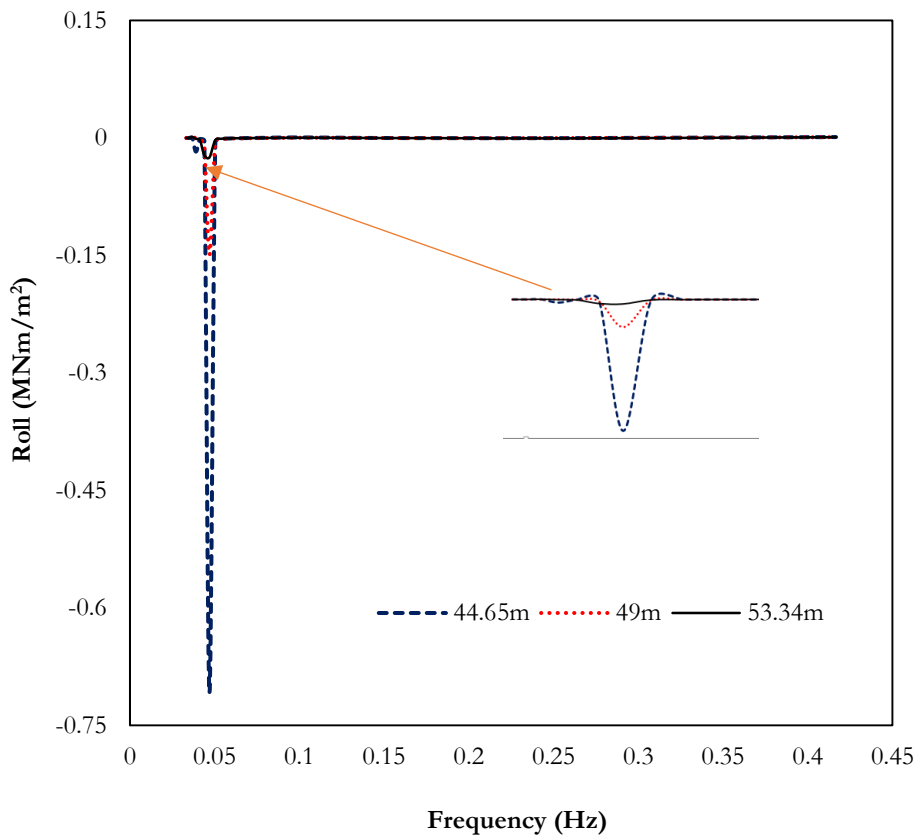


Figure 4.21 Drift roll moment

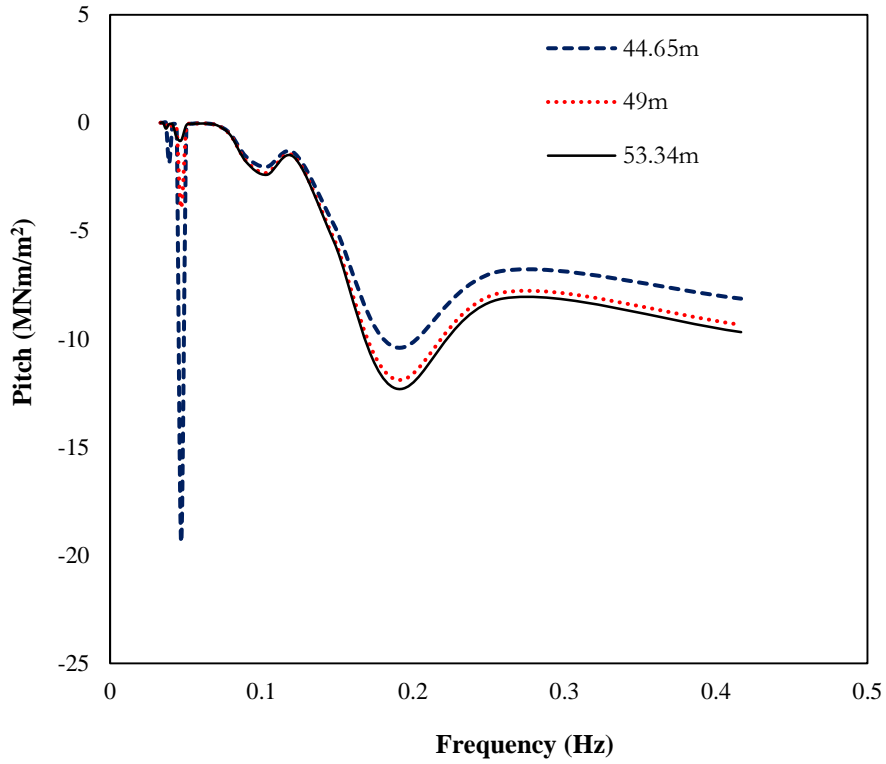


Figure 4.22 Drift pitch moment

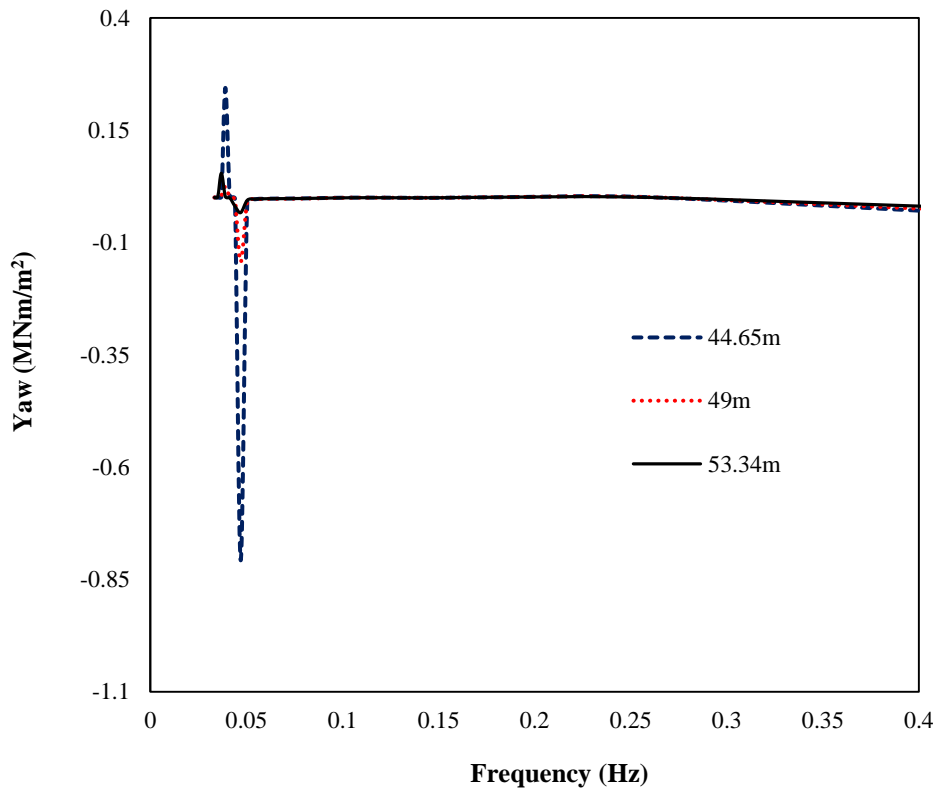


Figure 4.23 Drift yaw moment

The second order roll and pitch drift moments showed extreme sensitivity with draft size; Figure 4.21 and Figure 4.22. This result is very important in understanding and predicting the second order motion behaviour of the future design of PC-Semi. The result for roll moment presented in Figure 4.22 is in agreement with the experimental investigation on the low frequency mean roll moment of semisubmersibles presented in [110]. Findings from the experimental setup for roll investigation on conventional four column semisubmersibles suggested that almost 400% in roll drift moment for a 13% increase in draft size. The percentage increase observed from Figure 4.21 (between 49m and 53.34m draft sizes) a bit more than what was recorded for conventional four column semisubmersible. The same phenomenon was recorded for pitch moment (see Figure 4.22). Further experimental investigation on the second order roll behaviour will be required to understand and circumvent the effect of this behaviour during shallow draft operations.

### 4.6.3 Added Mass

The effect of added mass on the submerged part of the hull was investigated for irregular wave condition, at 0° flow angle, and the results are presented from Figures 4.24 to 4.29. At zero degree flow, the hull formation is symmetrical in the X and Y direction; i.e., the total surface area is the same. This creates similar hydrodynamic behaviour in the surge and sway directions of the hull.

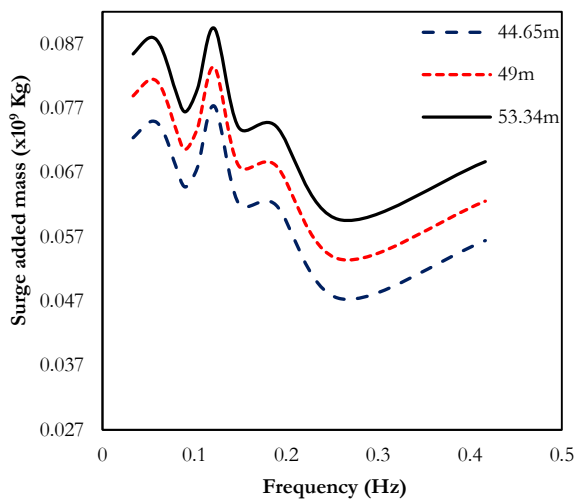


Figure 4.24 Surge added mass

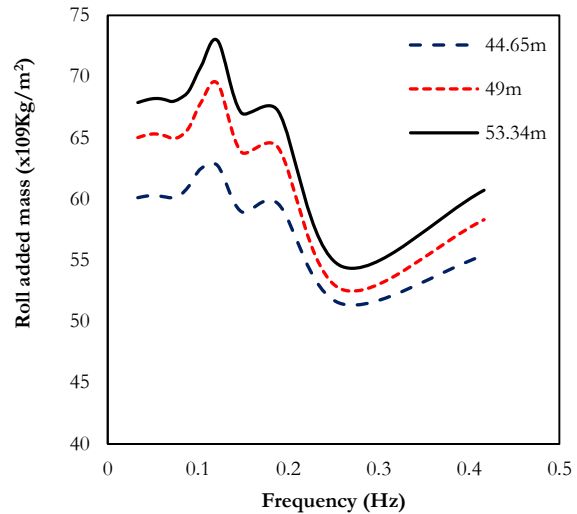


Figure 4.25 Roll added mass

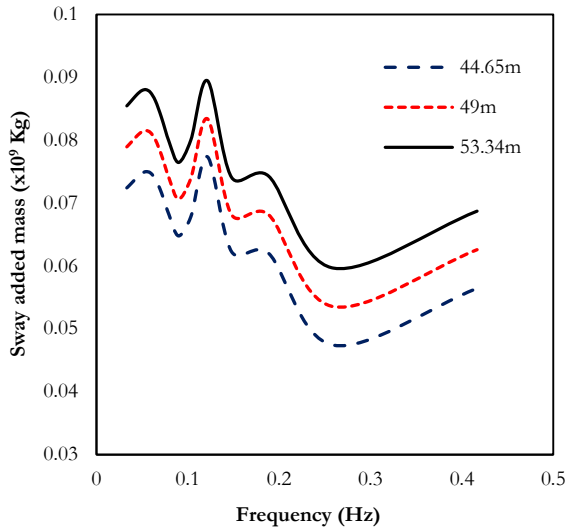


Figure 4.26 Sway added mass

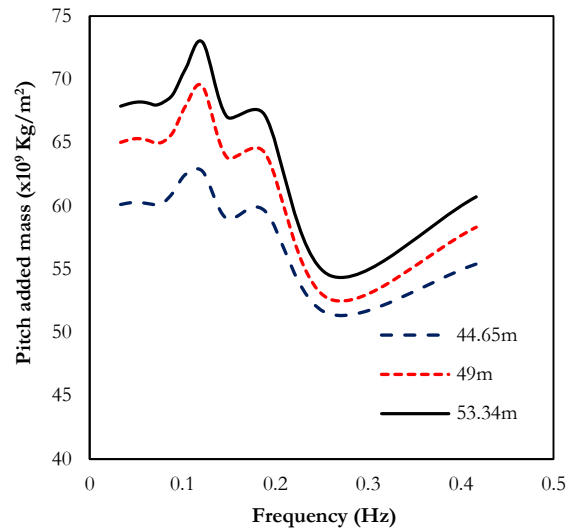


Figure 4.27 Pitch added mass

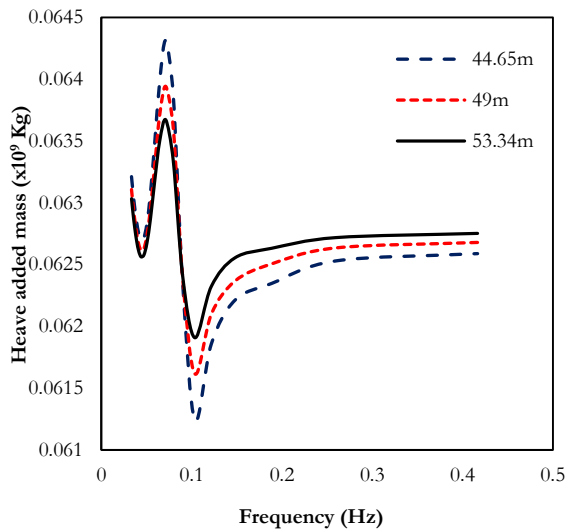


Figure 4.28 Heave added mass

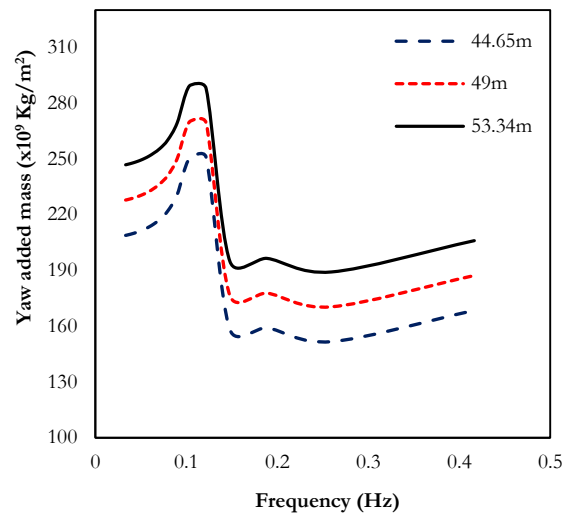


Figure 4.29 Yaw added mass

Figure 4.24 to Figure 4.29 (with the exception of Figure 4.28) shows that an increase in draft size will lead to a corresponding increase in the added mass (which is expected), but an increase in wave frequency gradually reduces this behaviour. It is imported to mention that the added mass component for the rotational components of the surge and sway motions are almost 15 times greater than their translational components. This parameter might be required to understand the influence of altering the hull's natural frequency in the later part of this thesis.

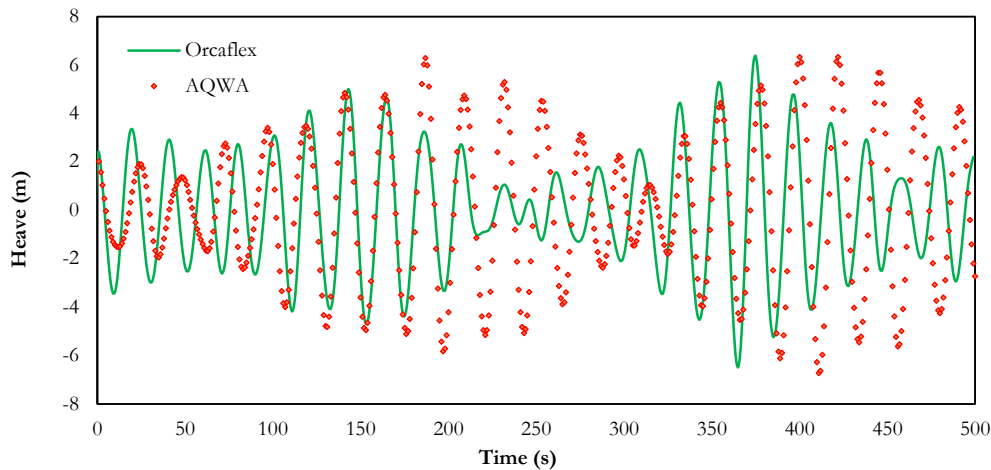
#### 4.6.4 Motion Test (Extreme and Survival Conditions)

We have presented met-ocean criteria for survival and extreme conditions in the G.O.M in Table 4.7. The standard has been designed with 1000yrs wave return period for survival conditions, and 100yrs wave return period for extreme conditions to guarantee the safety of the structure for

extreme conditions. The motion offset study was carried out using time series analysis set up in [139] and Orcaflex. Both solvers were developed using the basic equation of motion as described section 4.2.3. The results were studied and compared for both packages and no significant variation was observed for the maximum values.

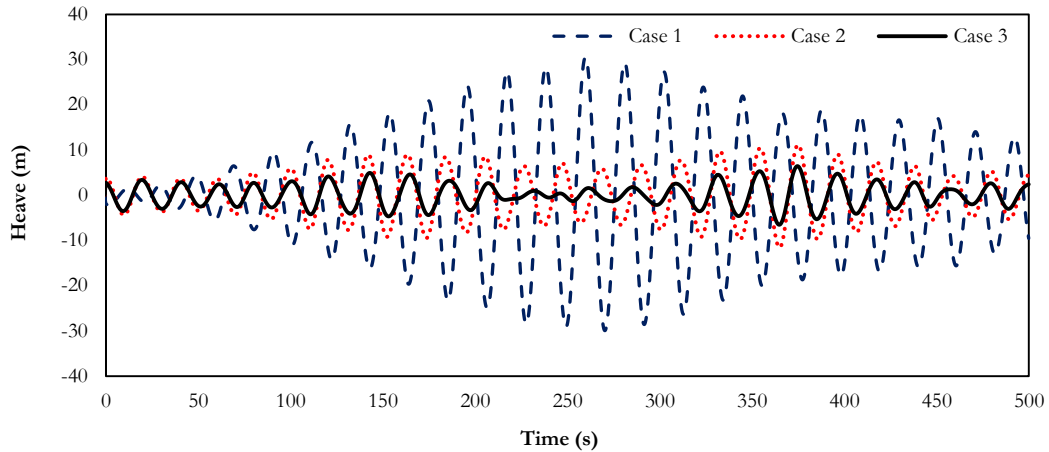
#### 4.6.4.1 Heave offset

Figure 4.30 shows a comparison made between the results obtained for heave motion from both packages for survival conditions, at  $0^\circ$  flow orientation.



**Figure 4.30 Comparison between ANSYS and Orcaflex**

Both solvers showed agreement for maximum heave offset for a period 500 seconds (6.45m). Although, the ANSYS solver was observed to have an early developed flow period ( $<350s$ ), when compared to the Orcaflex solver, 470s. The Orcaflex solver was more time effective, as compared to the ANSYS solver, and most of our results were computed using it, for this reason. The heave offset was studied for  $0^\circ$  flow angle, considering weather conditions for both extreme and survival cases. The heave study showed a high sensitivity to weather conditions and draft size. The application of top-tension riser to this hull system is very much dependent on these findings. The time required for a fully develop heave motion response reduces with a reduction in draft size for survival condition. But for extreme conditions, it takes almost the same period. For an increase in weather conditions from H13.1 T15.1, to H16.1 T16.7, the hull attained 3 times its motion response for all three drafts conditions. A study of the line plots presented in Figure 4.31 and Figure 4.32 shows this. For a draft size of 44.65m (case 1), the maximum heave motion increase from 10m to almost 30m. This result suggests an impossible application of shallow draft for dry-trees installations because of the acceptable vertical displacement of TTR in the industry in less than 10m [67].



**Figure 4.31 Heave offset for survival conditions**

For survival conditions (Figure 4.31), the heave offset obtained at 49m draft size is just about the maximum allowable. This is acceptable for free floating hull design because the vertical stiffness offered by the incorporation of the mooring and risers will further drop the offset by 20% to 40%, depending on the type and strength of the attachment used.

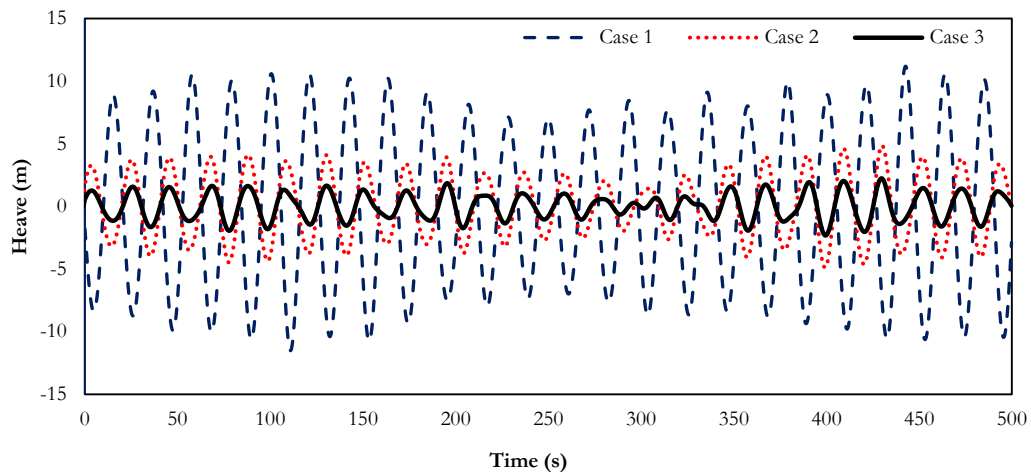


**Figure 4.32 Heave offset for extreme conditions**

#### 4.8.4.2 Surge Offset

Horizontal motions in semisubmersibles are greatly controlled by the slack level offered by the mooring lines. The mooring study on the VIV response for this hull system recommended taut mooring system [1]. The extent of the tension exerted on the taut mooring system will, therefore, be a function of the surge and sway offset. For  $0^\circ$  flow orientation, the sway motion is very small (almost insignificant), and therefore has been neglected in the analysis.

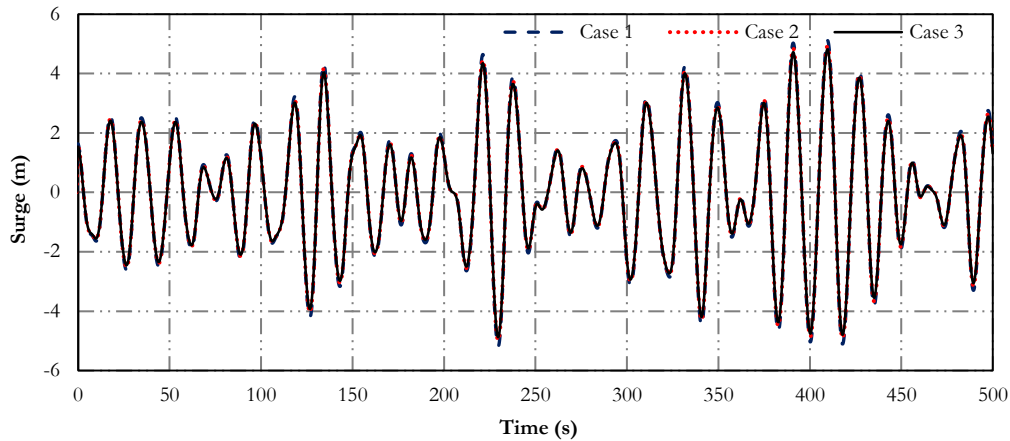


**Figure 4.33 Surge offset for survival conditions**

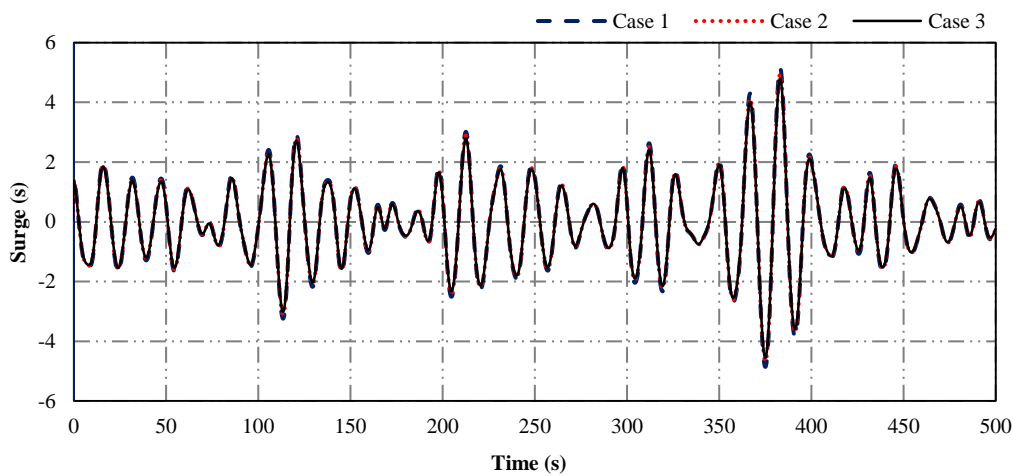


**Figure 4.34 Surge offset for extreme conditions**

The surge offset study presented in Figure 4.33 and Figure 4.34 did not show any significant difference in surge motion for draft size variation, neither does it show any difference for extreme and survival conditions. The single recommendation for mooring design can therefore be applicable for any form of application of PC-Semi; either for a drilling platform with moderate draft size or as a production platform with deep-draft configuration. Further invest

#### **4.8.4.4 Maximum rotation: pitch and roll offset**

The maximum rotation was studied for extreme and survival conditions, and the results are recorded in Table 4.14. For 5000 seconds, the wave effect was observed not to be symmetrical for intact position; i.e., the rotation +RY were not always equal to -RY, indicating that the righting moment is slightly more than the heeling moment in some cases, as shown in Figure 4.35. The unique feature about the rotational motion of the hull is that the maximum values don't necessarily take place at  $0^\circ$  flow angle. Investigating for these parameters, therefore, requires multiple series of test, considering different flow orientations. [4] recorded maximum rotation for this hull as  $7.75^\circ$

and  $6.66^{\circ}$  for survival and extreme conditions, both occurred at  $135^{\circ}$  flow orientation. In this study, we have shown that a reduction in draft size from 53.34m to 49.0m do not have a reducing effect on the rotation of the hull; as expected, but a further reduction in the draft size showed a significant reduction for its rotation.

**Table 4.14 Maximum offset summary**

Draft sizes	Conditions	Max. rotation
53.34m	Survival	$6.12^{\circ}$
	Extreme	$3.49^{\circ}$
49.0m	Survival	$6.17^{\circ}$
	Extreme	$4.06^{\circ}$
44.49m	Survival	$4.0^{\circ}$
	Extreme	$1.61^{\circ}$

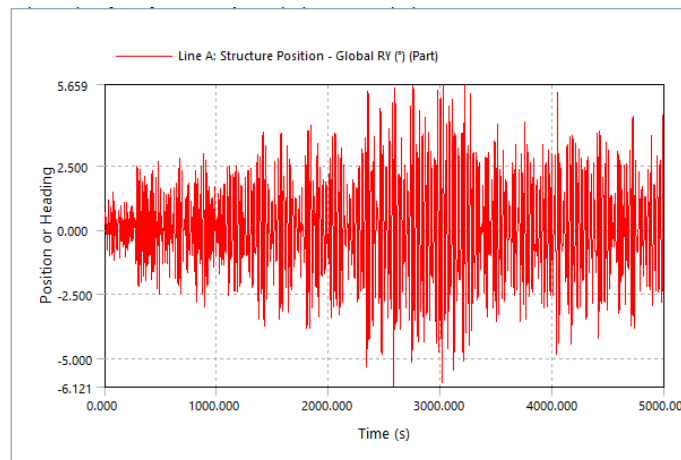


**Figure 4.35 Snap shot from ANSYS AQWA model for maximum rotation; 1000-years ( $^{\circ}$ )**

### 4.8.5 Current Effect

Recently, reports from weather conditions on floating buoys have shown a significant increase in sea current velocity. This is as a result of the increase in water level generated from global warming. This is why it is very important to investigate the effect of this high current velocities on newly developed structures, (and in some cases on already existing structures) to enable Offshore Monitoring Systems (OMS) to effectively predict their behaviour. [111] studied the effect of current velocities on the response of conventional semisubmersible hull system (four columns),



and documented very useful findings. He recorded that an increase in current velocity leads to a reduction in surge motion, irrespective of the mooring system. He also recorded a slight increase in pitch rotation and heave motion for an increase in current velocity from 0.6m/s to 1.2m/s. The effect of current velocity was investigated for regular wave conditions with forward speeds of 0.5m/s, 1m/s, 1.5m/s, 2m/s and 2.5m/s. The RAOs presented in this section are ordinarily expected to be different from the RAOs presented in the 4.6.1 because the hull responds differently for regular and irregular wave. The RAO plots reported in 4.6.1 are the highest possible response for the defined weather conditions.

### 4.8.5.1 Effect on RAO

We have investigated the effect of current-wave interaction (regular waves), on this unique hull system, and the results have been documented for each case study (draft size) with variable current velocities.

### Case 1 (44.65m draft size)

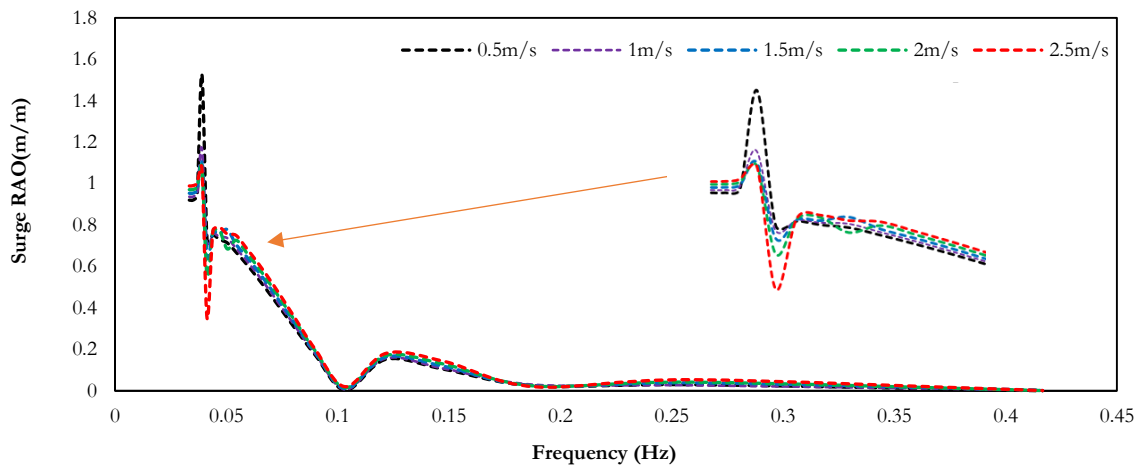


Figure 4.36 Effect of current velocity on the surge response of a PC-Semi of 44.65m draft size

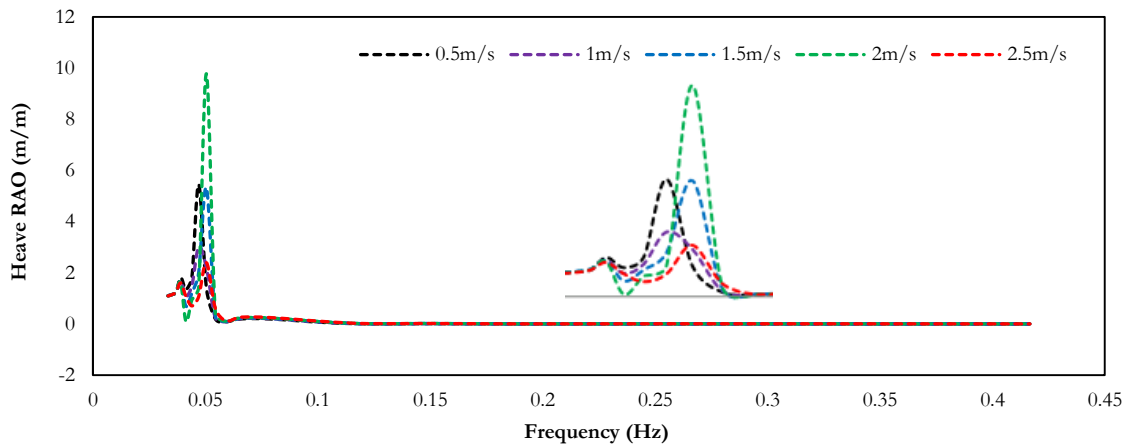


Figure 4.37 Effect of current velocities on the heave response of a PC-Semi of 44.65m draft size

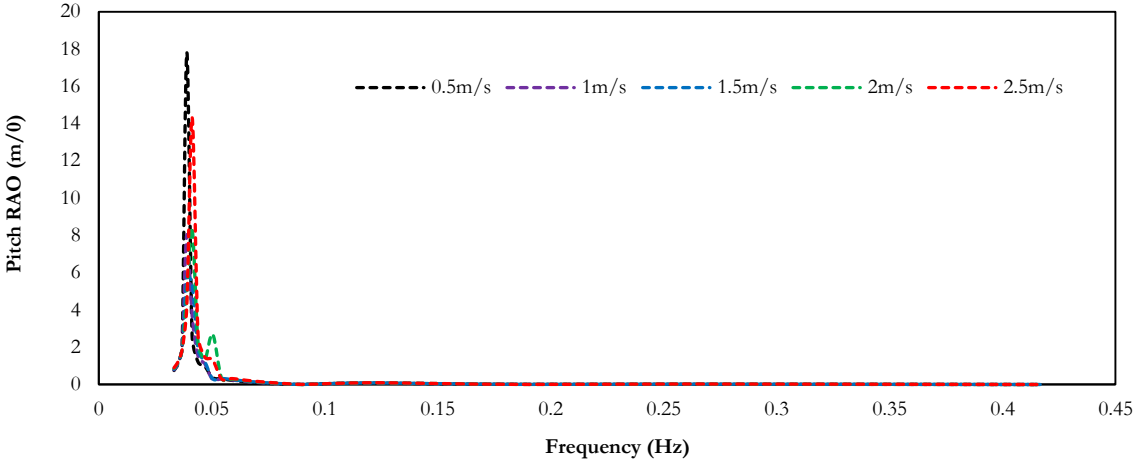


Figure 4.38 Effect of current velocities on the pitch rotation of a PC-Semi of 44.65m draft size

Case 2 (49m draft size)

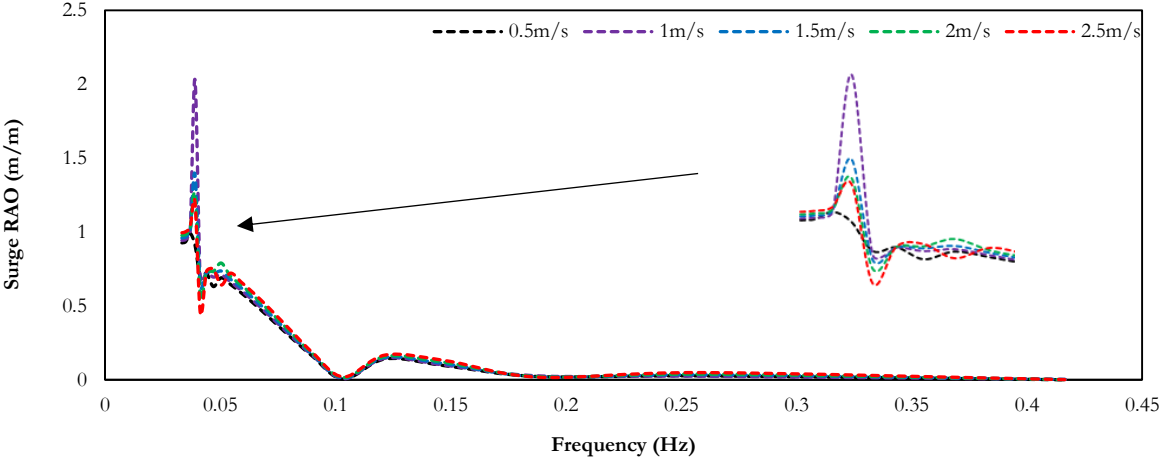


Figure 4.39 Effect of current velocities on the surge response of a PC-Semi of 49m draft size

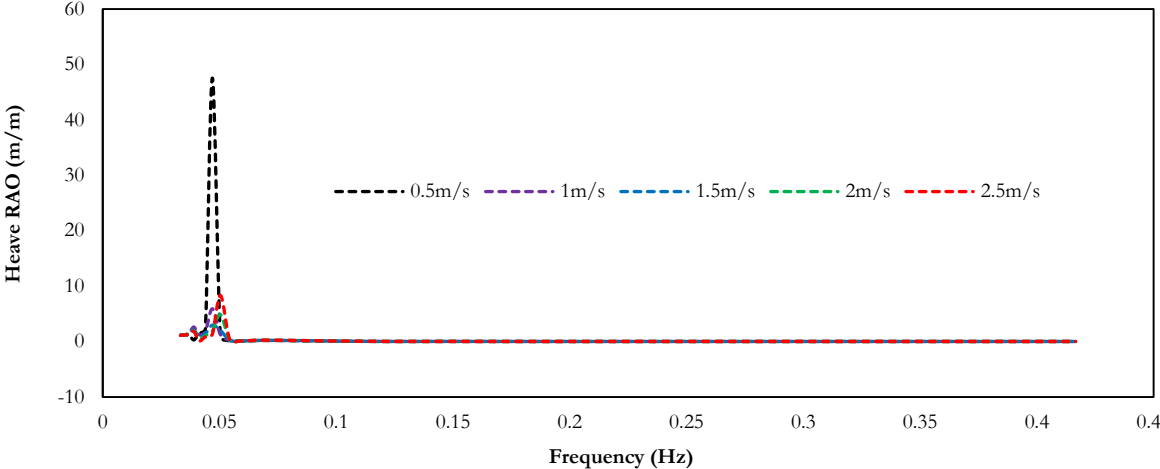


Figure 4.40 Effect of current velocities on the heave response of a PC-Semi of 49m draft size

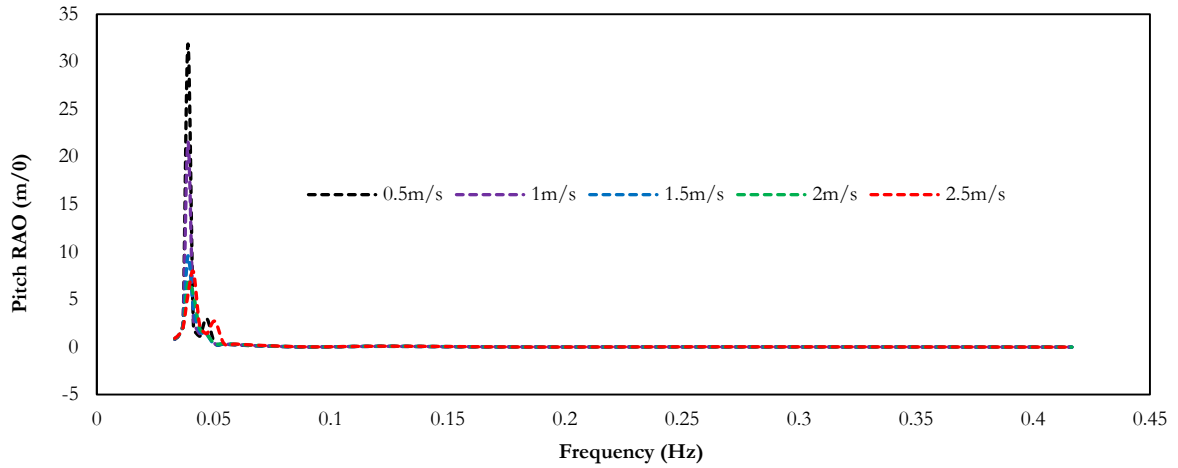


Figure 4.41 Effect of current velocities on the pitch rotation of a PC-Semi of 49m draft size

**Case 3 (53.34m draft size)**

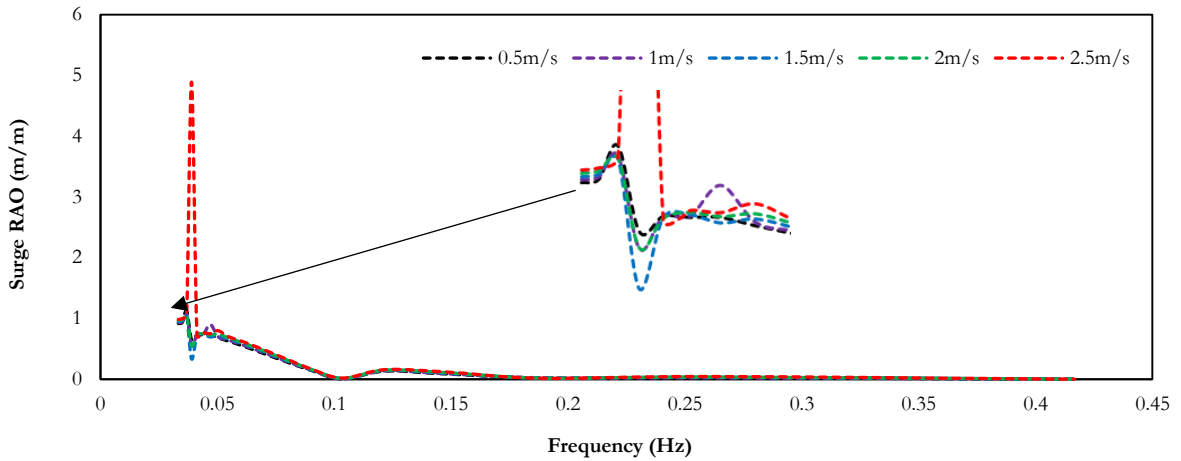


Figure 4.42 Effect of current velocity on the surge response of a PC-Semi of 53.34m draft size

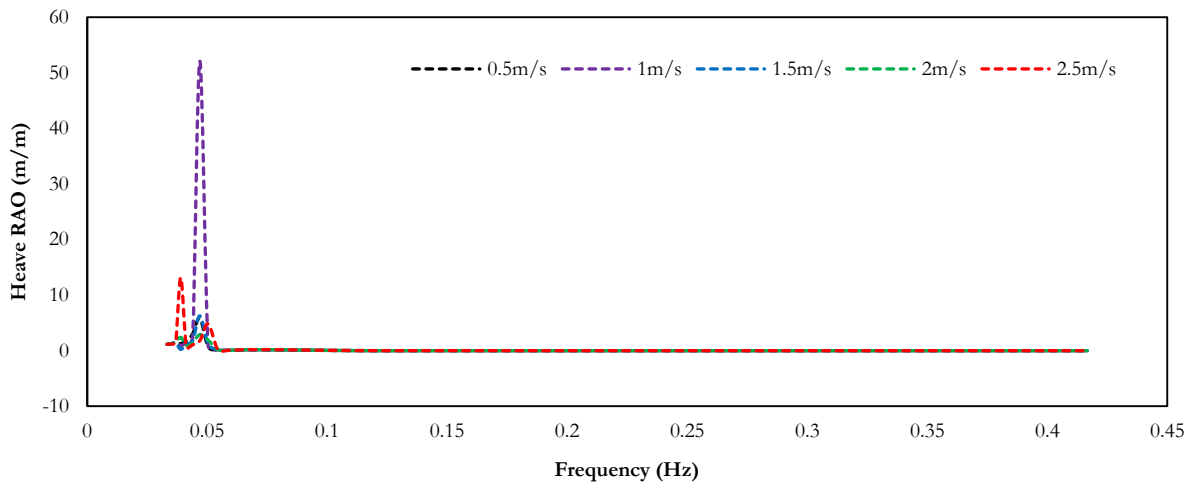


Figure 4.43 Effect of current velocity on the heave response of a PC-Semi of 53.34m draft size

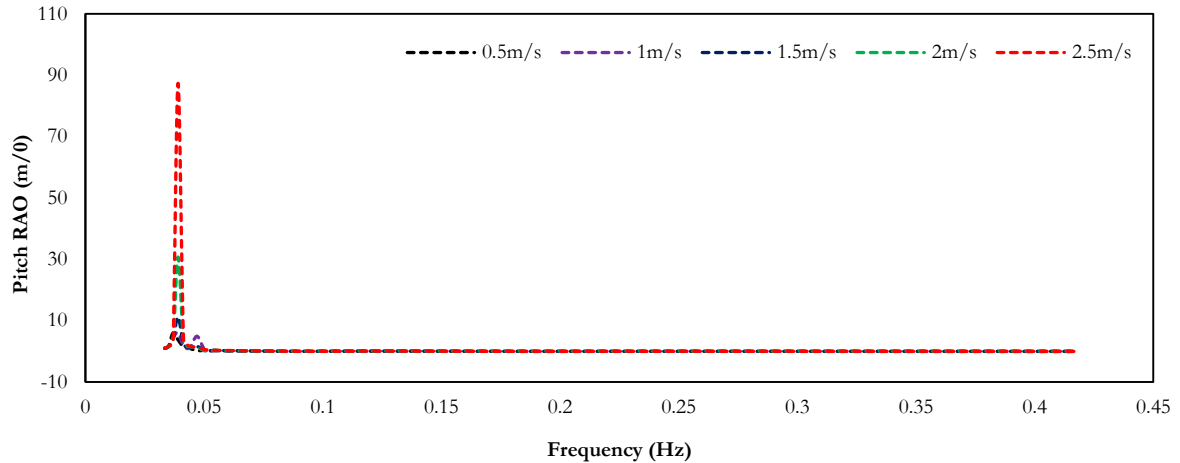


Figure 4.44 Effect of current velocities on the pitch rotation of a PC-Semi of 53.34m draft size

The surge RAO for the three draft cases presented in Figure 4.36, Figure 4.38, and Figure 4.41 showed different current effects on the hull. Maximum surge response was observed at 0.5m/s current velocity for draft size for 44.65m, for case 2 (49m draft size) maximum surge response was recorded for 1m/s current velocity, while for case 3 (53.34m draft size) maximum surge response was recorded at maximum current velocity of 2.5m/s. The maximum values for cases 1 and 2 have a similar relationship with the hull response for other current velocities, but the maximum value for case 3 (2.5m/s) have a highly significant difference with the response from other current velocities. Irrespective of these irregularities, maximum surge response for all three cases occurred at a resonant frequency of 0.039Hz. High current effect on deep draft PC-Semi might need careful investigation with a detailed FSI model, as the results suggest this. [111] presented a decrease in surge motion for an increase in current velocity for 0.6m/s to 1.2m/s. Figure 4.38 is in agreement with this theory. A clearer view of the low-frequency region shows there is a gradual decrease in surge response from 0.5m/s to 2.5m/s. For current velocity range of 1.5m/s and 2.5m/s, the decrease became very small. As the draft size increases from 44.56m to 49m, a slight alteration was observed in the hull response for low current velocities. For current velocities below 0.5m/s, the hull recorded very low surge response (Figure 4.39). The gradual decrease was recorded for current velocity range of 1m/s to 2.5m/s. As the draft size further increases from 49m to 53.34m, the maximum response at resonance frequency becomes very large for very high current velocities. The contributions from the vortexes generated in the wake formation can be traced to the source of the phenomenon. Details of this will be discussed in the next chapter of this thesis. For this draft size, apart from the response at 2.5m/s, all response of the hull for every other current velocity has a considerably low response. From a general point of view, the hull had a little increase in surge response from a draft size of 44.65m to 49m, but recorded a drop in surge response for

53.34m. Figure 4.37, Figure 4.40, and Figure 4.43 presents the effect of current velocities on the heave response for the different cases. The results recorded for all three cases have no similar behaviour, unlike that of surge response. Although on the average, the heave response increases with the increase in draft size. This is opposite to the results presented in Figure 4.12; for irregular wave study without current and wind contributions, the heave motion was discovered to reduce with increase in draft size. This is in agreement with previous studies [88]. From the results presented in all three cases, it is evident that high current velocities have a significant effect on the motion response of deep-draft PC-Semi. Results obtained for the pitch and surge motions for 53.34m draft establishes this fact

#### 4.9.6.2 Effect on first order forces

The effect of current velocity of the wave forces acting on a floating has previously been studied in different capacities in ocean engineering.

#### Case 1 (44.65m draft size)

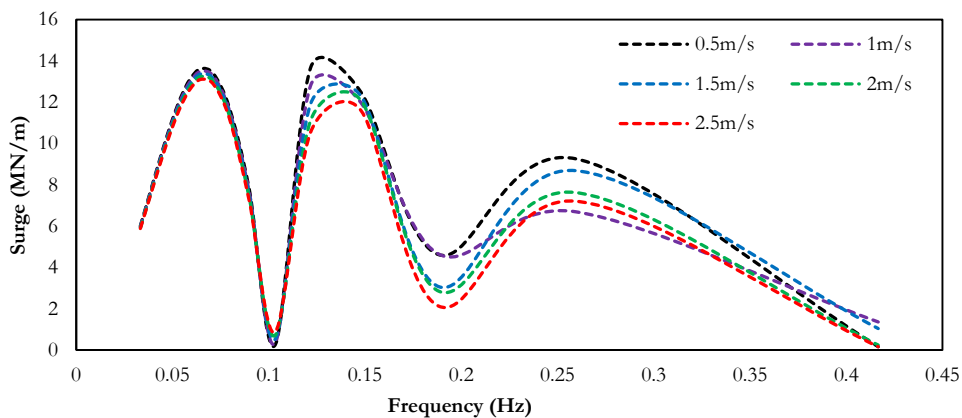


Figure 4.45 Effect of current velocities on the first order surge force on a PC-Semi for 44.65m draft size

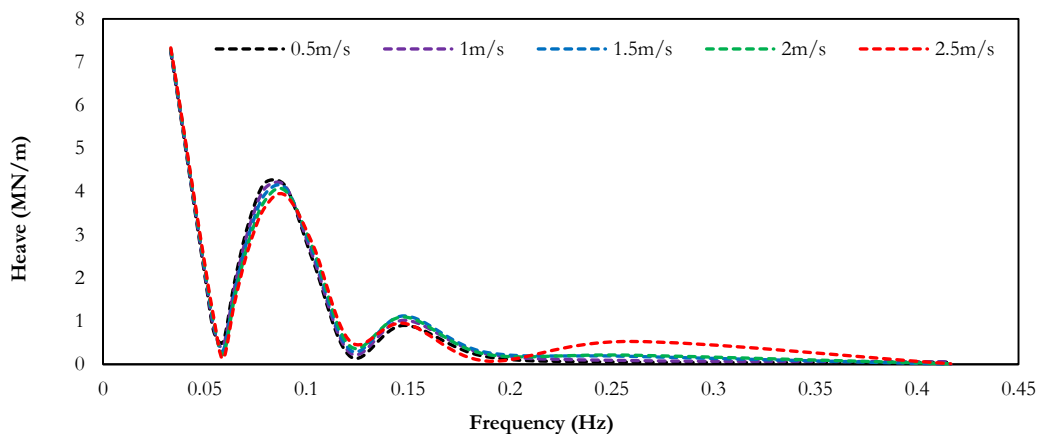


Figure 4.46 Effect of current velocity on the first order surge force on a PC-Semi for 44.65m draft size

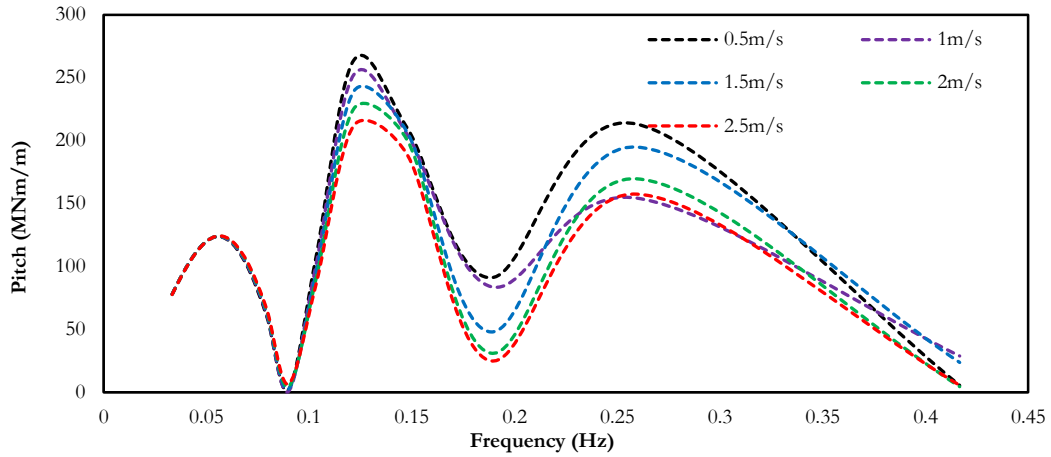


Figure 4.47 Effect of current velocities on the first order pitch moment on a PC-Semi for 44.65m draft

### Case 2 (49m draft size)

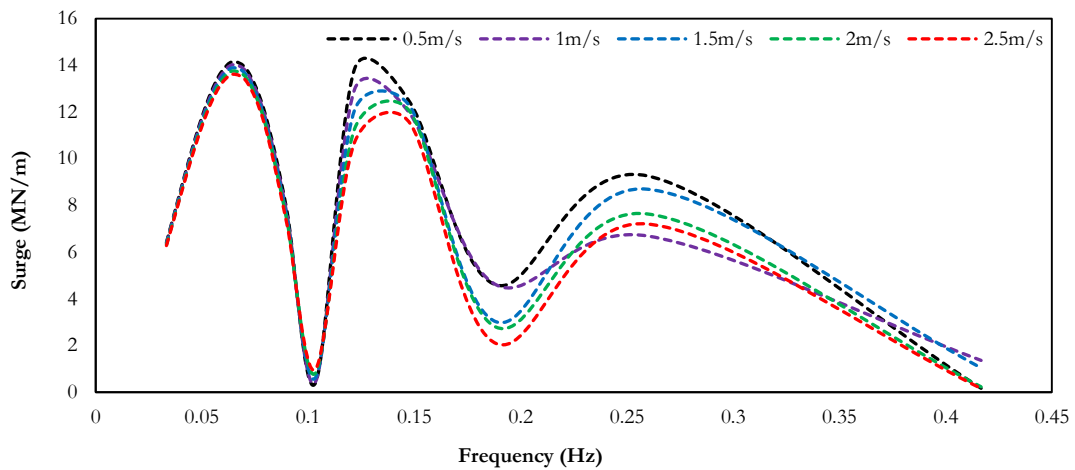


Figure 4.48 Effect of current velocities on the first order surge forces on a PC-Semi for 49m draft size

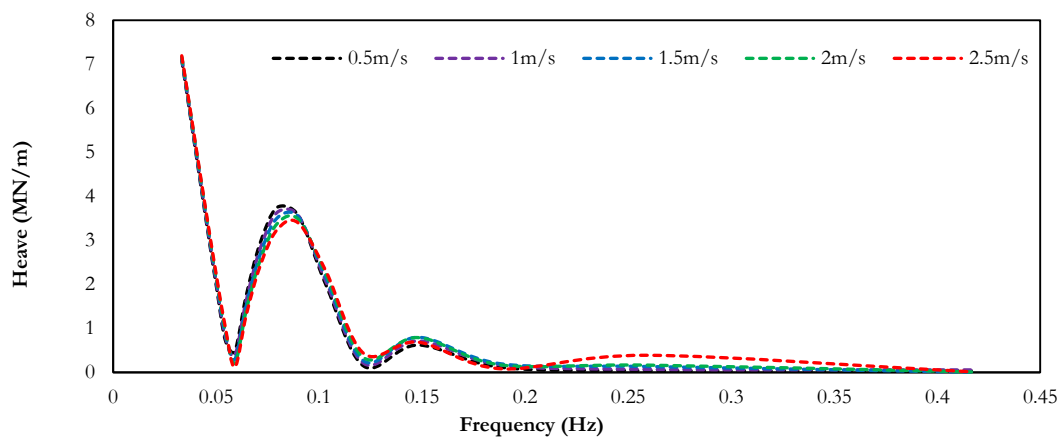


Figure 4.49 Effect of current velocities on the first order heave forces on a PC-Semi for 49m draft size

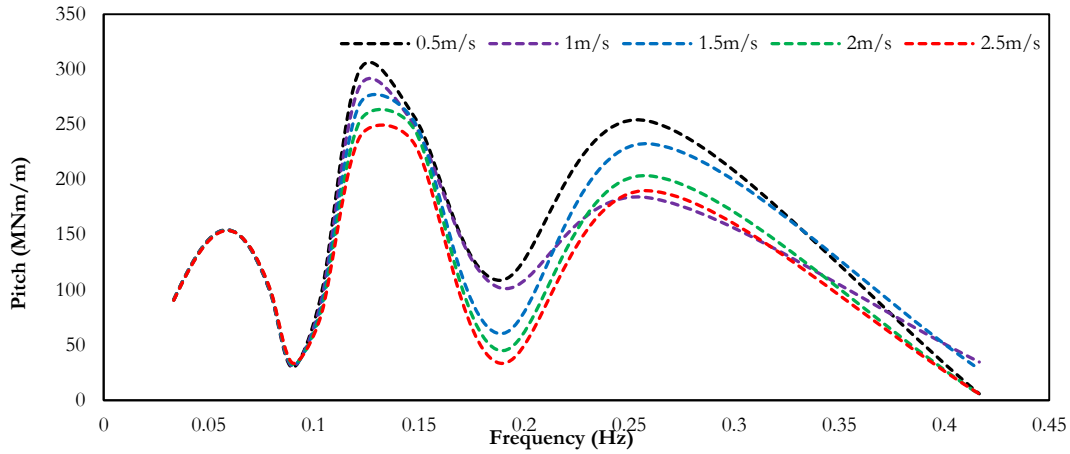


Figure 4.50 Effect of current velocities on the first order pitch moment on a PC-Semi for 49m draft

**Case 3 (53.34m draft size)**

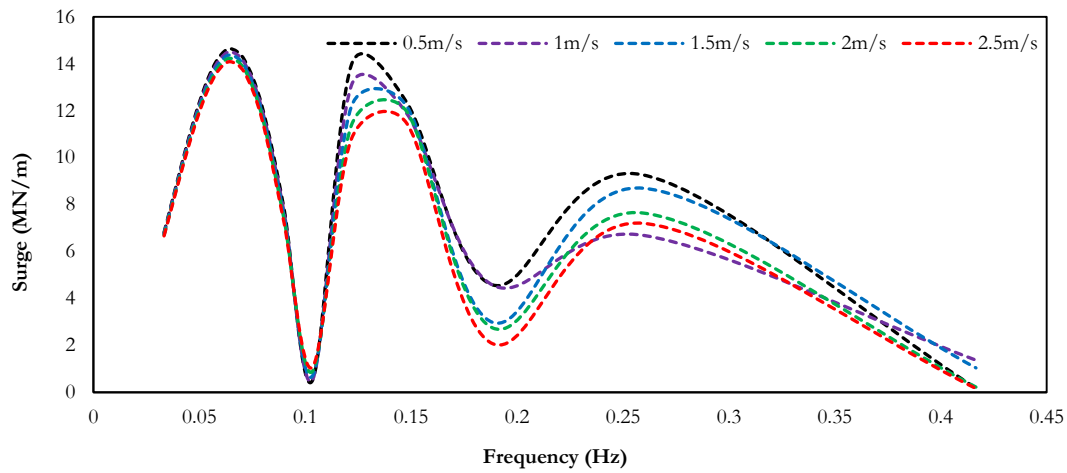


Figure 4.51 Effect of current velocities on the first order surge forces on a PC-Semi for 53.34m draft size

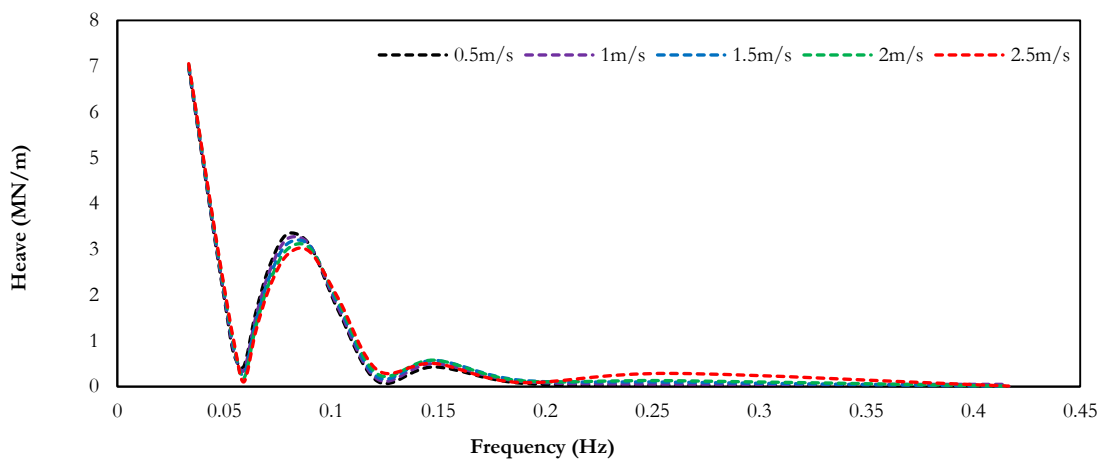


Figure 4.52 Effect of current velocities on the first order heave forces on a PC-Semi for 53.34m draft

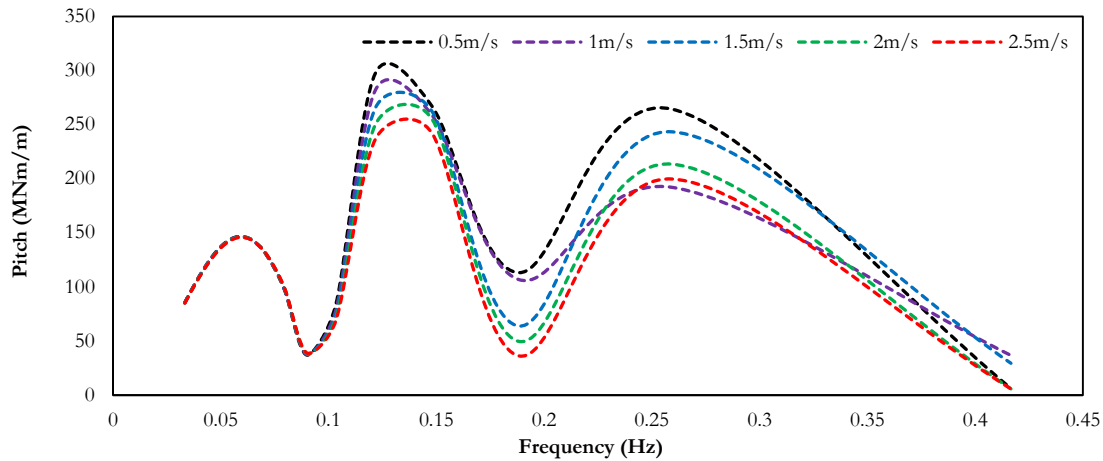


Figure 4.53 Effect of current velocities on the first order pitch moment on a PC-Semi for 53.34m draft

Figure 4.45, Figure 4.48, and Figure 4.51 presents the effect of current velocity on the first order surge forces on this hull system. For all three cases, the effect of current velocity do not necessarily have any effect on the relationship between the first order surge forces and wave frequency; the curve path is the same. This is in agreement with the conclusions made in [112], where the effect of wave-current interactions on three-dimensional floating bodies was studied. It was concluded that sea current does not affect the trend of the horizontal and vertical first order forces. On Figure 4.45 (case 1), between wave frequencies of 0.0333Hz and 0.104Hz, the relationship between the surge forces and the wave frequencies have a set of normal distribution curves, with an inversed relationship with the flow current velocity (low current velocity recorded higher forces). Within this frequency range (0.033Hz and 0.104Hz), maximum forces were recorded at 0.065Hz for all five velocity case studies. This relationship is opposite to the observation recorded for wave frequency range of 0.104Hz and 0.122Hz. For this frequency range, an inverse set of normal distribution curves were observed, which are direct proportionality with current velocity (increase in current velocity amount to increase in the surge forces). It is important to mention that the forces are very low for wave frequency range of 0.104Hz and 0.123Hz, when compared to 0.033Hz and 0.104Hz. Beyond 0.122Hz wave frequency, the wave surge forces maintain an inverse relationship with the current velocity, and the level/extent of proportionality varies for different frequencies. This behaviour is peculiar to what was observed for the other two draft sizes; 49m and 53.34m, but with a slight increase in the wave forces. Figure 4.46, Figure 4.49, and Figure 4.52 shows the effect of current velocities on the first other heave forces. As compared to the surge forces (Figure 4.45, Figure 4.48, and Figure 4.51), the effect of current velocity is less on the heave forces [113]. Figure 4.12 earlier showed that for high wave frequencies (above 0.3Hz), the heave wave forces (irregular waves) are very small, almost negligible. Similar finding was recorded for current effect. The effect of resonating references on the current behaviour is very



evident on the heave forces and it is on the surge forces, but the case of the heave force is more linear when compared with the horizontal forces. Figure 4.46 shows a significant change in the effect of current velocity on the heave forces at 0.1035Hz wave frequency. Between 0.0646Hz and 0.1035Hz wave frequencies, an increase in current velocity result to a decrease in the first order heave forces. For a wave frequency range of 0.1035Hz to 0.148Hz, this behaviour changes to the opposite; increase in current velocity amount to a corresponding increase in the heave forces. It is important to mention that the heave force decrease through the frequency range. For higher wave frequencies (0.15Hz and above), the relationship between the forces and the five current case studies of current velocities is very irregular. The behaviour for this case study (44.65m draft) is also peculiar for the other cases (49m and 53.34m draft sizes) as observed for surge forces, but for heave forces, they are an overall decrease in the first order heave forces with draft size. The results recorded for pitch moment are of high magnitude, and the line plots are similar to that of surge forces.

## **4.7 Chapter Summary**

The motion response of the newly developed paired column semisubmersible hull generated from ocean loadings and hydrodynamic interactions have been studied with numerical simulation, using diffraction and radiation method. The theories (diffraction and radiation) behind this method were explained with mathematical models, and their assumptions/limitations were clearly stated. Three cases were defined, relative to the hull draft size, as applicable for drilling, production, and support systems. Design standards for ocean conditions adopted were based on recommendations from the Oil and Gas industry. The selection of weather conditions for extreme, normal, survival and hurricane cases were based on recommended standards from Det Norske Veritas, American Petroleum Institute, and America Bureau of Shipping. The accuracy of our numerical model was verified by comparing our preliminary results with what was obtained from the experimental test. The comparison showed agreement for the motion response in all degrees of freedom for free floating hull analysis. The response amplitude operator for the heave, pitch, and surge responses were studied at  $0^\circ$  flow angle and the draft size was observed to have irregular behaviour for pitch rotation while a linear behaviour was recorded for heave motions. The hull was observed to experience about 80% increase in heave response for 8.14% reduction in draft size (from 53.34m to 49m), and over 450% heave motion increase for 16.26% draft decrease (53.34m to 44.65m). This excessive increase in heave motion for a shallow draft condition of this hull might restrict the future application of PC-Semi for deep-draft designs only. Although the behaviour for the pitch rotation was significantly different; the rotational behaviour for 8.14% reduction in draft size was

observed to be less. A reduction in draft size led to a higher rotation, but the reduction recorded between 53.34m draft and 49.0m draft is of important interest. Experimental studies have previously suggested that roll and pitch motions are mostly influenced by the second order drift forces, which are sometimes determined by the relationship between the draft size and the superimposed long crested waves [109]. The surge RAO indicated much-reduced motions in the horizontal direction when compared to traditional four-column semis. The design for mooring stiffness of a PC-Semi will therefore be based on its rotational motions (roll and pitch).

Results for the first order wave exciting forces were also presented in this chapter. In respect to the draft size, the wave oscillating frequencies have more effect on the behaviour of the heave forces and the pitch moment, when compared to the surges forces. As the wave frequency resonates with the natural frequencies of the hull (between 0.0450Hz and 0.0475Hz), the hull surge forces have a linear relationship with the draft size (more draft results to higher surge force). As the wave frequency further increases, the draft conditions have shown not to have any significant effect on the first order surge exciting forces. When the wave frequency is at resonance with the hull's natural frequency, the draft size the draft size was observed not to have any effect on the heave exciting forces. For all other wave frequencies, the heave forces were observed to increase with a reduction in draft size. For wave frequencies greater than 0.2Hz, the heave forces were observed to be negligible. The hull's draft size was observed to be an influencing parameter for its first order pitch moment, and this varies with different wave frequencies. For high wave frequencies, (between 0.2Hz and 0.42Hz,) the pitch moment increases with the draft sizes, whereas for very low wave frequencies (with the range of the hull's natural frequency), the irregular behaviour observed for pitch RAO was observed, with significant lower moment. This result suggests very favourable behaviour of pitch moment for resonance behaviour, for a PC-Semi.

The second order drift forces were also calculated for using the near-field method. The results obtained for roll and pitch moments were comparable with the results from an experimental setup developed in MARIN. The low frequency second order roll moment was observed to be very dominate for shallow draft condition, and very low effect for deep draft case for  $0^\circ$  flow angle. Maximum roll moment was recorded at  $90^\circ$  flow angle; symmetrical to the pitch moment. High roll/pitch moment was recorded for a wide range of wave frequencies, although maximum values were recorded at resonance frequency. For wave frequency above 0.08Hz, the drift roll/pitch moment was observed to increase with the draft size, with very significant values. This behaviour has influence our decision to optimize the hull performance, altering its weight distribution and geometric properties to help circumvent its rotational behaviour from drift forces/ improve its

stability. Details of this study are presented in chapter 7 of this thesis. The effect of the sway drift force was observed to be negligible. Results for the hull's added mass for the three cases were presented, and the added mass for the roll and pitch degrees of freedoms were observed to be the same for all three cases. As expected, the added mass was observed to increase with an increase in draft for five degrees of freedoms apart from heave. The heave added mass observed to be inversely proportional the draft size for low wave frequencies. As the frequency increase further beyond 0.1Hz, the added mass becomes directly related to the draft size.

The result for the time-response analysis was used to understand peak response of the hull, over a period of time. Comparison between ANSYS AQWA and Orcaflex showed agreement in predicting the response of the hull. The results obtained for heave offset showed considerable motions for all three draft cases for extreme weather conditions. The maximum offset was recorded as +10.21m for 44.65m draft size. For this weather conditions (extreme), a slight increase in draft size for our minimum draft case (44.65m) is recommended, to guarantee a safe application of top-tension risers on the hull. Industrial standard for heave motion/ stroke limit for TTR is about 9.14m. Different results were obtained for survival conditions; 44.65m draft size recorded maximum heave offset of -29.89m downward motion. This is over three times of the acceptable heave offset of this hull. 49m draft has a maximum offset of +10.3m. The acceptable draft size for this weather condition therefore above 49.0m, which is 54.87% ( $\approx 55\%$ ) of the entire hull size. The maximum surge response was observed to approximately be the same for all three draft cases, and for both survival and extreme weather conditions.

The effect of high current velocity on the response of the hull for regular wave case was studied, and the effect was observed to be dominating in the heave and pitch motions for deep draft case (53.34m draft size). The reverse case was recorded for the surge motion at the 44.65m draft size, at the resonance frequency, the hull responded to low current velocity, more than it did for high current. The effect of current velocity on the first order exciting forces was also studied, and results were recorded for heave, surge and pitch DOF, for  $0^0$  flow direction. The effect was observed to be dependent on the wave frequencies, for all three draft cases, especially for the heave force and pitch moment. The effect of the drag contribution of this force parameter is discussed in chapter five of this thesis.

# CHAPTER 5

## HIGHLIGHTS

- CFD Model for Vortex Phenomenon on a PC-Semi.
- 2D Simulation of Drag Effect on Eight Column Arrangement
- Relationship Between Current Velocity and Hull Drag
- Drag on Individual Columns for Different Flow Orientation

# Chapter 5: Effect of Vortex Shedding on a PC-Semi Hull Formation

## 5.1 Introduction

PC-Semi has a high tendency of been exposed to VIM behaviour because of the recently recoded high current velocities in deep sea. The slenderness ratio of the columns and its deep draft nature makes it prone to vortex induced movement when sea current passes through it. A further application of this hull formation for other areas in ocean engineering will require a complete knowledge of the relationship between the geometric properties and its reciprocating amplitude. In chapter 3 of this thesis, that relationship was experimentally investigated for PC-Semi. Apart from reciprocation, the sheared fluid generates other effect such 'drag' around the columns. In this study, we have presented results of the effects of the parameters in which vortex shedding depends on a paired column semisubmersible hull system. Parameters such as column shape (rectangular and square), inner/outer column distance, current velocity and flow orientation (angle) have been studied, and significant contributions were developed in future design of this hull. The results obtained from the series of experimental investigation on VIM response on a typical PC-Semi presented in the chapter 3 of this thesis were compared with the results obtained from our numerical study, and good agreements were recorded. Experimental and numerical studies recorded in [2, 13, 87] showed that PC-Semi has a reduced VIM amplitude when compared with conventional deep-draft semisubmersibles. Due to this development, we have only recorded results relating to the drag effect on the columns, to estimate for the force distribution.

Prerequisite of this study was generated from experimental results presented in [13] and [14, 25]. Background knowledge was also gathered from a wide range of sources, including that of single floating columns such as spar platforms, and conventional four column deep draft semisubmersible platforms.

At the end of this chapter we will be able to make conclusions on;

- i. whether a vortex supressing mechanism (such as strakes) will be required for any of the columns,
- ii. the require spacing between the inner and outer column for reduced VIM for this hull system,
- iii. the extent of drag contribution to the wave forces based on Morison equation,

- iv. the tendencies of destructive oscillating amplitudes in the transverse direction, and the effect of the wave inline motion on this,
- v. the flow effect of the columns on each pair.

## **5.2 Background Work**

The background study was carried in relation with the offshore industry, and with particular emphasis on semisubmersible platform. Bulk of the literature presented in this chapter is an extension of what was recorded in [114]. We have presented brief background work on vortex induced vibration in the offshore industry, on semisubmersibles hull systems, and on particularly on paired column semisubmersibles. It is important to mention that the effect of VIM on paired column semisubmersible is limited to few studies which were presented in chapter 3. Because this hull system is new, there no much studies on this area.

### **5.2.1 VIM in Offshore Industry**

VIM in the offshore industry spreads around structures, risers, mooring lines, tethers and other components with an elongated geometry. Early conventional spar platforms were faced with this challenge, and helical strakes were used to reduce the effect of this phenomenon. The strakes were placed in curved forms around the cylindrical hull, and they helped in altering the wake generated from the interaction of the hull and the fluid. This altered the frequency of the generated shed vortexes, preventing it from making resonance with the natural frequency of the hull. The evolution of truss and cell spars further helped to reduce the effect of vortex shedding on spar platforms. [115] and [116] explained the motion improvements in these structures. For simplicity, [86] performed an experimental investigation, using high Reynolds numbers, on the Vortex-Induced Vibration (VIV) of a cylinder with helical strakes. In their experiment, they compared the flow parameters and structural movements of a cylinder with and without strakes, from which significant reductions in VIV amplitude were recorded for the cylinder with strakes. Over the years, extensive research studies have been conducted on the effect of VIM on marine risers because of the extent of damage that has been recorded in the oil and gas industry. These movements occur at certain points during the flow when the vortex shedding frequency equals the natural frequency of the riser. This phenomenon cannot easily be predicted because the current velocity of flow on which the vortex shedding is completely dependent changes with the wind speed. The only way to identify when these movements are likely to occur is to ‘monitor’ the risers during operation. [117] developed a technique to monitor the extent of fatigue damage on marine risers, caused by VIM. [118] demonstrated the monitoring of VIV on a riser at Schiehallion, using realistic drilling and

production conditions. They used different methods in estimating the reduced velocity along different vibratory modes, and were able to make useful predictions using this tool.

Companies like MARIN, Technip, and Aker Solutions are known for their wide range of researches on vortex shedding phenomenon on ocean structures. Recommendation for further investigation on VIM on ocean structures can be found in reports presented by these companies, because their findings are recent.

### 5.2.2 VIM in Semisubmersibles

VIM in semisubmersible platforms became evident following the invention of the deep-draft concept. The design concept was created to help increase the stability of the structure by placing the centre of gravity below the centre of buoyancy. [119] experimentally investigated the effect of flow induced vibration on multi column floaters, using single and double pontoon semisubmersible for illustration. They evaluated the relation between the structural responses and the wave headings. [14, 26] presented a clearer view to this by considering the effects of surface waves, external damping and draft conditions. They [14, 26] showed that VIM in the transverse direction for a four cylinder semisubmersible platform arranged in a square configuration occurred at a reduced velocity range of  $4.0 \leq V_R \leq 14.0$ , while the maximum amplitude was observed at  $7.0 \leq V_R \leq 8.0$ . The enquiry into the effect of surface wave on VIM of offshore structures is very recent, since past researchers could not identify any significant effect this might cause. It was concluded that the VIM effect on large semisubmersible platform in regular waves is reduced, with no motions in the transverse direction, and no energy was dissipated on the natural frequencies in these nodes. It was also suggested that for this type of structure, VIM amplitude was dependent of the nature of in-line motions imposed by the incident waves. [24] investigated the motion response of a deep-draft semisubmersible platform and concluded that VIM was very pronounced for deep draft semis in irregular waves and the amplitude was larger for smaller waves. The external damping effects of VIM on semisubmersible structures have also been studied and different results have shown a reduction of amplitudes in certain directions, with an increase in damping. Structural attachments on offshore platforms such as risers and mooring lines act as external damping to the structure. Other recent contributors on surface wave effect include [23, 120, 121]. Most investigations that have been carried out on semisubmersible column arrangements have been done relative to their geometric parameters. The range of the oscillating frequency parameter (Reduced Velocity  $V_R$ ) from the shed vortexes is calculated relative to the distance between the centres of the columns  $\mathcal{S}$ , the thickness/width of the columns  $L$ , the height of the submerged part of the columns  $H_c^s$  (see Table 4.1), and the height of the pontoon  $H_p$ . Considering examples such

as [14, 23, 26, 122]. [122] experimentally studied the VIM behaviour of a prototype design of a multi-column semisubmersible postulated for MODU application. For a draft size and pontoon thickness of 150ft and 30ft, they observed VIM behaviour within a  $V_r$  range of 2.0 to 15.0. This is slightly different from what was recorded in other studies and the values for  $H_c^s$ ,  $H_p$ ,  $L$ , and  $S$  were different. Table 5.1 shows some recent results recorded by academic and industrial researchers on the correlation between the geometric parameters of semisubmersible platforms and the reduced velocity. Table 5.1 also includes the obtained  $V_r$  from our research for the specified geometry shown in Figure 5.1.

**Table 5.1 Geometric parameters of semisubmersible platform and  $V_R$**

References	$\frac{H_c^s}{L}$	$\frac{S}{L}$	$\frac{H_c^s}{H_p}$	$V_r$
[122]	1.74	3.20	4.0	2.0 – 15.0
[23]	1.71	4.04	3.04	5.0 – 9.0
[14, 26]	1.14	3.76	1.98	2.5 – 20.0
<b>Current work (2015)</b>	2.34 & 2.57	4.95 & 5.42	5.73	2.0 – 10.0

### 5.2.3 VIM in Paired Column Semisubmersible.

There are few reports that describe VIM of PC-Semis, as the design is relatively new in ocean engineering, although the deep draft nature, eight columns arrangement and its physical parameters (slenderness ratio) makes it respond to flow in a vibratory manner. As concluded in [24, 25, 27], deep-draft semis will experience VIM when they are exposed to high current velocities. The nature of flow around a paired column semisubmersible platform in relation to the angle of incidence ( $\alpha$ ) is characterized by complex wake interference because of its ability to be positioned simultaneously in in-line and staggered arrangement for a single flow angle; and also because of its varying column diameters. This exerts an unusual / uneven hydrodynamic force around the hull of the structure which in turn alters its stability. The available reports on the VIM behaviour of Pc-Semi have previously been discussed in chapter 3 of this thesis.



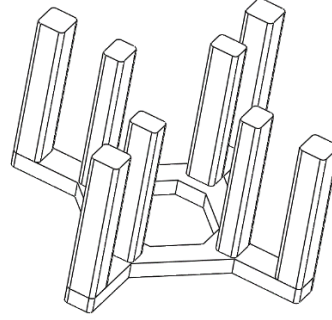


Figure 5.1 Schematic Diagram of a PC-Semi

## 5.3 Mathematical Formulation

Vortexes are basically formed as a result of instabilities generated from flow separations, as they travels through the hull. The flow is assumed to be incompressible; i.e., the energy of the vortexes are allowed to continuously increase or damp away, depending on the situation. The Euler equation for incompressible flow is presented in Equation 4.1. The CFD study was carried out for incompressible unsteady flow using continuity equations. The dimensionless vector form of the continuity equations can be written as

$$\frac{\partial\{u\}}{\partial t} + \{u\} \cdot \nabla\{u\} + \{\nabla p\} - \frac{1}{Re} \nabla^2\{u\} = 0 \quad [5-1]$$

The Reynold's number  $Re$  is a measure of the flow velocity, the column diameter and the kinematic viscosity of water. The hydrodynamic drag in the X- direction is calculated as

$$F_d = \frac{1}{2} \rho A U^2 C_d \quad [5-2]$$

$$C_d = \frac{2F_d^i}{\rho A U^2} \quad [5-3]$$

However, considering the Keulegan Carpenter number  $KC = U/f_w L$ , which is a function of the frequency of the oscillating wave  $f_w$ , VIM can be measured thereby making surface wave a vital parameter.

## 5.4 CFD Model

### 5.4.1 Description

Computational fluid dynamics is one of the most reliable tool for predicting the effect of vortex shedding on a set of multiple array of columns. The complexities associated with the flow separation which eventually leads to recirculation and oscillation in multiple directions can be

analyse in 2D and 3D cases. For vortex phenomenon; apart from visualization advantage, there is no significant difference between the results obtained for 2D and 3D simulation [84]. 2D has a comparative advantage of lesser simulation time. We have carried out simulation for both 2D and 3D in this study, but have recorded most results for the 2D cases. One of the early challenges faced was how to develop numerical setups with accurate turbulence models and mesh standards to represent real live scenarios in deep sea. [87] earlier used the results obtained from experimental test to check the contribution of turbulence model and mesh refinement on this hull, and the detached eddy simulation technique was discovered to be more effective in predicting the vortex shedding behaviour when compared to the Reynolds average Navier-Stokes. We have made use of this finding in carrying out our 3D models.

#### 5.4.2 Case Study

The cases that were studied for VIM were defined relative to the hull's geometric parameters, as mentioned in chapter 4. The postulated rectangular columns were studied in comparison with square columns, which are generally the geometric configuration for deep-draft semisubmersible platforms. The geometry adopted for the rectangular columns in this study are presented in the last two previous chapters, while the square columns were designed in relation with the surface area of the rectangular ones. Early results recorded for VIM amplitude and drag coefficient showed no comparative advantage of square columns over the rectangular ones. Due to this development, the results for square columns have not been recorded in this thesis. The flow angle of this hull system is significantly different from that of a conventional four or six columns arranged in-line with each other, as the inner and outer columns of this hull are arranged in staggered array at  $0^\circ$  flow angle, shown in Figure 5.4. This showed that the characteristic length  $L$  (which has previously been defined as the thickness of the column) is different for the inner and columns, and it gradually reduced from  $0^\circ$  to  $45^\circ$ , as shown in Figure 5.2

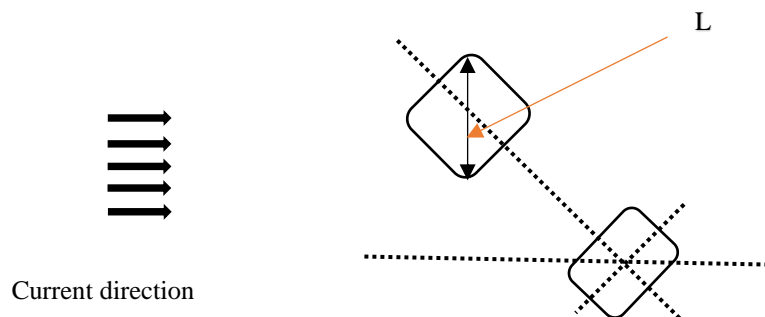
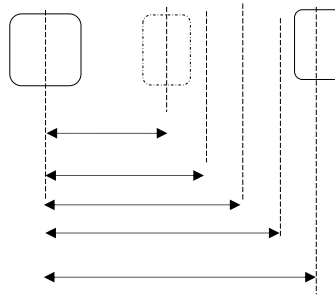


Figure 5.2 Definition of current angle

The effect of the spacing between the inner and outer columns was also investigated, as illustrated in Figure 5.3. The outer column was kept in place, while the distance inner column distance was varied between 12.4m and 32m.

12.4m, 16.8m, 20.4m, 24m, 26m, 28m, and 32m.



**Figure 5.3 Definition of inner/outer column spacing**

Figure 5.4 shows the direction of the flow the relationship between the direction of flow and the column arrangement at  $0^\circ$  and  $45^\circ$  flow angles respectively.

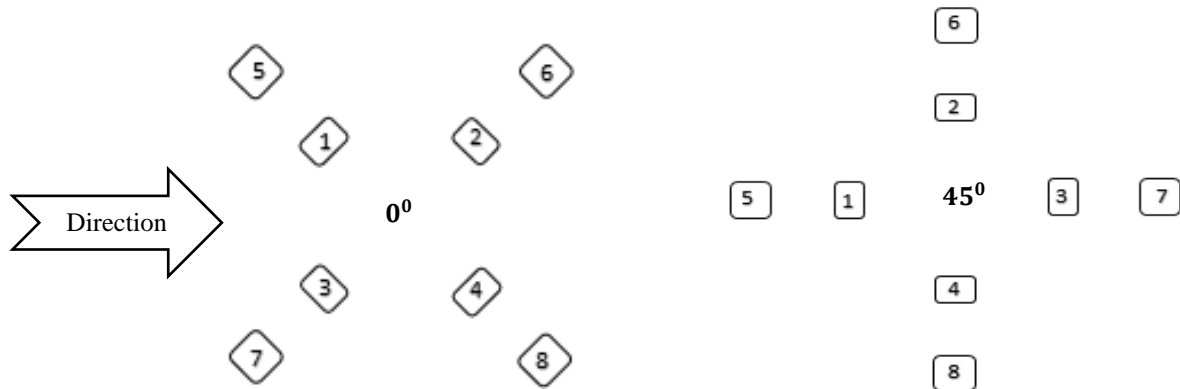


**Figure 5.4 Column numbering**

### 5.4.3 Flow Domain and Setup

The Cartesian coordinate use in creating the flow analysis is based on three coordinates; x, y & z, as explained in chapter 4. In creating a flow domain, factors such as simulation / computation time, cost, complexity, and computer type were considered in obtaining accuracy with the results. The domain is measured relative to the column's diagonal/characteristic length  $L$ . The columns of a PC-Semi are arranged diagonally; placing the inner columns at angle  $45^\circ$  to the outer column. Practically, the flow does not make contact with the same cylinder diameter, i.e.; the cylinder diameter changes at different flow angles, creating an irregular variation of the Reynolds number.

This phenomenon will be investigated in later studies, but in this case  $L$  was considered as the largest possible length the flow can make with the column; which is the diagonal length of the outer column (19m). Different researchers have recommended different flow domains for a typical square configuration of multi cylinder arrangement. [84] recommended a  $24L \times 24L$  flow domain for a four circular cylinder arranged in a square configuration, making the upstream distance as  $8L$ , while the downstream is  $16L$ , not placing the arrangement at the middle in the horizontal plane. This is a bit different from the recommendation presented by [123], with a computational domain of  $30L \times 20L$ , with  $16L$  upstream,  $14L$  downstream, while the up and down are  $10L$  respectively. In this case a mesh study was conducted to help increase the result accuracy. An unstructured triangular mesh was used to increase the possibility of analysing the pictorial results from the curvy edges of the columns. Apart from the simplicity of this type of meshing system, the shear layer created around the columns takes place from their curvy edges, which might be too complex for a quad mesh to resolve.

#### 5.4.4 Mesh Study

A mesh study was conducted for the 2D-case to investigate the effect of the mesh size on the nature of vortex formation around the array of columns. The mesh was gradually refined using smooth transition method from the column wall to the edges of the domain.

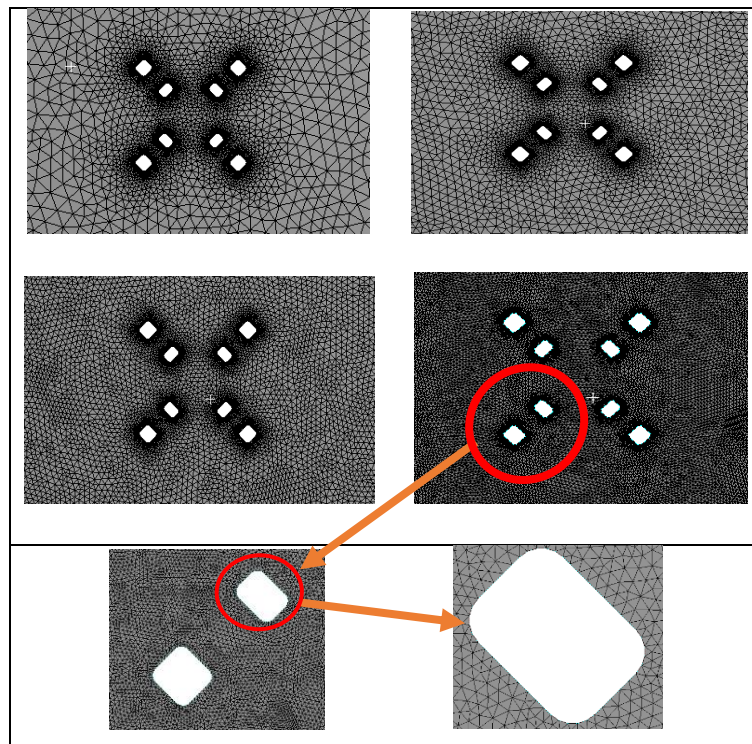


Figure 5.5 CFD mesh study

### **5.4.5 Boundary Conditions**

This analysis was carried out on Ansys workbench. Four simple boundaries were selected for this study;

- Inlet
- Outflow
- Sysmetry
- Wall

The domain upstream and downstream edges were designated as ‘inlet and outflow respectively, while the up and down edges were labelled ‘symentry’. The columns itself were labelled ‘wall’, with a bit of mess refinement around them to give a clearer contour display of the point of flow separation during the postprocessing; (see Figure 5.5). For vortex identification, a traiscient based solver was selected, under a well calculated time step.

### **5.4.6 Model Validation**

The model was validated with experimental results for drag coefficients presented in [1, 13]; as presented in chapter 3. The relationship between the hull drag and reduced velocity was investigated for  $0^0$  and  $45^0$  flow angles. Maximum hull drag for both flow orientation was recorded as 1.47 and 0.975 , and occurred at the same reduced velocity; 6.7.

## **5.5 Drag Study**

The drag was studied for current velocities ranging for 0.5m/s to 2.5m/s, as discussed in the previous chapter, and the results were recorded for 2.4m/s, because it the maximum value for current velocity recorded in deep sea, in the Gulf of Mexico, for hurricane conditions. The results presented in this study were recorded in relation with the flow angle. The reason for this is because numerical simulation has shown that the variation of viscous drag on an array of columns is relative to the nature of the incidence flow stream and the wake formation from the layers of shed vortexes. In this study we have assumed that the flow stream is undisturbed before it makes contact with the columns, which is usually the case in operating conditions. We carried out a preliminary study on the effect of flow angle on the average drag on the columns for 31.65m spacing between the inner/outer columns. The columns numbering is presented in Figure 5.4.

Results from experimental studies presented in the chapter 3 of this thesis showed an improvement in the VIM motion amplitude for PC-Semi, when compared with conventional deep-

draft semisubmersibles (Figure 3.2). The preliminaries of this finding is documented in [13], further investigation and confirmation is documented in [1], and CFD models built using Large Eddy Simulation technique also confirmed this [87]. The vortex effect on this hull have therefore been studied in relation with the drag effect on the columns. The recommendation for drilling hull application for this hull requires knowledge and understanding of the wave forces, and the drag coefficient have been recorded to be the major factor of that; from Morison's Equation [124].

### 5.5.1 Relationship between average hull drag, current velocity and inner/outer column spacing.

The test for the relationship between high current velocity and the hull drag was studied, and an increase in current velocity led to increase in hull drag. Figure 5.6 shows the relationship between the column drag and current velocity, for different inner/outer column distance. The result shows that the average drag around the columns changes with the spacing between the inner and outer columns.

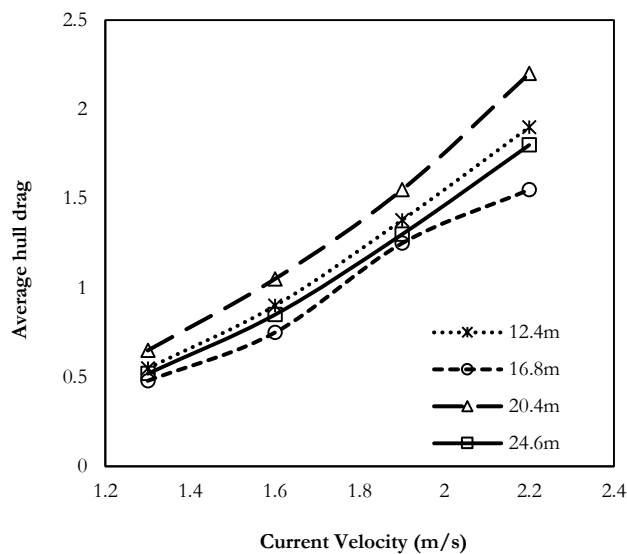


**Figure 5.6 Relationship between hull drag and high current velocity**

With the hull highest and lowest drag recorded as 20.4m and 16.8m respectively, a non-linear relationship between the shed vortices generated in the wake formation and the column spacing is evident. The extent of the non-linearity on each of the columns will describe the drag force nature on the hull. As flow travels through the hull, each of the columns has the tendency of behaving as a single structure, depending on the incident flow angle.

### 5.5.2 Relationship between flow angle and average hull drag

Figure 5.7 presents the relationship between flow angle and drag on each of the columns. It is evident from the curves that the position of the columns greatly affect the level of viscous drag around them, but the average drag around the entire hull reduces from  $0^\circ$  to  $45^\circ$ .

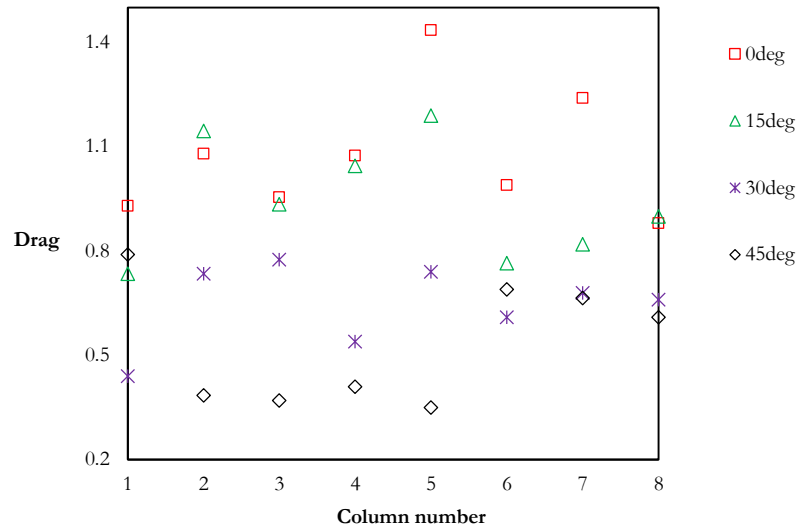
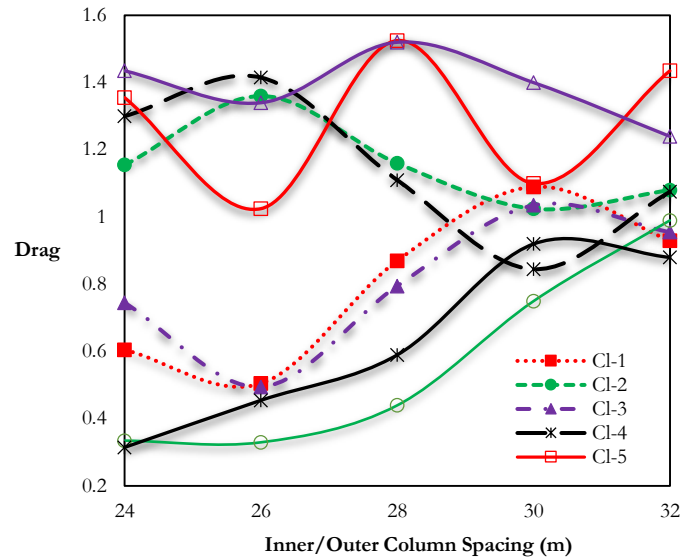


Figure 5.7 Flow angle and column drag

### 5.5.3 Individual column drag at $0^\circ$ flow angle: staggered pattern

At 0 degrees flow angle, the front pair columns are in-line with the downstream columns; but the inner columns are at staggered pattern with each other. The phenomenon of shared layer of vortices from the upstream column rapping round the downstream column as described by [84] does not occur, despite the fact that the rear columns are in-line with the leading ones. The reason for this can be found in the conclusions made by [125], in an experimental investigation of current-induced drag on two columns placed at staggered arrangement. It was concluded from the experiment that the intersection between a layer of shed vortices from the leading column and a layer of shed vortices from the rear column creates a stream of irregular wake. These irregular wake formations restrain the rear column from developing any form of regular vortex, thereby reducing the viscous drag effect on it. The extent of this wake collision between the columns in a pair was observed to be relative to the distance between them. This phenomenon was observed around the columns at  $0^\circ$  flow angle, as all four inner columns are arranged in staggered configuration with their outer columns. The distance between the front four columns and the rear ones will therefore determine the effect of the front irregular wave on the rear columns.



**Figure 5.8 Column  $C_d$  at  $\alpha = 0^\circ$**

Figure 5.8 shows the drag effect on each column for  $0^\circ$  flow angle. The effect of irregular wake formation postulated by [125] is evident on columns 1, 3, 6 and 8. The wake disturbance from column 5 mixes with the flow that impinges on column 1, and reduces the drag on column 1. But as the distance between the columns (1 and 5) gradually increases from 26m to 32m, the behaviour changes; column 1 receives more uninterrupted flow from the stream, which increases the amount of drag on it. Similar behaviour was observed between column 2 and column 6, but in this case the difference the drag on the columns at any point is much larger than the difference between column 1 and column 5. With regards to size, column 6 is bigger than column 2, the drag on column 2 is much higher than column 6 for small inner/outer column spacing. But as the spacing reduced, the drag on column 6 gradually starts increasing, while the drag on column two drops. The reason for the drop can be traced to the reduction in the disturbance level created in the wake, which is originally caused by the presence of column 6 in it (for small inner/outer column distance). Column 7 and column 3 behave in a similar manner as column 1 and column 5, while column 4 and column 8 behave like column 2 and column 6.

Apart from the unique nature of the drag pattern around the columns, another every important observation was recorded for this flow orientation. As the flow/disturbance travels through the arranged columns, the eight columns shed their vortexes individually. The nature of the reciprocating vortexes shed by the outer columns is significantly different form the reciprocating vortexes shed by the inner columns. The cause of this can be traced to the difference in their characteristic length (the diagonal distance between two corners of each column). The characteristic length of the inner column is different from that of the outer column. The imbalance



created as a result of this, might be the cause of the reduced Max. A/D recorded for PC-Semi, when compared to conventional deep draft semisubmersibles.

### 5.5.4 Individual column drag at 45° flow angle: diamond pattern

When the columns are arranged in such a way that the pairs make an angle of 90° to each other, they are said to be in a diamond configuration; ‘diamond’ in the sense that the shape of the arrangement is in form of placing two triangles together. The inner and outer columns of the leading and rear pair are in-line with each other, and the pairs are also in-line with each other as shown in Figure 5.4.

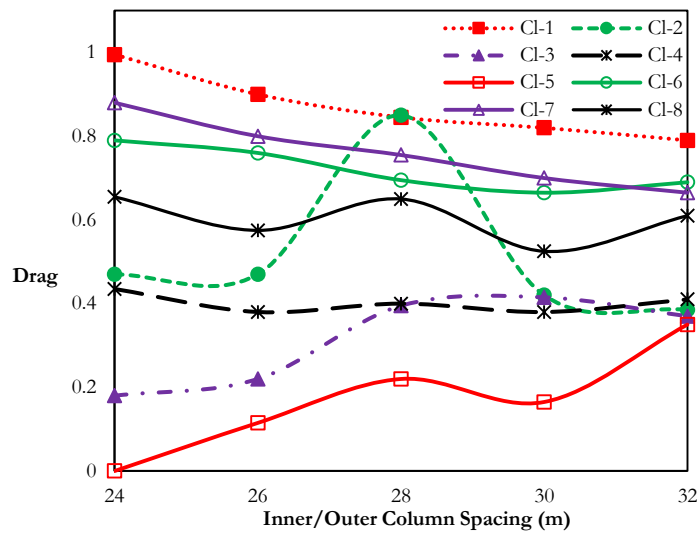


Figure 5.9 Column  $C_d$  at  $\alpha = 45^\circ$

Figure 5.9 presents the drag effect on the columns at 45° flow angle. Relative to Figure 5.8, the line plots on Figure 5.9 are widely spread apart. Because of the tangential distance between the leading pair and side pairs, there is hardly any significant interference between the shed vortices generated from the leading pair and the side pairs, even with an increase in inner/outer column spacing. The drag on each column on the side pairs is therefore independent of the shed vortices from the leading pair. From the arrangement of the columns (Figure 5.4), column 1 is just behind column 5, and column 7 is just behind 3.

As the flow travels through the columns, column 1 is therefore buried in the stream of wake generated from regular vortices developed from column 5. This drastically increases the drag force on column 1. This is also the case with columns 3 and 7. Columns 2, 6, 4 and 8 are the side columns. They have limited effect on each other. But this effect increases as the distance between them reduces from 24m to 26m. These observations are in agreement with the conclusion recorded

in [126] on the nature of drag on columns placed in-line with each other. A better understanding of this will be discussed in the contour study. A study of the contour plot for the flow pattern showed that there is a progressive transformation of interference between each pair, which creates a vortex rotation, exerting drag on the columns. The top and bottom pairs are in cross pattern with each other, which the front and rear pairs are in-line with each other, creating a high variation of drag for the columns.

### **5.5.5 Individual column drag at 15° and 30° flow angles: inclination**

We also investigated the nature of flow for two angles (15° and 30°) between 0° and 45°, and the results have been presented in Figure 5.10 and Figure 5.11. As  $\alpha$  increase from 0° to 30°, columns 2 and 4 get exposed to more direct unaltered flow (without getting contact from the upstream columns). This direct contact to undisturbed flow helps to gradually reduce the drag on them. This reduction is not linear because the nature of wake formed from the front pairs when  $\alpha$  is 15° is very unique, it impinges on the rear columns in a manner that exerts high drag on them. A good understanding of this type of flow can be found in [127].

It is also very important to note the manner in which the flow exerts drag on column 7. In both cases, (15° & 30°), column 7 seem to be the first column that creates contact with the fluid. At 0°, the flow shears at the midpoint of the curved edge of the column, creating an even distribution of wake on the two inclined edges of the column. But as the structure rotates to make 15° flow incidence angle, the shear point shift downward a bit, (just before the point where the curved edge begins).

On further rotation, from 15° to 30°, the share point moves to the point where curve begins; creating a fine sweep of wake at the top of the column. This helps to reduce the drag on the column by over 50%. Although on further rotation, the shear point moves closer to the centre of the line edge just in front of the flow, re-establishing a sharp flow separation which in turn leads to huge amount of drag on it. Just as it was with 0° flow incidence, the column drag at 15° and 30° is also affected by the nature of flow interaction in-between each pair.

This flow interaction is controlled by the centre-to-centre distance the inner column makes with the outer one. The graphs below illustrate that relationship.

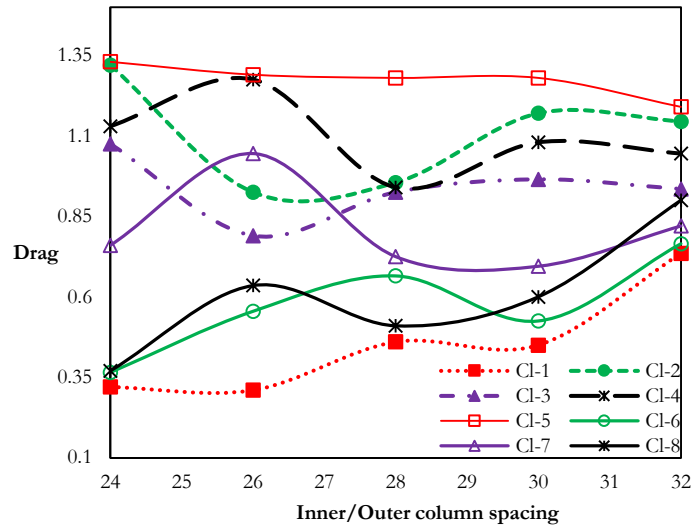


Figure 5.10 Column  $C_d$  at  $\alpha$  is  $15^\circ$

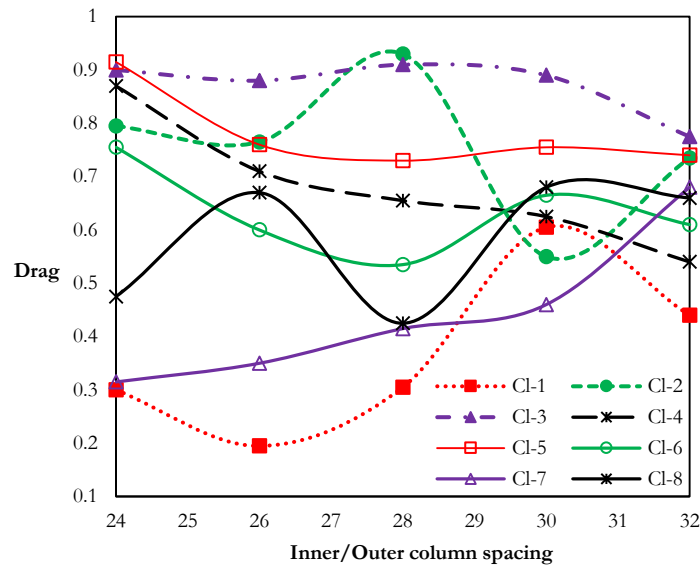


Figure 5.11 Column  $C_d$  at  $\alpha$  is  $30^\circ$

### 5.5.6 Pair Analysis

Different experimental and numerical studies on the nature of ocean forces on conventional semisubmersible hulls have recorded uneven/nonlinear force distribution around the hull for certain wave and current parameters [128]. This uneven force distribution phenomenon increases the instability of the hull. Early drag studies presented from Figure 5.7 to Figure 5.11 suggest the possibility of this on a PC-Semi. We have therefore studied the drag around each corner/pair of the hull. Table 5.2 shows the pair arrangement. Columns 1 and 5 are denoted as pair 1, 2 and 6 are pair 2, 3 and 7 is pair 3 while 4 and 8 are pair 4.

Table 5.2 Pair definition

Pair	1	2	3	4
Columns	1 and 5	2 and 6	3 and 7	4 and 8

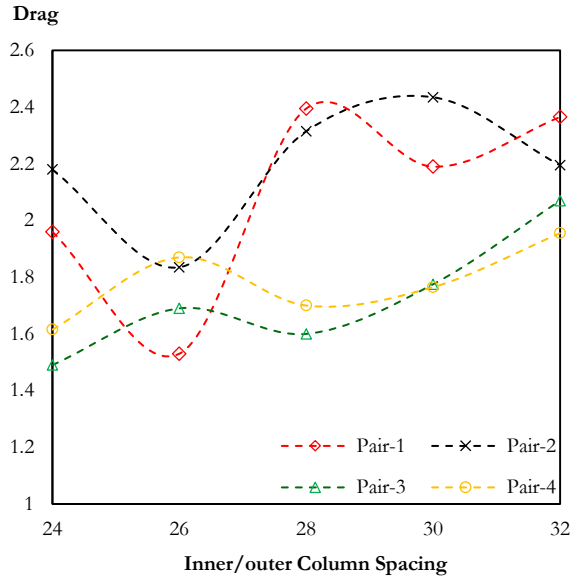


Figure 5.12  $C_d$  on Pairs at  $\alpha = 0$

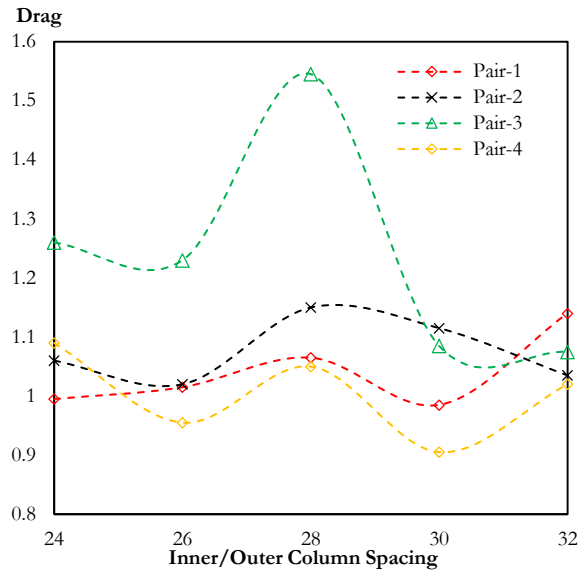


Figure 5.13  $C_d$  on Pairs at  $\alpha = 45^\circ$

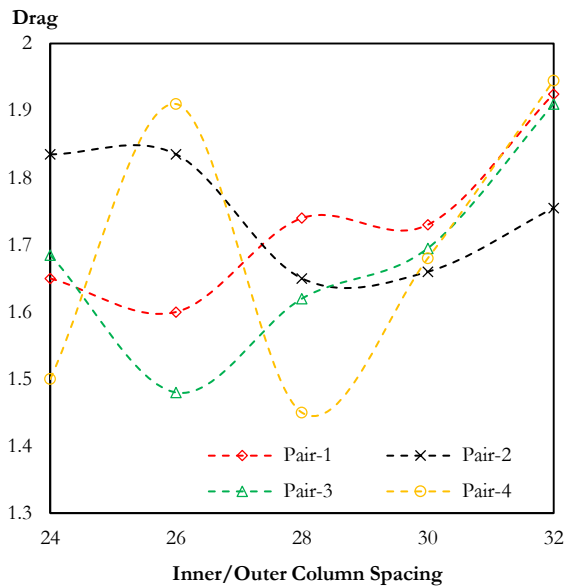


Figure 5.14  $C_d$  on Pairs at  $\alpha = 15^\circ$

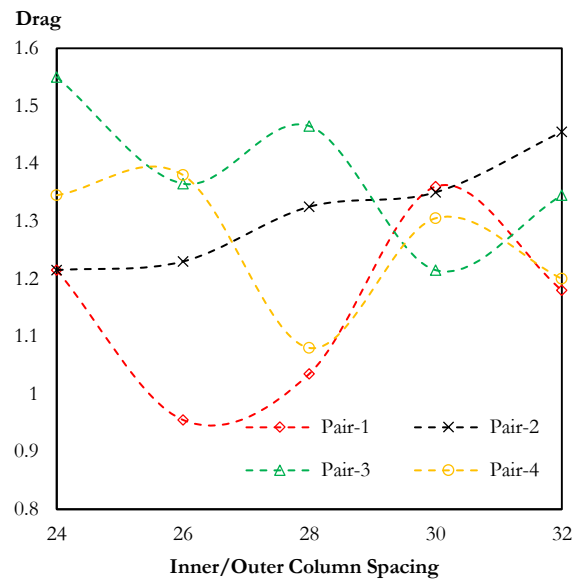


Figure 5.15  $C_d$  on Pairs at  $\alpha = 30^\circ$

Figure 5.12 to Figure 5.15 shows the drag around each pair of the hull for the different cases of flow angles. From the four plots (Figure 5.12 to Figure 5.15), we can conclude that the drag force around the hull will be uneven for any inner/outer column spacing. The results showed that if the flow disturbance between each pair is altered by a certain degree, the drag around the four

edges (pairs) will gradually balance itself. For the structural dimensions presented in this study, an inner/outer column spacing between 29.6m to 31.8m is recommended, because at every flow angle, the hydrodynamic drag around the pairs have a lower gradient. For design recommendation, a mechanism for circumventing this challenge will need to be developed, especially for the deep-draft application of this hull system. GVA Consultants have previously employed different methods in eliminating this phenomenon for conventional semisubmersibles. In the optimization of GVA4000 NCS, a set of cross and horizontal bracing system were used to reduce the possibility of this uneven drag phenomenon during transit [129]. This will be commended for further studies

### 5.5.2 Contour Study

The contour plots present a visual descriptive illustration of the flow paths around the columns and the wake region. The images were extracted from ANSYS FLUENT solver.

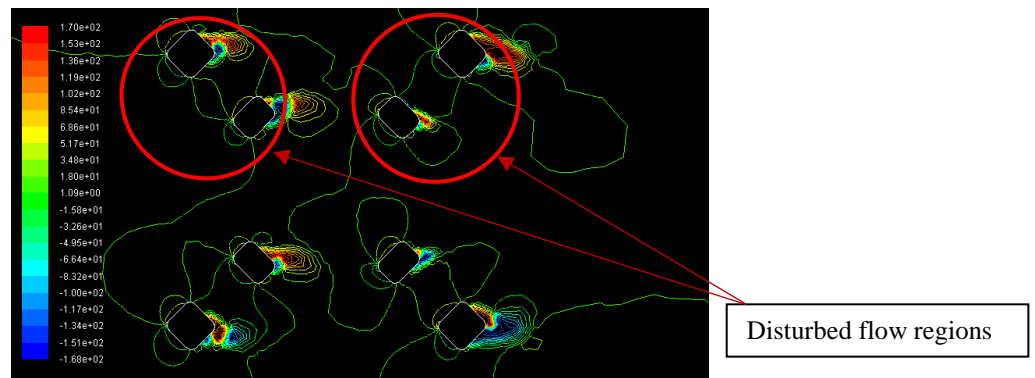


Figure 5.16 Velocity direction for  $0^\circ$  flow heading, 32m inner/outer column spacing, and 1.8m /s current velocity

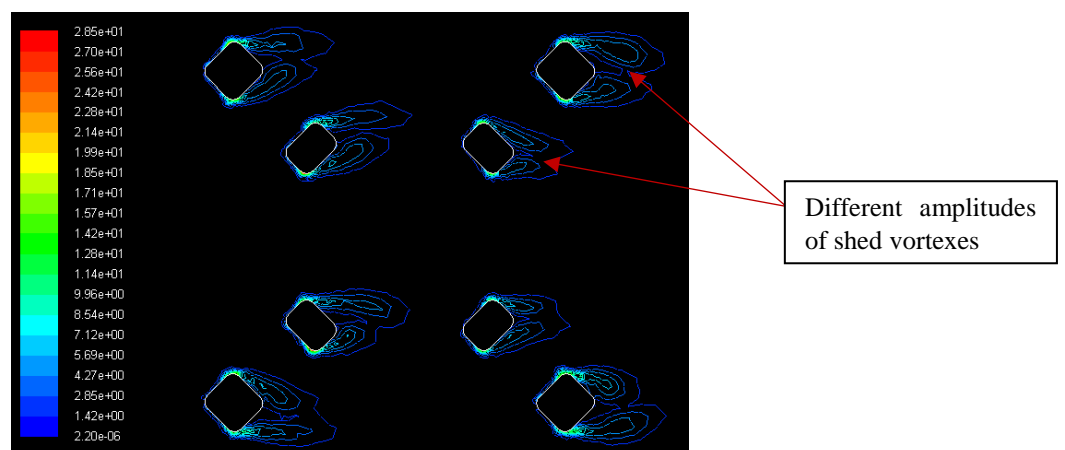
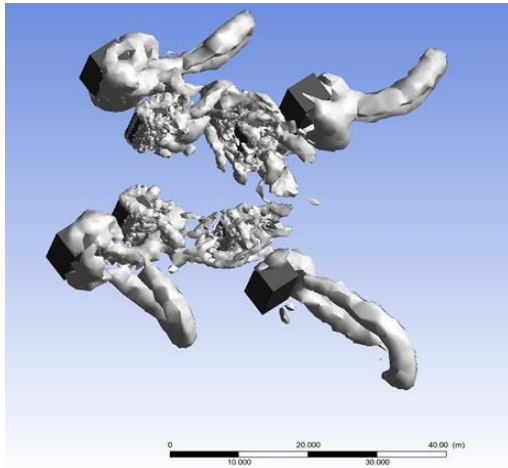


Figure 5.17 Vorticity magnitude for  $0^\circ$  flow heading, 32m inner/outer column spacing, 1.8m/s current velocity

An example of the flow part for velocity direction is presented in Figure 5.18. From the image, it is evident why columns 1, 3, 6 and 8 have low drags for  $0^\circ$  flow angle; their incident flows are significantly affected by the shed vortexes from their leading columns.

Figure 5.19 shows the image of vorticity magnitude (near the columns) of the shed vortexes for  $0^\circ$  flow angle. All eight columns can be observed to have different patterns of shed vortexes; the very reason why the nature of drag forces exerted on them are different in the first place. Outside that, a significant observation was recorded; that the amplitude of shed vortexes from the inner columns is smaller than that from the outer columns. From this observation, we can suggest that the reduction in vortex shedding amplitude of PC-Semi to deep draft semisubmersibles recorded in [1] could be as a result of this. To investigate this, a 3D study was carried out for two geometric configurations for inner and outer columns; circular-rectangular and rectangular-rectangular, and the observations are presented in Figure 5.20 and Figure 5.21.



**Figure 5.18 Rectangular-rectangular**

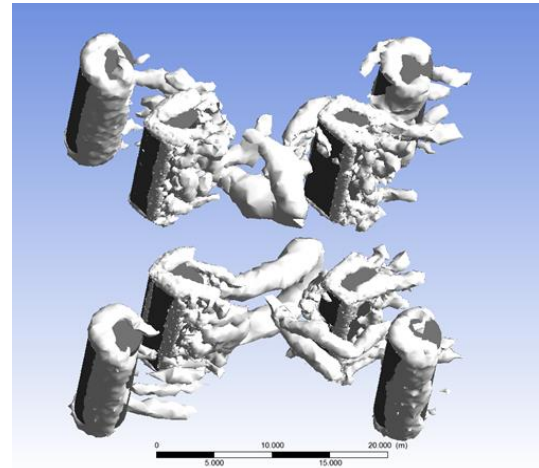


**Figure 5.19 Circular-rectangular**

The results showed that the amplitude of the shed vortexes from the inner columns are significantly different from that of the outer columns; as shown in Figure 5.20. The collision of both vortexes in the far stream generates a set of reciprocating vortexes with reduced amplitude. When the outer columns are replaced with circular ones (Figure 5.21), the amplitude of the shed vortexes drops further. A possible recommendation for circular outer columns might be considered in the later stage of this design process because of the comparative advantages it might offer in relation with the flow induced motion of this unique hull system. The extraction of the vortexes in far field (wake region) is based on Q-criterion developed by Hunt, and it identifies the vortex regions on a flow stream, by extracting the areas with reduced strain and pressure. Mathematically, it is expressed as;

$$Q = \frac{\partial U}{\partial x} \frac{\partial V}{\partial y} - \frac{\partial U}{\partial y} \frac{\partial V}{\partial x} \quad [5-4]$$

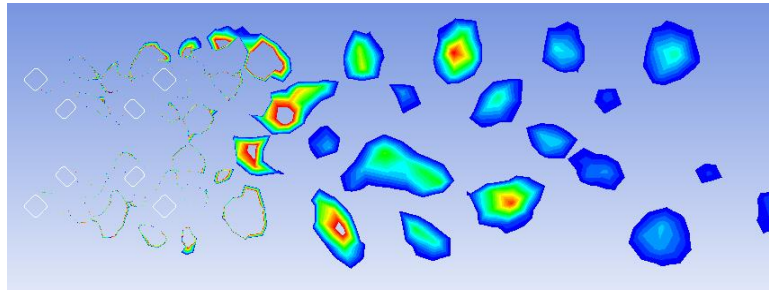


**Figure 5.20** Wake vortex identification at 0° flow angle

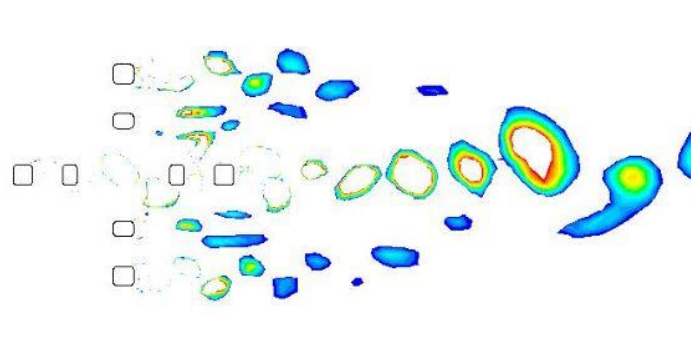


**Figure 5.21** Wake vortex identification for 45° flow angle

Figure 5.20 and Figure 5.21 shows the reciprocating vortices generated in the wake, at 0° and 45° flow angles respectively. From the images, it is evident that the reciprocating amplitude of the vortices generated from 0° flows is larger than that of 45°.

## 5.6 Summary

A CFD model developed in ANSYS release 16.0 was used to investigate the effect of vortex shedding on an array of eight columns, arranged in form of the newly developed paired column semisubmersible hull, and the effect of flow drag (pressure and viscous) on each of the column was recorded, and presented in this chapter. The Contour plots of the vortex formation were also studied for different column geometries, and significant findings were recorded. The drag was studied for a spacing range between 12.4m and 20m, and for 0° flow angle. The drag coefficient on each column was studied for different inner/outer column spacing, and the results were recorded accordingly. The result presented in this chapter showed that spacing between the inner/outer columns is a significant factor in estimating the average drag on the hull, because it creates a nonlinear relationship with the total hull drag.

# CHAPTER 6

## HIGHLIGHTS

- Time dependent Finite Element Analysis.
- Mass calibration for free floating hull.
- APDL finite element model; solid and shell elements.
- Formulation of boundary conditions for dynamic load cases.
- DNV and ABS standards for stress evaluation of column stabilized semisubmersible.



# Chapter Six: Non-Linear Finite Element Modelling of PC-Semi for Hull Reinforcement

## 6.1 Introduction

The unique column arrangement creates flow circulation within the hull structure which in turn generates an uneven drag force around the hull; as recorded in chapter 5. These circulations coupled with the hydrodynamic load from high wave amplitude, topside integration, and other structural attachment, generates an unusual load pattern on the columns and unconventional stress and deformation profile of the hull. The strength of the hull can, therefore, be guaranteed from understanding its deformation/buckling tendencies, alongside reinforcement, where required. In this chapter, we have addressed the nature and effect of fluid interaction from the nonlinear flow behaviour on the hull structure using finite element approach. The study also described a detailed understanding of the effect of the wave and topside loadings alongside the effect of the structural attachments. Most importantly, we have identified areas around the columns where high steel reinforcement will be required for any application of this hull formation in deep sea, to avoid failure at any point around the hull. We have also investigated the effect of structural responses discussed in chapter 4 on the stress distribution and possible buckling tendencies of the columns and the pontoon section. For future design, the sizing of braces, connections, fairleads, and plate thickness will be based on recommendations from this study. At the end of the first stage of the analysis, design engineers will be able to carry out effective selection for stiffener parameters (spacing, thickness, length and material) for the column reinforcement.

The development of this finite element model involved integrating hydrodynamic loads and the hull's mass distribution. This was not a straight-forward process as it involve writing some APDL codes to couple both set of equations. The formulation of boundary conditions for the different sea states was also a complex problem that was careful resolved in this chapter. The method adopted in this chapter is very much recommended to future design engineers.

## 6.2 Component Description

The hull model presented in Chapter 3, 4 and 5 consist of only two components; columns and pontoon, because the effect of hydrodynamic loading are controlled by them. Apart from the columns and pontoon, the hull has other components (see Chapter 1; Figure 1.1 and Figure 1.2), which include;

- Inner columns brace
- Inner/outer column connections
- Column/pontoon joints
- Topside integration points
- Deck truss supports
- Deck plates

Figure 6.1 show shows some of those parts. Two cases of topsides was used in this study, as shown in Figure 6.2. The inclusion of these sub-structures enabled us to introduce other external loads (mooring loads, riser loads, and top-deck loads).

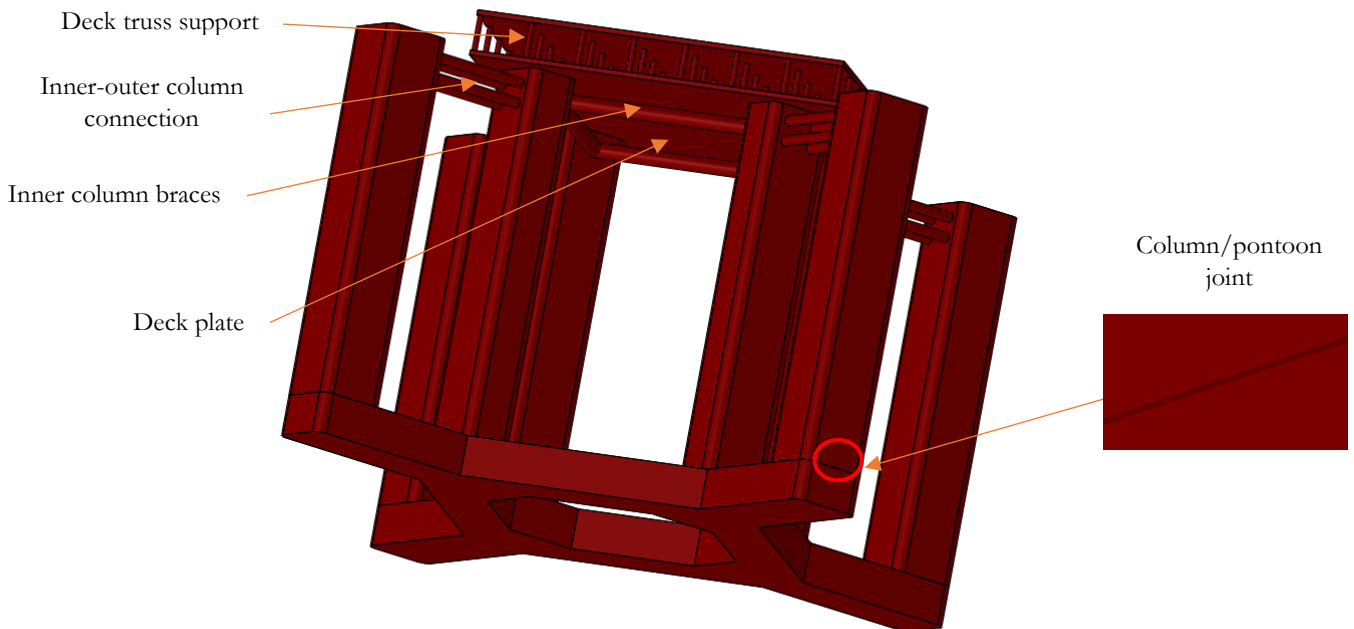


Figure 6.1 Semisubmersible parts

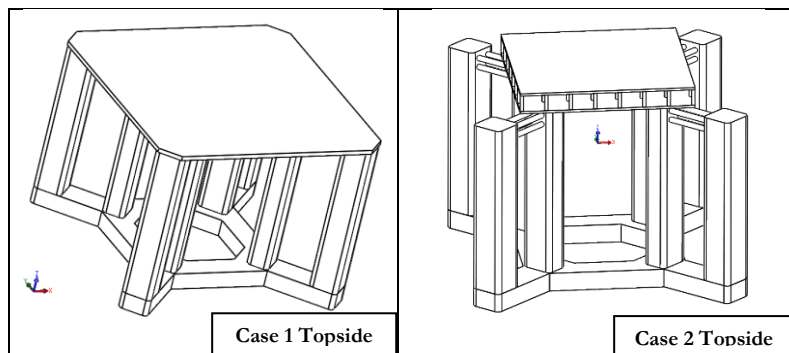


Figure 6.2 Case definition

## 6.3 Load calibration

A typical offshore structure has multiple load sources, but for assessing their strength and fatigue behaviour, the most critical loading scenarios are investigated on. Literature and industrial standards on acceptable loading conditions for assessing the strength of offshore platforms are presented in [15, 47, 130]. The loading system is addressed in their static and dynamic phases. ABS 2004 presented generally acceptable loading conditions for Mobile Offshore Units (MODU) and Floating Production Installations (FPI). The static and combined loadings are basically required for MODU, while the normal operation and severe storm scenarios are investigated for FPI; as presented in Table 6.1.

The dynamic loads are as a result of environmental conditions (wave, current and wind), while the static loads are defined with the uneven mass distribution around the structure.

**Table 6.1 Loading conditions for MODU and FPI**

Static	Combined	Normal operation	Severe storm
Forces to be considered include the mass of hulls structure and the operational loads. No water motion is considered.	The inclusion of environmental loadings to static loadings.	Considering of all working conditions; inclusion of all possible topside loads, live load, dead loads and all other operating loads.	Loadings from harsh or rough weather conditions. 100 and 1000 wave return period are considered in this case.

### 6.3.1 Mass calibration (Static loads)

The mass calibration was carried out considering two reference points; the centre of gravity and the buoyancy centre. The gravity centre been the point where the downward forces were computed from and the centre of buoyancy is where the upward thrust is calculated from. The masses are categorized into five groups;

- Buoyancy mass
- Deck mass (Materials and Facilities)
- Mass of hull steel (columns, pontoon, and internal reinforcement)
- Topside steel
- Additional mass

It is important to mention that at equilibrium (no ocean loading), the summation of the reaction forces from the mass distribution equals zero at the cut water plane, i.e., the mass of the entire structure equals the mass of the displaced volume (Archimedes principle).

### 6.3.1.1 Buoyancy mass

The mass of the displaced volume of water is regarded as the *buoyancy mass* in this case. It is a function of the density of sea water ( $1025\text{kg/m}^3$ ) and the volume of the submerged hull. The upward buoyancy force is calculated with this mass. It is denoted as  $m_b$

$$M_b = \rho_{sw} * Vol \quad [6-1]$$

$\rho_{sw}$  is the density of sea water, while  $Vol$  is the volume of the displaced water.

### 6.3.1.2 Deck mass (Materials and Facilities)

A conserved analysis was used in this study, with the basic assumption that the weight on the deck (platform) is evenly distribution at every point in time. This might not necessarily be the case during operation as the staff working on-board might move equipment around with time, but the top-deck designers we contacted during this study explained that the design is done to obtain even weight distribution. The error margin that might result from this is negligible.

A study into existing semisubmersibles was carried out to be able to effectively estimate the total amount deck mass for this study. The drilling rig and the house quarters are usually the heavy components associated with the deck mass. Recently developed semisubmersibles used for drilling purpose were designed for high payload; like Ocean Apex and Ocean Baroness were designed to accommodate 140 and 138 personnel respectively [131].

### 6.3.1.3 Mass of hull

The mass of the hull steel is the mass of steel required to build/fabricate the columns, braces, welds, and pontoon section. This involves the amount of steel plate and internal reinforcement (scantling) used. It is important to note that the liquid content within the hollow section of the hull (such as blast liquid and dead oil) are not considered.

### 6.3.1.4 Topside steel (Deck structure)

The weight of the deck structure was estimated to be between  $5.2 \times 10^6\text{Kg}$  and  $6.3 \times 10^6\text{Kg}$ . This estimation was done from the deck type selected. [132] presents the sizes (weight) of the recently installed offshore structure.

### 6.3.1.5 Additional mass

Every other mass that has not been listed in 2.1 to 2.5 above was classified under *additional mass*. Materials such as the weight of ballast liquid and riser liquid are considered as an additional mass. In this study, the value for additional mass was varied, depending on the functionality the hull was designed for. In our result analysis, we stated the occasions where additional mass were included in the analysis. Table 6.2 shows the summary of the mass calibration used in this study.

**Table 6.2 Summary of mass calibration**

Mass	Component	Magnitude
Buoyancy	Mass of the displaced water	$96.5 \times 10^6$ Kg
Deck	Facilities and utilities	$(25.1 \text{ to } 34) \times 10^6$ Kg
Hull steel	Columns, pontoon, braces & internal reinforcement	$26.72 \times 10^6$ Kg
Topside steel	Truss and plate	$9.1 \times 10^6$ Kg
Additional	Ballast liquid, dead oil,	$4.5 - 11.0 \times 10^6$ Kg
Attachments	Mooring and Risers	$10.1 \times 10^6$ Kg

### 6.3.1.6 Steel Properties

The offshore industry recommends between grades 50-80 steel for constructing drilling and production semisubmersible hull systems. The yield stress of this steel grade range is 350MPa to 550MPa. In this study, we considered the least strength; 350MPa, for safe design. Table 6.3 shows the properties of the steel material selected for the construction of the hull, for all application, discussed in this thesis.

**Table 6.3 Properties of steel**

Particular	Amount
Strength	350MPa
Density	$7850 \text{ Kg/m}^3$
Young's modulus	201GPa

### 6.3.2 Environmental load

The data for the environmental load (wind, current and wave) used in this study has been earlier discussed in Chapter 4, section 4.6. For bending and stress analysis, we have considered only wave and current loads, the effect of wind loading was assumed not to be significant in estimating/calculating the strength of the hull for MODU and FPS applications. The vortexes

generated as a result of the flow current also generate an uneven drag around the hull; as demonstrated in chapter 5.

### 6.3.3 Yield Assessment

The material yield was analysed using von Mises stress, as recommended in DNV [16].

$$\sigma_e = \sqrt{\sigma_x^2 + \sigma_y^2 - \sigma_x \sigma_y + 3 \tau_{xy}^2} \quad [6-2]$$

$\sigma_x$  = Normal stress in the X-direction,  $\sigma_y$  = Normal stress in the Y-direction and  $\tau_{xy}$  = Shear stress in the XY plane

## 6.4 Modelling

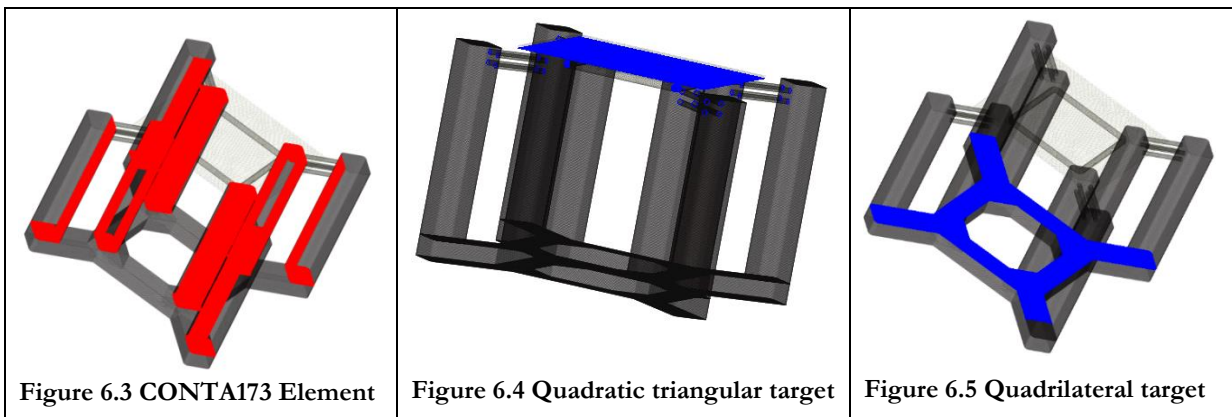
Finite element analysis was adopted in analysing the strength of the hull during rough sea weather conditions. Unlike the numerical models used for hydrodynamic response and the vortex shedding phenomenon, the model used for analysing the strength of this hull has no ‘benchmark results’ (experimental). The development of the numerical model was done in conjunction with the hydrodynamic model presented in chapter 4. In carrying out hydrodynamic analysis, the loading and boundary conditions impose challenges such as fluid separation, radiation, viscosity, but diffraction helps to simplify the effect of these challenges [61]. Some theories have been developed over the years to help circumvent the effect of these challenges; as discussed in chapter 4. The hydrodynamic diffraction model creates a set of ocean pressure on each node, as developed in chapter 4. After hydrodynamic pressures are developed, they were transferred via a script file into APDL. There is no direct recommended process of transferring hydrodynamic diffraction loadings for static analysis as it requires developing script files in text formats, and applying the pressure loading in an ocean environment via FORTRAN language. The study was carried out for shell thickness range between 0.01m to 0.05m and round fillet edges of radius 2.05m were introduced to increase the result accuracy and distribute the stresses around the plate. This will be recommended during the construction stage of this hull.

### 6.4.1 Description of ANSYS Finite Element Model

The FEA model was developed in ANSYS APDL. It is made up of a shell, 3D-solid, contact, surface, and target elements. SHELL181 was used for columns and pontoon plate, while SURF154 for surface ocean loading. The braces, inner/outer column connections, fairleads and topside trusses, were built with SOLID187, while CONTA173 and TARGE170 are used to define the interface between the bodies to take their deformation into account.

SHELL181 is a 4-node 3-D element with six degrees of freedom. Its formation is based on the fundamental thin-wall shell theories recorded in [133-136]. Some researchers have employed the use of this type of element to analyse the behaviour of plate structures exposed to ocean loadings. [137] used a 4-node shell element (S4) to investigate the buckling failure mode of semisubmersible columns under ocean loadings. The numerical set-up was developed in ABACUS, alongside an experimental study. With the element, they were able to effectively study the buckling mode of a stiffened semisubmersible column. [138] also made use of elements developed from thin-wall shell theories to investigate the hydro-elastic behaviour of ships. It also has a unique quality of easy convergence during simulation and allows easy identification of the effect of pressure distribution, the reason why it was preferred to other shell elements. The effect of plate thickness can easily be studied because it allowed alteration during coding. SOLID187 is advantageous for an irregular grid (mesh); the reason why it was used for this analysis, because of the geometric complexity experience from the inclusion of the connections, braces, topside-beams, and fairleads. Further description and functionalities of this element can be found in ANSYS release 16 reference documentation.

CONTA173 is a 3D element with 3 degrees of freedom. It was used to define the surface contact between the solid and shell elements, i.e., between shell-to-shell contact, shell-to-beam contact, and beam-to-beam contact. Figure 6.3 shows the areas around the hull where the contact elements applies. The contact elements were represented by TARGE170 as shown in Figure 6.4 and Figure 6.5. Figure 6.4 shows surface of shell-to-beam contact; columns and topside / connections. Quadratic triangular meshes where employed around these regions. For Figure 6.5, regions are shell-to-shell contacts; columns and pontoon. Linear quadrilateral meshed were used on these surfaces.



## 6.4.2 Developing Boundary Conditions

The stress distribution and concentration are controlled by the nature of boundary conditions around the hull. Developing the accurate boundary conditions for structural analysis of a semi-submerged free floating structure can be very tricky as there is no basic form of constraint on any part around the structure apart from the added mass and damping effect on the submerged part section, and the loadings around the structural component is not the same (static and dynamic cases). The outer columns receive the mooring loadings at the fairleads and have no direct contact with the topside (for case 2 topside), while the inner columns have direct loadings from the topside and no connection with the mooring weight. The ocean loading cuts through the columns 28.04m from the top at base case configuration (deep-draft), and the wave forces are distributed around the structure from this plane. The motion in the 6 degrees of freedom and the stiffness in each of these directions are therefore considered to be the factors responsible for controlling the boundary condition for an accurate structural analysis.

### 6.4.2.1 Displacement

We considered the translational and rotational displacement components for dynamic load condition. The reason for this was that the response analysis showed movements from the cut-water plane and the hull base; explained in chapter 4. The displacement parameters were computed using time series method carried out in Orcaflex and AQWA, and the results were recorded over a specific time period. The data was arranged in a tabular form, (as presented in Figure 6.7) converted to an 'xml' file and used as boundary conditions during the build-up of the numerical model. This form of boundary condition involves motions in all 6DOF, and this replicates the actual scenario of the structure during environmental loading. Figure 6.6 and Figure 6.7 shows the setup for displacement measured from the cut-water plane, for 100 seconds, at  $0^\circ$  flow angle. The motion was extracted from the response analysis computed in ANSYS. Figure 6.8 shows a snapshot from ANSYS of the horizontal displacement of the hull in the X-direction for 2000 seconds, using a time-step of 0.01 (for which Figure 6.6 was extracted.) From this result, it is evident that the hull experiences a nonlinear displacement.

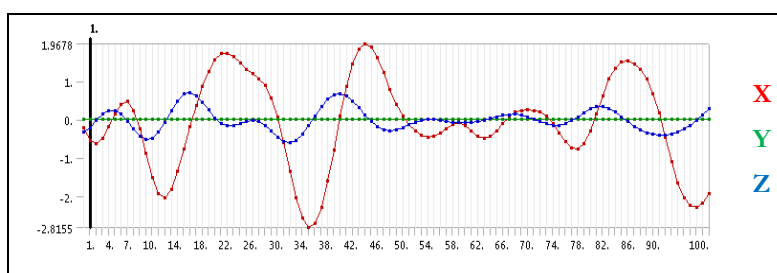


Figure 6.6 X, Y and Z response for 100 seconds (m)



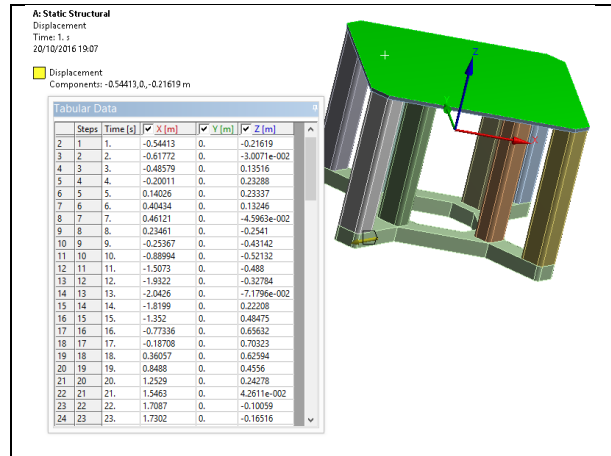


Figure 6.7 Nonlinear boundary displacement in X, Y and Z direction for 0° flow angle

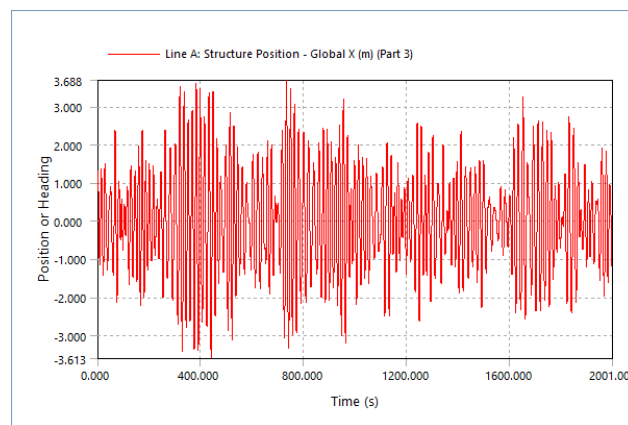


Figure 6.8 Displacement in the X-direction; Snapshot from ANSYS time response analysis (m)

#### 6.4.2.2 Hydrostatic Stiffness: Cut-Water Plane, COG, and Column Base

The cut water plane stiffness shows the resultant relationship between the structural load and the weight generated from its displacement (also known as buoyancy) to the motion characteristics (heave, roll and pitch) from the centre plane to which all the forces act. It is derived from the early analytical formulation of the equation of motions governing a single degree of freedom system. For a rigid body motion analysis, the stiffness is a fundamental property which is required as a boundary condition around the affected area. The resultant equation is made of a 3 X 3 matrix, derived from a 6 X 6 matrix, as shown in Equation 6.2 [139]. The zero elements recorded in the surge, sway and yaw (1, 2 and 6) describe the hydrostatic stiffness on the horizontal plane of a free floating body.

$$K_{hys} = \begin{bmatrix} 0 & 0 & 0 & 0 & 0 & 0 \\ 0 & 0 & 0 & 0 & 0 & 0 \\ 0 & 0 & K_{33} & K_{34} & K_{35} & 0 \\ 0 & 0 & K_{43} & K_{44} & K_{45} & K_{46} \\ 0 & 0 & K_{53} & K_{54} & K_{55} & K_{56} \\ 0 & 0 & 0 & 0 & 0 & 0 \end{bmatrix} \quad [6-3]$$

For a free floating hull system, when the stiffness is completely due to the hydrostatics (no mooring or riser system),  $K_{46}$  and  $K_{56}$  are equal to zero. Equation 6-3 reduced to Equation 6-4.

$$K_{hys} = \begin{bmatrix} K_{33} & K_{34} & K_{35} \\ K_{43} & K_{44} & K_{45} \\ K_{53} & K_{54} & K_{55} \end{bmatrix} \quad [6-4]$$

$$K_{33} = \rho * g * A_{ws}^z \quad [6-5]$$

Where  $K_{33}$  is the stiffness in heave degree of freedom and  $A_{ws}$  is the area of the submerged part of the hull (see chapter 4 Table 4.3)

$$K_{34} = \rho * g * A_{ws}^y * \delta_y \quad [6-6]$$

Where  $\delta_y$  is the distance between the mid-point of the cut water plane and the centre of gravity in the Y-direction.

$$K_{35} = \rho * g * A_{ws}^x * \delta_x \quad [6-7]$$

$\delta_x$  is the distance between the water plane mid-point and the centre of gravity in the X-direction.

$$K_{43} = K_{34} \quad [6-8]$$

$$K_{44} = \rho g \left[ \left( \int_{A_{ws}} y^2 dA \right) + (\delta_{zcg} * Vol.) \right] \quad [6-9]$$

Where  $\delta_{zcg}$  is the Z-distance from the centre of gravity to the cut-water-plane and *vol.* is the volume of the displaced hull.

$$K_{45} = \rho g \int_{A_{ws}} xy dA \quad [6-10]$$

It is important to note  $A_{ws}^x$  is equal to  $A_{ws}^y$ , and represented as  $A_{ws}$  in Equation 6-10.

$$K_{53} = K_{35} \quad [6-11]$$

$$K_{54} = K_{45} \quad [6-12]$$

$$\text{For a symmetric hull, } K_{55} = K_{44} \quad [6-13]$$

$K_{46}$  and  $K_{56}$  are the stiffness components offered by external components such as moorings and risers. Free-floating hull conditions have been considered in this study, the effect of  $K_{46}$  and  $K_{56}$  were therefore neglected. [4] modelled the cut-water plane stiffness on the heel of the columns. At the time of this research, we don't believe this is correct. The reason for this is because the hydrostatic stiffness at the cut-water level is different from the hydrostatic stiffness at the heel of the columns; from Equation 6-2 to Equation 6-11. The value for  $\delta_x$ ,  $\delta_y$  and  $\delta_{z_{cg}}$  are different for both planes. The stiffness at the heel of the columns was calculated, and the results are shown in Table 6.4.

The disadvantage of using stiffness method is that excessive deformation is experienced around the pontoon plate, because reinforcement was considered as distributed load (dead load) at this stage. The reason for this is that the set-up for this analysis was created to identify areas where high reinforcement will be needed and adequate material selection for it. For column analysis (where the effect of the pontoon is neglected), the stiffness was modelled at the heel of the columns as recommended by [4]. We compared the results obtained using this method and the displacement method (for column analysis), and the results were the same. But the advantage of using this method is that it takes less computational time when compared with the displacement method. We also considered the stiffness from the centre-of-gravity.

### 6.4.3 Joint Design

The 2014 DNV certification of PC-Semi for dry-trees installation in deep waters specified 'column-pontoon joint sizing' as a design phase that requires further investigation, because of the slenderness ratio of the columns. In our FE analysis, we have considered bonded-interface for the joints around the hull; no form of separation between them. The normal stiffness factor of the sort of contact type is generally determined by the weld type and strength. At the time of this study, no information was available on this. ANSYS 17.0 recommended a factor of 10 for normal stiffness for bonded contact, and we have adopted this value for our analysis.

**Table 6.4 Stiffness matrixes**

	Heave	Roll	Pitch
<b>Cut- Water Plane</b>			
<b>Heave</b>	12977894N/m	-0.034764N/°	-0.7288118N/°
<b>Roll</b>	-1.9918276N.m/m	-180024000N.m/°	52.457371N.m/°
<b>Pitch</b>	-42.757839N.m/m	52.457371N.m/°	-180024000N.m/°
<b>Centre of Gravity</b>			

<b>Heave</b>	12977894N/m	-0.034764N/°	-0.7288118N/°
<b>Roll</b>	-1.9918276N.m/m	347826000N.m/°	52.457371N.m/°
<b>Pitch</b>	-42.757839N.m/m	52.457371N.m/°	347826000N.m/°
	<b>Heel of Columns</b>		
<b>Heave</b>	12977894N/m	-0.034764N/°	12977894N/m
<b>Roll</b>	-1.9918276N.m/m	569193000N.m/°	-1.9918276N.m/m
<b>Pitch</b>	-42.757839N.m/m	52.457371N.m/°	569193000N.m/°

### 6.4.4 Mesh Study

The mesh study was developed to understand its effect on the result quality. The same element size was used for all the columns (Figure 6.9). The mesh size was gradually reduced from 1.15m to 0.25m, for a 0.15 interval, an recorded in Table 6.5. A variation in the maximum equivalent stress of 129MPa and 155MPa was recorded for static analysis, and the value of maximum equivalent stress gradually increased from 218MPa to 256 MPa for dynamic case. Table 6.5 shows a summary of the mesh study carried out for dynamic analysis. During the mesh refinement, the column elements were studied to ensure smooth transission around the curved edges and the joint areas. There is a densed element concentration on the columns from 1.15m element size to 0.25m element size, as presented in Figure 6.10 and Figure 6.11.

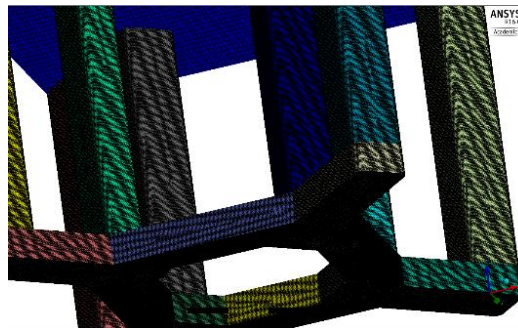


Figure 6.9 Hull mesh

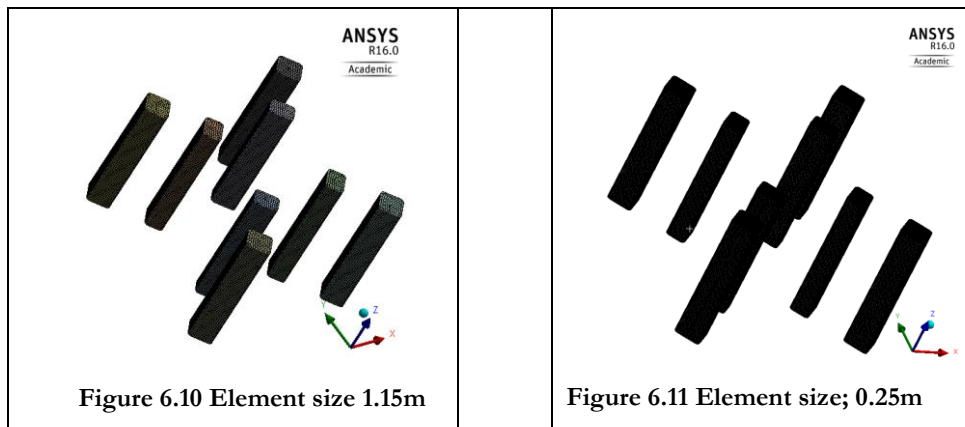


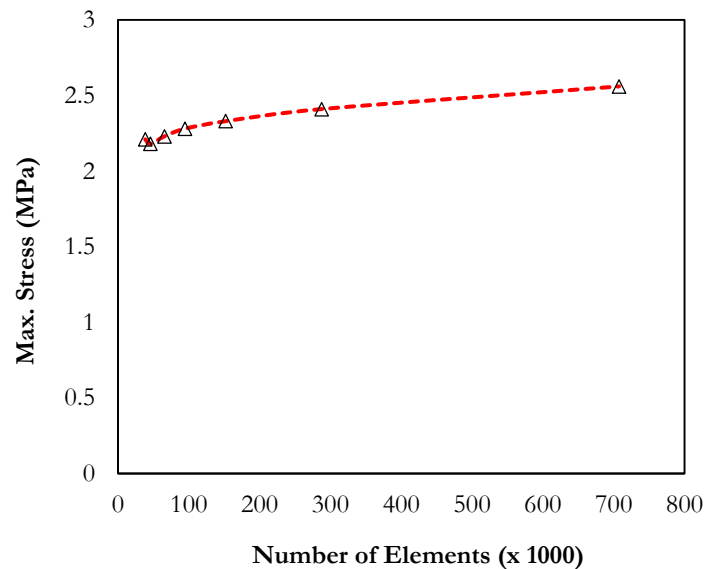
Figure 6.10 Element size 1.15m

Figure 6.11 Element size; 0.25m

**Table 6.5 Column mesh study for dynamic analysis**

Element size	No. of Nodes	No. of Elements	Max. Skewness	$\sigma_{e_{max}}$ (MPa)
1.15	48481	38507	0.8314	221
1.00	55618	45630		218
0.85	75672	65667		223
0.70	104297	94327		228
0.55	161912	151962		233
0.40	297197	287252		241
0.25	717390	707601	0.78329	256

Table 6.5 is graphically represented in Figure 6.12. The graph shows a steady small growth in maximum stress between one hundred thousand and seven hundred thousand elements. The range falls between 220MPa and 260MPa. A further increase in the number of elements will lead to significant increase in computation time and cost, with little effect on the maximum equivalent stress. The average value for mesh size (0.7m) was therefore adopted for this study, to help eliminate the excesses of further refinement.

**Figure 6.12 Column mesh study**

## 6.5 Loads on Columns

As earlier cited, the columns are hollow structures. The internal space is often partitioned into different sections, and is used for liquid storage (ballast liquid, drilling mud, dead oil). The stresses on the columns are therefore due to the internal and external forces. In this study, we have considered only the external forces, as the standard for designing semisubmersible hull in deep waters, recommends only the external loadings.

Figure 6.13 and Figure 6.14 shows schematic representations of the external loadings on the inner and outer columns respectively. The weld connections at the top and bottom of the columns were modelled differently. Ideally, the weld connection at the top ought to be modelled with the weld stiffness, at that joint. This again is relative to the type of topside used. For a truss-topside (where beams are used to construct truss frames between columns), there might be no centralized joint at the top of the columns. To circumvent for this complexity, a flexible approach was adopted. A bonded-interface was established between the bottom steel plate of the topside and the column top; for both topside cases. This implies that the columns and the topside act as a single unit at the top.

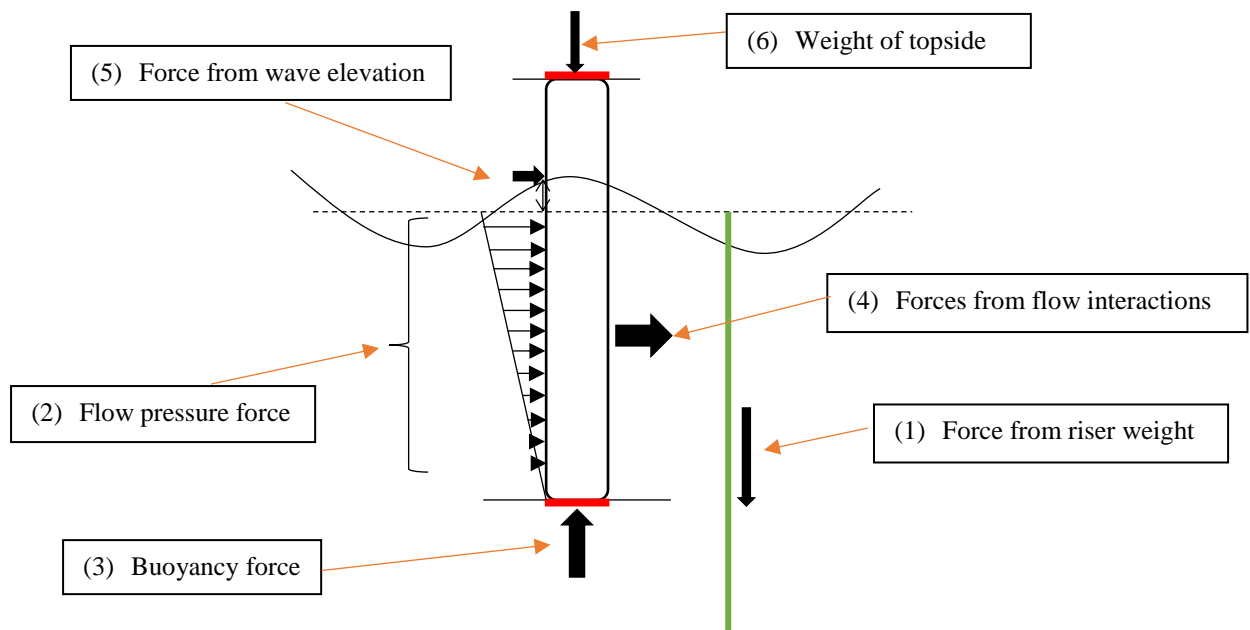
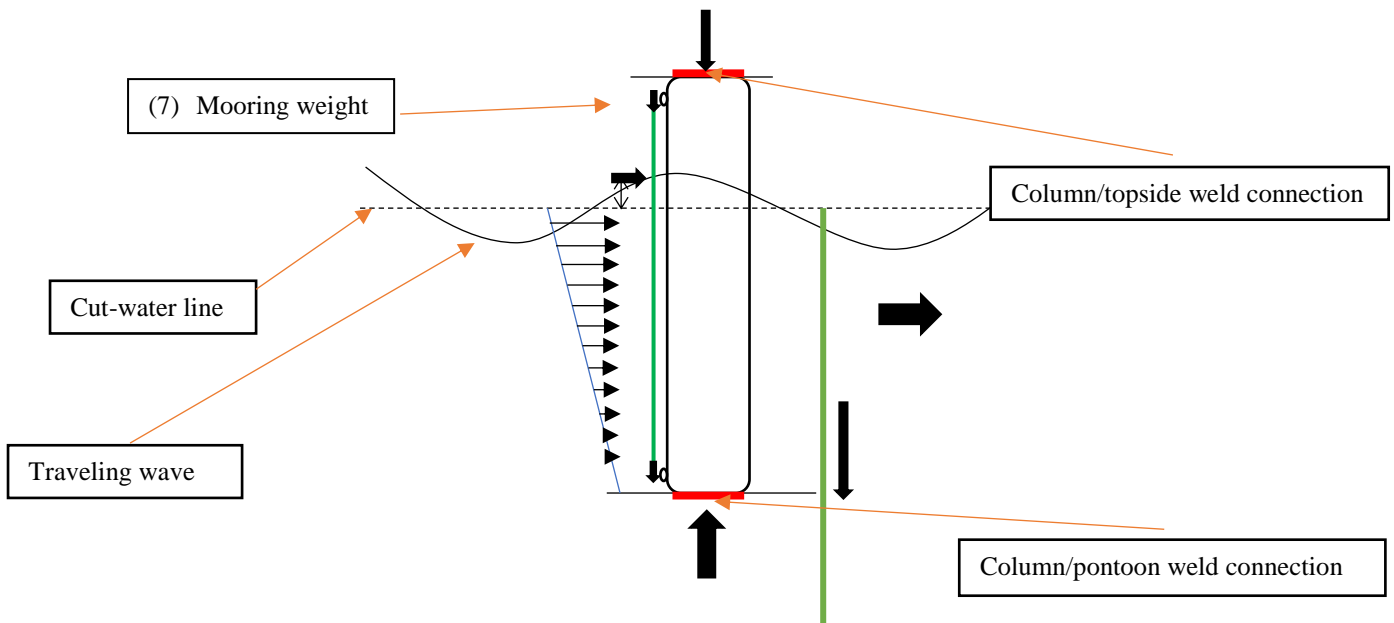


Figure 6.13 External force illustration on inner columns



**Figure 6.14 External force illustration on outer columns**

This wasn't the case for the weld between the pontoon and the column. Further studies have previously been recommended in [1, 4] on sizing this joint, because of the slenderness ratio of these columns, as wave loading will create significant bending on them, which will exert high stresses on this joint. As at the time of this research, there is nothing in the public domain that suggests the thickness and properties of this joint. Conventionally, design engineers try to relate the properties of the joint to the hydrostatic stiffness, because it is submerged in water. This is a very realistic approach; as the mass properties of an object in space is different from when it is in water. In this study, we developed the hydrostatic stiffness of the hull at that point (45.42m below the water plane; the result is presented in Table 6.4), and modelled the joint with it. The columns are fabricated from steel plates and are therefore represented as shell structures. Emphasis is placed on yielding and buckling stresses in calculating and estimating stability and failure modes.

## 6.6 Stress Assessment: Working Stress Design (WSD)

The offshore industry has different recommended methods for developing acceptable stress profile around a typical semisubmersible platform, to understand and assess its strength. [16] presented the Working Stress Design (WSD) method, where the stress generated at different load conditions are expected to be smaller than the product of the strength of the material and some usage factors which are basically a function of the material strength, its loadings and the buckling mode of deformation. The load resistance factor design approach (LRFD) is also a generally accepted method for determining the stress level on offshore structures. This method assesses

the level of safety of a structure by comparing the effect of the loadings and the structural resistance. The structure is categorized as ‘safe’ if the load effect is less than the structural resistance [140]. The Working Stress Design method was adopted for this study, because of the nature of the loading conditions considered. The permissible usage factor is obtained from the product of the basic usage factor presented in Table 6.6, and a range of coefficient as presented in Table 6.7.

$$\eta_p = \beta * \eta_0 \tag{6-14}$$

Five loading condition were defined in [16] when considering the Working Stress Design method.

L<sup>1st</sup>: Function loads

L<sup>2nd</sup>: Environmental loads and functional loads; environmental loads are defined in chapter 4

L<sup>3rd</sup>: Accidental loads and functional loads

L<sup>4th</sup>: Highest value of L<sup>2nd</sup> and L<sup>3rd</sup> per calendar year

L<sup>5th</sup>: L<sup>4th</sup> for heeling and flooding conditions

**Table 6.6 Basic usage factors**

Load Conditions					
Loads	L <sup>1st</sup>	L <sup>2nd</sup>	L <sup>3rd</sup>	L <sup>4th</sup>	L <sup>5th</sup>
<b>η<sub>0</sub></b>	0.60	0.80	1.00	1.00	1.00

**Table 6.7 β for shell buckling as presented in [16]**

Type of Structure	λ ≤ 0.5	0.5 < λ < 1.0	λ ≥ 1.0
Girders, beams stiffeners on shells	1.0	1.0	1.0
Shell of single curvature (cylindrical shells, conical shells)	1.0	1.2 – 0.4λ	0.8
Spherical shells	0.8	0.96 – 0.32λ	0.64

Where λ is the slenderness parameter, which is the ratio of minimum yield stress (f<sub>Y</sub>) and the elastic buckling stress (f<sub>E</sub>) for a particular mode.

$$\lambda = \frac{f_Y}{f_E} \tag{6-15}$$



On the buckling of the columns, an eigenvalue analysis is recommended to estimate the topside load effect on their failure mode. A complete hull scantling and reinforcement are required before buckling analysis can be carried out, and at the time of this research, ANSYS do not have the capacity to perform FEA on a completely reinforced PC-Semi. After the column reinforcement, the buckling stresses are less likely to exceed the specified minimum yield stress of the steel. Therefore, for this study, we have assumed that  $\lambda \geq 1.0$ ;  $\beta$  is therefore equal to 0.8.

## **6.7 Analysis and Description of the Hull Structure Finite Element Models: Column Stresses**

### **6.7.1 Case 1 Hull Type**

The columns were checked for yielding to identify areas where high reinforcement will be required. Maximum stresses ( $\sigma_e$ ) were observed around the pontoon section for this topside case; as shown in Figure 6.15. Some operating deep-draft semisubmersibles in deep waters are designed with this topside formation (Petrobras 55). Results from this study have shown that for a PC-Semi (during ocean loading conditions), more stresses are concentrated on the pontoon section for this topside design. Figure 6.15 showed that the columns do not necessarily achieve any reduction in stress level. Apart from the large topside associated with this topside type, the close distribution of stresses around the entire eight columns is also a significant advantage of this hull type, as suggested by Figure 6.15. Again, the round fillet edge was observed to be very helpful in distributing the stress on the plate. Similar behaviour can be observed for the rear edges of the outer columns. Another important finding is the stress pattern at the base of the inner columns. The effect of mesh refinement on the stress distribution on these areas was checked (Figure 6.16, Figure 17 and Figure 18), and some changes were observed on the stress pattern on the columns. As the mesh size gradually reduced (from 1.15m to 0.25m), the high-stress distribution observed at the base of the inner columns (case 1 topside) gradually concentrated around its edges. The mesh refinement around these areas showed very fine and smooth grid progression around the regions. It is important to mention that for a 0.05m plate thickness, and an overall topside weight of 26500metric tonnes, the maximum stress around the columns where observed to be below the steel strength, before the application of the WSD check, as recommend by [16]. This is the best possible situation, though, as the thickness of the steel plate used for construction does not exceed 0.05m.

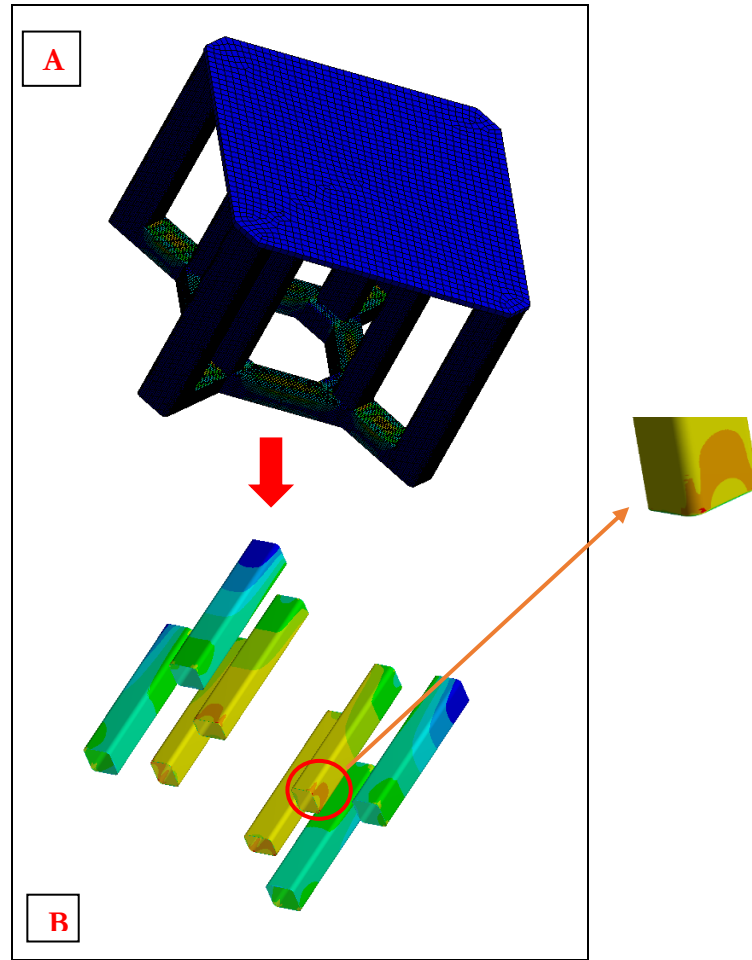


Figure 6.15 Column stress study for case 1 topside

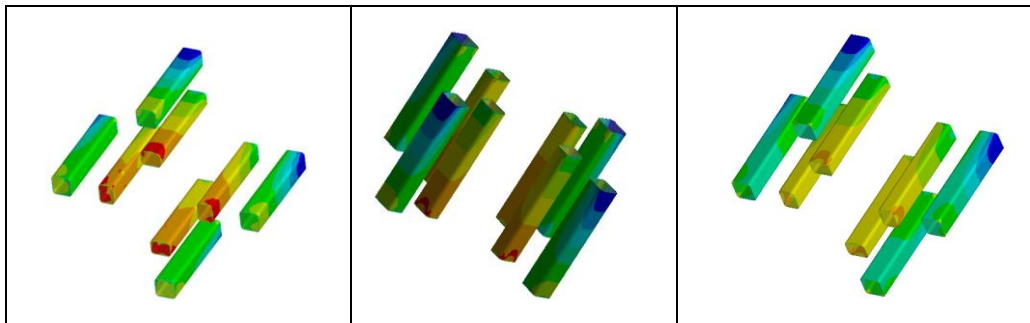


Figure 6.16 1.15m Mesh Size

Figure 6.17 0.70 Mesh Size

Figure 6.18 0.25 Mesh Size

### 6.7.2 Case 2 Hull Type

From the recommendations in [4], there is an inclusion of braces, introduction of inner/outer column connection, and a reduction in the topside operating area. Case 2 hull was built on that premise.

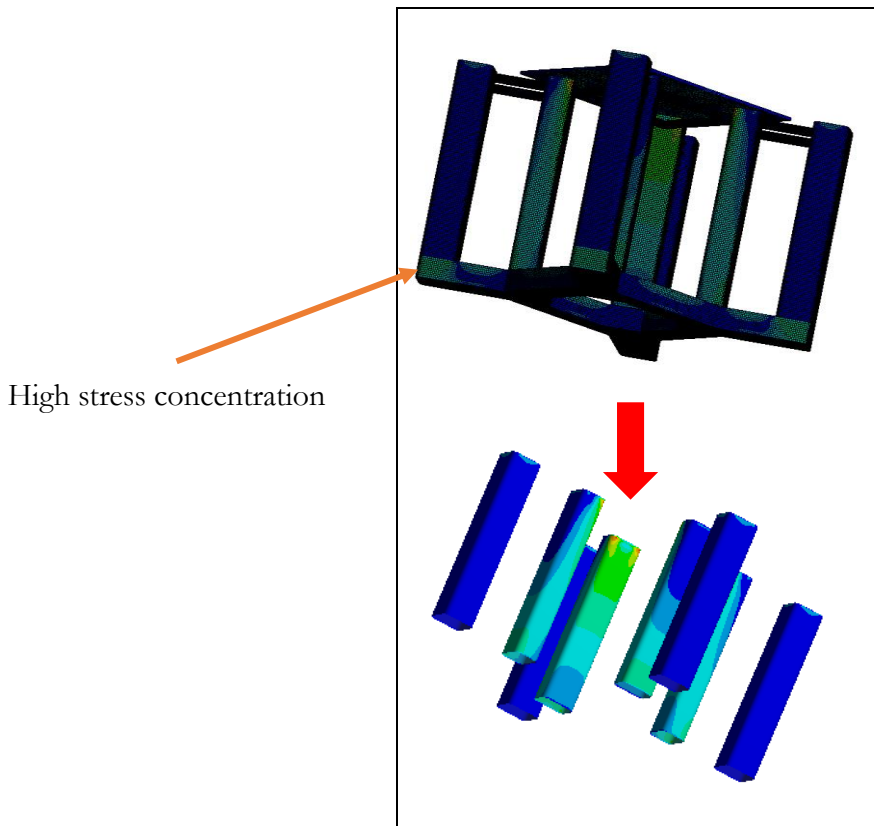


Figure 6.19 Hull stress distribution from case 2 topside

The results obtained from this study showed a significant reduction in the overall stress distribution around the eight columns, when compared with the previous analysis presented in Figure 6.15. Findings from this study have shown that these recommendations will lead to high-stress concentration on the pontoon section below the outer columns (see Figure 6.19). From series of visual/video studies, the bending and twisting created on the inner columns are transferred to the outer one through the connections, in turn creating high stresses underneath them.

## 6.8 Column Stress Assessment

The maximum equivalent stresses obtained on the columns from the mesh study for static analysis ( $L^{\text{st}}$  load case) ranges between 129MPa and 155MPa, while it falls within 218MPa and 256MPa for  $L^{\text{2nd}}$  load case. Their working stress is presented in Table 6.8

**Table 6.8 Working stresses for static and dynamic load cases.**

For load case L<sup>1st</sup>,  $\eta_0$  is 0.6. For  $\beta$  as 0.8, the permissible usage factor is  $0.6 \times 0.8 = 0.48$ . Considering the steel strength as presented in Table 6.3, the working stress for static analysis is expected to be  $\leq 0.48 \times 350 \times 10^6 = \mathbf{168MPa}$ .

For load case L<sup>2nd</sup>,  $\eta_0$  is 0.8. For  $\beta$  as 0.8, the permissible usage factor is  $0.8 \times 0.8 = 0.64$ . Working stress is  $\leq 350 \times 0.64 = \mathbf{224MPa}$

For load case L<sup>3rd</sup>, L<sup>4th</sup> and L<sup>5th</sup>,  $\eta_0$  is 1.0. For  $\beta$  as 0.8, the permissible usage factor is  $1 \times 0.8 = 0.8$ . Working stress is  $\leq 350 \times 0.8 = \mathbf{280MPa}$

The stress distribution on the columns exceeds the permissible stress level from environmental loading, for WSD assessment. Scantling will significantly reduce the level of stress around the columns.

## 6.9 Chapter Summary

A nonlinear finite element analysis has been presented in this chapter, to assess the strength of a PC-Semi under hydrodynamic and static operating loads. The amount of scantling and column reinforcement required will be estimated from the results obtained from this analysis.

The numerical model was developed with shell and solid elements, and CONTA173 and CONTA174 were used to model the surface contact between bodies. Novel boundary formulations that represent real life scenarios of offshore floating hulls were employed in this study. This involves the inclusion of the hydrostatic and hydrodynamics behaviours, of the hull during FE-analysis. The hydrostatic stiffness on the cut-water plane, the centre of gravity and the column heel, where modelled accordingly, and modelled on their respective plane. The hull response developed from time-response analysis was also included, to understand the effect of hydrodynamic response on the stress distribution of a PC-Semi.

The result showed a comparative advantage of small truss topside design to a fully covered design. The inclusion of braces and connections between the columns also helped to distribute the stresses around the structure. Apart from distribution, there was a significant reduction in the stress level on the columns for smaller topside than a bigger one, irrespective of the advantages (wider operating area) offered by the bigger topside. The less stress on the columns has suggested a reduced amount of steel will be required for reinforcement during scantling. Maximum stress

concentration was observed on the inner column for both topside cases, with extra reinforcement needed around the top and bottom sections, depending on the type of joint adopted during construction.

The Working Stress Design method was employed to assess the level of stress level on the hull as recommended by DNV. Apart from static load case where only the operating loads are considered, the stress distributions obtained around the hull for all other load condition indicated the need for adequate hull reinforcement. It also enabled us to highlight the regions where high steel reinforcements will be required.

# Chapter Seven: Recommendations for Design Improvement

## 7.1 Introduction

The design of paired column semisubmersible hull as presented by Houston Offshore Technology and Research Partnership to Secure Energy for America, cannot be used for sea depths below 2000 meters, and cannot be applied as foundation system to offshore floating structures such as wind turbine. But from the results presented in chapters 3, 4, 5 and 6, we might be able to recommend the draft design for these applications, as a more detailed description of its dynamics and operation has been studied. Furthermore, this project also involves ways of achieving weight reduction with semisubmersible hull formations. Offshore conventional practice applies the use of composite materials for the design of superstructures and topside facilities in achieving weight and maintenance reduction. Because the hull columns are load-carrying-structures, there is less possibility of replacing their steel plates with composite ones. A more realistic way of reducing the column weight is by 'using a light weight material for hull reinforcement (scantling)' during construction. The results recorded in chapter 6 can be used for such recommendation.

In this chapter, we have discussed future designs of PC-Semis with the results obtained from this study. Ways to improve its heeling moment (stability) for shallow draft scenarios have been highlighted, alongside its translational heave motions. Designs for scantling, joints, and topside weight were also discussed.

## 7.2 Improving Stability

The stability requirement for floating hull systems as recommended by HSE, ABS, IMO and DNV cited a positive metacentric height for all cases of hydrodynamic action on the hull, alongside a level of rotation (Figure 7.1 shows a description of the angle of rotation). These two parameters are controlled by the hull's translational motions in the X, Y, and Z directions, and the rotational behaviour around these directions. Results obtained from these motions have been presented in chapter 4 of this thesis. Table 7.1 shows a summary of that study.

**Table 7.1 Summary of global performance**

	Survival	Extreme
--	----------	---------

Case 1		
Maximum heave displacement	30.43m	11.18m
Maximum rotation	4.0 <sup>0</sup>	1.61 <sup>0</sup>
Case 2		
Maximum heave displacement	11.15m	4.85m
Maximum rotation	6.17 <sup>0</sup>	4.06 <sup>0</sup>
Case 3		
Maximum heave displacement	6.33m	2.22m
Maximum rotation	6.12 <sup>0</sup>	3.49 <sup>0</sup>
<b>Effect of wave-current interactions</b>		
<ul style="list-style-type: none"> <li>○ Non-uniform effect for hull RAO for all draft sizes; between 0.5m/s and 2.5m/s current velocities</li> <li>○ At resonance, heave response increases with draft size for wave (regular) - current interaction. Although this was observed to occur at different current velocities, for different draft sizes.</li> </ul>		

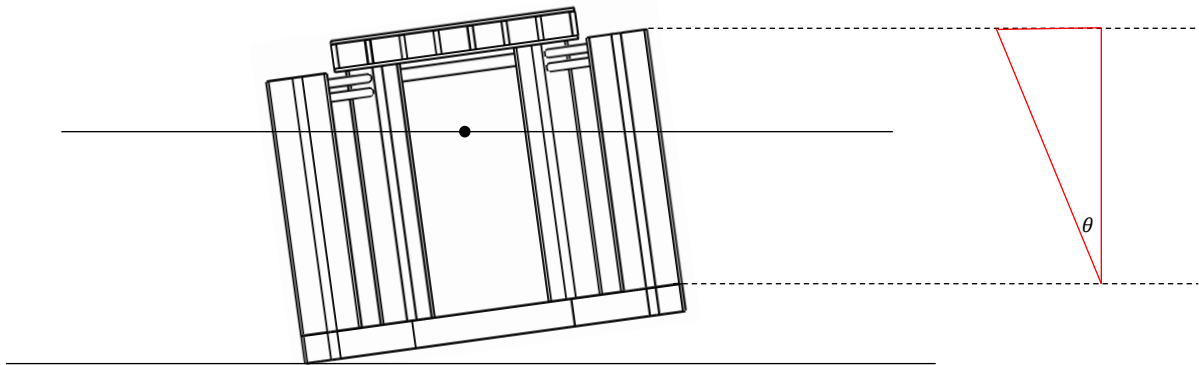


Figure 7.1 Calculating for rotation

### 7.2.1 Design alteration for roll improvement

Key observations;

- Motion increases between 0<sup>0</sup> and 90<sup>0</sup>, with maximum values recorded at 90<sup>0</sup>.
- RAO moment has nonlinear relationship with draft size.
- Satisfies HSE and DNV stability standard for heeling moment for intact condition.

High roll motions can lead to significant heeling angles, which can result in an overturning of the hull. [141]. For us to guarantee the stability of the hull under roll motion, we have investigated the parameters on which the roll motions depend. The first study conducted was the relationship between the roll RAO and the flow angle, it was observed that for low frequency wave motions (resonance frequency), roll moment increase from 0<sup>0</sup> to 90<sup>0</sup>, as illustrated in Figure 7.2. This is not necessarily the case for higher wave frequencies, but the extent of roll moments recorded at such

frequencies was observed not to be significant in estimating the stability of the hull. The symmetric nature of the hull geometry around its four corners generated an inverse relationship between the roll and pitch motions for one-fourth of the entire flow angle ( $90^\circ$ ). At  $90^\circ$ , the roll motions are the same as the pitch motion recorded at  $0^\circ$  flow angles. The inclusion of structural attachments such as moorings and riser might alter these dynamics but the alteration is expected to be small. Nonetheless, design engineers are advised to investigate the extent/effect of structural attachments on for any particular application of this hull, before proceeding to construction. From experimental and numerical investigations of low-frequency row motions of conventional four column semisubmersible, [110] concluded that roll angle is generated by the mean drift moment, and this has a linear relationship between 15m and 17m draft conditions; as the draft increases the roll moment reduced. This study has suggested that the case is not always linear for a PC-Semi, as discussed in chapter 4 of this thesis. Figure 7.4 shows the relationship between the Roll RAO for the three draft cases defined in chapter 4.

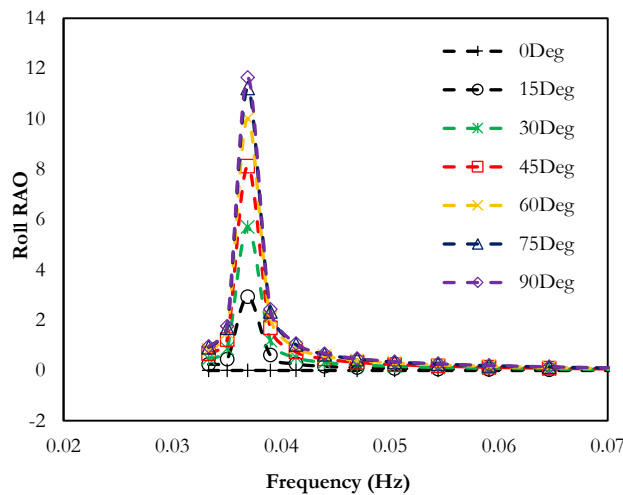


Figure 7.2 Relationship between flow angles and roll motion for 53.34m draft size

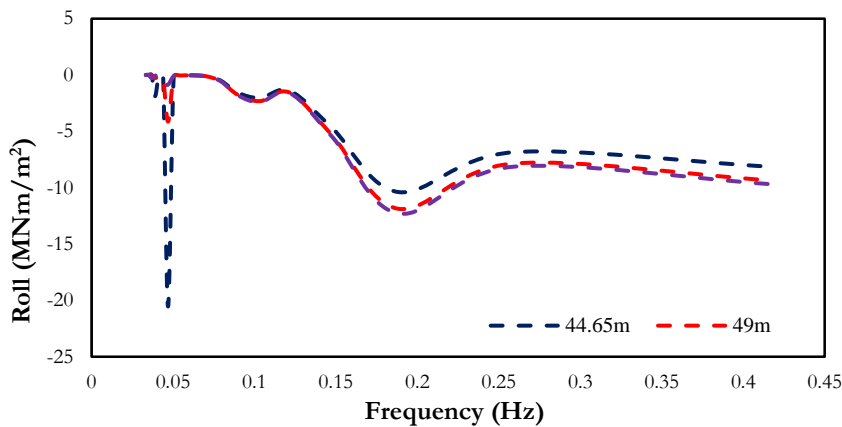
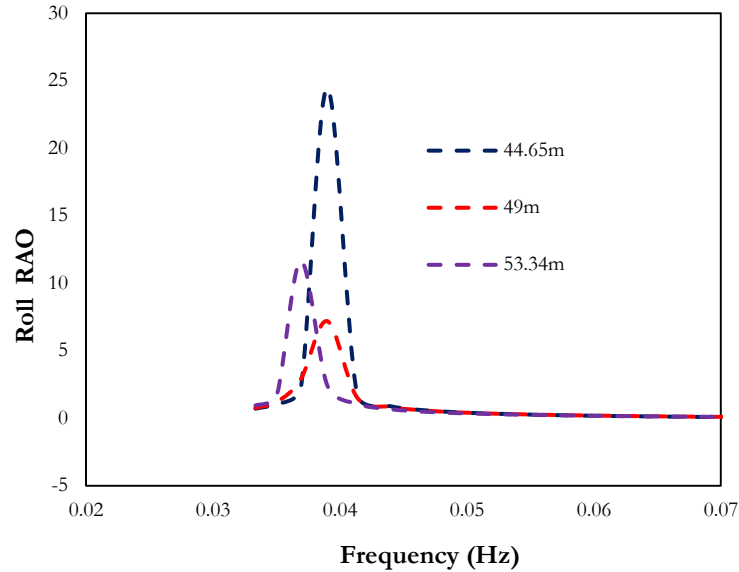


Figure 7.3 Drift roll-moment at  $90^\circ$  flow angle





**Figure 7.4 Draft effect on roll RAO for 90° flow angle.**

From Figure 7.3, it is evident that maximum roll moment does not occur for smaller draft size for all wave frequencies. Specifically, the maximum moment only occurs for smaller draft size at the resonance frequency; and very low wave frequencies (below resonance). For all other wave frequencies, smaller draft size is likely to have lesser roll moment. Reconfiguration for roll optimization is therefore done only for resonance frequency, and low-frequency wave responses, despite the fact that the hull is designed to operate outside the resonance frequency range.

After a careful study of the roll motions for different draft sizes, flow orientations and wave frequency range, it is confirmed that the roll performance of a Pc-Semi is highly favourable, when compared to any other form semisubmersible. Although in applications where roll improve is required, some recommendations have been postulated in this study.

- i. Load redistribution can significantly improve the roll performance of a PC-Semi.
- ii. The alteration of the draft size can also help to improve the roll performance of this hull.

### **7.2.2 Design alteration for heave improvement**

The results presented in this thesis (including other reports on this hull) have shown that reduced heave motion is obtained on a PC-Semi because of its dynamic behaviour from ocean loads. In reality, this is not actually the case for all draft sizes. To be specific, low heave displacement on a PC-Semi hull can only be obtained in its base-case or deep-draft configuration. Immediately the draft is altered, the response gradually becomes what is obtainable in conventional deep-draft semis. A summary of the results discussed in chapter 4 section 4.6.4, is presented in

Figure 7.5. Further reconfiguration or design alteration might, therefore, be required if it is to be applied for sea depths below 2000m, or for foundation systems.

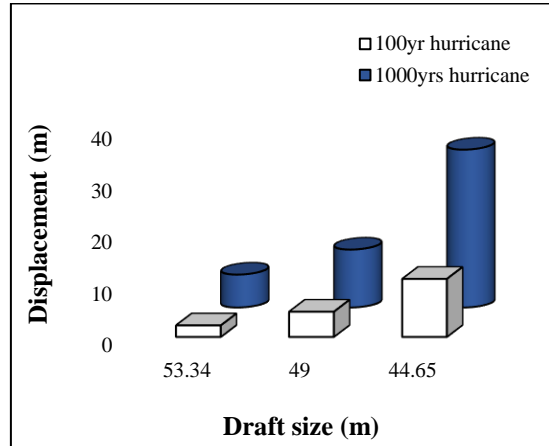


**Figure 7.5 Heave offset study for hurricane conditions; extreme and survival conditions**

Figure 7.5 shown 11.142m heave displacement for 1000-years hurricane weather conditions when the draft size is reduced from 53.34m to 49.0m. This value exceeds the stroke limit of top-tension risers. With this amount of downward displacement, the issue of deck slamming is of concern. Further reduction in heave motion on this hull can be achieved from the following;

**I. Column design recommended by [3]**

[3]presented a novel method for optimizing the weight and heave motion of a semisubmersible floating production unit, by altering the column geometric properties. The conventional straight column was sub-divided into 10 parts as shown in Figure 7.6. They estimated the size of each part for a set of mathematical relations, which they developed.

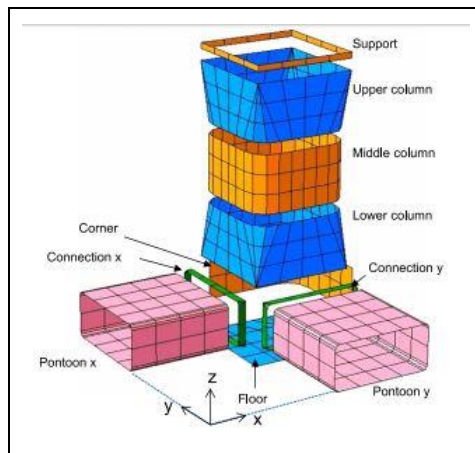


**Figure 7.6 Column design presented by [3]**

The report suggested that an increase in hull weight from column alteration can lead to a reduction in heave motion. As can be observed in Figure 7.6, the upper, middle and lower parts of the column are of different geometry. This will redistribute the added mass parameter around the submerged section, which will eventually create more mass/weight below the region of the submerged section. This method may be applied during the construction of PC-Semi.

## **II. Pontoon plate enlargement**

Apart from column alteration, another way to achieve heave reduction on a Pc-Semi is by improving the added mass parameters on the submerged part of the hull; i.e., pontoon enlargement. The discussions on drag effect on the hull presented in chapter 3 and chapter 5 cited the pontoon section to be responsible for one-third of the entire drag on the hull. The centralized nature of the pontoon system can remain the same with a slight increase in its top section. This can lead to a small increase on the columns/pontoon drag ratio, increase the plate-like behaviour of the pontoon, in turn, decreases the entire heave response of the hull.

At the time of this study, this is speculated as a recommendation from the results obtained for drag relationships. Further investigation will be required before any form of conclusive recommendation can be drawn from this.

## **7.3 Strength Improvement**

The columns have the ability to behave like independent structures from their uniaxial compressive loading conditions. This will reduce the overall strength of the hull. Jun Zou introduced inner column braces and connections between the inner and outer columns to help improve its strength (see Figure 7.7 and Figure 7.8). The FE analysis presented in chapter 6 showed that these inclusions can be very effective, although specifications for their design and construction have not been recommended in previous studies. In this study, we have adopted hollow steel circular tubes have been used for both reinforcements. It is more economical in terms of materials.

Figure 7.8 shows the stress study on the inner column braces. Stress concentration was recorded around the contact surface between the columns and the brace, for all four edges. Recommendation for material thickness is therefore required for this connection depending the payload adopted.

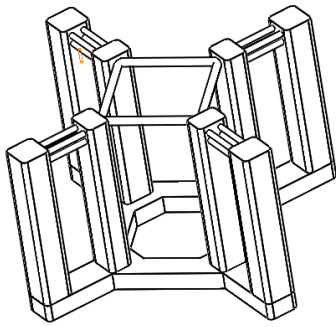


Figure 7.7 Hull frame

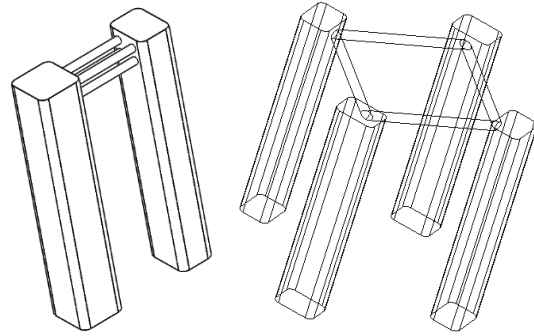


Figure 7.8 Connections and braces

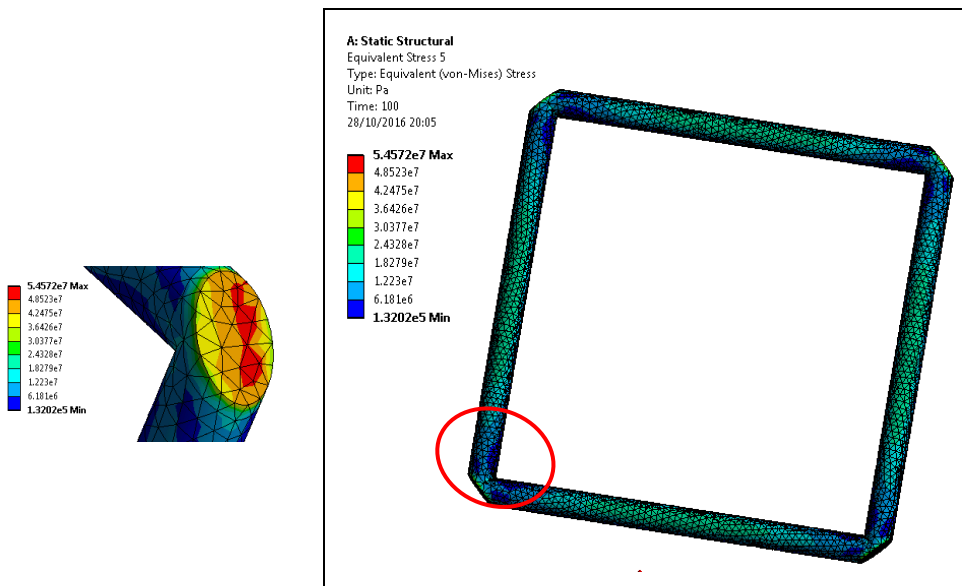


Figure 7.9 Stress on inner columns braces

### 7.3.1 Design for Columns under Uniaxial Compressive Loads

Recommendations for the redesign of the columns have been postulated to reduce heave response for draft variation (reduction), to help proliferate the application of PC-Semi. The stress on the columns for the original design presented in chapter 6 was studied. In chapter 6, it was mentioned that maximum equivalent stress was observed on the inner columns for both topside cases. Figure 7.10 and Figure 7.11 shows their independent von-Mises stress evaluation for dynamic load case, for a topside deck mass of  $34 \times 10^6$  Kg. It is important to mention that for this particular comparison, a very refined mesh was used, with element size 0.2m.

There is a slight difference between the maximum stresses on both columns, which is as a result of the high compressive stress concentration at the edge of the column for case 2 topside, represented in Figure 7.11. Apart from that, there is a lesser stress distribution around the column

for case 2 topside, which signifies it will receive less material for scantling and reinforcement, as compared to the on Figure 7.10.

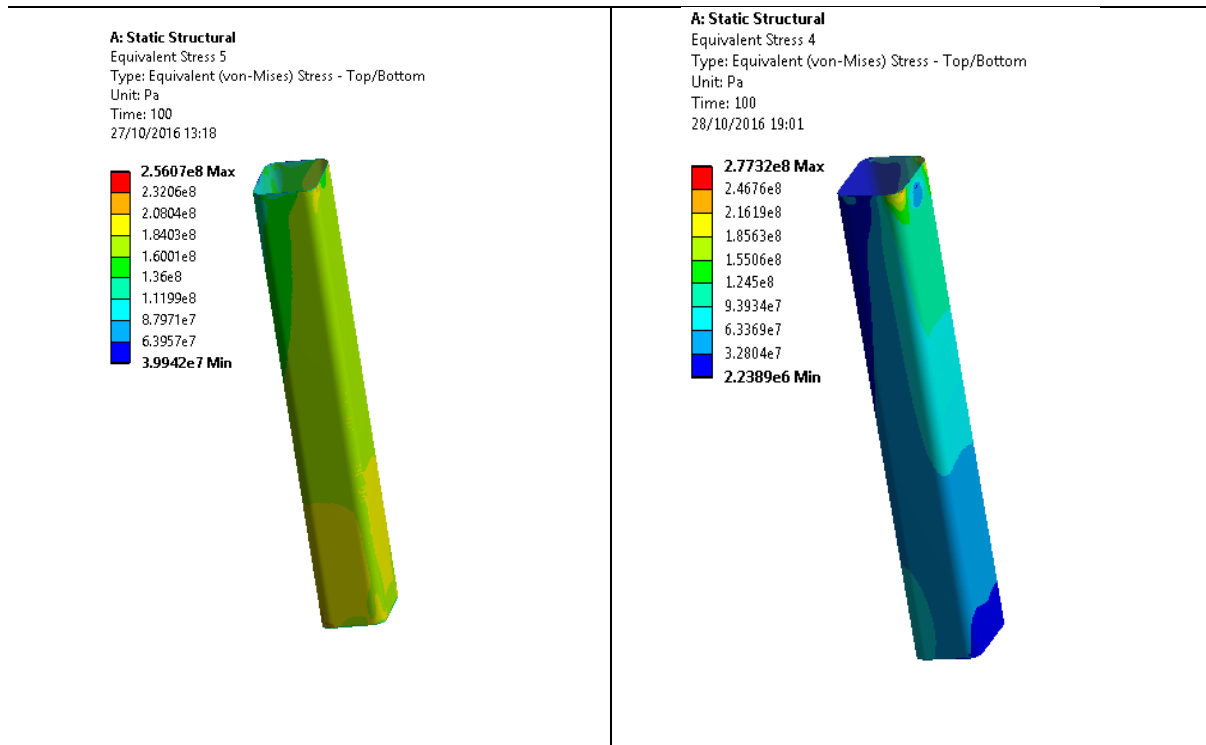


Figure 7.10 Inner column stress from case 1 topside

Figure 7.11 Inner column stress from case 2 topside

### 7.3.2 Joint Assessment and Recommendation

Sizing the different joints around the structure is of key interest in assessing the strength of the hull also depends on this. The column-pontoon connection and the connection at the inner column braces were considered to be of outmost importance in our analysis. This results obtained from column stress for case 1 topside (Figure 7.8 and Figure 7.9) can be used to select the most realistic joint and weld type suitable for the connection. Early studies presented in RPSEA 2009 first stage report suggested a slot-in type of connection with a sub-section protruding from the pontoon, creating little gap for welding (Tee-fillet weld); as described in Figure 7.12. A more effective joint type has been recommended from this study.

From the results obtained so far, the weld around the column-pontoon connection is likely to have very high-stress concentration, as high stresses have been obtained at the base of the columns. [142] presented recommended standards for developing joint/weld connections for floating hull systems. The standard cited a limit of 3mm for tee-fillet joints on floating hulls. The standard presented in [143] is equally to this effect. This is far less than the thickness of the column/pontoon plates, and also less than the spacing created between them. Considering the stress level recorded at the column base for both topside cases, the above joint type might not be valid. A tee-butt joint

(weld) has been recommended for this hull type. Figure 7.13 and Figure 7.14 shows the distinct difference between the two joints.

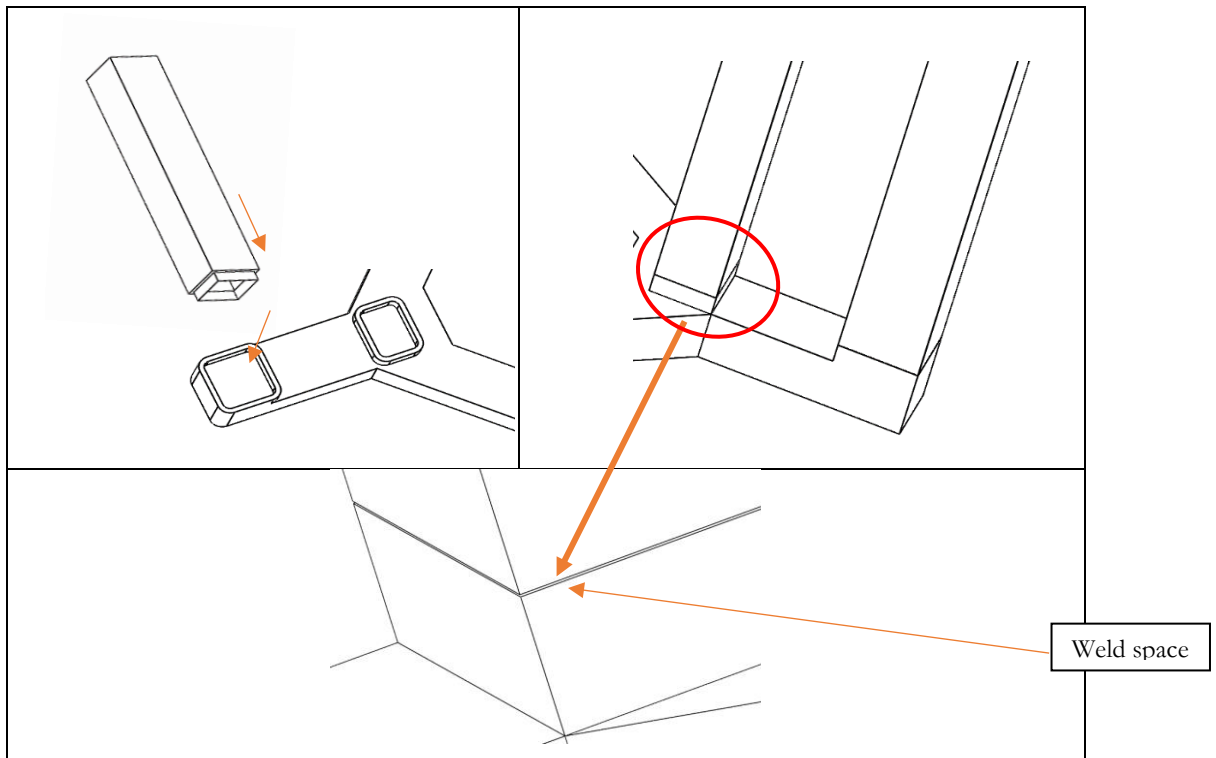


Figure 7.12 Column-pontoon assembly postulated by [4]. Tee-fillet joint

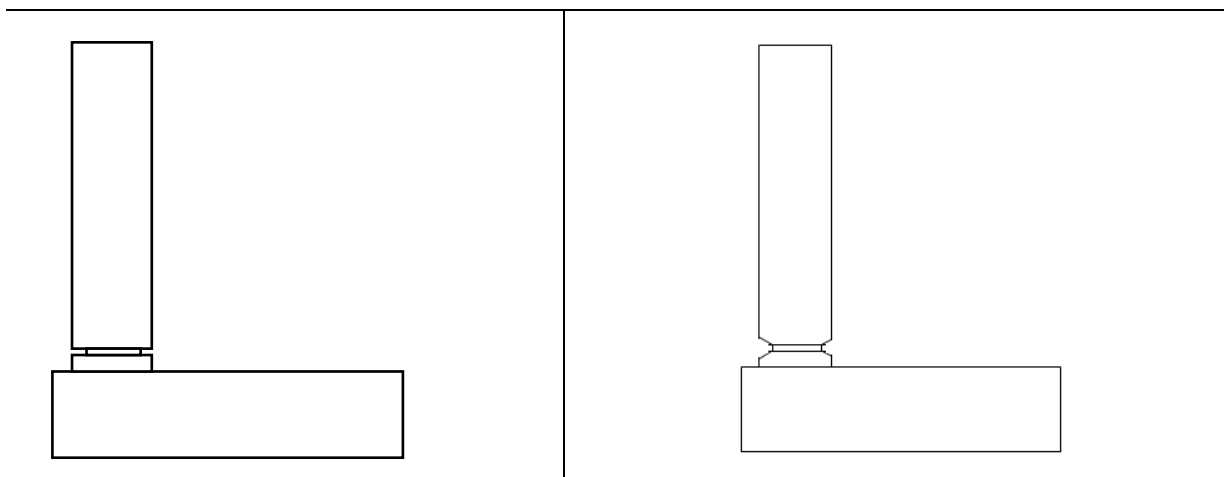


Figure 7.13 [4] recommended joint design

Figure 7.14 Recommended joint from current study

## 7.4 Recommendation for Payload

All floating systems are designed for their payloads, which is the amount of weight that can be put on them while they maintain their stability. From basic principle of floating bodies, the payload

is always a function of the displaced mass. Table 4.2 in chapter 4 reported a mass of  $96500 \times 10^3 \text{Kg}$  as the displaced mass of the hull for a draft size of 53.34m. Table 6.2 in chapter 6 shows how this mass was calibrated/allocated for different structural components of the. This mass allocation determines where the hull's centre of gravity will be located, which is responsible for the response and stability of the entire system. This implies that the amount of mass that can be allocated on the deck (facilities and utilities) will be reduced. After reviewing the payload / displaced mass ratio of 56 existing semisubmersibles in deep waters, we decided the most accurate deck mass for PC-Semi that would keep the centre of gravity around the point which we have presented in Table 4.3 should be between the ranges of  $25.1 \times 10^6 \text{Kg}$  to  $34.0 \times 10^6 \text{Kg}$ , and earlier presented in Table 6.2. (Some of the semisubmersibles studied can be found in [144] and [145]. Therefore, we've investigated the column stresses for different deck mass. Table 7.2 shows the effect on the topside mass on the stress distribution on the columns. For this stress study, we have considered the hull type described in case 1 and a coarse mesh, with element size 1.15, because it is more time effective. The relationship will be the same for a more refined mesh and for case 2 topside; irrespective of the value of stress level that will be recorded.

**Table 7.2 Effect of topside weight on maximum stress on columns**

Mass ( $\times 10^6 \text{ Kg}$ )	Weight ( $\times 10^6 \text{ N}$ )	Static Load Case	Dynamic Load Case
		$\sigma_{e_{max}}$ (MPa)	$\sigma_{e_{max}}$ (MPa)
25.1	246.23	147.24	201.92
26.0	255.06	153.52	205.50
28.0	274.68	164.25	213.46
30.0	294.30	175.98	221.45
32.0	313.92	184.71	229.38
34.0	333.54	191.34	237.32

Table 7.2 shows the effect of the topside weight on the maximum stresses (von-Misses) around the columns. A gradual progressive increase in  $\sigma_{e_{max}}$  was observed for both load cases. The wave and current loads were observed to have over 25% increase in the stress level on the columns. Figure 7.15 showed the linear relationship between the deck-mass and the maximum stress.

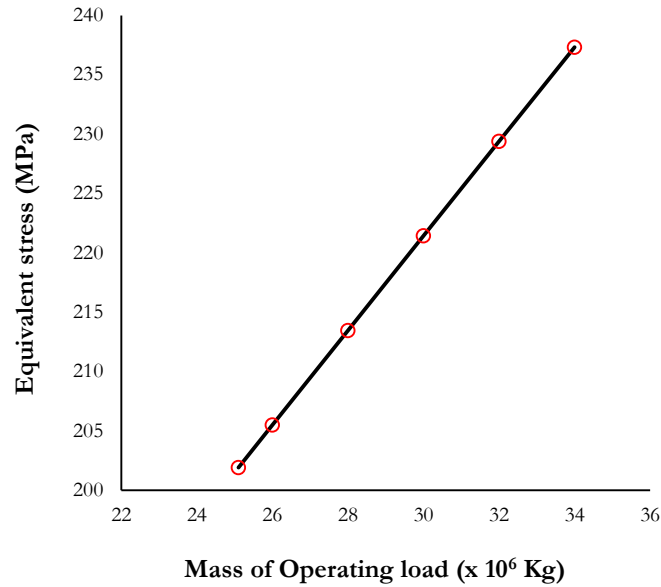


Figure 7.15 Effect of topside weight on the maximum stress on columns

## 7.5 Postulated Reinforcement

Hull scantling (including braces and flange design) is often the most critical stage in the design of floating hulls, to guarantee their strength in rough weather. The results presented in chapter 6 and the recommendations from this chapter can be used to postulate the internal reinforcement for the columns.

Previous company reports recommends uniformly distributed internal reinforcement for semisubmersible columns. From our results, non-uniform column reinforcement will significantly reduce the materials required for reinforcement, since there is a high disparity between the stresses recorded around them. An illustration has been reported in this study.

A set of ring and I stiffeners have been recommended for reinforcing the inner columns during scantling. This recommendation is based on (ABS, 2004) and (ABS, 2014) documentations. A set of 17 ring stiffeners (Figure 7.17) were designed for reinforcing the inner columns; as illustrated in Figure 7.16. From the top, the first five rings have a spacing of 2.81m, while the other 12 rings are 4.93m spaced. The formulation for spacing is due to the premise that the level of stress concentration is higher around the upper region of the column as reported in Figure 7.11.



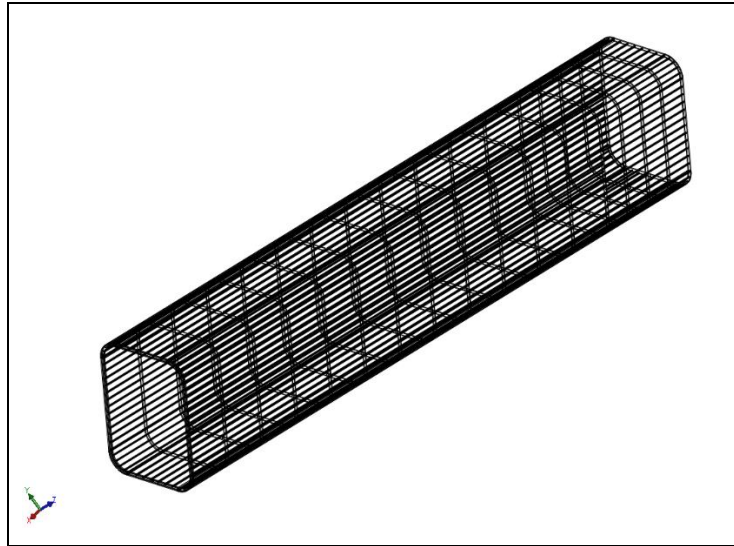


**Figure 7.16 Reinforcement for inner columns**

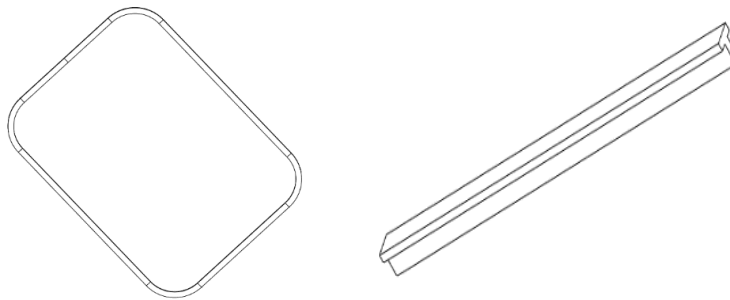


**Figure 7.17 Ring and straight stiffeners**

## **7.6 Applications**

One of the main objectives of this research is to be able to recommend the hull formation of a PC-Semi for different applications in ocean engineering. From our wide range of results presented in chapters 3, 4, 5, 6 and 7, we can give key recommendations for PC-Semis application for drilling, production, and support units.

### **7.6.1 Application for Support Systems; Accommodation and Luxury Cruise**

From the results obtained from this study, we can conclude that the numerous advantages of a PC-Semi will be better exploited when used to construct the hull of a support vessel where the high payload is required. The results for its motion characteristics presented in chapter 4 of this thesis showed very low rotational and translational response at base case configuration for 1000-years wave return period, for hurricane situation in the GOM. For normal operating condition, this will be over 10times lower. Result summary presented in Table 3.1 is evidence to this fact.) If these motion characteristics are compared to the size of the possible payload integration presented

in chapter 7, the size of the top-deck accommodation design can be very massive. For this reason, PC-Semi is highly recommended for any future design of floating accommodations and cruise vessels to operate in rough sea weather.

### **7.6.1 Application for FPS (Floating Production System)**

Another very useful application of this hull is the design of production platforms in deep waters. This is the function for which it was initially invented. The series of reports presented by RPSEA already showed how that design should be achieved. Achieving a positive metacentric height (as required by regulatory bodies for stability) for the hull is easy when it's used for production platform design. A positive metacentric height means the centre of gravity must always be below the metacentre. The additional weight integration offered by the production risers helps to place the centre of gravity further below the cut water plane. This advantage is only peculiar with production platforms, because drilling rigs only have 3 to 4 risers, while production platforms can operate with over 30 steel centenary risers, alongside over 40 top-tension risers.

### **7.6.2 Application for Foundation System**

For wind turbine foundation system, we still require a detailed knowledge of the regulatory policies in developing foundations systems for a wind turbine in different regions. As much as we know, the only functional semisubmersible foundation system used for wind turbines is the Dutch Tri-Floater. If the policy supports the application of other semisubmersibles outside the tri-floater, an experimental investigation still need to be carried out. Investigation on the effect of wind and maximum turbine rotation strength of a PC-Semi needs to be carried out before any form of recommendation can be made. In relation with the hull response, favourable response and turbine weight are compatible with PC-Semi for foundation system application.

### **7.6.3 Application for Drilling Rig**

This study has shown that although a PC-Semi can easily be used to develop production platforms for deep-water operations, same cannot be easily achieved for a drilling rig. The reason is that without the weight provision of production facilities (risers and umbilicals), achieving a lower centre of gravity will be restricted to the hull's weight distribution. From this study, a recommendation for hull design alteration (columns and pontoon) is required to attain the level of stability needed for a safe drilling operation. Further studies are required to come to any sort of precise conclusion on this.

## **7.7 Chapter Summary**

A detailed review of the results from hydrodynamics analysis and strength assessment presented in chapters 3, 4, 5, and 6, have been used to recommend design alterations to help improve the performance of the hull. These recommendations were discussed in this chapter.

A different form of column design was recommended to improve the heave motion for shallow and transient draft conditions. It involves increasing the area of the submerged part. An increase in pontoon surface area was also greatly encouraged, to help increase the vertical added mass parameter for dynamic cases. For roll and pitch improvement, weight redistribution was recommended for the outer columns, which will depend on the application of the hull. This concept is not particular to this study. Some researchers have previously recommended this sort of design to improve the roll behaviour of semisubmersible MODUs. The uniqueness of the case of a PC-Semi is that it meets the rotational criteria for intact condition required from floating structures for all draft cases. If there will any concern for roll improvement, it can only be the possible degree of rotation around the resonance frequencies, and the hull is designed to operate outside this range. In which case, no permanent mechanism is required for roll improvement. For extreme damage cases and for applications where rotation is required to significantly go below the required standard, weight redistribution can improve the roll performance of this hull.

Ways of improving the strength of this hull were also discussed in this chapter. The effect of inner columns braces and connections between inner/outer columns on the stress distribution was studied. The effect of hydrodynamic loads on the stress distribution on the columns was observed to be less with the inclusion there braces and connections.

# Chapter Eight: Conclusions and Recommendations for Future Studies

## 8.1 Conclusion

The conceptualization of this project is anchored on harnessing the advantages of a paired column semisubmersible hull system in the design and construction of floating platforms used for support vessels, drilling platforms and foundation systems, alongside production platforms for which it was initially designed. The research was structured in-line with industrial standards for designing offshore floating hulls, and prerequisite was taken from reports on the first PC-Semi design by presented H.O.E and RPSEA.

The most challenging aspect of this research is the process of coupling different numerical models, as the effect of the load; response and strength were developed differently. To numerically investigate the effect of wave in-line motions on the VIM response of the hull as recommended by [14], we had to integrate hydrodynamic model with CFD model. To evaluate its strength, we had to design for all load conditions, which means we had to integrate the hydrodynamic and CFD models to the FE-model.

A systematic literature review of the dynamics and functionalities of semisubmersible hulls in the offshore industry was carried out, alongside the origin and idealization for Pc-Semi. The review cited the flexibility of semisubmersibles and the series of optimizations that has been achieved as reasons for its high demand in the growing oil and gas industry. Structural attachments (such as mooring and risers) were discussed and the comparative advantages of semisubmersible hull over TLP with respect to these attachments were also discussed. In light of payload integration, the advantages of semisubmersible hull over Spar platforms were also cited. The review also discussed the recent demand of column stabilized semisubmersible hull in the design of mini floating island and cruise vessels. The review showed a significant knowledge gap in achieving high payload for floating semisubmersibles and less motion response, and some progress has been achieved on this over the years. The constant search for crude oil deposit in remote sea areas and the extreme weather conditions recorded as a result of global warming/increase in sea level demands novelties for motion reduction for semisubmersible hulls to meet regulatory standards. Conclusions from the review suggested that the vertical plane (heave, roll, and pitch) motion reduction for dry-trees compatibility achieved from the idealization of PC-Semi can be extremely useful in filling that knowledge gap. Further research was therefore required to understand the complete dynamics of

this hull, alongside a complete knowledge of its strength under combined loading. Considering industrial standards, this required us to develop series of numerical models to investigate and interpret before setting standards and recommending it for specific designs/applications.

Given the complex flow pattern associated with the unique PC-Semi column arrangement, an experimental setup was put together to investigate the motion response and hydrodynamic loadings of the hull in its free floating state. This was carried out alongside a numerical setup modelled on diffraction and radiation theories. The relationship between the flow angle and its hull motion amplitude was observed to be opposite to the conventional relationship for four column semisubmersibles operating in deep waters. Useful findings from previous studies were considered in developing the numerical setup. Some conclusions were made from the results obtained from the motion study;

- i. Low frequency heave response for PC-Semi was observed to be extremely favourable for deep-draft (base-case configuration) designs when compared to survival and tows draft cases; as the slender nature of the rectangular columns makes it unfavourable in such situations. Considering the standards for semisubmersible stability as set by the regulatory bodies and the requirement of stroke limit for top tension risers, the stability of this hull type/compatibility with top-deck well head installation for survival and extreme weather conditions can only be guaranteed in its deep-draft state. Again, this restricts its application to only deep-draft designs
- ii. There is an inverse relationship between the pitch and roll behaviour for  $0^{\circ}$  and  $90^{\circ}$  flow angles because of the symmetric nature of the hull, future operators of PC-Semis must take note of this. This hull type easily gains stability as required by recommended standards (IMO, API, DNV:  $7^{\circ}$  for intact state, and  $17^{\circ}$  for damage condition), irrespective of the draft condition, this was not the case for damage conditions. Although, this is not the case for the translational motions, for which its attachments (moorings, risers, and umbilicals) depends on. An overall hull reconfiguration might be required (specifically for heave reduction) for some future applications of this hull. Conventional four columns deep-draft semisubmersibles do not have this behaviour; reduced draft size normally leads to increase in hull rotation.
- iii. The effect of wave-current interactions on a PC-Semi is significantly different from what is obtained in conventional floating structures; this research has been able to establish that. Wave-current interactions will generate extremely high/destructive heave amplitude on

this hull for base-case configuration, at resonance frequency. A further investigation is required to gain a complete understanding of the parameters in which this unique behaviour depend on.

The drag effect of the flow on the hull was also investigated. An important reason for this investigation is its usefulness in industrial applications. A conserved approach is mostly adopted in industries for calculating and estimating the flow/wave forces on floating bodies; in which case, Morison's equation is applied (Equation 2-1 and Equation 2-2). The results recorded for drag coefficients; as present in chapter five can be applied to calculate for wave forces in situations where the 3D BEM is not available. It can also be used to estimates the effect of vortex formation on the hull. Useful conclusions on PC-Semi hull were obtained from the CFD model some of which includes;

- i. Maximum drag and vortex shedding amplitude have been observed to occur at  $0^0$  flow angle. Future operators of structures suspended on PC-Semi hull have to take note of this during installation and operations.
- ii. The spacing between the inner and outer column on each pair controls the flow drag (force) on the entire hull. This parameter has a unique nonlinear effect because of the superimposition of the wake transition behaviour around multiple arranged columns. For a PC-Semi hull design, the relationship will need to be investigated for all flow angles to select the most effective spacing for minimum drag distribution around the columns. In this study, we observed that the formation of irregular wake around the columns significantly reduces the level of drag around the hull.
- iii. A highly uneven drag force relationship was recorded for the four pairs for different inner-outer column spacing. This is an indication of the level of instability that can arise if the spacing between the columns is not appropriately selected. Since maximum response amplitudes and drag coefficients have been recorded for  $0^0$  flow angle, offshore engineers will be recommended to operate the hull for  $45^0$  current flow. For this flow orientation, a minimum of two times the length of the outer column is required for the spacing between the outer and inner column to effectively reduce the margin of the disparity between the drag on the each pair. This recommendation has to be strictly adhered to for any design of PC-Semi to obtain the required level of stability required for column stabilized unit.

- iv. A study of the vortex formation from the column boundary layer for different geometric configuration showed that despite the advantages offered by the rectangular columns, the design can be improved. A combination of circular outer columns and square inner columns is likely to be more favourable to design a vortex suppressed PC-Semi. Further research is required to gain a complete understanding of this unique combination.

The strength of the hull under combined loading was assessed with a finite element model. The result showed the advantages of smaller deck over a larger one. The inner column braces and load distribution by the inner/outer column connections helped to reduce the overall stress level around the columns. Less material will therefore be required for hull scantling, with the possibility of applying composite stiffeners and girders.

## **8.2 Recommendation for Future Studies**

### **8.2.1 Effect of fluid-structure interaction on column stress profile and hull deformation**

The set of flow equations used in estimating the hydrodynamic properties of the hull, presented in chapter 4, functions on single phase flow assumption. Figure 4.1 and Equation 4-1 clearly cited this. Due to this development, we were unable to predict the effect of backward-hydrodynamics and multi-phase flow scenarios on the stress and flexural properties on the hull. To gain a complete understanding of sloshing effect around the centralized area of the hull, a multi-phase hydrodynamic model will need to be developed. This will further aid material selection in the construction stage of this hull.

### **8.2.2 Design and sizing of Tee-Butt joint for column-pontoon connection**

The results presented on the stress distribution on the columns showed high stress concentration around the column-pontoon connection, and a joint type has been postulated to that regards. Further research is therefore required to effectively size this recommended joint, for different amount of payload and weather conditions. The FE-model presented in this study is capable of carrying out this task, but further improvement and company weld stiffness will be needed to advance the progress of this study

### **8.2.3 Design and development of PC-Semi for wind turbine foundation system**

The motion response of a Pc-Semi characterized in this study has shown high weight to motion response ratio for PC-Semi hull. This advantage can be very useful in designing foundation systems in the fast growing renewable energy industry. It is therefore recommended that the effect of wind turbine installation should be investigated on a PC-Semi hull. This will require the application of new set of standards. The motion and strength assessment presented in this thesis might not be valid for this application.

### **8.2.4 Hull Scantling**

The recommendations postulated for hull scantling in chapter 7 need to be investigated on.



## Reference

- [1] J. Zou, "VIM Response of a Dry Tree Paired-Column Semisubmersibles Platform and its Effects on Mooring Fatigue," in 19th Offshore Symposium, Texas USA, 2014: Society of Naval Architects and Marine Engineers.
- [2] Zou, J., Poll, P., Antony, A., Das, S., Padmanabhan, R., Vinayan, V. and Parambath, A., "VIM Model Testing and VIM Induced Mooring Fatigue of a Dry Tree paired Column Semisubmersible Platform," presented at the Offshore Technology Conference, USA, 2014.
- [3] Y. Park, B. S. Jang, and J. D. Kim, "Hull- form optimization of semi- submersible FPU considering seakeeping capability and structural weight," *Ocean Engineering*, vol. 104, pp. 714-724, 2015.
- [4] RPSEA, "Ultra Deepwater Dry Tree System for drilling and Production," ed: Research Partnership to Secure Energy for America, 2009.
- [5] J. Zou, "Dynamic Responses of a Dry Tree Semi-submersible Platform with Ram Style Tensioners in the Post-Katrina Irregular Seas.," in The Eighteenth International Offshore and Polar Engineering Conference, Vancouver, BC, Canada, 2008, vol. 2: The Eighteenth International Offshore and Polar Engineering Conference, International Society of Offshore and Polar Engineers. International Society of Offshore and Polar Engineers.
- [6] Lloyd's R. (2011, August 08th). Drilling in Extreme Enviroment: Challenges and implications for the energy insurance industry. Available:  
<https://www.lloyds.com/~ /media/lloyds/reports/emerging%20risk%20reports/lloyds%20drilling%20in%20extreme%20environments%20final3.pdf>
- [7] R. J. Erdbrink, "Semi-submersible crane vessel," USA, 1990.
- [8] T. Priest, "Extraction Not Creation: The History of Offshore Petroleum in the Gulf of Mexico," *Enterprise & Society*, vol. 8, no. 2, pp. 227-267, 2007.
- [9] N. S. Galgoul, "Fatigue Analysis of Offshore Fixed and Floating Structures ", ed, 2007.
- [10] B. Alexei, "Oil-Services Firms Take a Bath on Deep- Water Drilling --- Offshore Exploration Presents Higher Costs, Greater Technological Challenges," ed, 2001, p. B.4.
- [11] Makinson, K., Pearce, D., Hodgson, D.A., Bentley, M.J., Smith, A.M., Tranter, M., Rose, M., Ross, N., Mowlem, M., Parnell, J. and Siegert, M.J. "Clean subglacial access: prospects for future

- deep hot- water drilling," *Philosophical transactions. Series A, Mathematical, physical, and engineering sciences*, vol. 374, no. 2059, 2016.
- [12] C. R. Bentley and B. R. Koci, "Drilling to the beds of the Greenland and Antarctic ice sheets: a review," *Annals of glaciology*, vol. 47, no. 1, pp. 1-9, 2007.
- [13] J. Zou, P. Poll, D. Roddier, N. Tom, and A. Peiffer., "VIM testing of a paired column semi submersible," presented at the 32nd International Conference on Ocean Offshore and Arctic Engineering, Nantes, France, 2013.
- [14] R. T. Gonçalves, G. F. Rosetti, A. L. Fajarra, and A. C. Oliveira, "Experimental Study on Vortex Induced Motions of a Semi-Submersible Platform with Four Square Columns, Part 2: Effect of Surface waves, External Damping and Draft Condition," *Ocean Engineering*, vol. 62, pp. 10-24, 2012.
- [15] *Guide for Buckling and Ultimate Strength Assessment for Offshore Structures*, 2004.
- [16] *STRUCTURAL DESIGN OF OFFSHORE UNITS (WSD METHOD)*, 2011.
- [17] W. L. Leffler, *Deepwater petroleum exploration & production : a nontechnical guide (Deepwater petroleum exploration and production)*. Tulsa, Okla. : PennWell, 2003.
- [18] S. Akagi and K. Ito, "Optimal Design of Semisubmersible Form by Minimizing its Motion in Random Seas ", ed. Osaka, Japan: Department of Mechanical Engineering for Industrial Machinery, Faculty of Engineering,Osaka University., 1984, p. 8.
- [19] D. Knox, C. Smith, and A. Sedlmayer., "Revolutionary Design for Semisubmersible Hull Catamaran," ed: OSSeas Consulting, 2015, p. 3.
- [20] J. William T. Bennett and Alden J. Laborde, "Deep draft semi-submersible offshore structure," USA, 2001. Available: <http://www.google.co.uk/patents/US6190089>.
- [21] ABS. (2015, 1st February). *Offshore Innovation: A Histroy of Offshore Development*. Available: <https://www.eagle.org/eagleExternalPortalWEB/ShowProperty/BEA%20Repository/References/Capability%20Brochures/OffshoreInnovationCp>
- [22] A. U. Bindingsbo and A. Bjørset, "Deep draft semisubmersible," presented at the International Conference on Offshore Mechanics and Arctic Engineering, 2002.
- [23] O. Rijken, S. Schuurmans, and S. Leverette, "Experimental Investigations into the Influences of SCRs and Appurtenances on Deep-Draft Semisubmersible Vortex Induced Motion

response.," presented at the 30th International Conference on Ocean, Offshore and Arctic Engineering, USA, 2011.

[24] Y. Hong, Yongho Choi, u. L. and, and Y. Kim, "Vortex-Induced Motion of a Deep-Draft Semi-Submersible in Current and Waves," presented at the Proceedings of the Eighteenth (2008) International Offshore and Polar Engineering Conference, Canada, 2008.

[25] R. T. Gonçalves, G. F. Rosetti, A. L. Fujarra, and A. C. Oliveira, "Wave Effects on Vortex-Induced Motion (VIM) of a Large-Volume Semi-Submersible Platform," presented at the 31st International Conference on Ocean, Offshore and Arctic Engineering, Rio de Janeiro, Brazil, 2012.

[26] R. T. Gonçalves, G. F. Rosetti, A. L. C. Fujarra, and A. C. Oliveira, "Experimental study on vortex- induced motions of a semi- submersible platform with four square columns, Part I: Effects of current incidence angle and hull appendages," *Ocean Engineering*, vol. 54, pp. 150-169, 2012.

[27] Z. Bai, L. Xiao, Y. a. Kuo, and L. Yang, "Research on vortex induced motion of a deep draft semisubmersible with four rectangular columns," presented at the In The Twenty-third International Offshore and Polar Engineering Conference, 2013.

[28] J. Halkyard, *Floating Offshore Platform Design-Chapter 7*. Elsevier Ltd, 2005, pp. 419-661.

[29] H. Zhu, J. Ou, and G. Zhai, "Conceptual design of a deep draft semi-submersible platform with a moveable heave-plate," ed: *Journal of Ocean University of China*, 2012.

[30] Q. Xu, "A NEW SEMISUBMERSIBLE DESIGN FOR IMPROVED HEAVE MOTION, VORTEXINDUCED MOTION AND QUAYSIDE STABILITY," presented at the Proceedings of the ASME 2011 30th International Conference on Ocean, Offshore and Arctic Engineering, 2011.

[31] DiamondOffshore. (2016, 12th September). Deepwater Rigs: Ocean Apex & Ocean Onyx. Available: <http://www.diamondoffshore.com/video-360-degree-flyaround-of-the-ocean-apex>

[32] B. Malcolm and P. Dixon, "Column-stabilized offshore vessel," USA, 2001. Available: <http://appft1.uspto.gov/netacgi/nph-Parser?Sect1=PTO1&Sect2=HTOFF&d=PG01&p=1&u=/netahtml/PTO/srchnum.html&r=1&f=G&l=50&s1=20020090270.PGNR>.

- [33] R. Sharma, T.-W. Kim, O. P. Sha, and S. C. Misra, "Issues in offshore platform research - Part 1: Semi- submersibles," *International Journal of Naval Architecture and Ocean Engineering*, vol. 2, no. 3, pp. 155-170, 2010.
- [34] N. Srinivasan, "Column-stabilized floating structures with truss pontoons," USA, 2004.
- [35] S. Chakrabarti, J. Barnett, H. Kanchi, A. Mehta, and J. Yim, "Design analysis of a truss pontoon semi-submersible concept in deep water," *Ocean Engineering*, vol. 34, no. 3-4, pp. 621-629, 2007.
- [36] R. Sundaravadivelu, R. Kanotra, and N. Srinivasan, "Transportation Analysis of Dry Tree Semisubmersible," vol. 5, no. 2, pp. 105-116, 2014.
- [37] Y. a. S. Ding, W.L., "Truss semi-submersible offshore floating structure," USA, 2011. Available: <http://www.google.es/patents/US7871222>.
- [38] J. F. Wilson, *Dynamics of offshore structures*. New York : Wiley, 1984.
- [39] S. A. Mavrakos, V. J. Papazoglou, M. S. Triantafyllou, and J. Hatjigeorgiou, "Deep water mooring dynamics," *Marine Structures*, vol. 9, no. 2, pp. 181-209, 1996.
- [40] A. Sarkar and R. Eatock Taylor, "DYNAMICS OF MOORING CABLES IN RANDOM SEAS," *Journal of Fluids and Structures*, vol. 16, no. 2, pp. 193-212, 2002.
- [41] X. H. Chen, J.A. Zhang, and W. Ma., "Coupled Time-Domain Analysis of the Response of a Spar And Its Mooring System," presented at the The Ninth International Offshore and Polar Engineering Conference,, Brest, France 1999.
- [42] M. A. Jordán and R. Beltrán-Aguedo. "Nonlinear identification of mooring lines in dynamic operation of floating structures." *Ocean engineering*, vol. 3131, no. 3, pp. 455-482., 2004.
- [43]S. Chakrabarti. (2005, 16th September). *Handbook of Offshore Engineering (2-volume set)* [electronic resource].
- [44]M. Duan, Y. Wang, Z. Yue, S. Estefen, and X. Yang, "Dynamics of risers for earthquake resistant designs," *Pet. Sci.*, vol. 7, no. 2, pp. 273-282, 2010.
- [45]Y. Bai and Q. Bai, *Subsea Pipelines and Risers*. Elsevier Science, 2005.
- [46]S. Kaewunruen, J. a. Chiravatchradej, and S. Chucheepsakul, "Nonlinear free vibrations of marine risers/pipes transporting fluid," *Ocean Engineering*, vol. 32, no. 3, pp. 417-440, 2005.

- [47] DNV-RP-205, "Environmental Conditions and Environmental Loads," ed: Det Norske Veritas, 2007.
- [48] K. Qian and Y. Wang, "Wave load calculation of structural strength analysis for a semi-submersible platform. ," presented at the In The Twelfth International Offshore and Polar Engineering Conference., 2002 January.
- [49] S. Wu, Murray J.J., and G. S. Virk, "The motions and internal forces of a moored semi-submersible in regular waves. ," *Ocean Engineering*, vol. 24(7)24, no. 7, pp. 593-603, 1997.
- [50] API 2INT-MET, "Interim Guidance on Hurricane Conditions in the Gulf of Mexico," ed: American Petroleum Institute, 1997.
- [51] V. L. F. Matos, A. N. Simos, and S. H. Sphaier, "Second-order resonant heave, roll and pitch motions of a deep-draft semi-submersible: Theoretical and experimental results," *Ocean Engineering*, vol. 38(17)38, no. 17, pp. 2227-2243 2011.
- [52] J. H. Tan, F. Kiprawi, J. Kyoung, J. F. O Sullivan, and N. J. A., "Dry Tree Semisubmersible for Cost-Effective Deepwater Development," presented at the Offshore Technology Conference, Malaysia, 2016.
- [53] A. Hussain, E. Nah, R. Fu, and A. Gupta, "Motion comparison between a conventional deep draft semi-submersible and a dry tree semi-submersible.," presented at the 28th International Conference on Ocean, Offshore and Arctic Engineering, Hawaii, USA, 2009.
- [54] DNVGL-CG-0128 Buckling 2015.
- [55] Structural Design of Self-Elevating Units (LRFD Method), 2012.
- [56] E. E. Begnaud, C. V. Norton, B. Malcolm, and L. Friede & Goldman, "Dynamically positioned semi-submersible drilling vessel with slender horizontal braces," USA, 2002.
- [57] X. J. Chen, Y. S. Wu, W. C. Cui, and J. J. Jensen, "Review of hydroelasticity theories for global response of marine structures. ," vol. 33(3) ed: *Ocean Engineering*, 2006, pp. 439-457.
- [58] J. N. Newman, "Wave effects on deformable bodies," *Applied Ocean Research*, vol. 16, no. 1, pp. 47-59, 1994.
- [59] J. Xu and M. R. Haddara, "Estimation of wave- induced ship hull bending moment from ship motion measurements," *Marine Structures*, vol. 14, no. 6, pp. 593-610, 2001.

- [60] J. H. Kyoung, S. Y. Hong, J. W. Kim, and K. J. Bai, "Finite- element computation of wave impact load due to a violent sloshing," *Ocean Engineering*, vol. 32, no. 17, pp. 2020-2039, 2005.
- [61] M. Kashiwagi, "Hydrodynamic interactions among a great number of columns supporting a very large flexible structure," *Journal of Fluids and Structures*, vol. 14, no. 7, pp. 1013-1034, 2000.
- [62] *Offshore-Mag*. (2012, 05th August). Dry trees offer alternative for deepwater development. Available: <http://www.offshore-mag.com/articles/print/volume-72/issue-6/engineering-construction-installation/dry-trees-offer-alternative-for-deepwater-development.html>
- [63] R. R. API, "Design of Risers for Floating Production Systems (FPSs) and Tension-Leg Platforms (TLPs)," vol. Recommended Practice 2RD, ed. USA: American Petroleum Institute, 1998.
- [64] Q. Xu and L. Xu, "An Introduction to Extendable Draft Platform (EDP)," presented at the Fourteenth International Offshore and Polar Engineering Conference, Toulon, France, 2004.
- [65] J. Murray, "Extendable draft platform with buoyancy column strakes," 2004. Google Patent
- [66] Y. Hao, C. Yongjun, and C. Yujun, "State of the art dry tree semi technologies," *Engineering Sciences*, vol. 4, p. 14, 2013.
- [67] J. J. Murray, C. K. Yang, Chen C., and E. Nah, "Two Dry Tree Semisubmersible Designs for Ultra deep Water Post-Katrina Gulf of Maxico," ed: Ocean, Offshore and Arctic Engineering Division, 2008.
- [68] *Offshore-Technology*. (2013, 5th August). Blind Faith Subsea Development, United States of America. Available: <http://www.offshore-technology.com/projects/blindfaith/>
- [69] R. Zhang, Y. Tang, J. Hu, S. a. Ruan, and C. Chen, "Dynamic response in frequency and time domains of a floating foundation for offshore wind turbines.," vol. 60, , ed: Ocean Engineering, , 2013, pp. pp.115-123.
- [70] C. Michailides, Z. a. Gao, and T. Moan, "Experimental and numerical study of the response of the offshore combined wind/wave energy concept SFC in extreme environmental conditions." vol. 50,, ed: Marine Structures, , 2016. , pp. 35-54. .
- [71] M. Karimirad and C. Michailides, "V-shaped semisubmersible offshore wind turbine: An alternative concept for offshore wind technology," *Renewable Energy*, vol. 83 pp. 126-143., 2015.

- [72] J. M. Jonkman, Dynamics modeling and loads analysis of an offshore floating wind turbine. ProQuest, 2007
- [73] T. Ishihara, P. V. Phuc, H. Sukegawa, K. a. Shimada, and T. Ohyama. (2007, February 4th). A study on the dynamic response of a semi-submersible floating offshore wind turbine system Part 1: A water tank test. Available: <http://windeng.t.u-tokyo.ac.jp/ishihara/paper/2007-3.pdf>
- [74] P. Van Phuc and T. Ishihara, "A study on the dynamic response of a semi-submersible floating offshore wind turbine system Part 2: numerical simulation," ed. Cairns, Australia: ICWE12. , 2007, pp. 959-966.
- [75] CNN. (2015, 3rd March). Monaco Yacht Show 2015: Forget the boat, here's the island you can sail. Available: <http://edition.cnn.com/2015/09/24/sport/gallery/migaloo-submersible-yacht-floating-island/>
- [76] B. Li, K. Liu, G. Yan, and J. Ou, "Hydrodynamic comparison of a semi- submersible, TLP, and Spar: Numerical study in the South China Sea environment," J. Marine. Sci. Appl., vol. 10, no. 3, pp. 306-314, 2011.
- [77] A. Kareem, P. C. Lu, T. D. a. Finnigan, and S. L. V. Liu, "Aerodynamic loads on a typical tension leg platform.," Ocean engineering, vol. 14, no. 3, pp. 201-231, 1987.
- [78] I. Senjanović, M. Tomić, and S. Rudan, "Investigation of nonlinear restoring stiffness in dynamic analysis of tension leg platforms," Engineering Structures, vol. 56, pp. 117-125, 2013.
- [79] I. Senjanović, M. Tomić, and N. Hadžić, "Formulation of consistent nonlinear restoring stiffness for dynamic analysis of tension leg platform and its influence on response," Marine Structures, vol. 30, pp. 1-32, 2013.
- [80] M. M. Gadagi and H. Benaroya, "Dynamic response of an axially loaded tendon of a tension leg platform," Journal of Sound and Vibration, vol. 293, no. 1, pp. 38-58, 2006.
- [81] M. H. Patel, P. H.I., and "Dynamics of tension leg platform tethers at low tension. Part I- Mathieu stability at large parameters.," vol. 4, ed: Marine Structures, 1991, pp. 257-273.
- [82] J. Halkyard, "Spar Floating Drilling, Production, and Storage System: History and Evolution of Spar Platform," ed, 2012.
- [83] A. K. Jain and A. A. K., "Dynamic Analysis of Offshore Spar Platforms," Defence Science Journal, vol. 53, no. 2, pp. 211-219, 2003.

- [84] K. Lam, W. Q. Gong, and R. M. C. So, "Numerical Simulation of Cross-Flow Around Four Cylinders in an In-Line Square Configuration," *Journal of Fluid Mechanics and Structures*, vol. 24, no. 1, pp. 34-57, 2008.
- [85] D. Zhou, X. Gui, J. Tu, and Z. Han, "Numerical study of flow past four square-arranged cylinders using spectral element method," vol. 84, ed: *Journal of Computers and Fluids*, 2013, pp. 100-112.
- [86] T. Zhou, S. F. Razali, Z. Hao, and L. Cheng, "On the study of vortex-induced vibration of a cylinder with helical strakes," *Journal of Fluids and Structures*, vol. 27, pp. 903-917, 2011.
- [87] S. J. Kim, D. Spornjak, S. Holmes, V. a. Vinayan, and A. Antony, "Vortex-induced motion of floating structures: CFD sensitivity considerations of turbulence model and mesh refinement. ," presented at the 34th International Conference on Ocean, Offshore and Arctic Engineering, 2015.
- [88] D. R. Shields, R. F. Zueck, and W. J. Nordell, "Ocean Model Testing of a Small Semisubmersible," ed. USA: 19th Annual Offshore Technology Conference in Houston, Texas, 1987.
- [89] F. Tasai, K. Nemoto, H. a. Arakawa, and M. Kurihara, "A study on the motions of a semi-submersible catamaran hull in regular waves.," Japan1970.
- [90] O. Yilmaz and A. Incecik, "Extreme motion response analysis of moored semi-submersibles," *Ocean Engineering*, vol. 23, no. 6, pp. 497-517, 1996.
- [91] H. S. Chan, "A three-dimensional technique for predicting first-and second-order hydrodynamic forces on a marine vehicle advancing in waves " PhD, Department of Naval Architecture and Ocean Engineering, University of Glasglow, United Kingdom, 1490, 1990.
- [92] J. A. Pinkster, "Low frequency second order wave exciting forces on floating structures.," ed: PhD. Thesis, TU Delft, 1980.
- [93] C. A. Brebbia, *Dynamic analysis of offshore structures*. London ; Boston : Newnes-Butterworths, 1979.
- [94] N. D. e. Barltrop, "Floating Structures: a guide for design and analysis " vol. Vol. 1, ed: Oilfield Pubns Inc. 1998.
- [95] X. B. Chen, " 'The set-down in the second-order Stokes' waves'," presented at the Seventh International Conference on Hydrodynamics, The Island of ISCHIA, Italy, 2006.



- [96] C. H. Kim, *Nonlinear waves and offshore structures*. Hackensack, N.J. : World Scientific, 2008.
- [97] T. S. Sarpkaya, *Wave Forces on Offshore Structures* [electronic resource]. United Kingdom: Cambridge : Cambridge University Press, 2010.
- [98] C. Odijie and J. Ye, "Understanding Fluid-Structure Interaction for high amplitude wave loadings on a deep-draft paired column semi-submersible platform:a finite element approach," presented at the International Conference on Light Weight Design of Marine Structures, Glasgow, United Kingdom, 2015.
- [99] G. K. Batchelor, *An introduction to fluid dynamics*. Cambridge U.P., 1967.
- [100] M. Brorsen, "Slowly-varying 2. order wave forces on large structures. ," ed: Aalborg University, Department of Civil Engineering, 2006. .
- [101] R. S. Langley, "The statistics of second order wave forces," *Applied Ocean Research*, vol. 6, no. 4, pp. 182-186, 1984.
- [102] H. Yamaguchi, K. Endo, and H. Yamaguchi, "Wave drift forces and moments on two ships arranged side by side in waves," vol. 32, ed: *Ocean Engineering*, 2005, pp. 529-555.
- [103] M. McIver and P. McIver, "Second- order wave diffraction by a submerged circular cylinder," *Journal of Fluid Mechanics*, vol. 219, pp. 519-529, 1990.
- [104] G. X. Wu, "Second- order wave radiation by a submerged horizontal circular cylinder," *Applied Ocean Research*, vol. 15, no. 5, pp. 293-303, 1993.
- [105] J. Y. T. Ng and M. Isaacson, "Second- order wave interaction with two-dimensional floating bodies by a time-domain method," *Applied Ocean Research*, vol. 15, no. 2, pp. 95-105, 1993.
- [106] H. Kagemoto and D. K. P. Yue, "Interactions among multiple three- dimensional bodies in water waves: an exact algebraic method," *Journal of Fluid Mechanics*, vol. 166, pp. 189-209, 1986.
- [107] A. Biran and R. L. Pulido, *Ship hydrostatics and stability*. Ship hydrostatics and stability. . Butterworth-Heinemann. , 2013.
- [108] J. N. Newman and C. H. Lee, "Heave response of a semi-submersible near resonance," in *In Proceedings of 14th International Workshop on Water Waves and Floating Bodies*, Port Huron, USA., 1999.

- [109] M. Kashiwagi, "Wave drift force in a two- layer fluid of finite depth," J Eng Math, vol. 58, no. 1, pp. 51-66, 2007.
- [110] A. J. Voogt, Soles J.J., and D. R.V. (2002, 2002-JSC-285). Mean and Low Frequency Roll for Semi-submersibles in Waves. Available:  
[http://www.marin.nl/upload\\_mm/2/d/1/1806576740\\_1999999096\\_2002-ISOPE-JSC-285\\_VoogtSolesDijk.pdf](http://www.marin.nl/upload_mm/2/d/1/1806576740_1999999096_2002-ISOPE-JSC-285_VoogtSolesDijk.pdf)
- [111] A. H. Mohamed, "Hydrodynamic Loading and Responses of Semisubmersibles," Phd Thesis, School of Marine science and Technology, Newcastle University, Newcastle upon Tyne, United Kingdom, 2011.
- [112] Z. Liu, B. Teng, D.-Z. Ning, and Y. Gou, "Wave- current interactions with three-dimensional floating bodies," Journal of Hydrodynamics, Ser.B, vol. 22, no. 2, pp. 229-240, 2010.
- [113] J. Nossen, J. Grue, and E. Palm, "Wave forces on three- dimensional floating bodies with small forward speed," Journal of Fluid Mechanics, vol. 227, pp. 135-160, 1991.
- [114] C. Odijie and J. Ye, "Effect of vortex induced vibration on a paired column semi-submersible platform," International Journal of Structural Stability and Dynamics, vol. 15, no. 8, p. 1540019, 2015.
- [115] L. D. Finn, J.V. Maher, and H. Gupta., " The Cell Spar and Vortex Induced Vibration. ," ed. Proceedings of the Offshore Technology Conference, Houston USA. OTC 15244 2003.
- [116] V. Dijk, V. R. R., F. A., and S. Mirza, "The effect of mooring system and sheared currents on vortex induced motions of truss spars.," presented at the International Conference on Offshore Mechanics and Arctic Engineering. . In ASME 2003 22<sup>nd</sup> International Conference on Offshore Mechanics and Arctic Engineering (pp. 285-292). American Society of Mechanical Engineers Cancun, Mexico, 2003.
- [117] H. Mukundan, Y. Modarres-Sadeghi, J. M. Dahl, F. S. A. Hover, and M. S. Triantafyllou, "Monitoring VIV Fatigue Damage on Marine Risers," Journal of Fluid Mechanics and Structures, vol. 25, no. 4, pp. 617-628, 2009.
- [118] S. F. A. Cornut and J. K. Vandiver, "Offshore VIV Monitoring at Schiehallion-Analysis of Riser VIV Response," in In Proceedings of ETCE/OMAE 2000 Joint Conference: Energy for the New Millenium, New York, USA, 2000, pp. 14-17: Proceedings of ETCE/OMAE 2000 Joint Conference: Energy for the New Millenium (pp. 14-17).American Society of Mechanical Engineers.

- [119] O. J. Waals, A. C. Phadke, and S. Bultema, "Flow Induced Motions on Multi Column Floaters," presented at the 26th International Conference on Offshore Mechanics and Arctic Engineering, USA, 2007.
- [120] O. Rijken and S. Leverette, "Experimental Study into Vortex Induced Motion Response of Semisubmersibles with Square Columns," in 27th International Conference on Offshore Mechanics and Arctic Engineering, Estoril, Portugal. , 2008: In the Proceedings of the 27<sup>th</sup> International Conference on Offshore Mechanics and Arctic Engineering American Society of Mechanical Engineers.
- [121] M. Saito, Masanobu S., Taniguchi T., Otsubo K., Asanuma T., and M. K., "Experimental Evaluation of VIM on MPSO in Combine Environmental Conditions of Wave and Current," presented at the 31st International Conference on Ocean, Offshore and Arctic Engineering, Rio de Janeiro, Brazil, 2012.
- [122] A. Tahar and L. Finn, "VORTEX INDUCED MOTION (VIM) PERFORMANCE OF THE MULTI COLUMN FLOATER (MCF) – DRILLING AND PRODUCTION UNIT," presented at the Proceedings of the ASME 2011 30th International Conference on Ocean, Offshore and Arctic Engineering, Rotterdam, Netherlands, 2011.
- [123] T. Farrant, M. Tan, and W. Price, "A cell boundary element method applied to laminar vortex shedding from circular cylinders," *Computers & Fluids*, vol. 30, no. 2, pp. 211-236, 2001.
- [124] M. J. Terro and M. Abdel-Rohman, "Wave induced forces in offshore structures using linear and nonlinear forms of Morison's equation," *JVC/Journal of Vibration and Control*, vol. 13, no. 2, pp. 139-157, 2007.
- [125] R. Olsen, S. a. Huang, and N. Barltrop, "Steady Current-Induced Drag on Piggyback Risers.," presented at the In The Eleventh International Offshore and Polar Engineering Conference, Glasgow UK, 2001.
- [126] X. K. Wang, K. Gong, H. Liu, J. X. Zhang, and S. K. Tan, "Flow around four cylinders arranged in a square configuration," *Journal of Fluids and Structures*, vol. 43, pp. 179-199, 2013.
- [127] D. Sumner, S. J. Price, and M. P. Paidoussis, "Flow- pattern identification for two staggered circular cylinders in cross- flow," *Journal Of Fluid Mechanics*, vol. 411, pp. 263-303, 2000.

- [128] M. A. Benitz, D.P. Schmidt, M.A. Lackner, and G. M. Stewar, "Validation of Hydrodynamic Load Models Using CFD for the OC4-DeepCwind Semisubmersible," presented at the ASME 2015 International Conference on Ocean, Offshore and Arctic Engineering, St. John's, Newfoundland, Canada, 2015.
- [129] H. Lindekrantz, S. O., "IMPROVED COLUMN DESIGN ON A DP3 SEMISUBMERSIBLE UNIT," MSc, Department of Shipping and Marine Technology, CHALMERS UNIVERSITY OF TECHNOLOGY, Göteborg, Sweden 2014, 2014.
- [130] Y. Bai, Marine Structural Design [electronic resource]. Burlington : Elsevier Science, 2003.
- [131] DiamondOffshore. (2016, 26th August). Technical Report. Available: <http://www.diamondoffshore.com/fleet-overview>
- [132] WoodGroupMustang. (2015, 26th August). Offshore Topside Design Catalog: Reference designs to meet any project need. Available: [http://www.mustangeng.com/NewsandIndustryEvents/Publications/Publications/WGM\\_OffshoreDesignCatalogPreview051315.pdf](http://www.mustangeng.com/NewsandIndustryEvents/Publications/Publications/WGM_OffshoreDesignCatalogPreview051315.pdf)
- [133] R. Toscano and E. Dvorkin, "A shell element for finite strain analyses: hyperelastic material models," Engineering Computations, vol. 24, no. 5, pp. 514-535, 2007.
- [134] E. N. Dvorkin and K. J. Bathe, "A Continuum Mechanics Based Four-Node Shell Element for General Non-Linear Analysis," ed: Department of Mechanical Engineering, Massachusetts Institute of Technology, Cambridge USA., 1983.
- [135] R. D. Cook, Concepts and applications of finite element analysis, 2d ed. ed. New York : Wiley, 1981.
- [136] T. R. Chandrupatla, Introduction to finite elements in engineering, 3rd ed. ed. Upper Saddle River, N.J. : Prentice Hall, 2002.
- [137] T. P. Estefen and S. F. Estefen, "Buckling propagation failure in semi-submersible platform columns," Marine Structures, vol. 28, pp. 2-24, 2012.
- [138] I. Senjanovic, S. Malenica, and T. e. S., "Investigation of ship hydroelasticity," Ocean Engineering, vol. 35, pp. 523-535, 2007.
- [139] A. INC, "Aqwa Theory Manual," vol. Release 16.2, ed: Ansys, 2015, p. 174.
- [140] Design of offshore steel structures, general - LRFD method, 2016.

[141] J. M. J. Journée and J. Pinkster, INTRODUCTION IN SHIP HYDRO-MECHANICS. Netherland: Delft University of Technology, 2002.

[142] GUIDE FOR SHIPBUILDING AND REPAIR QUALITY STANDARD FOR HULL STRUCTURES DURING CONSTRUCTION, 2007.

[143] FABRICATION AND TESTING OF OFFSHORE STRUCTURES, 2010.

[144] DiamondOffshore. (2016, 29th October). Our Fleet.

Available: <http://www.diamondoffshore.com/fleet-overview>

[145] AkerSolutions. (2016, 26th October). Floater designs. Available:

<http://akersolutions.com/what-we-do/products-and-services/floater-designs/>

[146] ORCINA, “Orcaflex Manual” vol. 9.6. ed: Orcaflex, 2015.